Production of lactic acid from renewable resources using electrodialysis for product recovery

Garde, Arvid; Jørgensen, Sten Bay; Jonsson, Gunnar Eigil

Publication date:
2002

Document Version
Publisher's PDF, also known as Version of record

Production of lactic acid from renewable resources using electrodialysis for product recovery

Ph.D. Thesis

by

Arvid Garde

Department of Chemical Engineering
Technical University of Denmark

Supervisor: Ass. Prof. Gunnar Jonsson

Co-supervisor: Prof. Birgitte K. Ahring

December 2002.

ISBN 87-90142-84-5
Printed by Book Partner, Nørhaven Digital, Copenhagen, Denmark

Preface

This thesis presents the results of work done in The Membrane Group, Department of Chemical Engineering and in The Anaerobic Microbiology/Biotecnology Research Group, Department of Biotechnology, The Technical University of Denmark, in the period from January 1, 1998 to December 31, 2000 with Professor Gunnar Jonsson and Professor Birgitte K. Ahring as supervisors.

The work is carried out as part of the Danish research project “Biologically Based Packaging Materials for Foods” for which the main objective is to initiate development of a new generation of food packaging materials based on biomass originating from waste products from Danish crops, and to investigate the suitability of the biobased materials for packaging of foods.

The project “Biologically Based Packaging Materials for Foods” is focused on:

- Development of biobased packaging materials originating from potato starch.
- Development of biobased packaging materials originating from polylactic acid (PLA) produced by microbial fermentation of e.g. hemicellulose from wheat straw and brown juice from the green crop drying industry.
- Investigation of the suitability of the biobased packaging materials for packaging of foods.
- Optimization of the properties of the biobased packaging materials.
- Investigation of foodstuff packed in biobased packaging materials (e.g. mushroom, orange juice and mould ripened cheeses).

In this thesis “only” the fermentative production of lactic acid from agricultural crop residues (wheat straw) and agro-industrial waste (grass juice) are investigated in combination with product recovery using different membrane techniques. The thesis consists of a short summary, an introduction describing the motives for doing research within this field, a chapter describing the theory behind the different steps of the lactic acid process, a results section including research papers, a chapter concerning modeling of a special electro-membrane process, a chapter in which the economics behind a lactic acid plant is evaluated and finally concluding remarks.

Acknowledgement

I would like to thank Gunnar Jonsson and Birgitte K. Ahring for supervision, guidance and support. I would also like to thank pre- and present members of both the Membrane Group and The Anaerobic Microbiology/Biotecnology Research Group.

A special thank to Anette S. Schmidt, Plant Biology and Biogeochemistry, Risø National Laboratory, PO Box 49, DK-4000 Roskilde and Pauli Kiel, Centre for Agro-Industrial Biotechnology, University of Southern Denmark, Niels Bohrs Vej 9, DK-6700 Esbjerg for a good and fruitful collaboration.

Chr. Hansen A/S, Bøge Allé 10, DK-2970 Hørsholm is acknowledged for supplying lactic acid bacteria for the initial screening and Tokuyama Europe GmbH, Düsseldorf for supplying ionexchange membranes.

The Danish Ministry of Food, Agriculture and Fisheries is acknowledged for support of the work by grants from the program “Increased Utilization of Renewable Resources for Industrial Non-food Purposes (1997-2001)”.

Sammendrag

Hemicellulose fra hydrolyseret hvedestrå samt plantesaft (brunsaft) fra produktion af foderpiller blev benyttet som udgangsmateriale for produktion af mælkesyre. Gennem screening af forskellige mælkesyreproducerende bakterier, viste det sig, at en kombination af *Lb. pentosus* og *Lb. brevis* kunne udnytte samtlige sukkerkomponenter i hemicellulose hydrolysatet med et højt udbytte, nemligå 95 %. Bakterie kombinationen kunne gro på en blanding af hemicelulose hydrolysat og brunsaft uden tilsætning af yderligere vækst komponenter.

Ved at benytte kombinationen af *Lb. pentosus* og *Lb. brevis* var det muligt at ændre forbehandlingen af halmen, så vådoxideringen kunne forløbe uden brug af natriumkarbonat og ved et reduceret ilttryk på 6 bar uden negativ indvirkning på mælkesyre udbyttet. Det var herved muligt at reducere omkostningerne ved forbehandlingen.

Kontinuert mælkesyrefermentering af brunsaft i en Anaerobic Sludge Blanket (UASB) reaktor viste at blandingskulturen af *Lb. pentosus* and *Lb. brevis* var i stand til at danne granula og herved immobiliseres i reaktoren. Som følge af dannelsen af granula var det muligt at operere med hydrauliske opholdstider der var kortere end generationstiderne for bakterierne, hvilket medførte en maksimal produktivitet på 14.8 g/l/h ved en fortyndingshastighed på 1.07 h^{-1}. Det var dog ikke muliget at få omsat al sukkerstof i udløbet fra reaktoren.

Forskellige mulige processer til separation og videre oprensning af mælkesyre fra brunsaft fermentat er blevet undersøgt. Fælles for disse *flow sheets* er brugen af elektrodialyse med bipolære membraner (EDBM) til at generere og koncentrere mælkesyre ud fra laktat. Eksperimenterne viste at EDBM enheden var yderst effektiv med strømeffektiviteter nær det teoretisk maksimale og et energiforbrug fra 1.48-2.26 kWh/kg når mælkesyre oprenses fra en væske indeholdende laktat. En ulempe ved at benytte EDBM er kravet til en meget ren fødevæske, der ikke må indeholde celler, proteiner o. lign. Specielt tilstedeværelsen at selv små mængder calcium og magnesium kan betyde udfældninger af tungtopløselige hydroxider og irreversibel skade på membranerne. Den meget lave koncentration af divalente kationer i væsken fra fermenteret hvedemel gjorde det muligt at benytte mikro-/ultrafiltreret ferment direkte til forsøg med to- og trekammer EDBM. Forsøgene viste at trekammer konfigurationen havde en højere strømeffektivitet og lavere energiforbrug end tokammer konfigurationen. Dette skyldes hovedsageligt at der i tokammer EDBM

forekommer konkurrerende iontransport af laktat og hydroxid, hvilket ikke er tilfældet ved trekammer EDBM.

Nanofiltrering blev undersøgt som en mulig forbehandling for at imødekomme kravene om et lavt niveau af divalente kationer før behandling af fermenteringsvæske i en EDBM-enhed. Ved nanofiltrering af fermenteret brunsaft var det muligt at reducere indholdet af calcium med ca. 98 % og opnå en fuldstændig klar væske, men pga. et meget højt start niveau af divalente kationer kan det være nødvendigt at foretage to serielle nanofiltreringer. De bedste resultater blev opnået med en NF45 nanofiltreringsmembran fra DSS, Danmark. Permeatfluxen faldt fra 30 til 10 l/m^2h under en 6 gange opkoncentrering ved 30 bar. Der var ingen markant ændring ved at benytte fermenteret brunsaft der allerede var mikro- eller ultrafiltreret, hvilket kan skyldes det relativt lille volumen af fermenteret brunsaft i forhold til membranarealet som blev benyttet i forsøgene.

Der blev foretaget forsøg med en ny type neddyppet vibrerende mikrofiltreringsmodul med hule fibre, som udviste høj permeatflux under filtrering ved ekstrem lavt transmembrantryk (TMP). Af hensyn til sammenlignelighed med andet litteratur blev der under udviklingsarbejdet af modulet udelukkende benyttet modelopløsninger i form af gærsuspensioner. Ved vibrationer med en amplitude på 3 mm og en frekvens på 30 Hz var det muligt at opnå en kritisk flux på 68 $l/m^2/h$ under filtrering af en 5 g/l gær suspension ved et transmembrantryk på 6 mbar.

Længerevarende undersøgelser af mælkesyreekstraktion fra fermenteringsvæske med elektro-membran processer førte til udviklingen af en proces med indbygget anti-tilsmudsningsmekanisme. Processen er blevet døbt strømvendende elektro-forstærket dialyse og er beskrevet i en patentansøgning. Membranopsætningen svarer til opsætningen i en Donnan dialyse proces med anionbyttermembraner, men elektrisk strøm sendes gennem systemet for at forstærke iontransporten, der er kontrolleret af konkurrerende transport mellem laktationer og hydroxidioner ved skiftende pH-niveauer. Strømvending er inkorporeret for at destabilisere opbyggede lag af organisk tilsmudsning på membranerne.
Den strømvendende elektro-forstærkede dialyse proces blev testet på både model opløsninger og fermenteringsvæsker ved en opsætning, der simulerer en kontinuert fermentering. Tilfredsstillende laktatfluxe kombineret med høj tilbageholdelse af sukkerstoffer, calcium og magnesium blev konstateret. Procesfaktorer som strømeffektivitet og energiforbrug var ikke tilfredsstillende, men det blev anslået at optimering af udstyrsdesign og af operationsparametre gennem computersimulationer kunne bringe disse op på et økonomisk acceptabelt niveau.

Ved at indføre strømvending kunne processen køre uden stop over længere perioder, end hvis strømvending blev udeladt.
Strømvendingen medfører et effektivitetstab, der blev undersøgt ved konstruktionen af en matematisk model, der blev implementeret som et computerprogram. Dette program var i stand til at producere estimater for strømeffektivitet, samlet laktatflux, energiforbrug og nødvendigt membranareal for som funktion af strømvendingsfrekvens, laktat og hydroxid koncentrationer i føde og dialysat, samt strømdensitet.

Et anlæg til produktion af 10,000 tons mælkesyre (88%) om året blev designet baseret på kontinuert fermentering i en UASB reaktor og den strømvendende elektro-forstærkede dialyse proces ved at benytte procesestimater bestemt fra eksperimenter eller gennem simuleringer. Ekstraktionen af laktat fra fermenteringsvæske blev kombineret med elektrodialyse med bipolære membraner, afsaltning ved hjælp af elektrodialyse og inddampning for at opnå den ønskede renhedsgrad og koncentration. En økonomisk evaluering af produktionen blev foretaget, og den samlede investering blev vurderet til at være € 26,2 mio. Med en mælkesyrepris på 1,56 €/kg 88% mælkesyre blev tilbagebetalingstiden udregnet til 3,4 år og forrentningen til 35 %. Anlæggets økonomiske sensitivitet overfor udsving i mælkesyres salgspris og substratomkostninger blev ligeledes undersøgt.

Summary

Hemicellulose from hydrolyzed wheat straw and grass juice (brown juice) from production of fodder pellets was used as raw material for production of lactic acid. Through screening of a number of lactic acid producing bacteria a combination of *Lactobacillus pentosus* and *Lactobacillus brevis* was found to utilize all sugars in hemicellulose hydrolysate at high yield (95%). They also grew well on a mixture of hemicellulose hydrolysate and brown juice without addition of extra growth factors.

Lactic acid production from hemicellulose hydrolysate prepared by wet-oxidation at various process conditions showed that by using a co-culture of *Lb. pentosus* and *Lb. brevis* it was possible to omit the use of alkali and reduce the oxygen pressure in the wet oxidation process without adversely effecting utilization of hemicellulose. The cost of pretreatment could hereby be reduced.

Continuous lactic acid fermentation of brown juice using an Upflow Anaerobic Sludge Blanket (UASB) reactor showed that a co-culture of *Lb. pentosus* and *Lb. brevis* was able to form granules and immobilize in the reactor, and thus allowed operation with hydraulic retention times shorter than the generation time. The maximum productivity of lactic acid reached 14.8 g/l/h at a dilution rate of 1.07 h^{-1}, even though not all sugar components where fully utilized.

Different processes for recovery and purification of lactic acid from fermentation broth were investigated. In all the proposed process flow sheets electrodialysis with bipolar membranes (EDBM) was employed for generating the lactic acid and in most cases also for concentrating the acid. Experiments showed that the EDBM process was very effective with current efficiencies close to the theoretical maximum and energy consumption from 1.48-2.26 kWh/kg when lactic acid was recovered from a stream containing lactate. However, a major disadvantage of using bipolar membranes is the need of a very pure feed stream. The feed must be free of cells and proteins, but most important, the level of calcium and magnesium ions must be below approximately 2-5 ppm to minimize the risk of irreversible damage to the membranes, caused by precipitations of hydroxides. The very low level of divalent cations in the broth of fermented wheat flour enabled experiments with EDBM directly on MF/UF permeates to compare two-, and three-compartment setup. It was found that the three-compartment cell exhibited higher current efficiency leading to lower power consumption than in the two-compartment cell, since competition between hydroxide and lactate ions can be avoided in the three-compartment cell.

One way to insure safe operation of the EDBM-unit is by subjecting the fermentation broth to different membrane filtrations. A completely clear feed solution with a reduction in calcium by approx 98% could be obtained by nanofiltration of the fermented brown juice. However, the high amounts of calcium and magnesium in brown juice makes one single nanofiltration step insufficient for reducing the concentration of divalent cations to an acceptable level. The best results were achieved with an NF45 nanofiltration membrane from DSS, Denmark with a permeate flux dropping within 55 min. from 30 to 10 l/m^{2}h when upconcentrating by a factor of 6 at 30 bar. No marked difference in the performance of the nanofiltration process could be observed when the broth was pre-filtered using ultra- or microfiltration membranes. However, since only screening experiments where performed with relatively small volumes of fermented brown juice compared to membrane area, nothing conclusive can be said about the need for MF/UF pre-filtration.

A novel membrane filtration system employing a submerged vibrating hollow fiber module was evaluated for microfiltration at very low trans-membrane pressures of (0-25 mbar). The filtration system was tested with baker's yeast suspensions at different amplitudes and frequencies of the vibration. At an amplitude of 3 mm and a frequency of 30 Hz a critical permeate flux of 68 l/m^2/h at a trans membrane pressure of 6 mbar was obtained.

An alternative to filtration for preparing the fermentation broth for EDBM was found through lengthy investigations of electro-membrane processes for direct lactate recovery. These investigations lead to invention of a process with a built-in anti-fouling mechanism and has been submitted as patent application. We entitled the process "reverse electro-enhanced dialysis" (REED) as it resembles a Donnan dialysis setup with anion-exchange membranes, but with an overlaid electrical migration for increased total flux, and reversed at short intervals for destabilization of a built-up fouling film. The electrical migration is controlled by competitive transport between lactate and hydroxide ions at different pH-levels.
The reverse electro-enhanced dialysis process was extensively tested on both model solutions and fermentation broths, simulating continuous fermentation operation. Lactate fluxes combined with high retention of sugars, calcium, and magnesium was found to be satisfactory. Even with calcium and magnesium levels in the brown juice of approx. 700 and 400 ppm, respectively, no calcium or magnesium could be detected in the dialysate after a 2 hours run. Process factors such as current efficiency and energy consumption were evaluated and found to be initially unsatisfying. It was estimated that optimization of equipment and of operation

parameters by computer simulations could improve the overall process economics. The process was able to run for prolonged operation times when the current was reversed every 10 seconds compared to similar runs without current reversal.
The efficiency loss incorporated by the frequent current reversals in the reverse electro-enhanced dialysis process was examined by mathematical simulation, implemented in a computer program. The program was able to estimate values for current efficiency, overall flux, energy consumption and necessary membrane area as functions of current reversal frequencies, lactate and base concentrations in feed and dialysate streams, and current densities.

A plant able to produce 10,000 tons lactic acid (88%) annually was designed, incorporating the reverse electro-enhanced dialysis process with process parameters estimated from experiments and simulations. The extraction of lactate from fermentation broth through the reverse electro-enhanced dialysis unit was combined with an electrodialysis with bipolar membranes, an electrodialytic desalination unit and an evaporator system for final purification. An economic evaluation of the lactic acid plant showed that a total capital investment of € 26.2 mill. had a break even time of 3.4 years and an internal rate of return of 35% when the selling price of 88 % lactic acid is 1.56 €/kg. The sensitivity of plant economics to lactic acid prices were also evaluated.

Contents

1

INTRODUCTION

The rapid increase in worldwide consumption of fossil fuel resources poses a potential threat to the environment and time is not too distant before depletion begins to adversely affect reserves. Known global reserves of oil are expected to run dry in approximately 40 years and natural gas in 60 years, but the economical impact of their depletion could hit much sooner (Klass 1998). In the last decades increasing concern for environmental issues, not to mention economical issues, has made researchers all over the world focus on sustainable production of chemicals and energy.

Conversion of agricultural crop residues and agro-industrial waste streams into lactic acid is a process with several beneficial effects. On one hand agricultural waste poses an environmental threat and on the other hand it represents an abundant renewable raw material for several value-added products *e.g.* biogas, ethanol, fibers and different organic acids such as lactic acid. Lactic acid is an important chemical used in a variety of industrial and food applications, but its main potential is as intermediate for manufacture of the biodegradable polymer, poly(lactic acid) (PLA). PLA is a bio-based, and biodegradable polyester that can replace traditional plastics synthesized from fossil hydrocarbon resources in many industrial applications including packaging of foods, and hence solve many waste problems related to packaging materials.

The art of producing lactic acid by fermentation has received much attention in the past decade and judging by the number of recent patents and scientific articles research has been especially tense in the past 3-5 years. There are several vital factors affecting large scale fermentative production of lactic acid. The choice of substrate, LAB species, operating conditions and separation processes are a few of the main factors of importance for commercial production.

One major hurdle in fermentative production of lactic acid from agricultural waste is finding a recovery process that is economically viable.

In the present study, focus will mostly be on the membrane process in direct contact with the fermentation broth, as this unit encounters a very impure stream with a high fouling potential and faces some strict requirements for purity, set by the subsequent bipolar electrodialysis.

2

PROJECT AIMS

The overall aim of this project was to investigate the use of agricultural wastes and residuals for lactic acid production, as outlined below:

- Investigate the suitability of hemicellulose from wheat straw and grass juice as fermentation substrates for lactic acid production.

- Find microorganisms, able to utilize all the different sugar components of the hemicellulose at high yield.

- Investigate different membrane techniques for separation and purification of lactic acid from the fermentation broth.

- Based on the results, suggest a process for commercial production of lactic acid.

- Evaluate the economy behind a lactic acid production facility based on the “best technology” found in this work.

3

THEORY

The task of designing an entire process to convert agricultural crop residues to a purified lactic acid product requires multidisciplinary insight. This chapter will provide insight into the technology and fundamentals behind the many unit operations involved in the process, as well as the chemistry/biochemistry behind the substrates and their utilization by lactic acid bacteria. The present market and future potential of lactic acid production are discussed to draw a picture of the commercial motivation for the project.

3.1 Lactic acid

3.1.1 Properties

2-hydroxypropanoic acid, better known as lactic acid, is a chiral molecule with two optically active forms, L(+)-lactic acid and D(-)-lactic acid, as shown in Figure 3.1.1. Lactic acid is the simplest and most widely occurring hydroxy carboxylic acid found in most living organisms, from anaerobic prokaryotes to humans (Datta 1995). Small amounts of L-lactic acid occur in body fluids and organs. Primarily muscle tissue produces the L-lactic acid while obtaining energy by metabolizing sugar in the absence of oxygen.

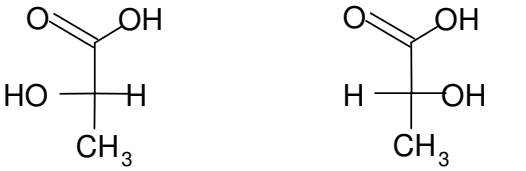

Figure 3.1.1 The two optically active forms of lactic acid.

In the pure anhydrous form lactic acid is a white crystalline solid with a melting point of 52.7-52.8 °C for either pure isomer and 17-33 °C for the racemic mixture. The pure form is quite difficult to obtain and for industrial purposes lactic acid is handled in

concentrated aqueous solutions. The consistence is syrupy, and depending on how the liquid is produced it can be colorless or be slightly yellow. Lactic acid has a pKa-value of 3.88 at 25 °C, resulting in the curve in Figure 3.1.2 where the degree of dissociation is plotted as function of pH. It can be seen that below pH=2 virtually all of the acid is undissociated and above pH=6 it is almost totally dissociated.

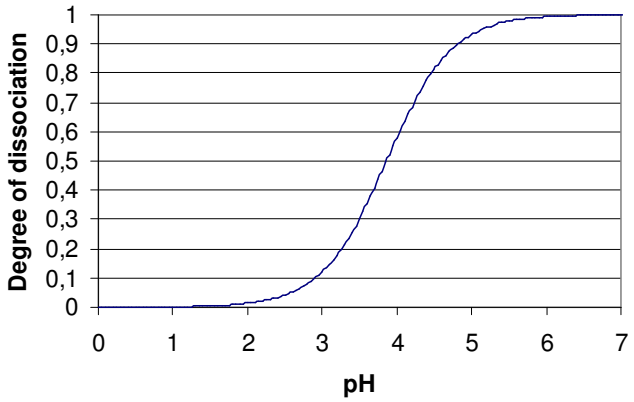

Figure 3.1.2. Degree of dissociation of lactic acid as function of pH.

As a bulk chemical lactic acid is available in technical, food and pharmaceutical grade at concentrations of typically 50, 80 or 88%. Pharmaceutical grade lactic acid satisfies United States Pharmacopoeia (USP) or European Pharmacopoeia (Ph. Eur.), which dictates the strictest requirements regarding the purity. The food grade must live up to the requirements of the E270 number in Europe, but no particular restrictions apply to technical grade lactic acid, other than those set by the buyers. The lactic acid used for production of PLA must be the very pure Pharmaceutical grade.

3.1.2 Production

There are two main routes for producing lactic acid, synthetically by the hydrolysis of lactonitrile or through fermentation of carbohydrates by lactic acid bacteria.

The synthetically production of lactic acid is carried out according to Figure 3.1.3 where a fossil feedstock is converted into ethylene which is oxidized to form acetaldehyde. Lactonitrile is produced by base catalyzed addition of hydrogen cyanide to acetaldehyde and after distillation the crude lactonitrile is hydrolyzed to a racemic lactic acid by either hydrochloric or sulfuric acid. The crude lactic acid is further purified through esterfication with methanol, which is then distillated and re-hydrolyzed by acid catalyzed addition of water (Datta 1995). The lactic acid produced in this way is heat stable, meaning that it can be heated with reflux at 180 °C in 20 min. without undergoing side reactions.

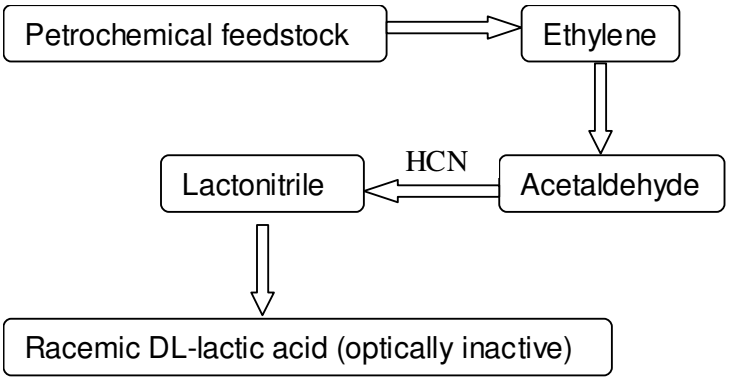

Figure 3.1.3. Petrochemical route to lactic acid.

With the shutdown of the Sterling Chemical, USA 8600 t lactic acid plant in 1995, Musashino Chemical Laboratory Ltd., Japan is presently the sole company still using the synthetic route for production of racemic lactic acid (Lunt 1998).

By and large the commercial production of lactic acid is based on glucose fermentation using homofermentative lactobacilli, particular strains of *Lactobacillus delbruckii* and *Lb. helveticus*. Like the synthetic route, fermentative production of lactic acid requires a series of unit operations before reaching a concentrated and purified product. However, production of lactic acid by fermentation offers some advantages over the chemical synthesis. Substrate for the fermentation process can be chosen from a variety of different carbon sources, which gives the opportunity to select the feedstock depending on availability and price. Furthermore, it is possible to obtain the pure D- or L-lactic acid by selecting specific strains of bacteria. The configuration of the lactic acid molecule is a very important parameter when for instance PLA is produced. However, it should be mentioned that it is possible to combine the synthetic route with action of microorganisms to produce optically active lactic acid, but the economics behind such a process is questionable. By subjecting DL-lactonitrile to the action of microorganisms, which are capable of stereospecifically hydrolyzing a nitrile, D- or L-lactic acid can be produced in a predominant proportion (Endo *et al.* 1992).

In the scientific literature, and in particularly the patent literature, the typical fermentative route to lactic acid starts with some sort of substrate pretreatment, either just addition of essential growth components e.g. suitable mineral and proteinaceous nutrients, or in addition, mechanical treatment combined with chemical/enzymatical hydrolysis. The required pretreatment depends primarily on the feedstock and to some extent on which kind of lactic acid bacteria that is employed. The purpose of

the pretreatment is to make the carbon source available for fermentation with LAB, which in case of most renewable resources means, hydrolyzing the polymeric carbohydrate constituents to form monomeric sugars.
Aiming for high productivity and yield, lactic acid fermentation is commonly carried out by a bacterial strain chosen of from the genus *Lactobacillus*, the species depending on the type of substrate and desired lactate configuration. The fermentation can be performed in several ways but three principal methods can be distinguished: batch (Zayed and Winter 1995), fed-batch (Roukas and Kotzekidou 1998) or continuous (Ohashi *et al.* 1999;Tejayadi and Cheryan 1995;Zayed and Winter 1995) fermentation. Regardless of the mode of operation the lactate must be separated from the fermentation broth and here microfiltration (Borgardts *et al.* 1998b;Boyaval *et al.* 1996;Kulozik 1998) or ultrafiltration (Van Nispen et al. 1991) seems to be the method of choise. The type of unit operations needed for further purification strongly depends on which kind of impurities the initial feedstock contains, but processes such as reverse osmosis (Liew *et al.* 1995;Timmer *et al.* 1993;Timmer *et al.* 1994), nanofiltration (Jeantet *et al.* 1996;Mani and Hadden 1998;Miao 1997;Timmer *et al.* 1993;Timmer *et al.* 1994), diffusion dialysis (Portner and Markl 2001) Donnan dialysis (Zheleznov *et al.* 1998), electrodialysis (Boniardi *et al.* 1996;Boniardi *et al.* 1997a;Boniardi *et al.* 1997b;Borgardts *et al.* 1998a;Borgardts *et al.* 1998b;Czytko *et al.* 1987;de Raucourt *et al.* 1989;Hongo *et al.* 1986;Lee *et al.* 1998;Mani and Hadden 1998;Miao 1997;Nomura *et al.* 1987;Van Nispen et al. 1991;Vonktaveesuk *et al.* 1994), ion exchange (Beschkov *et al.* 1995;Mani and Hadden 1998;Miao 1997;Rincon *et al.* 1997), carbon adsorption for decoloration, extraction (Kleerebezem *et al.* 2000;Scholler *et al.* 1993;Siebold *et al.* 1995), evaporation as well as esterification combined with distillation and hydrolysis of the ester has been suggested (Eyal *et al.* 1998).

The conventional method for producing lactic acid consists of a 4-6 days batchwise fermentation with pH control using calcium carbonate where the lactic acid concentration reaches around 10 wt % (Datta 1995). The broth is filtered to remove biomass, treated in carbon columns, evaporated and acidified using sulphuric acid to convert the calcium lactate to lactic acid and insoluble calcium sulfate. There are several drawbacks to this conventional process. In the carbon columns impurities are retained and new active carbon must be purchased, but more important, for every ton of lactic acid produced one ton of gypsum is generated as waste.

A commercially used alternative to the gypsum precipitation is extraction using a trialkyl amine in an organic solvent as employed by Cargill (Bizzari *et al.* 1999). (Eyal *et al.* 1998) disclose a technique where a lactic acid containing feed solution (broth)

is contacted with an extractant composed of 47 wt% tricapryl amine, 33 wt% octanol and 20 wt% kerosene. Lactic acid is hereby extracted to the organic phase and after separation of the two phases the organic phase can be added butanol and heated to form butyl lactate. Butyl lactate can be recovered from the organic phase by distillation at reduced pressure and if lactic acid is the desired product the ester can be hydrolyzed to form a very pure product.

Being the main issue of this thesis, each step of the fermentative production route with subsequent product recovery using membrane techniques will be described in details in chapter 3.2-3.5.

3.1.3 Market and Applications

The predominant part of the lactic acid production is done by carbohydrate fermentation, which is the preferred technology when it comes to meeting the future demands for lactic acid. The worldwide consumption of lactic acid has increased significantly over the past decade and was in 1999 rated at 130,000 to 150,000 tons per year with an expected annual growth rate of 5 to 8 percent (Mirasol 1999). Of this annual capacity around 65,000 tons was in the form of lactic acid and the rest was different derivatives hereof. Figure 3.1.4 shows how the consumption in the U.S. has climbed since 1978 without the domestic production being able to fully keep up. In 1998 this led to an import of 22.8 thousand tons of lactic acid from primarily Spain and the Netherlands. Even though the demand has increased, the price of lactic acid has decreased over the past 5-6 years due to toughened competition (Mirasol 1999), see Figure 3.1.5. The current price (Dec. 2000) in U.S. for 88% food grade and 88% technical grade are 70-80 cent/lb and 72-85 cent/lb, respectively. In Europe the prices are generally lower than the U.S. level, which could be due to a cheap Chinese product entering the European market and plenty of product available. Prices on 88% material have been as low as 50 or 60 cent/lb and the 80% Chinese-grade sells at roughly 52 cents/lb in Europe (Mirasol 1999).

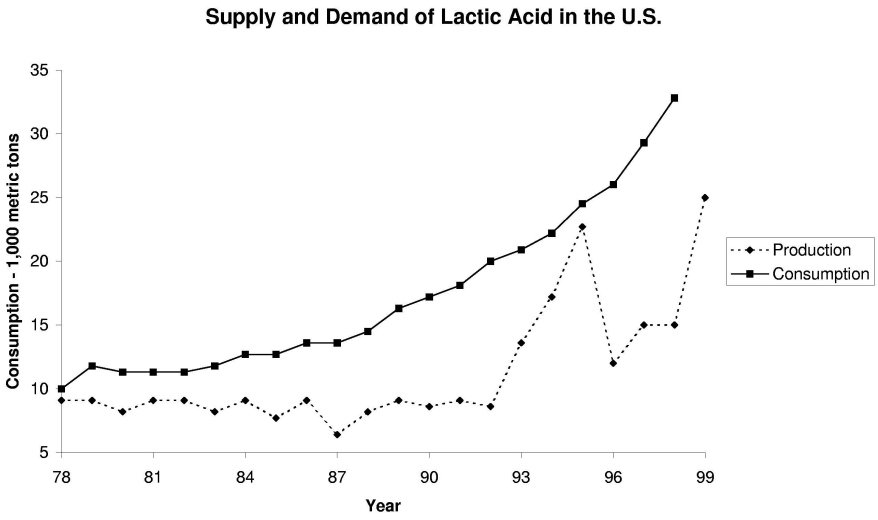

Figure 3.1.4. Production and consumption of lactic acid in US. The drop in supply after 1995 was due to the shut down of the Sterling Chemical plant. Data adapted from (Bizzari *et al.* 1999).

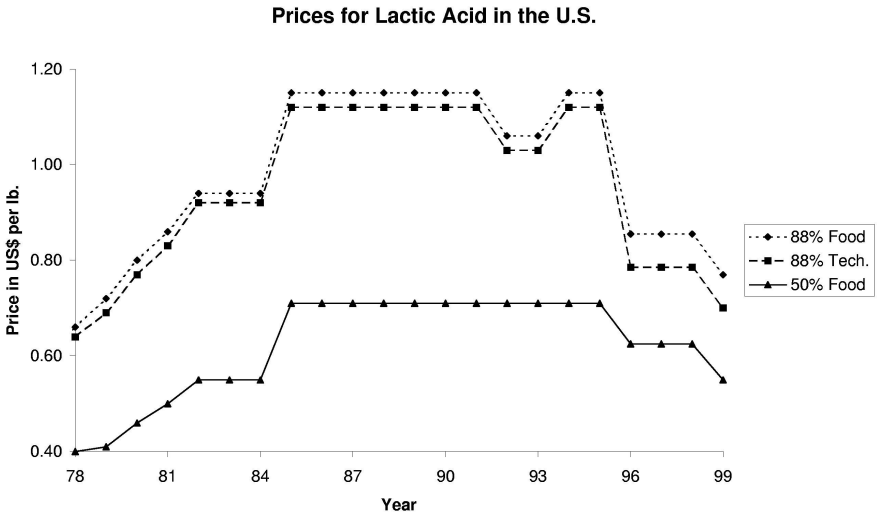

Figure 3.1.5. Prices for lactic acid in the U.S. Data adapted from (Bizzari *et al.* 1999).

The main producing countries are the U.S., China, and Western Europe (Spain, Netherlands and Belgium) and the most active players operating on the lactic acid market includes Purac (Netherlands), Archer Daniels Midland Company (US), Musashino (Japan), Mitsui Chemicals (Japan), Galactic (Belgium) and Cargill-Dow Polymers (US). A more extensive list of companies involved in production and/or end use of lactic acid can be found in appendix A.

Lactic acid is a versatile compound used in a wide variety of applications within both food and non-food areas. The beneficial properties of lactic acid in foodstuff include:

- **pH regulation.**
  Controlling the pH can extend the shelf life. Lactic acid based acidulants are for instance used in salads and dressings.

- **Flavoring.**
  Enhanced and protected meat flavor. The mild acidic flavor is used in candy, soft drinks, beer, soups, dairy products etc.

- **Antimicrobial action**
  Controlling pathogenic bacteria such as *E. coli, C. botulinum, L. monocytogenes* in foodstuff.

- **Pickling agent.**
  Sauerkraut, olives and pickled vegetables are conserved in lactic acid containing brine.

- **Emulsifying agents.** (Esters of lactic acid and long-chain fatty acids)
  Particularly used in bakery goods

- **Animal feed supplement**
  Stabilize gastro-intestinal function of dairy, beef, pork, poultry and pet animals. Protect the animal from pathogenic bacteria by creating a favorable microflora.

Food and beverage applications accounts for approximately half of the total lactic acid consumption, not counting the amount of lactic acid that is produced *in situ* by adding LAB starter cultures to foodstuff such as yoghourt and other dairy products.

One of the relatively new areas with a huge growth potential is the use of lactic acid ferment as animal feed supplement. Studies on pigs have shown that the general well-being of the animal improves and the need for antibiotics diminishes when lactic acid is feed to the pigs. Lactic acid has a positive effect on growth performance and gastrointestinal environment in pigs resulting in higher daily weight gain (Scholten *et al.* 1999).

Within the non-food area the applications for lactic acid and its derivatives are extremely diverse. Some examples are given below:

- **Pharmaceuticals.**
  Electrolyte solutions e.g. for artificial kidney machines, lactate salts of magnesium, zinc and iron lactate for deficiency therapy.

- **Cosmetics.**
  pH-regulator in shampoo and soap, moisturizing and anti-wrinkling agent in many skin care products, anti-tartar agent in toothpastes and mouthwashes

- **Solvents.**
  Paint & Ink thinners, high-purity rinsing solvents for electronics, detergents, metal complexing agent in Ni-plating processes and cleaning solutions with strong degreasing ability.

- **Biodegradable polymers – Poly(lactic acid) (PLA).**
  Surgical sutures, implantable medical devices, pharmaceutical controlled drug delivery systems, and especially packaging materials, films, fibers, and yarns for manufacturing of clothing.

Of the many different non-food applications biodegradable polymers and solvents made from lactic acid are especially exciting due to an enormous market in substituting conventional solvents and polymers. Realization of the intrinsic properties of polymers of polylactic acid and cheap production of monomer from renewable feedstock has led to increasing commercial interest in PLA products.

Cargill Dow Polymers (CDP), a 50-50 joint venture between Cargill Inc. and Dow Chemical Company have spend more than $300 million on building a 140.000 tons

per year PLA plant in Blair, Nebraska that came on stream in late 2001. Lactic acid for the PLA production will come from fermentation of corn, but other materials such as wheat and sugar beet can also be used. Eventually, bio-waste such as rice hulls and corn stalks will be used as feedstock in the fermentation process as well. CDP anticipate building subsequent plants every 18-24 month if demand warrants, with the first plant being placed in Europe. CDP expect a selling price for the so called NatureWorks™ PLA resin in the range of 50 cent to $1 per pound and have already lined up commitments from several companies to develop products made from PLA (Brown 2000). CDP is confident that PLA will ultimately compete on cost/performance with PE, PP, PS, and PET as well as paper and cellophane (Matthew 1998).

CDP is a market leader when it comes to PLA production, but among the few competitors with smaller production capacities are Mitsui Chemicals (Japan), Shimadzu Corp. (Japan) and Chronopol Inc. (U.S.). Mitsui Chemicals produce PLA under the brand name Lacea™ through a new manufacturing technology using direct condensation polymerization. Lacea™ is based on lactic acid from fermented starch, which enables the use of other renewable resources as feedstock. The company claims to be able to economically produce PLA that can be extruded and injection molded like conventional polyester with properties comparable to PET. Since 1996 Lacea™ has been made in a 500 tons/year semi-commercial plant and as is the case for most of the competitors, Mitsui Chemicals has ambitious plans for a fully commercial plant. An estimated selling price would be around $1.4/lbs for material produced in a factory with a capacity of several tens of thousand tons/year (Warmington 1999).

Shimadzu Corp. also uses a fermentation process to produce lactic acid for their poly-L-lactic acid resin called Lacty™. The company has a 100 tons/year pilot plant built in 1996 and a several hundred tons/year plant built in 1997 together with Kobe Steel. Among others Lacty™ has been developed to make fibers for clothing textile. The fiber material, called Lactron™, is similar to other synthetic fibers in terms of processability and physical properties but after use it can be completely decomposed into water and CO2 in soil or sea water. (Warmington 1999)

In 1998 Chronopol Inc. came on stream with a 1000 tons/year PLA plant in Golden, Colorado producing Heplon™ at a selling price around $5/lbs. Chronopol expect to build a 50.000-70.000 tons/year plant in 2002, which will lower the price on resin to $1.50-2/lbs.

Much attention has been drawn towards lactate esters because they are nontoxic, biodegradable, and have excellent solvent properties. Especially methyl-, ethyl- and butyl lactate have strong degreasing ability that enables them to substitute toxic and halogenated solvents in many industrial and consumer applications (Musashino Chemical Laboratory 2001). Until now they have been too expensive for widespread use but if the price gets down from the current $1.60 - $2.00/lb a huge market will open up. In Table 3.1.1 Argonne estimated the market for different applications at varying selling prices where the Argonne Process is expected to cut the current price be in half (Argonne National Laboratory 2001).

Table 3.1.1. Applications and Markets for Lactate Esters adapted from (Argonne National Laboratory 2001).

If the price of lactate esters is	$1.60-$2.10/lb	$1.25/lb	$0.85-$1.00/lb
and the total market is projected to be	For solvents and chemicals: 20 million lb/year	For solvent replacement: 120 million lb/year	For solvent replacement: 5 billion lb/year worldwide
then substitution of lactate esters will become cost-effective in the following applications:	Specialty chemicals manufacture/formulation High-end electronics Chiral synthesis Specialty cleaning Food emulsification agents	Specialty electronics and semiconductors Specialty water-based coatings Specialty paint stripping Specialty de-inking formulations High-purity specialty cleaners High-solids coatings	General-purpose industrial and household cleaners and degreasers Semiconductor chip manufacturing De-inking for recycled paper Metal cleaners Blended solvents Paints and coatings Print shop cleaners Aerosols Adhesives Other Applications Biodegradable polymers for films, packaging: more than 1 billion lb/yr Oxygenated chemicals: more than 6 billion lb/yr

The applications of lactic acid and its derivatives are numerous and the potential market is enormous, especially when it comes to PLA, lactate esters and lactic acid

ferment as animal feed supplement. Lactic acid is ubiquitous in nature, so the production and use of large quantities in various applications should not pose any danger to human health or the environment.

3.2 Renewable resources

As previously stated, the fermentative route for production of lactic acid can carried out utilizing a variety of different resources. Especially agro-industrial waste streams and agricultural crop and forestry residuals are interesting because they are abundant and renewable. The term renewable covers the fact that these residuals or waste streams are generated, if not constantly, when at least once a year from a non-fossil carbon source. This is in contrast to the fossil-fuel-based sources that aren't renewed and now are being depleted at a fraction of the time required for its formation. So, to find a viable resource and still be able to produce lactic acid, as well as other chemicals, in an economical fashion, we have to look at the potential of our vast amounts of renewable waste. Several factors affect the choice of feedstock for fermentative production of lactic acid:

- **Bioconversion potential.**
  A fermentable carbon source should be present in reasonable concentration.

- **Cost of raw material.**
  In the case of waste biomass the cost is often negligible or even negative.

- **Local availability.**
  Large quantities and low value of substrate do not allow for costly transport.

- **Continuous supply**
  The lactic acid plant must not stand still if the biomass is unavailable.

- **Required pretreatment.**

  Some resources necessitate extensive processing and addition of growth factors before the carbohydrates are fermentable – some need no pretreatment.

- **Impact on product separation and purification.**

  Impure feedstock can complicate the recovery of product and raise the cost of down stream processing.

- **Cost of waste disposal**

  Even though the COD in the initial waste biomass has been decreased there is still a waste stream to take care of.

A number of different renewable resources have been found to have potential as feedstock for production of lactic acid, a review is given in (Hofvendahl and Hahn-Hagerdal 2000). The compounds in crop residuals and agro-industrial waste, which are fueling the formation of lactic acid are most often hemicellulose, cellulose, starch, or in some cases readily available mono- and disaccharides. Knowledge of the chemical composition of the feedstock and structure of the carbon source is important for implementing the right pretreatment and product recovery processes, as well as for choosing the right fermenting microorganism(s).

The full economic impact of the choice of feedstock on the production price of lactic acid is complicated to analyze. The initial cost per kg of carbohydrates is important but far from determining for which kind of substrate that should be exploited. Utilization of residuals and waste streams has to compete with the use of refined beet or cane sugar (sucrose). The price of carbohydrates are higher, when using pure sugar instead of residuals, but the use of pure sugar will reduce the need for extensive pretreatment and reduce the complexity of recovery processes. The separation and purification processes are the most expensive part of fermentative lactic acid production, which is especially pronounced with the most impure substrates.

As with other chemical plants, to run most efficiently, a lactic acid plant must have as little downtime as possible. Therefore, continuous access to fermentation substrate is vital for the economics of the plant. However, most agricultural crop residuals are produced during a short period of time once per year, which necessitate storage facilities in addition to storage stability of the residual. The residuals should furthermore be generated close to the lactic acid plant to minimize costly transport.

Properties of the bioreactor effluent from the lactic acid plant depend on the nature of the substrate. The purge will contain some cell material together with a residue of organic compounds that the lactic acid bacteria don't utilize. For most substrates the level of COD and nitrogenous compounds in the discharge will be too high for direct disposal, and this nessessitates an investment in waste treatment. However, this does not necessarily mean a setback for the overall economy of the plant. On the contrary, a Danish company, Bioscan A/S, has shown, that by treating the effuent from a lactic acid plant based on whey substrate in a biogas reactor and utilizing the resulting energy, the extra capital investment will have a payback time of 3-4 years.

3.2.1 Lignocellulose

Lignocellulosic biomass is the most abundant organic resource in the biosphere. In the lignocellulosic biomass hemicellulose and cellulose are infiltrated with the stiffening bonding material lignin, which is an aromatic biopolymer rich in phenolic components. Hemicellulose and cellulose are both polysaccharides, constituting the main part of the flexible fibers of plants trees. The lignocellulosic crop residuals include various straws, bagasse, corn stoves and the like. The lignocellulosic complex is quite resistant to conversion by microorganisms but can be broken down by different acid or alkali catalyzed thermal hydrolysis methods. Mild hydrolysis using wet oxidation or steam explosion will solubilize the hemicellulose and make the solid cellulose fraction susceptible to enzymatic hydrolysis.

Cellulose is composed of glucose units in β-(1,4) glucosidic linkage with a degree of polymerization of 8000-15000, see Figure 3.2.1 (Wayman and Parekh 1990).

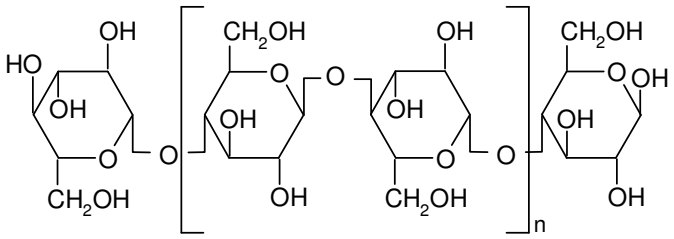

Figure 3.2.1. Cellulose – D-glucose in β-(1,4) linkage.

Cellulose is a linear polymer with a crystalline structure due to H-bonding within the cellulose fibers. It is insoluble in water, but can be enzymatic hydrolysis to yield D-glucose by cellulase and beta-glucosidase according to the following reaction:

$$\text{Cellulose} \xrightarrow{\textit{Cellulase}} \text{Cellubiose} \xrightarrow{\textit{Beta-glucosidase}} \text{Glucose}$$

Hemicellulose, (or rather hemicelluloses) is a complex collection of polysaccharides with an average size of 150-200 sugar monomers (Goden 1993). Unlike cellulose, hemicelluloses can be highly branched and are soluble in dilute alkali. They are classified on the basis of the dominant monomer, which most often is a β-(1,4) linked xylose backbone as shown in Figure 3.2.2.

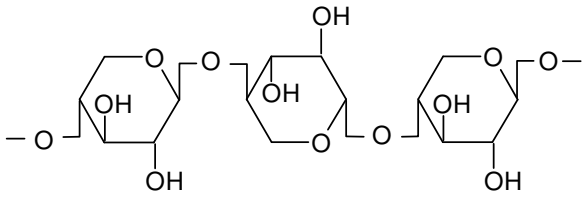

Figure 3.2.2. Xylan, a Hemicellulose backbone composed of D-xylose in in β-(1,4) linkage

The xylan chain usual bears mono- or oligosaccharides containing different amounts of arabinose, glucose, mannose, galactose or galacturonic and glucuronic acids. Hemicellulose can be hydrolyzed to the monomeric constituents by enzymatic or acidic treatment. In the present work hemicellulose from wheat is used as substrate for lactic acid fermentation.

3.2.2 Starch

Starch is the nutritional reserve in plants occurring in the form of minute granules in seeds, tubers, and is an important constituent of corn, beans, potatoes, rice, wheat and other biomass foodstuff. Polymerized chains of D-glucose make up starch, but in contrast to the structure of cellulose the glucose units are linked mostly by α-(1,4) linkage. Starch is composed two forms of chains, a linear chain with up to 100,000 glucose residues called amylose and a chain branched by one α-(1,6) linkage for every 20-40 α-(1,4) linkage called amylopectin, see Figure 3.2.3.

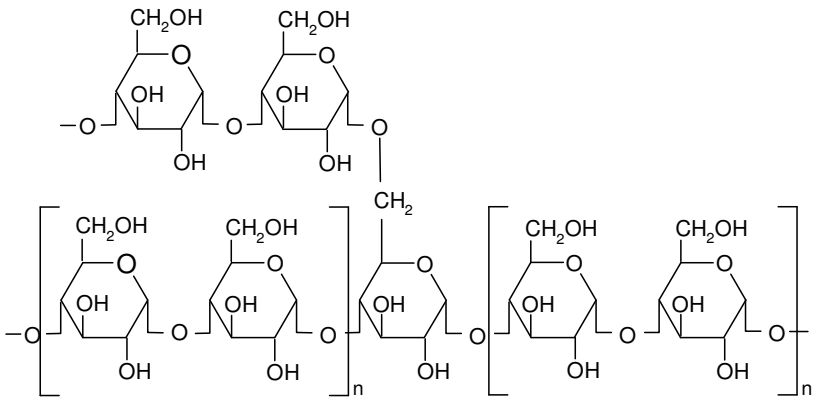

Figure 3.2.3. Amylopectin cross-linkage, n is around 10-20.

Amylose is soluble in water and can be separated from amylopectin by controlled heating to 90-100 °C where amylopectin stays insoluble. Both fractions can be saccharified to fermentable sugars by either acid hydrolysis or by a dual enzyme system in which the liquefying enzyme is alpha-amylase and the saccharifying enzyme is glucoamylase (Wayman and Parekh 1990).

3.2.3 Fructans, mono- and disaccharide

Agro-industrial waste streams, such as whey, molasses, and plant juice are examples of renewable resources that contain mono- and/or disaccharides. Whey, a by-product from cheese manufacturing industry, contains about 4-6% lactose (see Figure 3.2.4), which can be supplemented with a nitrogenous source and fermented to lactic acid (Borgardts *et al.* 1998b;Kulozik 1998;Kulozik and Wilde 1999;Roukas and Kotzekidou 1998;Tejayadi and Cheryan 1995;Zayed and Winter 1995). Apart of lactose, whey also contains potassium, calcium and chloride ions, which makes separation of the lactic acid more difficult. The annual worldwide production of whey is 40 mill. tons of which a large portion is treated by ultrafiltration to produce whey protein concentrate (Tejayadi and Cheryan 1995).

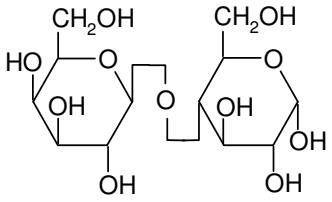

Figure 3.2.4. Lactose (galactose-β(1,4)-glucose)

Whey has very low storage stability, but as it is produced continuously throughout the year, lengthy storage can be avoided.

Molasses is typically the liquid waste from refining of cane or beet sugar and contains about 50% fermentable sugars, mostly sucrose (see Figure 3.2.5), but it can also consist of a syrupy liquid of pentose originate from wood pulping. Molasses often contains high levels of inorganic ions such as potassium and calcium together with ash and coloring agents. Molasses is used for production of fuel ethanol and in fodder for farm animals. By treatment with lime, part of the impurities can be precipitated and removed. Thereafter growth factors can be added and the sugars fermented to lactic acid (Ohashi *et al.* 1999).

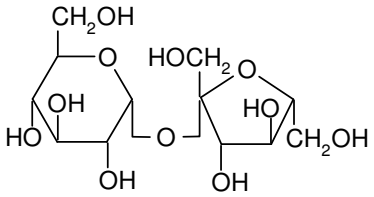

Figure 3.2.5. Sucrose (glucose-α(1,2)-fructose).

The seasonal productions of molasses requires storage facilities to level out the supply for the lactic acid plant between seasons. But as a result of the high sugar content, molasses can be stored for longer periods without deteriorating.

Plant juices are produced when plants are pressed and dried for various purposes. In the production of fodder pellets, different grasses are pressed resulting in large volumes of grass juice. Glucose, fructose, sucrose and fructans constitute the main carbohydrate source in grass juice, in combined concentrations around 2%. Fructans are polysaccharides, witch have a general structure of a glucose linked to multiple fructose units. In plants up to 200 fructose units can be linked in a single fructan-molecule. The type of fructan most often found in grasses, which are also referred to as the graminan type, have both β(2,1) and β(2,6) linkage bonds between the fructose units, and thus contain branches as shown in Figure 3.2.6. (Ebskamp 2001).

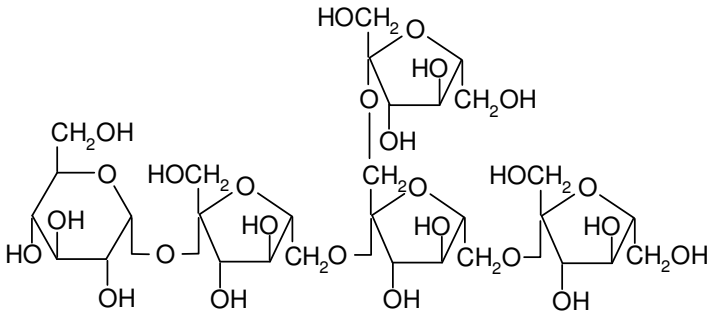

Figure 3.2.6. Fructan - graminan type.

Grass juice can be used as fertilizer, but in Denmark it is only allowed to spread plant juice on green fields in early autumn and not in the period between October 1st and February 1st. As the production of plant juice is confined to a limited time of the year, a method for both conservation and lactic acid production has been developed (Andersen and Kiel 2000). The juice is pre-fermented using LAB to lower the pH and hereby improve stability so storage is possible until the final fermentation and separation. Unlike many of the previously described substrates grass juice support

growth of LAB without addition of any growth factors (Andersen and Kiel 2000). In the present work brown juice, which is produced from pressing of green biomass at 80°C, is used as substrate for lactic acid fermentation. As with whey and molasses, grass juice contains relatively high amounts of potassium and calcium ions.

3.3 Lactic acid bacteria (LAB)

The realization of LAB as a distinct group of microorganisms is old – the unconscious use of LAB in foodstuff is ancient. In the late 19th century the first isolation of pure bacterial culture, *Bacterium lactis* was done and starter cultures were used for cheese and sour milk production (Stiles and Holzapfel 1997). Later, in the beginning of the 20th century development of taxonomic classification of LAB was pioneered by Orla-Jensen (Orla-Jensen 1919;Orla-Jensen 1924). For at least five thousand years the excellent properties of lactic acid has been exploited in connection with food preparation and food storage. Existence of fermented dairy products such as cheese, yoghurt, and butter is documented in archaic texts from Uruk/Warka (Iraq), dated around 3200 B.C. and the Babylonians exported ethanol/lactic acid fermented beer around 3000 B.C. (Stiles and Holzapfel 1997). In our days there are a multitude of food-associated uses of LAB, especially within the dairy industry, where these microorganisms are used for production of an enormous variety of fermented dairy product, some other uses have already been mentioned in chapter 3.1.3.

3.3.1 Characterization and taxonomy

Different tools are used for classification of LAB. Some are based on phenotypic properties, including carbohydrate fermentation patterns, resistance to different NaCl concentrations, growth at defined temperatures, arginine hydrolysis, acetoin formation, bile tolerance, production of extra cellular polysaccharides, growth factors requirement, presence of certain enzymes (example: β-Galactosidase and β-Glucoronidase), and resistance against antibiotics. More recent taxonomic methods rely on both phenotypic characterization, such as cell wall composition, and genotypic analysis based on mol% G+C (Guanine plus Cytosine) in the DNA, DNA:DNA hybridization studies and, structure and sequence of ribosomal RNA (Hofvendahl and Hahn-Hagerdal 2000).

Lactic acid bacteria belong to the Clostridium subdivision of the Gram-positive bacteria having a DNA base composition of less than 55 mol% G+C (Stiles and Holzapfel 1997). They are non-sporulating, catalase-negative, devoid of cytochromes, of anaerobic nature but aero tolerant, fastidious, acid tolerant and with

lactic acid as the major end product during sugar fermentation (Axelsson 1993). Today LAB consists of the genera(Stiles and Holzapfel 1997):

- *Carnobacterium (Carn)*
- *Enterococcus (Ent)*
- *Lactobacillus (Lb)*
- *Lactococcus (Lc)*
- *Leuconostoc (Leu)*
- *Oenococcus (Oen)*
- *Pediococcus (Ped)*
- *Streptococcus (Str)*
- *Tetragenococcus (Tetr)*
- *Vagococcus (Vag)*
- *Weissella (Wei)*

LAB differ in their morphology with a clear-cut difference between *Carnobacterium* and *Lactobacillus* that are rods, and the rest of the LAB, which are cocci.

3.3.2 Sugar Utilization

3.3.2.1 Sugar transport

The rapid growth of LAB requires an efficient transport system for the uptake of substrates. Sugar transport in LAB can be divided into two categories, Proton Motive Force symport (H+-symport) and translocation via the phosphoenolpyruvate: phosphotransferase system (PEP:PTS). Heterofermentative LAB use H+-symport where a specific membrane associated protein (carrier, permease) translocates the sugar across the membrane in symport with a proton. The driving force is generated by a proton exporting ATPase (Axelsson 1993). Homofermenters use the PEP:PTS, to at the same time translocate and phosphorylate sugars by a complex series of enzymes, a review is given in (Reizer *et al.* 1988). It is generally agreed that the presence of PTS is highly correlated with the ability to ferment substrates through the Embden-Meyerhof pathway, i.e. glycolysis (Axelsson 1993).

3.3.2.2 Catabolic pathways

LAB utilizes sugars through a limited number of pathways, resulting in homo-, hetero- or mixed acid fermentation, see Figure 3.3.1. The homofermentative lactic acid bacteria (Lactococcus, Pediococcus, streptococcus, Enterococcus and homofermentative Lactobacillus) metabolize glucose primarily to lactic acid via the Embden-Meyerhof pathway. The homofermentation involves splitting of fructose 1,6-

diphosphate (derived from glucose), catalysed by an aldolase, into two triose phosphate moieties (glyceraldehydes 3-phosphate and dihydroxyacetone phosphate). These trioses are further converted to pyruvate, which is reduced to lactate in order to maintain the electron balance. The reduction of pyruvate is brought about by a NAD^+-dependent lactate dehydrogenase (LDH), thereby reoxidizing the NADH formed during the earlier glycolytic steps. A net yield of two moles of ATP and two moles of lactate per mole of hexose fermented is achieved (Kandler 1983). At sub-optimal conditions, e.g. glucose limitation, relatively low intracellular levels of fructose 1,6-biphosphate which is an essential activator of LDH might cause some homofermentative LAB to produce ethanol, formic acid, and acetic acid in addition to lactic acid (mixed acid fermentation)(Thomas *et al.* 1979).

The heterofermentative LAB (Leuconostoc, Oenococcus, Weissella and heterofermentative lactobacillus) ferment glucose via the phosphoketolase pathway (PK), initiated by the oxidation of glucose 6-phosphate to 6-phosphogluconate, followed by decarboxylation of the hexose moiety. The resulting xylulose 5-phosphate is split by the phosphoketolase enzyme into glyceraldehydes 3-phosphate and acetyl phosphate. The acetyl phosphate is hydrolized to acetic acid or it is reduced by dehydrogenases to acetaldehyde and further to ethanol, depending on the hydrogen acceptors available. A net yield of only one mole of ATP, one mole of lactate, one mole of carbon dioxide and one mole of acetate/ethanol is produced per mole of hexose utilized in the PK (Kandler 1983). Usually most heterofermentative lactic acid bacteria can metabolize pentoses to lactate and acetate/ethanol according to the PK pathway, an example is given in Figure 3.3.1 for assimilation of the pentose xylose. The facultative heterofermentative LAB can catabolize glucose through the Embden-Meyer pathway like homofermenters and hereby exclusively produce lactic acid.

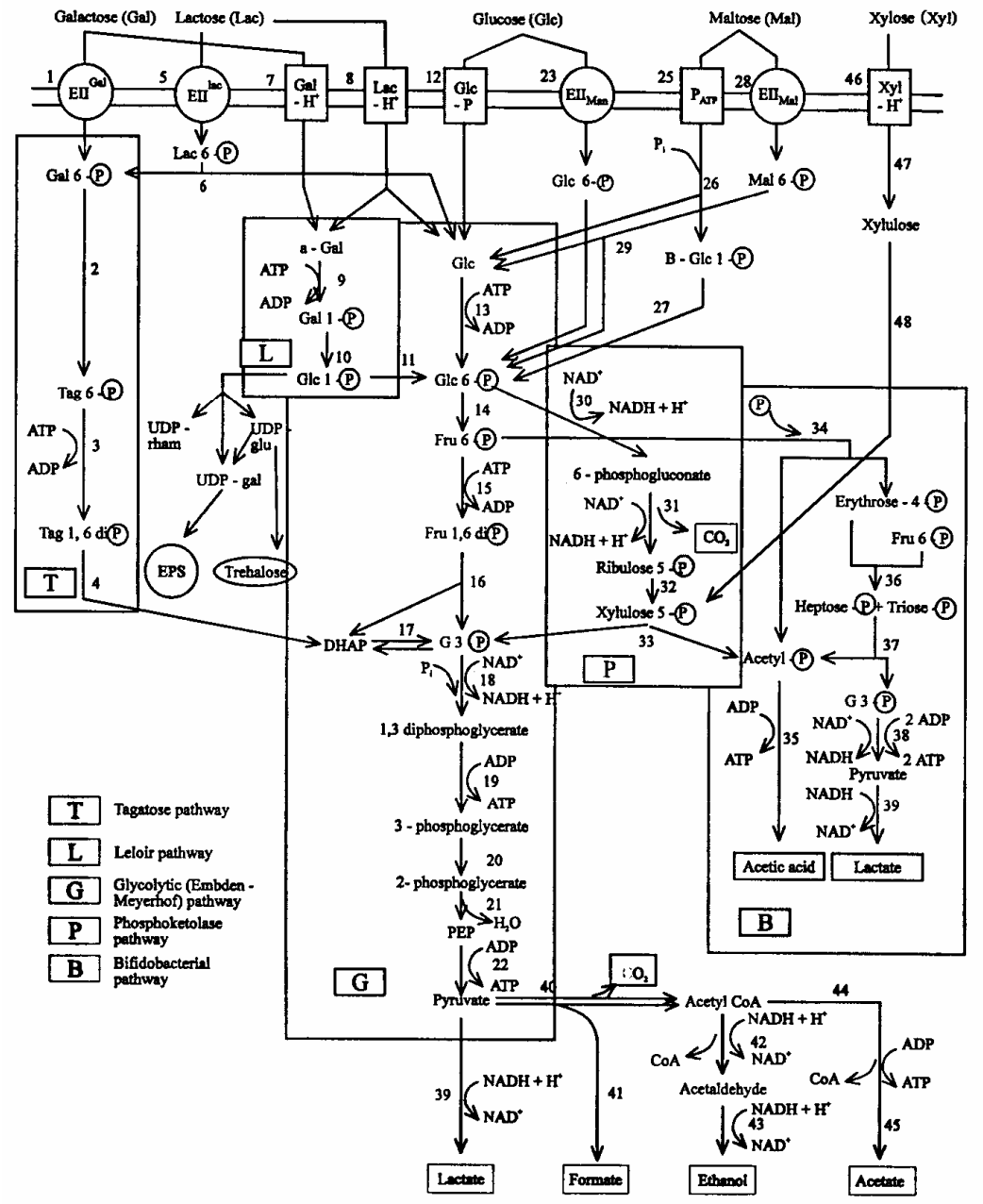

Figure 3.3.1. Metabolic pathways in LAB adapted from (Bunte 1998).

1. (PTS galactose)
2. galactose 6-phosphate isomerase
3. tagatose 6-phosphate kinase
4. tagatose 1,6-diphosphate aldolase
5. (PTS lactose)
6. phospho-β-galctosidase
7. (galctose-H+ symport)
8. (lactose-H+symport)
9. β-galactosidase
10. Several enzymatic steps via UDP sugars
11. α-phospho-glucomutase(α-PGM)
12. (non-PTS glucose transport)
13. glucokinase(GK)
14. phosphohexoisomerase
15. phosphofructokinase(PFK)
16. fructose bisphosphate aldolase
17. triose phosphate isomerase(TPI)
18. glyceraldehyde 3-phosphate isomerase
19. phosporglycerate kinase (PK)
20. phosphoglyceromutase
21. enolase
22. pyruvate kinase(PK)
23. (PTS mannose (affinity for glucose))
25. (ATP hydrolyzing maltose transport)
26. maltose phosphorylase(MP)
27. β-phosphoglucomutase(β-PGM)
28. (PTS maltose)
29. maltose hydrolase (maltase)
30. glucose 6-phosphate dehydrogenase
31. 6-phosphogluconate dehydrogenase + lactonase(2 steps)
32. ribulose phosphate-3-epimerase
33. transketolase
34. fructo 6-phosphate phosphoketolase
35. acetokinase
36. transaldolase
37. transketolase
38. glycolytic steps(18-22)
39. lactate dehydrogenase(LDH)
40. pyruvate dehydrogenase
41. pyruvate formate lyase
42. aldehyde dehydrogenase
43. alcohol dehydrogenase
44. phosphate acetyl transferase
45. acetokinase
46. (xylose-H+symport)
47. xylose isomerase
48. xylulose kinase

The configuration of the produced lactic acid is strain-dependent and is primarily determined by the stereo specificity of the LDH, as racemases only have been isolated in few species e.g. *Lb. curvatus* and *Lb. sake* (Garvie 1980). The ratio of the two isomers can be changed during batch growth by *P. pentosaceus* and many lactobacilli. In this case L-lactic acid is the major form produced in the early growth phase and D-lactic acid in the late to stationary phase. The activities of LDHs and thus the ratio of the isomers at different growth phases are both influenced by pH and the internal pyruvate concentration (Garvie 1980).

Three different genera of lactic acid bacteria, *Lactobacillus, Streptococcus*, and *Pediococcus* were studied in this thesis. The strains in focus within these genera were *Lb. plantarum, Lb. Pentosus, Lb. Brevis, Lb. Sake, S. thermophilus* and *P. pentosaceus*.

3.4 Fermentation

3.4.1 Batch mode

Fermentation, carried out in a closed system where all the nutrients initially are present in limited amounts, is called batch fermentation. After inoculation with LAB the composition of the fermentation broth will change throughout the process, lactic acid will be formed as the sugar is consumed and the concentration and activity of the bacteria will vary as well. In batch mode the growth of bacteria will pass through different phases, see Figure 3.4.1.

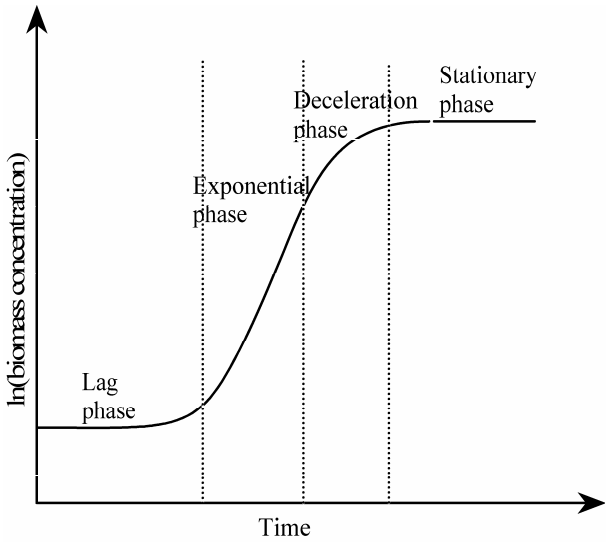

Figure 3.4.1. Typical bacterial growth curve in batch conditions.

During the lag phase the bacteria will acclimatize to the environmental conditions of the production medium. The duration of this phase can be minimized by inoculating with bacteria in the exponential phase and by using the same medium for inoculum as for the production, or at least ensuring high degree of similarity between the two media (Lincoln 1960). In the following exponential phase, the cell growth at a constant maximum specific rate described by the equation:

eq. 3.4.1 $$\frac{dx}{dt} = \mu \cdot x$$

Where x is the concentration of microbial biomass, t is time in hours and μ is the specific growth rate in hours^{-1}. On integration and taking the natural logarithm,

eq. 3.4.1 becomes:

eq. 3.4.2 $$\ln x = \ln x_0 + \mu \cdot x$$

A plot of the natural logarithm of biomass concentration against time should yield a straight line with slope μ, hereby determining the maximum specific growth rate μ_{max} for the prevailing conditions. At incipient substrate depletion the growth will enter the deceleration phase where the concentration of substrate no longer is high enough to sustain the maximum specific growth rate. The duration of this phase is influenced by the bacteria's affinity for the limiting substrate; a high affinity will result in a short deceleration phase and a low affinity will result in a long deceleration phase. In the stationary phase the growth rate has decreased to zero, but the bacteria are still metabolically active.

Batch mode is the simplest way of carrying out fermentations, but there are some limitations to production of lactic acid by batch fermentations, e.g. low productivity mainly caused by product inhibition in the end of the fermentation.

A variation of the batch process is the fed-batch fermentation where the fermentation initially is started in batch mode and is then fed continuously or sequentially with the limiting substrate, resulting in an increased volume. An advantage of the fed-batch is the possibility of maintaining a low substrate level, thus avoiding the repressive effect of high substrate concentration (Stanbury *et al.* 1995).

3.4.2 Continuous mode

Ideally, continuous lactic acid fermentation is a steady state conversion of substrate into lactic acid, e.g. there are no changes in the chemical/biological composition of the reaction medium and the feed flow rate is balanced by effluent flow rate. In it's simplest form, continuous fermentation consists of a vessel containing the microorganisms, a feed inlet, and a product outlet as shown in Figure 3.4.2.

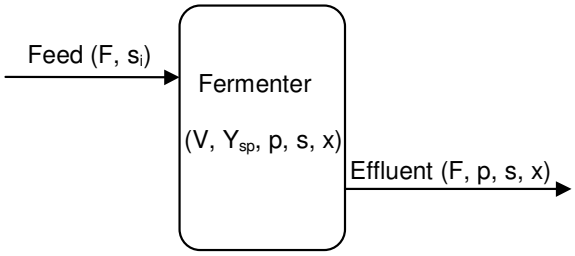

Figure 3.4.2. Simple model of continuous fermentation. F = feed flowrate, s_i = substrate concentration in the feed, V = volume of vessel, Y_{sp} = yield factor (g product produced g^{-1} substrate consumed), p = product concentration, s = residual substrate concentration, and x = biomass concentration.

An important parameter in continuous fermentation is the dilution rate D (h^{-1}), defined as:

eq. 3.4.3 $$D = \frac{F}{V}$$

To insure high productivity P (g product l^{-1} h^{-1}) the dilution rate should be as high as possible, but still meet the terms of near total substrate conversion. If the dilution rate is kept below μ_{max} the loss of biomass in the effluent stream will be balanced by formation of new cells and a steady state reached (D = μ). However, if D is set higher that μ_{max} the cells will be flushed out of the fermenter. The loss of active cells in the effluent stream is a major drawback of this system as energy is lost for production of new cells.

The use of immobilized cells or cell recycling circumvents this difficulty and enables very high cell densities in the fermenter at dilution rates above μ_{max}. Cell recycling can be accomplished in an external loop by different membrane processes, typically microfiltration (Borgardts *et al.* 1998b;Boyaval *et al.* 1996) or ultrafiltration (Van Nispen et al. 1991). A more energy efficient way of insuring a high biomass concentration is by immobilizing the bacteria culture, which could be done in an Upflow Anaerobic Sludge Blanket (UASB) reactor.

Successful operation of an UASB reactor is based on formation of compact sludge aggregates called granules (Schmidt and Ahring 1996). Because the cells are immobilized in/on granules the media that flows up through the fermenter will not flush them out. Pioneering work in the use of UASB methods was undertaken at the Dutch Agriculture University of Wageningen in the late 60's and later the Dutch beet

sugar firm, CSM, developed the basic technology to commercial application as they applied it for waste treatment within several of their sugar factories (2001). Today the UASB reactor has become the most popular high-rate reactor for anaerobic biological treatment of wastewater in the world (Schmidt and Ahring 1996).

3.5 Membrane separation

Membranes are (not surprisingly) always the key element in membrane separation processes. The IUPAC definition describes membranes as: 'structure, having lateral dimensions much greater than its thickness, through which mass transfer may occur under a variety of driving forces'. According to Dr. Mulder of the University of Twente (Mulder 1991) the definition of a membrane is: a selective barrier between two phases.

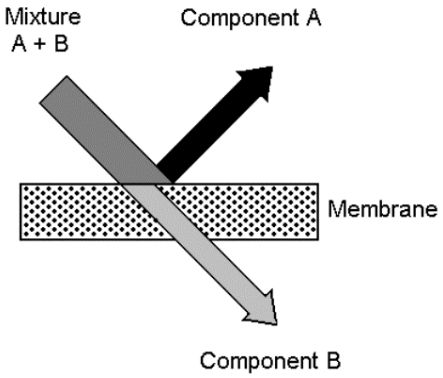

Figure 3.5.1 Ideal membrane separation.

Membranes come in many forms: porous or non-porous, polymeric or ceramic, natural or artificial. The selectivity that is their main advantage depends both on the size of the pores and on the membrane material. Some kind of external driving force like a pressure gradient, concentration gradient or electrical field acting across the membrane is required for a separation to take place. In Table 3.5.1 is given a list of some typical membrane processes and their driving forces.

Table 3.5.1. Overview of different membrane processes and the corresponding driving forces and typical poresizes. [a] Not directly pressure driven.

Membrane Process	Driving Force	Typical Poresize
Microfiltration	Pressure	0,05 – 10 µm
Ultrafiltration	Pressure	1 – 100 nm
Nanofiltration	Pressure	0,1 – 2 nm
Reverse Osmosis	Pressure[a]	Nonporous
Gas Separation	Pressure[a]	Nonporous (or < 1 µm)
Pervaporation	Pressure[a]	Nonporous
Dialysis	Concentration gradient	1-5 nm or nonporous
Electrodialysis	Electrical field	Nonporous
Liquid Membranes	Concentration gradient	Nonporous (liquid)
Membrane Distillation	Temperature	0,2 – 1 µm

The pressure driven membrane filtrations are often categorized according to the type of membrane used, with reverse osmosis (RO), nanofiltration (NF), ultrafiltration (UF), and microfiltration (MF) as the four common processes. This division is in fact very fuzzy because no sharp distinction can be made between adjacent membrane types where their poresize and hereby separation properties overlap. Typically, poresize or molecular weight cutoff (MWCO) is used to distinguish between MF, UF and NF but when it comes to differentiating NF from RO another approach is useful. Due to their dense nature, the NF/RO membranes are instead characterized in terms of salt (Na^+ and Ca^{2+}) rejection as well as organic (dextran) rejection. So, there is no clear-cut definition between RO and NF except the relative rejection capabilities. In Figure 3.5.2 the effect of different poresizes is demonstrated for the four pressure driven processes. Open membranes with large pores only reject bacteria-sized or larger particles, while very dense (nonporous) membranes reject even salts.

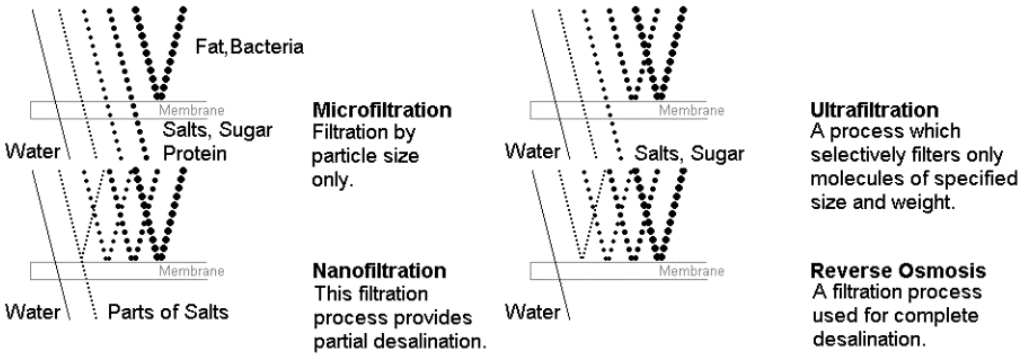

Figure 3.5.2. Comparison in particle rejection by membranes for four types of separation. (•••) Fats, bacteria, (•••) Proteins, vira, (•••) Sugars, amino acids, (···) Salts, (—) Water.

The definition of dialysis and electrodialysis are more clear-cut even though both terms cover several sub-processes. Dialysis is a membrane process in which transport is driven by concentration differences, rather than by pressure or electrical-potential differences across the thickness of the membrane (Koros *et al.* 1996). Dialysis is probably best known from treatment of blood in *hemodialysis* where undesired metabolites and toxic by-products such as urea and creatine are transported across a membrane between the blood and a refreshing solution under the action of a concentration gradient. In a special type of dialysis, called *Donnan dialysis*, ionexchange membranes are used, which primarily facilitate transport of charged molecules, e.g. lactate. Electrodialysis is a membrane-based separation process in which ions are driven through an ion-selective membrane under the influence of an electric field (Koros *et al.* 1996). A more detailed description of the studied membrane processes is given in the subsequent sections.

3.5.1 Micro- and ultrafiltration

The separation process of both MF and UF is based on particle size differences. However, other parameters such as shape of molecules and interactions between the membrane and solutes have an impact on separation characteristics. In the case of MF trans-membrane pressure (TMP)is commonly less than 2 bar, while for UF it is between 1 and 10 bar. Despite the larger driving force in UF, the flux through the membrane is generally larger in MF due to higher permeability, and the flux is perhaps the single most important design variable in membrane filtration. The magnitude of the flux governs the size, and therefore to a great extent the cost, of an application. Concentration polarization and especially fouling can lead to a severe decrease of flux over time and this must be addressed to maintain a feasible operation. The choice of membranes, module design, and mode of operation are tools with which fouling and polarization can be held in check. This section presents theory on transport in porous membranes, concentration polarization and fouling, and a short description of membranes and modules.

3.5.1.1 Membranes

Micro- and ultrafiltration membranes are porous membranes, which can be synthesized from organic (polymer) and inorganic materials. The membrane material is not important for the separation as such, it is the dimension and shape of the pores and the porosity that mainly determines the selectivity and flux, respectively. However, the choice of material affects phenomena such as adsorption and chemical stability. The choice of material is primarily based on preventing fouling and on recovery of the membranes (by chemical agents) after fouling

(Mulder 1996). A list of materials used for MF membrane manufacturing is shown in Table 3.5.2.

Table 3.5.2. Membranes materials and properties (Mulder 1996)

Properties	Material
Hydrophobic polymeric membranes	Polytetrafluoroethylene (PTFE, Teflon)
(General with an high protein binding)	Poly(vinylidene fluoride) (PVDF)
	Polypropylene (PP)
	Polyethylene (PE)
Hydrophilic polymeric membranes	Cellulose esters
(Low protein binding)	Polycarbonate (PC)
	Polysulfone/poly(ether sulfone) (Psf/PES)
	Polyimide/poly(ether imide) (PI/PEI)
	(Aliphatic) polyamide (PA)
	Polyetheretherketone (PEEK)
Ceramic (inorganic) membranes	Alumina (Al_2O_3)
(Medium protein binding)	Zirconia (ZrO_2)
	Titania (TiO_2)
	Silicium carbide (SiC)

The tendency of the material to bind to certain organic substance such as proteins is related to the hydrophobicity of the membrane material. When a membrane is hydrophilic a layer of water covers the membrane, preventing until a certain limit the adsorption of proteins on the membrane surface. Hydrophobic membranes generally have a higher tendency to foul, especially in the case of proteins.

In general ceramic membranes are highly thermally and chemically resistant compared to polymer membranes. The chemical stability is an advantage in many applications as cleaning at high or low pH after fouling is necessary for continuous use of the membranes. In this respect the lifetime of ceramic membranes is greater than of polymeric membranes, but the main drawback to the use of ceramic membranes has been a marked difference in the price per membrane area compared to polymer membranes (Mulder 1996).

The efficiency of a given membrane is determined in particular by two parameters: selectivity and flow through the membrane. Both are determined by the membrane structure, which again is a function of polymer material and preparation technique. The morphology of a membrane can be very diverse as can be seen from the schematic drawing of the Figure 3.5.3.

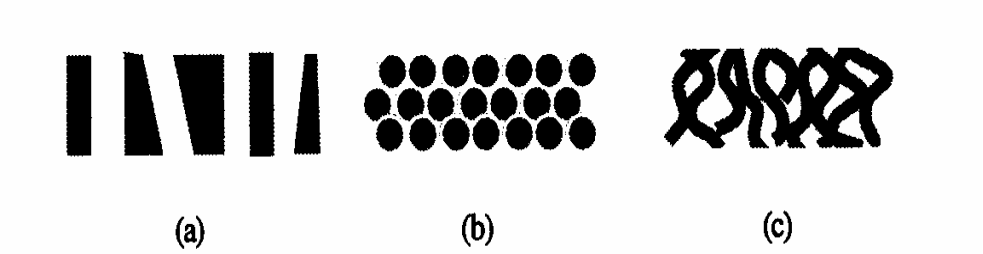

Figure 3.5.3 Some characteristic pore geometries found in porous membranes (Mulder 1996)

The simplest structure is one in which the membrane is considered as a number of parallel cylindrical pores perpendicular to the membrane surface (a). The length of the pore is more or less equal to the membrane thickness. This type of membrane can be prepared by the track-etched technique. Another structure is one of closed packed spheres (b), which can be prepared by the sintering technique. The third structure is a sponge-like structure (c), which normally is the structure in membranes prepared by the phase inversion technique.

Membranes can also be classified according to their symmetry across the membrane thickness, as a porous membrane is either symmetric or asymmetric. A *symmetric* membrane has a uniform pore size across the membrane thickness and the “functional” pore space consists of the total thickness. An *asymmetric* membrane has a thin skin layer (0.1-0.5 μm thickness) and much thicker support layer (50-150 μm thickness) where the pores in the support layer are much larger than the pores in the skin layer. In asymmetric membranes the skin layer controls the performance of the membrane with respect to selectivity and permeability. Thus the skin layer can be characterized as the “functional” pore space. The support layer is necessary for mechanical strength and thus it can be characterized as the bulk or “non-functional” pore space. Asymmetric membranes normally exhibit a much higher permeability compared to symmetric membranes because the resistance to flow is inversely proportional to the thickness of the “functional” pore space.

The pore size distribution is an important parameter for the particle retention of the membrane. For a given membrane a nominal or an absolute pore size is provided by manufactures. With an absolute rating, every particle or molecule with a size equal or larger as this pore size is retained. A nominal rating indicates that a percentage (95 or 98%) of the particles or molecules of that size or larger is retained. But often a broad distribution of pore sizes is present in the membrane.

3.5.1.2 modules

A membrane module can be defined as a manifold assembly containing one or more membranes in order to separate the feed, permeate and retentate stream (Koros *et al.* 1996). The module design is an important variable in improving the filtration performance. The main factors effecting the choice of membrane modules are:

- manufacturing costs
- effect on fouling and concentration polarization
- surface area to volume ratio *(packing density)*
- hydraulic resistance
- cleaning ability
- life cycle
- ease of membrane replacement

Depending on the type of membrane two main categories of modules can be distinguished: tubular or plain. The plain module basically consist of three components: 1) flat sheet membranes, 2) spacers that define the flow path and keeps adjacent membranes apart at a fixed distance, and 3) a housing, whereas the tubular modules have cylindrical membranes placed in a housing, without spacer-support.

Plate-and-frame and spiral wound modules are two typical plain modules. The plate-and-frame module, as shown in Figure 3.5.4 has rather low packing density of about 100-400 m^2/m^3 and relatively high manufacturing costs. However, the design is easy to scale up and allows an easy replacement of membranes and a good control of concentration polarization.

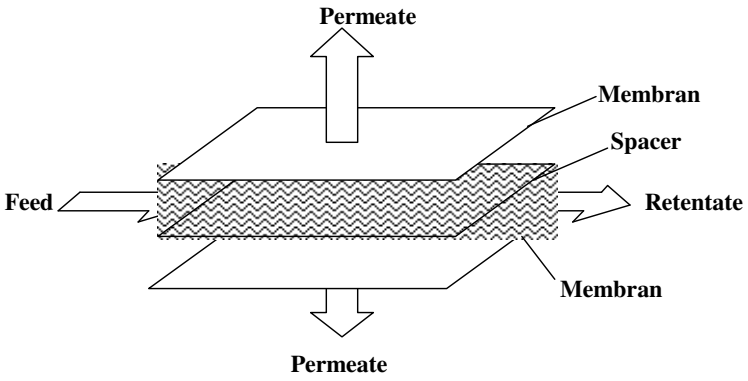

Figure 3.5.4. Schematic drawing of a plate-and-frame module.

The spiral-wound module is essentially a plate-and-frame system wrapped around a central pipe where permeate is collected. An advantage of the spiral-wound module compared to a plate-and frame is a higher packing density around 300-1000 m^2/m^3 and lower manufacturing costs.
The tubular membrane modules can be characterized according to the size of the cylindrical membranes (see Table 3.5.3).

Table 3.5.3 Size and packing density (membrane surface area per module volume) for different tubular modules. Adapted from (Mulder 1996)

Type	Diameter (mm)	Packing density (m^2/m^3)
Tubular	> 5.0	<300
Capillary	0.5 - 5	300 to 1200
Hollow fiber	< 0.5	< 30000

Two different configurations of the capillary and hollow fiber modules can be identified. When the feed is in the lumen of the fibers, the configuration is called “inside-out” (tube side feed). If the feed enters into the shell and the permeate exits from the fibers the configuration is called “outside-in” (shell side feed) as shown in Figure 3.5.5 Tubular modules (diameter > 5 mm) are generally operated inside out.

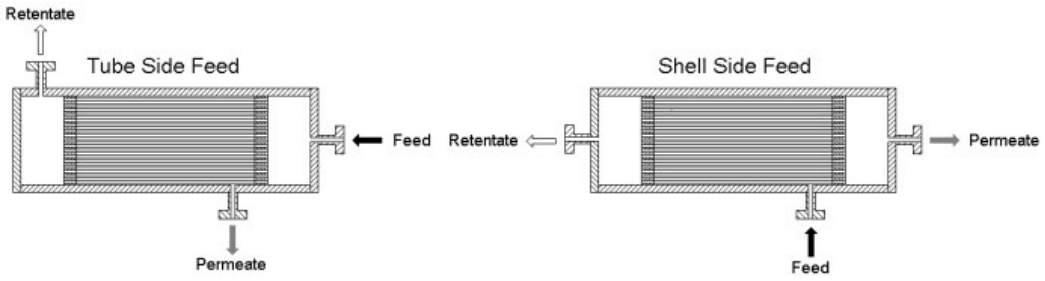

Figure 3.5.5. Possible configurations of capillary/hollow fiber module.

3.5.1.3 Mechanism of Micro- and Ultrafiltration

A distinction between two separation mechanisms can be made for MF and UF. When a membrane with pores smaller than the retained particles is used then a sieving mechanism applies. This, the basic mechanism of both MF and UF, is referred to as a *surface filtration*. If a membrane has pores that are larger than the retained particles, the particles enter the porous structure and the mechanism is referred to as a *depth filtration*

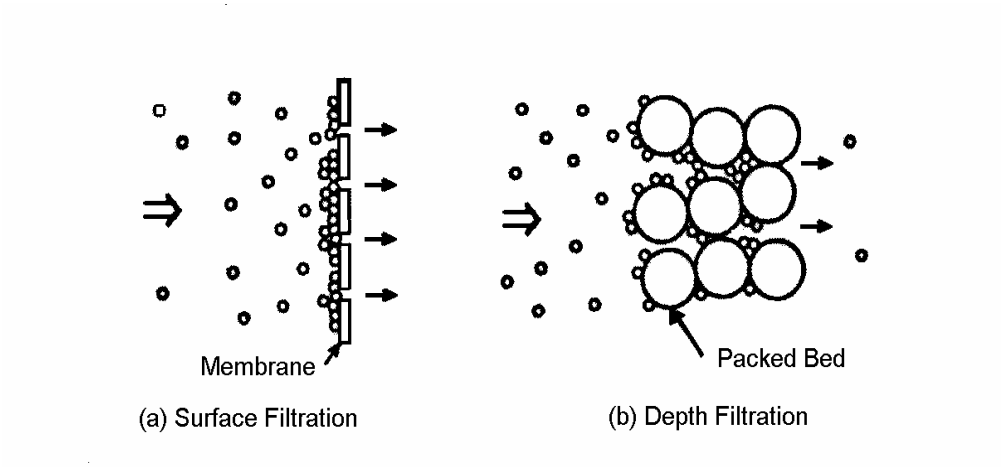

Figure 3.5.6 Schematics of surface filtration and depth filtration (Davis 1992).

Since both MF and UF apply porous membranes, flux can generally be described as a function of trans-membrane pressure according to Darcy's law:

eq. 3.5.1 $$J_v = L_p \Delta P$$

where J_v is volumetric flux ($m^3\ h^{-1}\ m^{-2}$), L_p is hydraulic permeability of a membrane ($m^3\ h^{-1}\ m^{-2}\ bar^{-1}$), and ΔP is TMP (bar). The permeability constant L_p can easily be determined experimentally as the slope of a flux-pressure plot. The pure water flux is a linear function of the TMP with a permeability of around 300-3000 and 3000-30000 $l\ h^{-1}\ m^{-2}\ bar^{-1}$ in UF and MF, respectively. However, in practice the permeability will always be lower than the pure water permeability due to the viscosity of permeate, fouling, and concentration polarization and it will typically decrease over time. The pure water permeability can be evaluated as a function of pore size distribution and porosity of the membrane. Commonly two approaches can be applied depending on membrane morphology.

For a nodular morphology comparable with a system of closed packed spheres, the Kozeny-Carman equation can be used are used to describe L_p:

eq. 3.5.2 $$J = \frac{\varepsilon^3}{K \cdot \mu \cdot S^2 \cdot (1-\varepsilon)^2} \cdot \frac{\Delta P}{\delta_m}$$

where ε is porosity (-) K is Kozeny-Carman constant, μ is solvent viscosity (kg m^{-1} s^{-1}), S is internal surface area (m^2), δ_m is membrane thickness (m), and ΔP is the TMP (bar)
The flux through a membrane prepared by sintering can be assumed to follow this expression as the morphology is nodular.

An alternative approach is to use the Poiseiulles law when a parallel array of uniform cylindrical pores perpendicular to the membrane surface can be assumed in the membrane. The volumetric flux J_v can then be described by (Mulder 1996):

eq. 3.5.3 $$J_v = \frac{\varepsilon r_P^{\,2}}{8\mu\tau}\frac{\Delta P}{\delta_m}$$

where r_P is pore radius (m), ε is surface porosity (-), μ is permeate viscosity (kg m^{-1} s^{-1}), ΔP is TMP (bar), τ is tortuosity factor (-), and δ_m is membrane thickness (m) with the porosity expressed as:

eq. 3.5.4 $$\varepsilon = n_p \pi r_P^2$$

where n_P is number of pores per square meter membrane (m^{-2}), and r_P is pore radius (m).

The flux through a track-etched membrane can be assumed to follow this expression as the morphology resembles a parallel array of cylindrical pores perpendicular to the membrane surface.

Again, it must be stressed that the permeability constant L_p expressed by the Kozeny-Carman equation or Poiseiulles law is used to summarize the influence of membrane structure and not time dependent change in overall resistance due to fouling and polarization.

3.5.1.4 Concentration polarization and membrane fouling

Concentration polarization is defined as a concentration profile that has a higher level of solute near to the upstream membrane surface compared with the more-or-less well-mixed bulk fluid far from the membrane surface (Koros *et al.* 1996).

Fouling is defined as a process resulting in loss of performance of a membrane due to the deposition of suspended or dissolved substances on its external surfaces, at its pore openings or within its pores (Koros *et al.* 1996).

Both concentration polarization and membrane fouling can be thought of as a resistance that adversely affects the actual membrane performance and causes flux to decrease considerably during MF and UF. (see Figure 3.5.7)

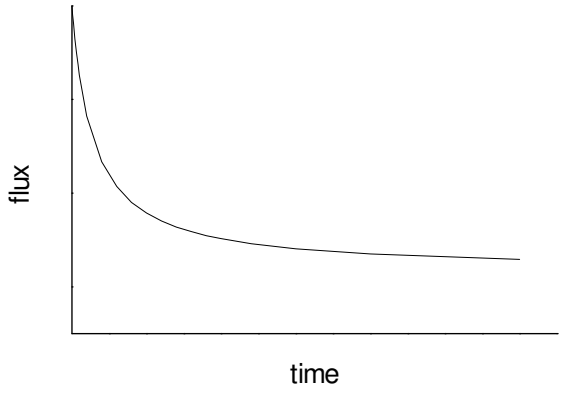

Figure 3.5.7 Flux behavior as a function of time

In an alternative expression of eq. 3.5.1 Darcy's law gives the flux as a function of resistance:

eq. 3.5.5 $$J_v = \frac{\Delta P}{\mu R_t(t)}$$

where R_t is total resistance (m^{-1}) towards flux, μ is the kinematic viscosity ($m^2\ s^{-1}$). The total resistance is time dependent can be expressed as the sum of the individual resistances:

eq. 3.5.6 $$J_v = \frac{\Delta P}{\mu\left(R_m + R_{cp}(t) + R_{fouling}(t)\right)}$$

Where R_m is the membrane resistance (m^{-1}); R_{cp} is the concentration polarization resistance (m^{-1}) and $R_{fouling}$ is the fouling resistance (m^{-1}) Membrane resistance is normally regarded as constant with time, however for high-pressure applications such as reverse osmosis a phenomena referred as "membrane compaction" will increase the membrane resistance with time. Fouling resistance can be expressed as a sum of the individual resistances caused by various fouling phenomena's such as adsorption, cake layer formation and pore plugging:

eq. 3.5.7 $$R_{fouling} = R_{pore\ blocking} + R_{adsorption} + R_{cake}$$

Where $R_{pore\ blocking}$ (R_{pb}) is the pore blocking resistance [m^{-1}]; $R_{adsorption}$ (R_{ads}) is the adsorption resistance (m^{-1}) and R_{cake} (R_c) is the cake resistance (m^{-1}). Pore blocking and cake layer formation is normally due to the retention of particles, whereas adsorption normally is due to the presence of macromolecules, e.g. proteins, in the suspension that can adsorb on the surface of the membrane and/or on the inner walls of the pores in the membrane.

Apart from flux reduction due to the mentioned resistances, the flux can also be decreased by action of an osmotic pressure difference caused by a difference in concentration of solutes in the permeate and in the film layer at the membrane surface on the retentate side. The main contribution to osmotic pressure arises from the low molecular weight solutes, so the osmotic pressure is often neglected in MF and UF. However, for the more dense UF membranes at high flux value and high rejection levels the osmotic pressure at the membrane surface must be taken into account. Flux equations which accounts for osmotic pressure are discussed later in relation to nanofiltration.

Concentration Polarization

During filtration solvent permeates through the membrane while solutes are (partly) retained, leading to an increased concentration at the membrane surface. At steady state the convective flow of particles towards the membrane will be balanced by the diffusive transport of particles away from the membrane. The concentration profile under steady-state conditions is depicted below.

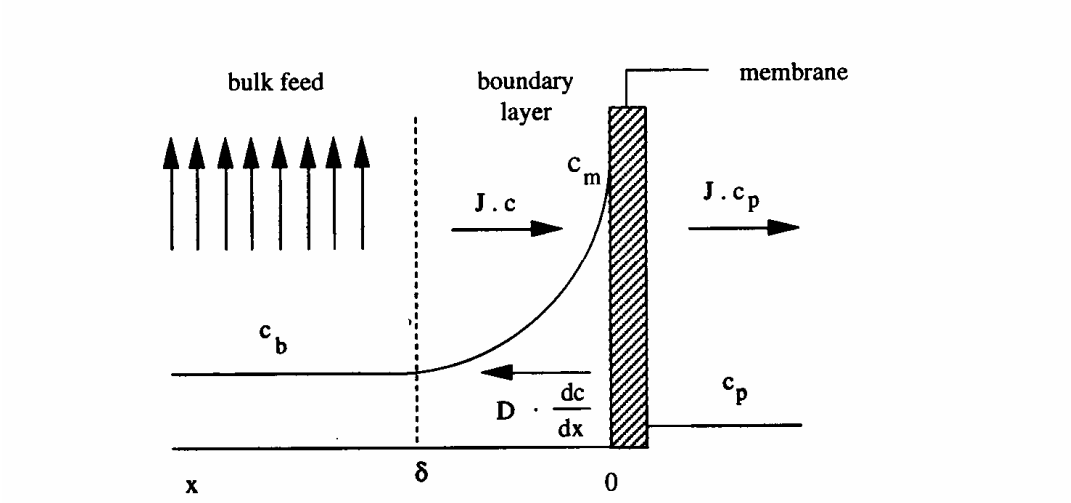

Figure 3.5.8. Polarization profile across laminar boundary layer at membrane surface during a pressure driven filtration process. C_b, C_m, and C_p are the solute concentrations respectively in the bulk of the feed solution, at the membrane surface, and in permeate. δ is the boundary layer thickness. (Mulder 1991):

Assuming:

- steady state,
- a boundary layer of thickness δ exists,
- Fickian Diffusion,
- no chemical reaction,
- the concentration gradient parallel to membrane can be neglected,
- the density is constant, and
- the diffusion coefficient is independent of the solute concentration,

a mass balance of the feed side on the membrane can be obtained:

eq. 3.5.8 $$J_v c + D\frac{dc}{dx} = J_v c_p$$

With the boundary conditions:

$$x = 0 \quad \Rightarrow \quad c = c_m$$
$$x = \delta \quad \Rightarrow \quad c = c_b$$

where J_v is volumetric flux ($m^3\ h^{-1}\ m^{-2}$), D is Brownian diffusion coefficient ($m^2\ s^{-1}$), c_p is permeate concentration (kg m^{-3}), c_b is feed concentration (kg m^{-3}), c_m is concentration at membrane surface (kg m^{-3}), c is local concentration (kg m^{-3}), δ is boundary layer thickness (m), and x (m) is distance from the membrane. Integration of equation eq. 3.5.8 using the boundary conditions gives:

eq. 3.5.9 $$\ln\left(\frac{c_m - c_p}{c_b - c_p}\right) = \frac{J_v \delta}{D}$$

or

eq. 3.5.10 $$\frac{c_m - c_p}{c_b - c_p} = \exp\left(\frac{J_v \delta}{D}\right)$$

The ratio of the diffusion coefficient and the thickness of the boundary layer is called the mass transfer coefficient $k = D/\delta$. If the solute is retained completely, as often is the case with particles in MF and UF, then eq. 3.5.10 becomes

eq. 3.5.11 $$\frac{c_m}{c_b}=\exp\left(\frac{J_v}{k}\right)$$

The ratio c_m/c_b is called the concentration polarization modulus. It is possible, by optimizing system hydrodynamics for a higher mass transfer coefficient k, to decrease concentration polarization and hereby also lowering the resistance R_{cp} in eq. 3.5.6. A lot of various correlations for different module configurations and flow regimes are available to determine the mass transfer coefficient. They have the general form:

eq. 3.5.12 $$Sh=a\mathrm{Re}^b Sc^c\left(\frac{d_h}{L}\right)^d$$

where a, b, c, and d are constants, Sh is Sherwood number, Re is Reynolds number, Sc is Schmidt number, d_h is hydraulic diameter [m], and L is length of tube or channel [m]. The same expression with the given expressions for Sh, Re, and Sc is:

eq. 3.5.13 $$\left(\frac{kd_h}{D}\right)=a\left(\frac{\rho v d_h}{\mu}\right)^b\left(\frac{\mu}{\rho D}\right)^c\left(\frac{d_h}{L}\right)^d$$

where ρ is density (kg m^{-3}), v is crossflow velocity (m s^{-1}), and μ is viscosity (kg m^{-1} s^{-1})

The empirical constants a, b, c, and d can be determined for different module types and flow regimes (see Table 3.5.4). A more extensive review of the different correlations can be found in (Gekas and Hallstrom 1987)

Table 3.5.4. Variables a, b, c, d for the Sherwood correlation, eq. 3.5.13.

System	a	b	c	d	Flow Regime	Reference
Tube	1.62	0.33	0.33	0.33	Laminar	(Mulder 1996)
	0.04	0.75	0.33	-	Turbulent	(Mulder 1996)
Plate and frame	1.615	0.33	0.33	0.33	Laminar	(Spang 1994)
	0.026	0.8	0.3	-	Turbulent	(Fiebig 1992)

The mass transfer coefficient k is an increasing function of the cross-flow velocity *v* in laminar and turbulent flow regimes but the dependence is strongest for turbulent flow. Laminar flow is prevailing below Re numbers of 2000 whereas turbulent flow is prevailing above.

The disadvantage of increasing the cross-flow velocity is an increasing pressure drop along the flow path and thus increasing energy expenditure. For turbulent flow compared to laminar flow the dependence upon flow velocity is much stronger. It is possible to estimate the pressures drop using the Fanning equation (Hughes and Brighton 1999):

eq. 3.5.14 $$\Delta P = f\left(\frac{SL}{A}\right)0.5\rho v^2$$

Where S is circumference or perimeter (m) and A is cross sectional area (m^2); L is the length of tube or channel (m) and f is the friction factor that is dependent on the geometry of the modules on the roughness of the membrane and the flow regime (see Table 3.5.5).

Table 3.5.5. Friction factors in various systems (Mulder 1996)

	Channel	Tube
Laminar	$f=24Re^{-1}$	$f=16Re^{-1}$
Turbulent	$f=0,133Re^{-0,25}$	$f=0,079Re^{-0,25}$

Concentration polarization can cause

- lower observed retention because the concentration at the membrane surface is higher than the bulk concentration and assuming that the real (membrane) retention is constant.
- higher observed retention in filtration of mixtures of macromolecules due to the formation of a dynamic membrane consisting of higher molecular weight solutes that causes increased retention of lower molecular weight solutes.
- lower flux because of an additional resistance due to concentration polarization.

In short, concentration polarization is very severe in MF and UF as the fluxes initially are high and the Brownian diffusivities of particles are very small. The high concentration of particles at the membrane surface results in a formation of a cake layer, which will be explained in the following.

Membrane fouling

It is important to understand the mechanism of membrane fouling in order to minimize its unwanted effects. While concentration polarization is a reversible boundary layer phenomenon, fouling can have an irreversible character due to

specific physical and chemical interactions between the feed particles and the membrane. Thus membrane fouling eventually will require cleaning of the membrane implying less time available for filtration.

Four different basic fouling mechanisms have been recognized, complete pore blocking, internal pore blocking, partial pore blocking and cake filtration (see Figure 3.5.9).

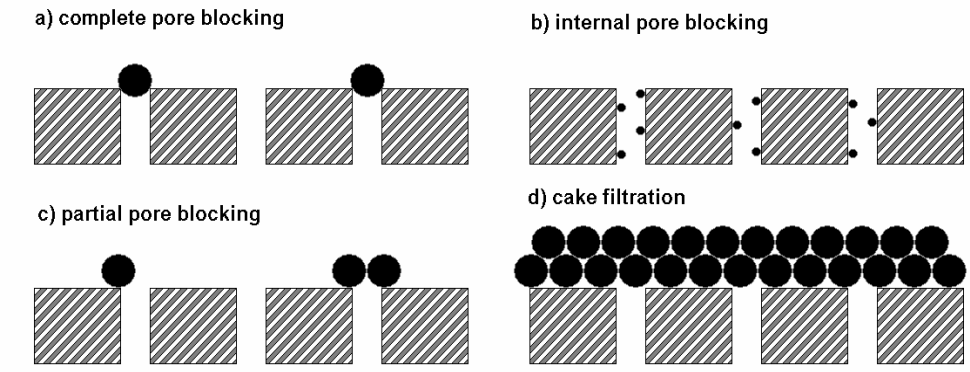

Figure 3.5.9. Schematic drawing of the fouling mechanisms assumed: (A) complete blocking, (B) standard blocking, (C) intermediate blocking and (D) cake filtration. (Modified from Bowen et al., 1995).

The fouling mechanism **complete blocking (A)** assumes that each particle reaching the membrane participate in blocking a pore on the membrane surface. This is a fouling mechanism that requires that the foulant (solute or particle causing fouling) is bigger than the pore size. Possible foulants of this size in microfiltration would be particles or aggregates of macromolecules. The complete blocking mechanism is likely to take place in the beginning of a filtration where all the pores are accessible for flow.

The fouling mechanism **standard blocking (B)** assumes that the fouling takes place on the pore walls decreasing the pore radius. It is a likely mechanism for adsorption of macromolecules in microfiltration, as the solute has to be small enough to enter the membrane pores.

The fouling mechanism **intermediate blocking (C)** is a less restrictive version of the complete blocking as particles are allowed to settle on each other as well as blocking pores. This model can be seen as an intermediate or transition state between complete blocking and the fourth fouling mechanism.

The fouling mechanism **cake filtration (D)** assumes that particles reaching the membrane form a cake layer on the membrane surface. This is often the main mechanism in microfiltration as retained particles accumulate on the membrane surface.

General equations for all four mechanisms and their influence on flux described for the case of dead-end MF at either constant pressure (eq. 3.5.15) (Hermia 1982) or constant flux (eq. 3.5.16) (Hlavacek and Bouchet 1993)

eq. 3.5.15 $cons\tan t\ pressure$ $$\frac{d^2t}{dV^2}=k\left(\frac{dt}{dV}\right)^n$$

eq. 3.5.16 $cons\tan t\ flux$ $$\frac{d^2t}{d(\Delta P)^2}=k\left(\frac{dt}{d(\Delta P)}\right)^n$$

Where V is the permeate volume (m^3); k is constant specific for each fouling mechanism and n is exponent specific for each fouling mechanism. For the values of k and n see Table 3.5.6.

Table 3.5.6 Values for n in the general expression for the blocking (Hlavacek and Bouchet 1993)

Blocking law	n (Const. flow)	n (Const. pressure)
Complete	3/2	2
Standard	5/3	5/3
Intermediate	2	1
Cake	-	0

(Bowen *et al.* 1995) have used the general expression for constant pressure dead-end microfiltration of protein solutions to determine the fouling mechanism. By rewriting eq. 3.5.15 to the following:

eq. 3.5.17 $$\ln\left(\frac{d^2t}{dV^2}\right)=\ln(k)+n\ln\left(\frac{dt}{dV}\right)$$

, and plotting $\ln(d^2t/dV^2)$ versus $\ln(dt/dV)$, n can be determined as the slope and thus it is possible to identify the fouling mechanism. If the n value lies between the value of two different fouling mechanisms, e.g. complete blocking and standard blocking, both fouling mechanisms occurred during the filtration (Bowen *et al.* 1995).

Tracey and Davis (1994) (Tracey and Davis 1994) used the equations to determine whether fouling could be characterized as internal or external. If internal fouling is occurring then resistance increases with increasing slope or (positive derivative) whereas if external fouling is occurring then resistance increases with decreasing slope (negative derivative).

3.5.2 Nanofiltration

As a filtration process, the Nanofiltration (NF) process lies somewhere between Reverse Osmosis and Ultrafiltration. Nanofiltration allows higher fluxes than Reverse Osmosis, but still demonstrates good retention towards multivalent salts and large molecules. NF is "defined" by a high selectivity between mono- and multivalent ions such as sodium (low retention) and calcium (high retention), and the retention of salts is caused by Donnan exclusion as most NF membranes are charged. Hence, the retention of charged molecules by NF membranes is dependent of charge, while the retention of non-charged molecules is highly dependent on their molecular size and shape. This theory section is mainly concerned with the mechanisms of polarization, and the difference between observed and true retention.

The volume flux through nanofiltration (and reverse osmosis) membranes can be described by the osmotic pressure model (Mulder 1991):

eq. 3.5.18 $$J = L_p\left(\Delta P - \sigma \cdot \Delta\pi\right)$$

J is the volume flux (m/s), which is considered equal to the solvent flux. ΔP is the transmembrane pressure (Pa) and $\Delta\pi$ is the osmotic pressure difference across the membrane (Pa). L_p can be regarded as the solvent permeability (m/s/Pa) and is composed of different solvent properties such as diffusion coefficient, concentration at the membrane surface, and molar volume. σ is a reflection coefficient that takes the small flux of solutes into account. The reflection coefficient is a measure of the degree that the solutes are retained:

$\sigma = 1$	*Ideal membrane, no solute transport*
$0 < \sigma < 1$	*Membrane not totally semipermeable, some solute transport*
$\sigma = 0$	*No selectivity, no retention of solute*

A_w can be experimentally determined by measuring the pure water flux of a clean membrane ($\Delta\pi = 0$) as function of the transmembrane pressure.

According to traditional membrane technology, the solute flux, J_s, can be described by (Mulder 1991):

eq. 3.5.19 $$J_s = c_{\ln,s} \cdot (1-\sigma) \cdot J_w + \omega \cdot \Delta\pi$$

$c_{ln,s}$ is the mean logarithmic mass concentration (g/l) and ω is the solute permeability.

The osmotic pressure for a component *i*, π_i, can be deduced by chemical potential calculations, but is most often derived from the simplified van't Hoff equation (Mulder 1991):

eq. 3.5.20 $$\pi_i = C_i RT = \frac{c_i}{M_i} RT$$

This equation is only valid for dilute solute concentrations, though often used for approximations.

By rearranging eq. 3.5.19 and replacing osmotic pressure with equation eq. 3.5.20 the following expression can be found:

eq. 3.5.21 $$\frac{J_s}{\Delta c} = \omega RT + (1-\sigma) \cdot J_w \cdot \frac{c_{\ln}}{\Delta c}$$

Δc and c_{ln} is respectively the concentration difference and the mean logarithmic concentration between the feed and permeate side of the membrane. By plotting experimental values of $J_s/\Delta c$ versus $J_w \cdot c_{ln}/\Delta c$, the reflection coefficient and the solute permeability can be found as shown on Figure 3.5.10.

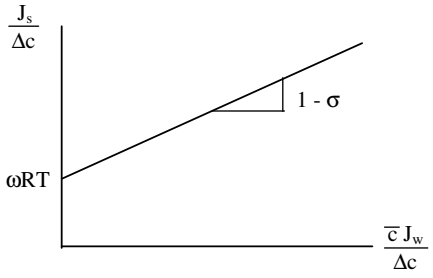

Figure 3.5.10 Experimental determination of σ and ω.

Polarization must often be considered a main factor that lowers the performance of NF separation and the concentration gradient across the boundary layer must be taken into consideration. The polarization at the surface of a NF membrane is equivalent to what happens in MF and UF as sketched on Figure 3.5.8.

The retention S of a solute *i* is defined as:

eq. 3.5.22 $$S_i \equiv 1 - \frac{C_{p,i}}{C_{b,i}}$$

S is called the *observed* retention, because it is calculated from the measurable concentrations of *i*. The *true* retention R of *i* by the membrane is defined as:

eq. 3.5.23 $$R_i \equiv 1 - \frac{C_{p,i}}{C_{m,i}}$$

The observed retention depends not only of the membrane, but also very much on the system's flow conditions. On the other hand, the true retention depends only on the membrane properties, and is a much more comparable parameter, when investigating the feasibility of a NF process. Since C_m ordinarily cannot be measured directly, an approximation is necessary to find R_i.

Equation (eq. 3.5.10) can also be written in the following form (Jonsson and Boesen 1977):

eq. 3.5.24 $$\ln\left(\frac{c_m - c_p}{c_b - c_p}\right) = K\frac{J_v}{v^b}$$

Where the crossflow velocity *v* that is part of the Reynolds number, and hence risen to an exponent *b*. The exponent is either 0.33 for laminar or 0.80 for turbulent flow conditions as summarized in Table 3.5.4. Substituting the concentration terms in eq. 3.5.24 with equations eq. 3.5.22 and eq. 3.5.23 yields:

eq. 3.5.25 $$\ln\left(\frac{1-S}{S}\right) = \ln\left(\frac{1-R}{R}\right) + K \cdot \frac{J_w}{v^a}$$

Thus, by plotting experimental values of ln((1-S)/S) versus J_v/v^b, a straight line should be obtained intersecting the ordinate axis at ln((1-R)/R). Hence the true retention, and from that C_w, can be deduced. The constant K can be determined as the slope of the plotted line.

3.5.3 Electrodialysis

Electrodialysis is an electromembrane process in which charged species are transported through ion permeable membranes from one solution to another under the influence of an electrical potential gradient. Since the membranes have the ability to selectively transport ions having positive or negative charge and reject ions of the opposite charge, concentration, removal, or separation of electrolytes can be achieved. The charged species must be mobile, and the separation media must be able to transfer electrical current with relatively low resistance. Electrodialysis is used widely for production of potable water from sea or brackish water, electroplating rinse recovery, desalting of cheese whey, production of ultrapure water etc.

Conventional electrodialysis, or desalting electrodialysis, is carried out by applying a voltage drop across a membrane stack with alternating cation-, (CEM) and anion-exchange membranes (AEM), forming concentration, and dilution chambers (see Figure 3.5.11).

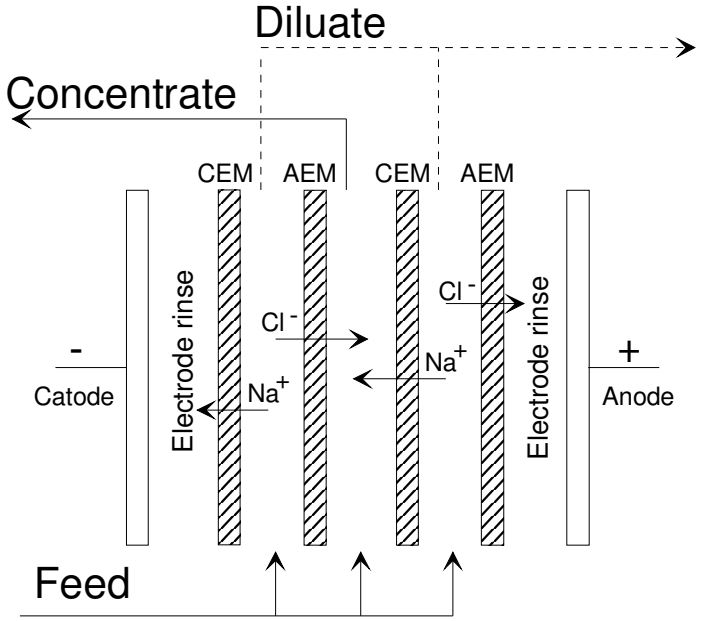

Figure 3.5.11. Conventional electrodialysis for concentration/desalination of a feed stream containing sodium chloride.

3.5.3.1 Ionexchange membranes

Charged polymer membranes have been investigated for well over 100 years. Most natural and artificial membranes consist of polymers and the porous membranes investigated in the past inherently carry at least some ionizable groups (except in a few instances) and are therefore charged (Sollner *et al.* 1973). The basis of classic electrochemistry was founded around the turn of the 20th century with capacities like Ostwald, Nernst and Donnan being some of the most notable forerunners. Charged membranes have been investigated ever since, and while the results obtained in this field were most confusing during the 19th century, a still greater understanding of charged membranes and their basic functions have developed during the 20th century.

Commercially created ion exchange membranes (IEM) are normally composed of crosslinked polymeric gels with fixed positive or negative charges. The fixed, immobile charge must be balanced by a dissolved mobile ion of opposite charge to preserve electroneutrality. Hence, to avoid crystallization of the ionic groups inside an ion exchange membrane, it is necessary to keep the membranes constantly wetted to preserve functionality. The polymers with high ion exchange capacity has a strong tendency to swell, which is held in check by a high degree of crosslinking (Kesting 1985).

Two general different types of ion exchange membranes exist. An ion exchange membrane with fixed positive charges allows primarily negative ions to enter and pass through the membranes internal matrix. This is then named an Anion exchange membrane (AEM). Typical fixed charges in anion exchange membranes are (Strathmann 1992):

$$-NH_3^+ \quad -RNH_2^+ \quad -R_3N^+ \quad =R_2N^+ \quad -R_3P^+ \quad -R_2S^+$$

Similarly, a membrane with fixed negative charges allows the free passage of cations and is hence named a Cation exchange membrane (CEM). Fixed charges commonly used in cation exchange membranes are:

$$-SO_3^- \quad -COO^- \quad -PO_3^{2-} \quad -HPO_2^- \quad -AsO_3^{2-} \quad -SeO_3^-$$

Normally the most strongly acidic or basic groups like the quaternary ammonium group ($-R_3N^+$) or the sulfonic group ($-SO_3^-$) are preferred in commercial membranes, since they are completely dissociated over nearly the entire pH-range.

The name "ion exchange membrane" is perhaps a little misguiding, since ion exchange membranes work quite different from ion exchange *resins*, normally employed in ion exchange columns. In ion exchange resins, ions of opposite charge are replaced by other ions of same general charge, while ions of the same charge as that of the resin are allowed free passage. An example on this is the demineralization of water, where calcium and magnesium ions are replaced by hydrogen or sodium ions, while anions like chloride and sulfate pass right through. In ion exchange membranes ions of opposite charge than the membranes fixed charges (counter-ions) can jump from one fixed group to the next and are hence mobile inside the membrane, while ions of same charge as the membrane (co-ions) are electrically repulsed by the fixed charges. The co-ions are still mobile inside the ion exchange membrane, but because of the repulsion and the necessity of preserving electroneutrality, the concentration of co-ions is much lower compared to that of the counter-ions. The principle is sketched on Figure 3.5.12 with a polymer carrying fixed sulfonic groups.

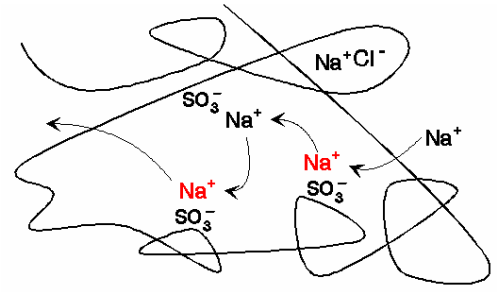

Figure 3.5.12 Migration of sodium ions through a cation exchange membrane

The mobile ions are respectively sodium (counter-ions) and chloride (co-ions). The sketch shows how the sodium ions migrate through the polymer by "jumping" from one fixed sulfonic group till the next, while chloride needs to keep in contact with an otherwise unoccupied sodium ion at all time. The mechanism of excluding co-ions from ion exchange membranes is referred to as Donnan-exclusion and is elaborated on in section 3.5.3.2.

The Donnan exclusion and the selectivity of an ion exchange membrane depend on different factors (Strathmann 1992). Both properties *increase* with:

- the concentration of fixed charges,
- increasing valence of the co-ions,
- decreasing valence of the counter-ions,
- decreasing electrolyte concentration,
- decreasing affinity of the of the exchanger groups with respect to the counter-ions.

Other important parameters for the ion exchange membrane's properties include the density of the polymeric network, the hydrophobic and hydrophilic properties of the polymer matrix, the distribution of the charge density, and the morphology of the membrane.
To be most effective an ion exchange membrane should have the following properties:

- *High permselectivity*. The ion-exchange membrane should be highly permeable to counter-ions and impermeable to co-ions.
- *Low electrical resistance*. The permeability for the counter-ions driven by an electrical potential gradient should be as high as possible.

- *Good mechanical and form stability*. The membrane should be mechanically strong to withstand handling during equipment assembling/disassembling as well as minor pressure changes during operation. Also a low degree of swelling or shrinking in transition from dilute to concentrated electrolyte solutions is important to preserve form and avoid equipment leakage.
- *High chemical stability*. The membrane should be inert to the electrolyte solutions and their electrolysis products. This means stability in the pH-range of 0-14 and resistance to oxidizing agents.

It can be difficult to optimize properties of ion exchange membranes because the parameters involved most often works in opposite directions. Higher degree of cross-linking, for instance, improves mechanical stability, but increases the electrical resistance as well. Higher concentration of fixed charges causes lower electrical resistance, but increases swelling, hence lowering mechanical stability.
Hence, commercial ion exchange membranes are usually designed with different special properties. Membranes with increased chemical resistance, mechanical stability, or low diffusion rates can be obtained as needed for a given process. Monovalent selective membranes, that are permeable to monovalent counter-ions while excluding multivalent counter-ions as well as co-ions, are also available. These special grade membranes are for example used in table salt production, when sodium chloride is concentrated from seawater with electrodialysis, thus only concentrating the sodium and chloride ions without the sulfate-, calcium-, or magnesium ions normally present in seawater.

A special type of ion exchange membrane is the bipolar membrane. The bipolar membrane is composed of two halves: an anion exchange film and a cation exchange film connected by a very thin (about 1 nm thick) interface junction. A bipolar membrane is sketched on Figure 3.5.13. When the membrane is placed in an electrical field water is split into hydroxide ions and protons.

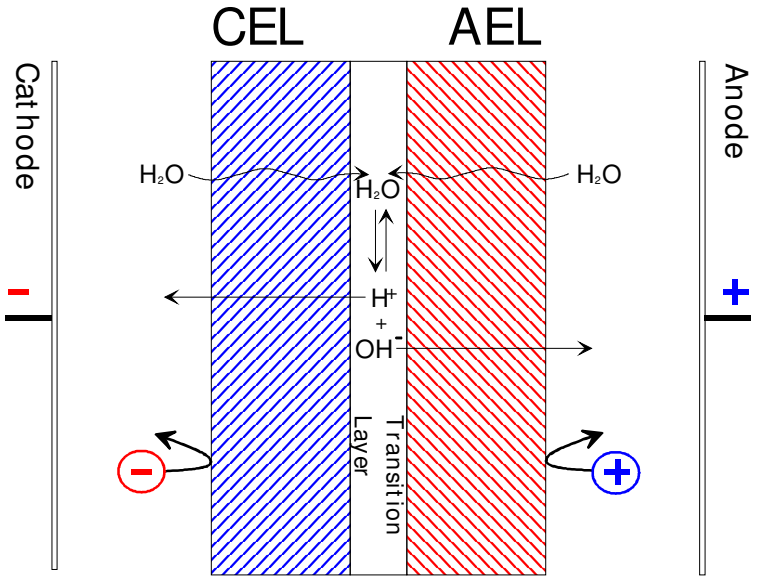

Figure 3.5.13. Watersplitting in a bipolar membrane.

3.5.3.2 Donnan exclusion

To explain the mechanisms of the ion exchange membrane's selective behavior towards positive and negative ions, consider a *cation exchange membrane* in contact with a dilute electrolyte solution as sketched on Figure 3.5.14.

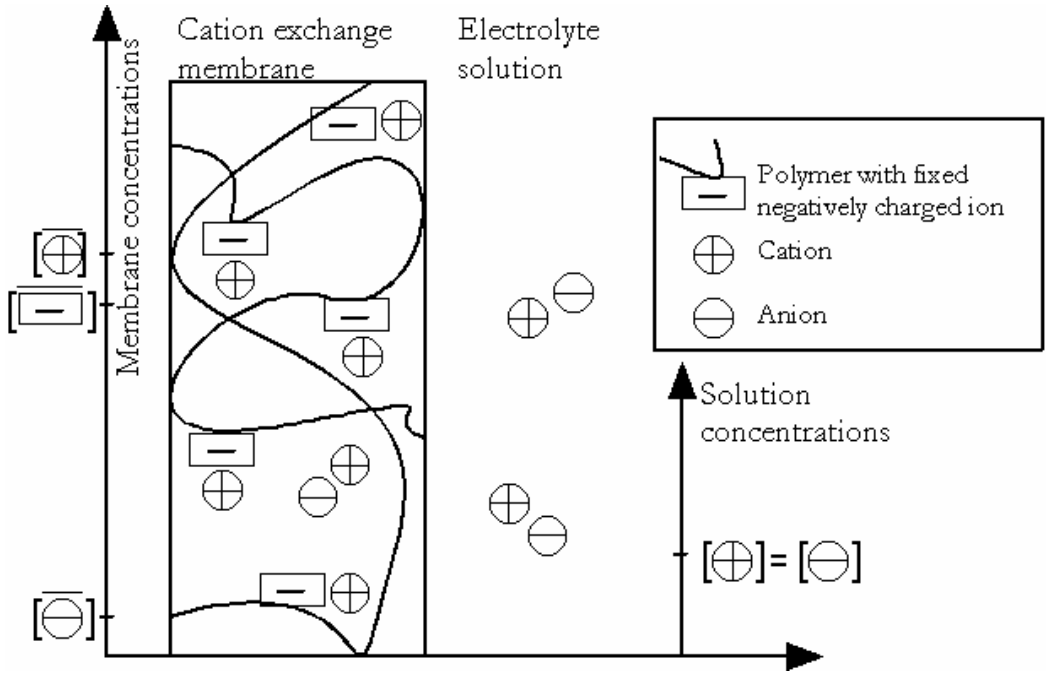

Figure 3.5.14. The distribution of cations and anions between a cation exchange membrane and a dilute electrolyte solution. Inside the membrane fixed negative charges are balanced by mobile counter-ions (cations). The axis gives a rough estimation of the concentration levels of the ions inside the membrane (indexed with ¯) and in the solution at equilibrium.

In this case the *cations* are the *counter-ions* and the *anions* are the *co-ions*. The concentration of cations inside the membrane is much higher than in the dilute solution because of the presence of the fixed negative groups. The concentration of anions, however, is much smaller (if existing) inside the membrane than in the solution.

For neutral molecules ordinary diffusion would take place, but since the cations and anions all carry charges, attempts to level off concentration differences are disturbing electroneutrality both in the membrane and in the solution. Diffusion of cations out of the membrane and into the solution and anions from the solution into the membrane would create a positive surplus of charge (space charge) in the solution and a negative space charge in the membrane. This creates an electrical field across the membrane-solution interface that is directed opposite to the diffusional flow as shown of Figure 3.5.15.

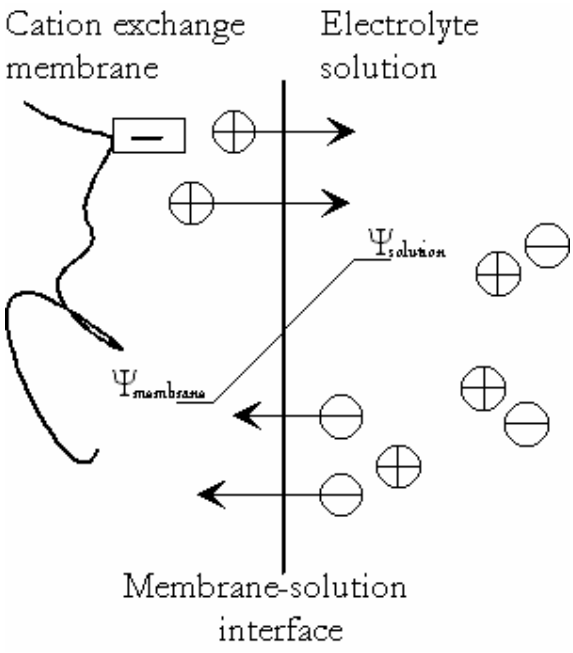

Figure 3.5.15. Cations trying to diffuse out while anions tries to diffuse inside the membrane creates an electrical field $\Delta\Psi = \Psi membrane - \Psi solution$ to balance out the driving diffusion forces.

At electrochemical equilibrium named the Donnan equilibrium this electrical field balances the driving diffusion forces of the ions. This potential allows the counter-ion concentration to be higher, and the co-ion concentration to be lower inside the membrane than in the external solution. Since the co-ions are repelled from the membrane, the electrolyte itself is too, because of the electroneutrality requirement.

This exclusion of electrolyte is called Donnan exclusion in honor of his pioneer work in this area (Donnan 1911).

The electrical potential that arises can be calculated from the electrochemical potentials μ of the mobile ions. Neglecting pressure differences between phases, the electrochemical potential for *i* can be expressed:

eq. 3.5.26 $$\mu_i = \mu_i^o + RT \ln a_i + z_i F \psi$$

μ° is the chemical standard potential, R is the Gas constant (8,31 J/mol·K), and T the temperature (K). a_i and z_i are the activity and ionic charge respectively of *i*. F is the Faraday number (96485 C/eq.) and ψ the electrical potential.

At steady state conditions the chemical potential for *i* will be equal on both sides of the electrolyte solution and membrane interface. Using index *m* for membrane conditions and *s* for solution conditions, this can be expressed as:

eq. 3.5.27 $$\mu_i^{o,m} + RT \ln a_i^m + z_i F \psi^m = \mu_i^{o,s} + RT \ln a_i^s + z_i F \psi^s$$

At equilibrium the chemical standard potential μ°_i is equal in both phases. Hence the potential difference between membrane and solution Δψ that arises can be calculated by rearranging the previous equation to:

eq. 3.5.28 $$\Delta\psi = \psi^m - \psi^s = \frac{RT}{z_i F} \ln \frac{a_i^s}{a_i^m}$$

Δψ is named the Donnan potential, E_{Don}. Since the E_{Don} that arises from the distribution of the cations must be equal to the potential that arises from the anion distribution, and then:

eq. 3.5.29 $$\frac{RT}{z_+ F} \ln \frac{a_+^s}{a_+^m} = \frac{RT}{z_- F} \ln \frac{a_-^s}{a_-^m}$$

which rearranges into:

eq. 3.5.30 $$\left(\frac{a_+^s}{a_+^m}\right)^{1/z_+} = \left(\frac{a_-^s}{a_-^m}\right)^{1/z_-}$$

Example A: For a single monovalent salt ($z_+ = 1$, $z_- = -1$) like sodium chloride in a dilute (0,01 M) solution ($\gamma_\pm \approx 1$) and a little rearrangement eq. 3.5.30 becomes:

eq. 3.5.31 $$\frac{C_+^m}{C_+^s} = \frac{C_-^s}{C_-^m}$$

In the solution $C_+^s = C_-^s$ = 0,01 M. For a cation exchange membrane, we assume that the membrane's ion exchange capacity (concentration of fixed ionic groups) is 1 M, which means that C_+^m is around 1 M to balance the fixed charges. From eq. 3.5.31 it then follows that C_-^m must be in the region of 0,0001 M. From this example can be seen that the membrane's concentration of cations is about 10.000 times larger than the concentration of anions, meaning the selectivity of this membrane in this solution is 99,99%.

From eq. 3.5.31it is clear that the higher the counter-ions' concentration ratio between membrane and solution (C_+^m/C_+^s), the higher the ratio of the solution/membrane concentration of the co-ions (C_-^s/C_-^m). This results in higher selectivity. The opposite is also the case. The lower the counter-ion ratio, the lower the co-ion ratio, which results in low selectivity. Ion exchange membranes generally perform poorly in high electrolyte concentrations.

Example B: In a dilute electrolyte solution with both monovalent and divalent cations in contact with a cation exchange membrane, eq. 3.5.26 can still be used to obtain the membrane/solution concentration ratios of the ions. Consider an electrolyte solution with 0,01 M sodium chloride and 0,005 M calcium chloride. The charge equivalent concentrations of both cations are the same (0,01 N), and the Donnan potential that arises at equilibrium affects both ions. From eq. 3.5.26 following the same routine as before and still neglecting activity coefficients, we obtain that:

eq. 3.5.32 $$\left(\frac{C_+^m}{C_+^s}\right)^2 = \frac{C_{2+}^m}{C_{2+}^s}$$

This equation shows that the ratio of the divalent cation concentration between membrane and solution will be the square of monovalent cation's concentration ratio. E.g. if the sodium concentration inside the membrane is 10 times higher than in the solution, the membrane's calcium concentration would be 100 times larger than in the solution.

The higher the ionic charge of a counter-ion, the more readily it will enter and fill the membrane's capacity spots.

To calculate the intermembrane concentration of counter- and co-ions more precisely, consider the need for electroneutrality of both phases in the system at equilibrium. For a salt in the initial solution:

eq. 3.5.33 $$\sum_i z_i C_i^s = 0$$

The same equation can be set up inside the membrane when the membrane's ion exchange capacity C_R (the concentration of fixed charges) is included:

eq. 3.5.34 $$\sum_i z_i C_i^m + z_R C_R = 0$$

Example 1.C: For monovalent electrolyte solution in contact with a cation exchange membrane (z_R = -1) equation and becomes:

eq. 3.5.35 $$C_+^s = C_-^s \qquad and \qquad C_+^m = C_-^m + C_R$$

Combining these two equations with the Donnan exclusion condition of equation eq. 3.5.31, the co-ion membrane concentration C_-^m can be obtained from the following expression:

eq. 3.5.36 $$\frac{C_-^s}{C_-^m} = \sqrt{\frac{C_R}{C_-^m} + 1}$$

For dilute solution $C_R/C_-^m >> 1$ and equation can be simplified to:

eq. 3.5.37 $$C_-^m = \frac{\left(C_-^s\right)^2}{C_R}$$

Equation 3.5.37 confirms the estimation of the co-ion concentration inside a cation exchange membrane with a capacity of 1 M and a 0,01 M monovalent electrolyte in example A.

3.5.3.3 Ion transport

Ion transport can in most cases be broken into three contributions: convective transport, diffusive transport and migration:

eq. 3.5.38 $$J_i = vC_i - D_i \frac{dC_i}{dx} - \frac{z_i F C_i D_i}{RT} \cdot \frac{d\psi}{dx}$$

J_i, C_i, D_i, z_i are respectively the flux, the concentration, the diffusion coefficient and the ionic charge of component *i*. *v* is the convective flow velocity, F the Faraday number, R the Gas constant, T the temperature and ψ the electrical potential.

According to the Einstein relation, the ionic mobility of component *i* u_i can be introduced into 3.5.38 as (Atkins 1992):

eq. 3.5.39 $$u_i = \frac{z_i F D_i}{RT}$$

Ion exchange membranes are generally nonporous, hence the convective ion transport can be neglected and reduces to the Nernst-Planck equation (Mulder 1991):

eq. 3.5.40 $$J_i = -D_i \frac{dC_i}{dx} - u_i C_i \frac{d\psi}{dx}$$

Two large applications incorporating ion exchange membranes are (Donnan) dialysis and electrodialysis. In dialysis the diffusional flux is the dominant ion transport, while in electrodialysis processes an electrical field is exerted across the membranes promoting the migration transport. In electrodialysis the diffusional flux often works counter to the desired separation direction.

Equation eq. 3.5.40 shows that non-charged molecules are only subject to diffusion through ion exchange membranes, but solvent transport must still be considered. For aqueous solutions, three different conditions affect the solvent. In the case of electrodialysis ions are driven through ion exchange membranes against their concentration gradient to create concentrated and diluted product streams. The concentration difference between the separated electrolyte solutions creates an osmotic pressure gradient that moves the solvent in an attempt (by Nature) to establish equilibrium. Since the dissolved ions coordinate solvent molecules to stay dissolved while being transported, a significant amount of solvent is moved by electroosmosis. And in some instances, high polarization effects at the membrane surfaces promote the "water-splitting" effect, causing water molecules to dissociate into hydrogen and hydroxide ions. The five different transport effects are schematically shown on Figure 3.5.16.

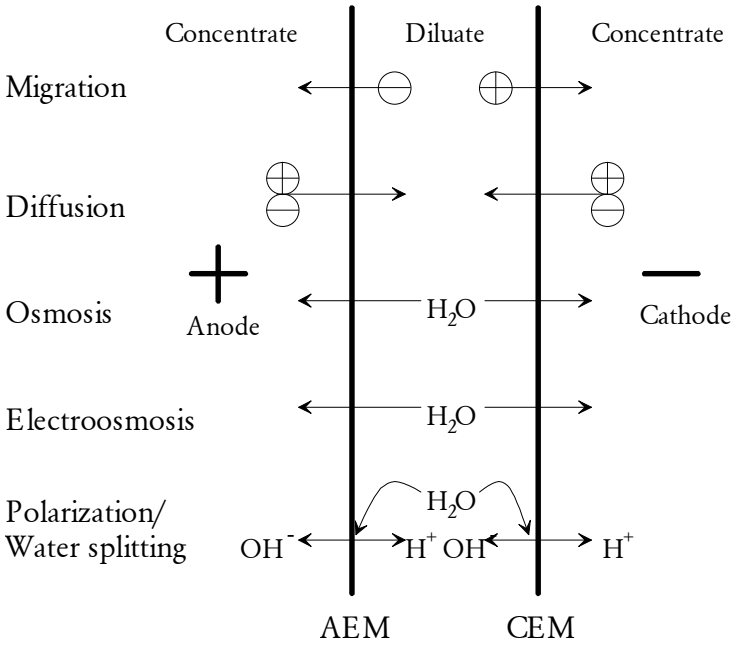

Figure 3.5.16 Transport mechanisms across ion exchange membranes in electrodialysis. AEM indicates an anion exchange membrane and CEM a cation exchange membrane.

A theoretical value for the transport of a given ion *j* species can be expressed by a transport number *t*, which is defined as the fraction of total current *i* carried by the ion:

eq. 3.5.41 $$t_j \equiv \frac{i_j}{i}$$

If the interaction between ions is neglected the transport number in diluted solutions can be expressed by:

eq. 3.5.42 $$t_j = \frac{|z_j| u_j C_j}{\sum |z_k| u_k C_k}$$

Where *z* is the charge, *u* is the mobility, and C is the concentration of the ion. The denominator is a summation of all ionic species present. For a monovalent salt, e.g. NaCl the transport number of Na^+ and Cl^- in solution is 0.39 and 0.61, respectively, while for KCl the transport number of both K^+ and Cl^- is approximately 0.5. However, inside e.g. the anion exchange membrane the transport number of Cl^- would approach unity for a very dilute outer solution (see Donnan exclusion). Likewise, the transport number inside a cation exchange approaches unity for either Na^+ or K^+

3.5.3.4 Polarization

Like in the filtration processes, polarization is an essential limiting factor in the performance of an electrodialysis process. Polarization in a boundary layer arises from the difference between the transport number of an ionic species in the membrane and in the solution. Figure 3.5.17 shows the concentration profiles in the boundary layer for two different current densities where cations are entering the cation exchange membrane.

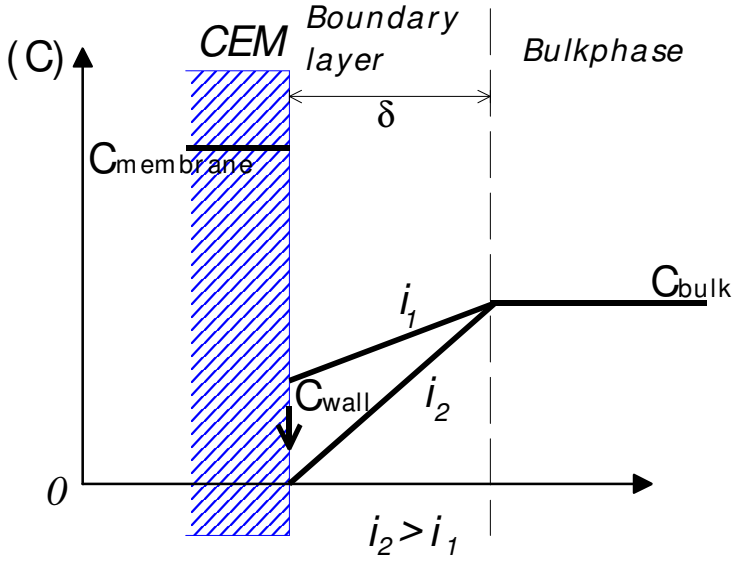

Figure 3.5.17. Concentration profile in the boundary layer of an ionic species entering the membrane. The two profiles are shown for different current densities where i_2 is equal to the critical current density.

As the current density is increased wall concentration drops until a critical (or limiting) value of the current is reached where $C_{wall} \approx 0$. At this point a further increase in the current density would result in the excess current being carried by H^+ and OH^- generated by the splitting of water at the membrane surface. The highest attainable current density before watersplitting sets in, depends on the bulk concentrations and hydrodynamics of the process streams, as given by the following equation:

eq. 3.5.43 $$i_{Crit} = \frac{z \cdot D \cdot F \cdot C_b}{(t^m - t) \cdot \delta}$$

Where z is the charge, D is the diffusion coefficient, F is Faradays number, C_b is the bulk concentration, δ is the boundary layer thickness, and t^m and t are the transport numbers in the membrane and solution, respectively.
Electrodialysis processes should be operated such that watersplitting is avoided at the membrane surfaces, typically at 80-90% of the critical current density.

3.5.3.5 Energy consumption

The energy needed for transferring a given amount of the targeted ionic species across a membrane from a feed solution to a product stream is an important parameter in evaluating the suitability of an electrodialysis process. The thermodynamic minimum work required for separating a monovalent salt is given by the Gibbs free energy (Strathmann 1992):

eq. 3.5.44 $$W_{\min} = \Delta G = 2RT(C_f - C_d)\left(\frac{\ln\frac{C_f}{C_d}}{1-\frac{C_f}{C_d}} - \frac{\ln\frac{C_f}{C_c}}{1-\frac{C_f}{C_c}}\right)$$

Where C_f is the feed concentration, C_d and C_c are the concentrations in the diluate and concentrate, respectively. ΔG is the Gibbs free energy required for producing 1 liter of diluate.
However, the actual energy consumption (kWh/kg recovered product) required for a separation is considerable higher due to:

- Ohmic resistance in the solutions and membranes.
- Polarization effects.
- Resistance in electrode system.

- Resistance in external electrical system.
- Current efficiency that is less than 1 per cell pair.
- Pumping energy for circulating the process streams.

The ohmic resistance of the electrolytes R_s can be calculated from:

eq. 3.5.45 $$R_S = \frac{1}{\kappa}\frac{l}{A}$$

Where κ is the conductivity of the solution, *l* is the height of the flow channels (distance between membranes) and *A* is the active membrane area. The resistance in the membranes R_m is depends on the membrane type and the concentrations in the flow chambers. Typical values for the specific membrane resistance can often be found in supplier's data-sheets or by measuring the difference in the conductivity across an electrolyte with and without a membrane inserted. For a bipolar membrane and extra resistance is encountered as a result of a minimum potential drop across the interface layer, required for watersplitting to take place.
Polarization effects as described in the previous section can cause the specific resistance of the boundary layers R_p to differ significantly from the resistance of the bulk solutions, especially at currents near the critical current density. The overall cell resistance can be expressed as the summation over the resistance of solutes, membranes and polarization layers:

eq. 3.5.46 $$Rcell = \sum Rs + \sum Rm + \sum Rp.$$

Resistance in the electrode system and the external electrical system is often neglected, because of the insignificant contribution to the overall resistance in a stack composed of 200-300 cell pairs.
The current efficiency has a major effect on the energy consumption, e.g. if the current efficiency is halved, the energy consumption is doubled. The current efficiency is influenced by the selectivity of the membrane (Donnan exclusion), the ratio between the targeted ion and co-ions in the feed solution, back diffusion of already transferred ions, and also current leakage in the manifold system. The current efficiency η can be defined as the number of equivalent targeted ions transferred from the feed per current equivalent, expressed by:

eq. 3.5.47 $$\eta = -\frac{z \cdot F \cdot Q_F \cdot \Delta C_F}{n \cdot I}$$

Where z is the charge of the targeted ion, F is Faraday's number, Q_F is the feed flow rate (m^3/s), ΔC_F is the difference between the feed inlet and outlet concentration (mol/m^3) from the stack, n is the number of cell pairs in the stack, and I (A) is the electrical current across the stack.

The energy input needed for pumping the different process fluids *i* can be estimated from:

eq. 3.5.48 $$W_{pump} = \sum k_i Q_i \Delta p_i$$

Where *k* is a constant related to the efficiency of the pump, *Q* is the volume flow, and Δp is the pressure difference between pump inlet and discharge.

Disregarding energy loss in the electrode system and external electrical system the energy consumption *E* (kWh/kg recovered product) can be expressed as:

eq. 3.5.49 $$E = \frac{I^2 R_{Cell} + W_{Pump}}{\left(I \cdot \eta / z_i \cdot F \right) \cdot MW_i}$$

Where MW_i is the molar weight of the product.

3.5.3.6 Fouling

Membrane fouling, scaling and poisoning are major problems in electrodialysis operations that must be avoided whenever possible.

Membrane fouling is used as a term to describe the adsorption of macro-particles or bio-matter like proteins on membrane surfaces. Large, charged molecules (MW > 1000) are generally retained by ion-exchange membranes because of their size, but their charges are attracted by the oppositely charged ion-exchange membranes and layers on top of the membranes often start to build. When oppositely charged proteins cling to the surface of an ion-exchange membrane, they affect the Donnan exclusion by neutralizing a number of fixed ions, and thus lowering the selectivity of the membrane. When the bio-matter fouling becomes more extensive, large surface areas are no longer effective for ion transport and electrical resistance increases. Build-up of bio-matter in electrodialysis also presents another problem by clogging up equipment and obstructing the flow. pH, bio-matter concentration and ionic

strength of the fouling matter all affects how the process is influenced (Mulder 1991). In case of oppositely charged matter with dense charge concentration (approximately as large as the membrane capacity) fouling an ion-exchange membrane, a situation is created that resembles the bipolar membrane. This can cause increased water-dissociation, which results in energy loss, lower efficiency and pH-changes (Ramirez *et al.*1992).
Membrane fouling is often reversible, and cleaning the system with alkaline and/or acidic agents often regenerates the membranes to the initial state of operation. The speed of the rebuilding of fouling layers on the membranes determines how often operation has to be interrupted for cleaning. By increasing the Reynolds number of the process streams through the membrane stack, it is possible to maintain a continuous removal of fouling matter that builds up and a steady-state of the fouling is reached.
The following process parameters can be changed to reduce fouling (Chiao *et al.*1991):

- Increasing flow velocity.
- Utilizing spacer design with channels that promotes turbulence.
- Periodically stopping in the electrical current.
- Periodically alternating flow chambers and reversing current direction (*reverse electrodialysis*).
- Periodically cleaning the system.
- Pretreatment of fouling content (precipitation, filtration, enzyme treatment).

In some commercial membranes like the Neosepta® AMX anion-exchange membrane (Tokuyama Corp., Japan), the length and degree of crossbinding have been adjusted to allow larger molecules to pass through the membrane (Strathmann 1992). This reduces the fouling build-up of small particles.

Membrane scaling commonly occurs when the feed contains fair amounts of multivalent cations, especially calcium and magnesium. When divalent cations like calcium and magnesium passes through cation-exchange membranes into an alkaline solution, they immediately precipitate on the membrane surface as their respective hydroxide salts ($Ca(OH)_2$, $Mg(OH)_2$). This scaling affects the process fast by reducing effective membrane area, and increasing electrical resistance.

Membrane poisoning occurs when charged ions in the process streams react irreversibly with the membrane. The reaction can be a chemical reaction that changes the membrane and the membrane properties. When poisoning degrades the membranes, membrane maintenance and replacement must occur at regular

intervals, which is a heavy expense. Only in exceptional cases (e.g. highly valuable products) can membrane poisoning be tolerated for lengthy operations.

3.5.3.7 Module configuration

The modules used in electrodialysis are of the plate and frame type, where flat sheet membranes, separated by spacers, are placed in parallel throughout the membrane stack. To transfer the electrical current to the electrolytes, electrodes are positioned in special chambers at each end of the membrane stack. To avoid deterioration, the anode is typically made of platinized titanium or mixed metal oxides (MMO), whereas the cathode can be made of less expensive materials, such as stainless steel. Circulation of e.g. Na_2SO_4 solution facilitate current transport across the electrode chambers and removes oxygen and hydrogen gas produced at the anode and cathode, respectively. To promote a good mass transfer from process stream to membrane surface, turbulent flow inside the spacers between membranes is provoked by adding *nets* (see Figure 3.5.18) to the spacers or constructing channels that cause the flow to take a longer path along the membrane surface (tortuous path).

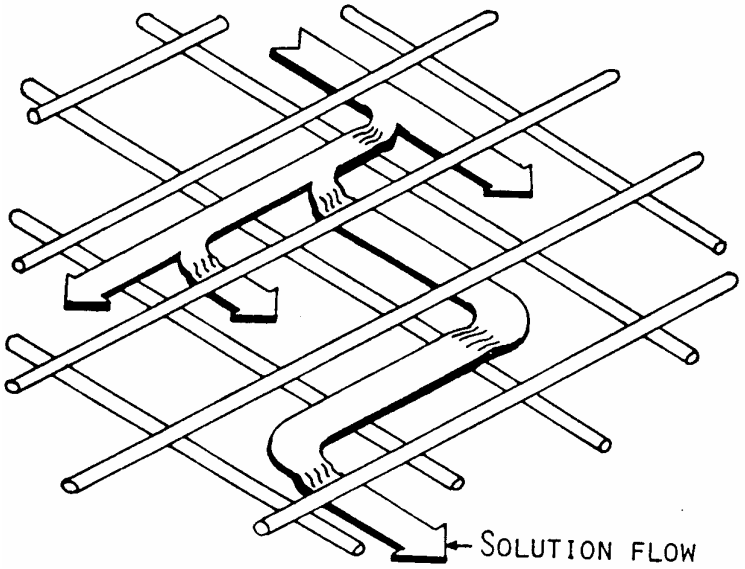

Figure 3.5.18. Solution flow in net-spacer.

The conventional ED-module as shown in Figure 3.5.11 can be combined with means for reversing the direction of the electrical current as well as interchanging the inlet and outlet of concentrate and diluate – leading to a process called Electrodialysis Reversal (EDR). By this configuration it is possible to diminish the unwanted effects of fouling as the large charged particles that, in one interval, fouled the diluate chambers are lifted off the membrane and flushed way with the

concentrate stream in the next interval. Typically, there would be 2-4 current reversals per hour depending on the liquid to be desalted. Furthermore, the anti-fouling effect can be enhanced by blowing gas into the diluate chambers at regular intervals to create high turbulence.

Modules for electrodialysis with bipolar membranes (EDBM) can be configured as either three-compartment cell, two-compartment anion cell or two-compartment cation cell, see Figure 3.5.19. In the three-compartment cell both the corresponding acid and base are generated from a solution of salt, e.g. citric acid and potassium hydroxide from potassium citrate as shown in the example.

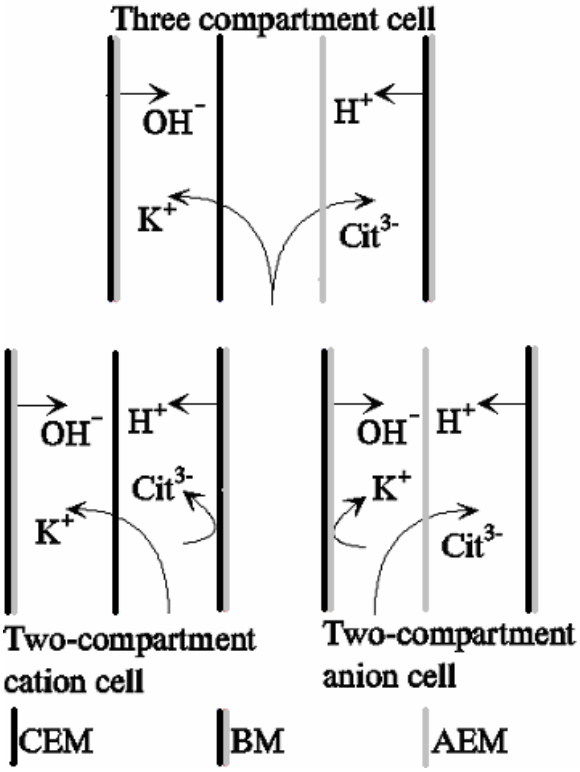

Figure 3.5.19. Different configurations of EDBM.

The two-compartment cation cell produces a pure base stream and lowers the pH of the feed stream at the same time, whereas the two-compartment anion cell produces a pure acid stream and increases pH of the feed stream.

There are other module configurations, as it will be shown in the experimental section of this thesis, but the above mentioned units covers the majority of commercial applications - yet!

3.5.3.8 Applications

Many applications of electrodialysis exist and even more are possible. Electrodialysis for table salt production has been well established in Japan for almost 40 years and desalination of sea water or brackish water are being employed in different places around the world, where ground water is sparse. Industrially, electrodialysis is mainly utilized for recovering ionic components from waste streams in order to obey environmental legislation and recycle valuable components. Electrodialysis is also utilized in food industry for removal of salts and organic acids. However, to ensure further exploitation of electrodialysis within areas of chemicals and pharmaceuticals, food, industrial & municipal effluent treatment etc. slight modifications in the conventional processes as well as extensive R&D work is required.

The following are some new business opportunities in ED (including EDBM) separation process (G. Srikanth, http://www.tifac.org.in/news/memb.htm, 2002):

- De-ionized water from conductive spacers
- Radioactive wastewater treatment by using radiation resistant membranes
- Deacidification of fruit juices
- Heavy metal recovery
- Recovery of organic acids from salts
- pH control without adding acid or base
- Regeneration of ion-exchange resins with improved process design
- Acid recovery from etching baths etc.

An example of how a slight modification of conventional ED can lead to a new process can be in the case of salt metathesis: A reaction of two salts to give two new salts with changed ion pairs, e.g.:

Sodium Gluconate + Hydrochloric acid -------> Sodium Chloride + Gluconic acid

Diluate 1 Diluate 2 Concentrate 1 Concentrate 2

Salt metathesis can be achieved through a special electrodialysis process in which two diluate process streams and two concentrate process streams are used. Except for the introduction of an extra set of flow circuits the module configuration is the same as in conventional ED with alternating cation and anion exchange membranes. The repeated unit only now contains four compartments.

More extensive research can lead to alternative applications of electrodialysis, e.g. the process described in this thesis, paragraph 5.2.

4

FERMENTATION

4.1 Screening

Screenings were performed to identify bacterial strains suitable for converting sugars of the wheat straw hemicellulose to lactic acid and to determine the best lactic acid producers on a feed of hemicellulose hydrolysate and brown juice.

4.1.1 Materials and methods

4.1.1.1 Microorganisms and cultivation

Lactic acid bacteria were selected based on literature studies and obtained from Chr. Hansen laboratories. One LAB strain, Lactobacillus salivarius, was obtained from Centre for Agro-Industrial Biotechnology, University of Southern Denmark where it was isolated from brown juice. Different thermophilic bacterial strains isolated from hot springs in Iceland by Sonne-Hansen et al. (Sonne-Hansen *et al.* 1993) were also evaluated for production of lactic acid. Table 4.1.1 lists the studied bacteria and classification of the LAB according to mode of fermentation is shown in
Table 4.1.2 Taxonomically, the thermophilic strains are most similar to Clostridium thermohydrosulfuricum (Sonne-Hansen *et al.* 1993).
.

Table 4.1.1. List of bacteria used in screenings.

Strain	Type
I01R2	Thermophilic strain
I06R1	Thermophilic strain
I07R2	Thermophilic strain
I08R1	Thermophilic strain
I14R1	Thermophilic strain
I24R1	Thermophilic strain
I25R1	Thermophilic strain
I72R1	Thermophilic strain
I72R2	Thermophilic strain
I73R1	Thermophilic strain
I78R1	Thermophilic strain
I78R2	Thermophilic strain
CHCC 2102	Lactobacillus plantarum
CHCC 2238	Lactobacillus plantarum
CHCC 2365	Lactobacillus plantarum
CHCC 3511	Lactobacillus plantarum
CHCC 2355	Lactobacillus pentosus
CHCC 2097	Lactobacillus brevis
CHCC 4006	Lactobacillus sake
CHCC 2133	Streptococcus thermophilus
CHCC 2328	Streptococcus thermophilus
CHCC 2354	Pediococcus pentosaceus
BC 1001	Lactobacillus salivarius

Table 4.1.2. Classification of the LAB according to fermentation mode

Strain	Fermentation mode
CHCC 2102	Facultative heterofermentative
CHCC 2238	Facultative heterofermentative
CHCC 2365	Facultative heterofermentative
CHCC 3511	Facultative heterofermentative
CHCC 2355	Facultative heterofermentative
CHCC 2097	Obligately heterofermentative
CHCC 4006	Facultative heterofermentative
CHCC 2133	Homofermentative
CHCC 2328	Homofermentative
CHCC 2354	Homofermentative
BC 1001	Obligately Homofermentative

As described in Paper I the LAB were grown in MRS media for 5 h at their optimum temperature, which is 40 °C for *Lb. Salivarius*, 37 °C for *Lb. pentosus* and *Str.*

thermophilus, and 30 °C for the rest of the LAB before being used as inoculum. The thermophilic bacteria were grown in BA media as described by Angelidaki et al. (Angelidaki *et al.* 1990) at 70 °C for more that 24 h before used as inoculum.
All experiments were performed as batch fermentations at strictly anaerobic conditions with 10 ml sterile liquid medium in 20 ml tubes, using 5% (v/v) inoculum where nothing else is stated.

4.1.1.2 Substrates

Hemicellulose hydrolysate from wheat straw was prepared by wet oxidation with low oxygen pressure (WOL) in a loop-reactor at Department of Plant Biology and Biogeochemistry, Risø National Laboratory as previously described in (Paper II). The hemicellulose hydrolysate was dispersed into test tubes, which were gassed (N_2 + CO_2), sealed and autoclaved. Enzymatic treatment was applied in order to release the fermentable sugars, using either a commercial enzyme product (Celluclast®, Novo Nordisk) or an enzyme product produced at Risø National Laboratory. The enzymatic hydrolysis with Celluclast® was performed by aseptically adding 1% (v/v) to the substrate. The mixture was incubated for 4 hours at 40°C and pH 4.4 before inoculated with the particular LAB.
Brown juice (produced from pressing of green biomass at 80 °C) with a dry matter content of 41.5% was received from Centre for Agro-Industrial Biotechnology, University of Southern Denmark. Depending on the nature of the experiment concentrated brown juice was either diluted with water or autoclaved and aseptically added to the hemicellulose test tubes to obtain a solution with 2 wt-% brown juice. The brown juice/water mixture was dispersed into test tubes, which were gassed (N_2 + CO_2), sealed and autoclaved. A buffer (K_2HPO_4) was added in a concentration of 16 g/l when fermentations were performed with a combination of hemicellulose hydrolysate and brown juice.

4.1.1.3 Analytical techniques

Dry matter content was determined by drying samples in a laboratory oven at 105 °C until constant weight.

Growth rates were monitored by optical density (OD_{578}) measurements using a Spectronic 301 (Milton Ray) spectrophotometer at a wavelength of 578 nm.

Samples taken during fermentation were diluted by a factor of 10 with 4 mM H_2SO_4 before being cooled to 0°C and centrifuged using an IEC Micromax centrifuge at 10.000 rpm for 10 min. to remove solids. The supernatant was stored at –18°C until analysis. Analysis was performed at 35°C with HPLC equipped with an Aminex HPX-87H column

(Biorad) using 4 mM H_2SO_4 as eluent at a flow rate of 0.6 ml/min. Sugars and ethanol were detected on a Waters 410 Differential Refractometer and carboxylic acids were detected on a Waters 486 tunable absorbance detector at 210 nm. Waters Millennium Chromatography Manager Software was used for quantification.

4.1.2 Results and discussion

4.1.2.1 Growth on model medium

An important trait of the lactic acid producing bacteria is the ability to utilize xylose as a substrate, as this is the most abundant sugar component of hemicellulose (see chapter 3.2.1.) An initial and simple way to determine the growth is by monitoring the optical density of the broth during fermentation. Figure 4.1.1 shows how the thermophilic cultures grow on an initial xylose concentration of 10 g/l. The three strains I01R2, I14R1, and I73R1 have the highest growth rate, but turned out to produce only 1-2 g/l of lactic acid from 10 g/l of xylose. The very low yield of lactic acid makes these thermophilic strains uninteresting for commercial lactic acid production.

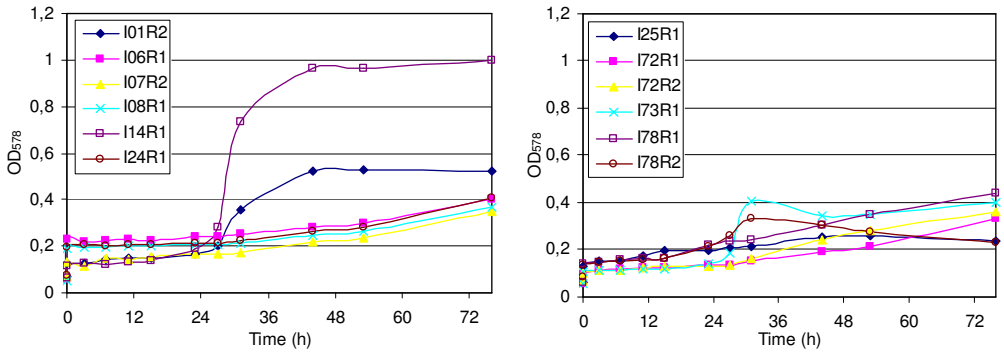

Figure 4.1.1. OD578 measurements during xylose fermentations using the thermophilic bacteria.

All of the selected LAB strains have the ability to grow well on xylose (10 g/l), see Figure 4.1.2. The optical density was measured throughout the fermentations as shown in but for clarity only the values before and after inoculation with 10 vol-% of the given bacteria, as well as after 71 hours are plotted.

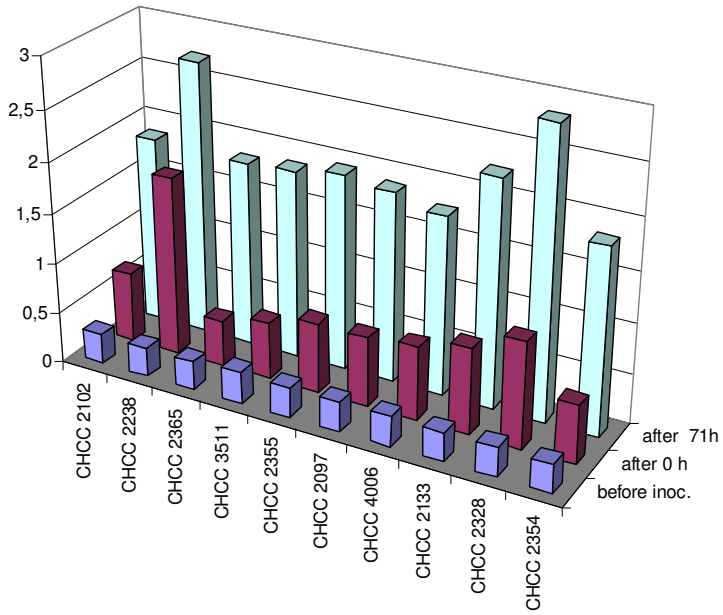

Figure 4.1.2. OD_{578} measured before and after inoculation , as well as after 71 hours fermentation on MRS medium supplemented with 10 g/l of xylose.

Lb. salivarius was not available at the time of these experiments and was only tested in connection with later brown juice fermentations.

Of the tested LAB, *Lb. pentosus (CHCC 2355)* and *Lb. brevis (CHCC)* had the highest growth rate on xylose (data not shown), and were chosen for further experiments with hemicellulose hydrolysate (see Garde *et al.* 2002).

4.1.2.2 Growth on hemicellulose/brown juice

Hemicellulose hydrolysate from wheat straw does not support growth of lactic acid bacteria without addition of extra growth factors. Therefore, it is important to have a cheap source of essential amino acids and vitamins to be able to produce lactic acid from hemicellulose in a cost effective manner. Andersen and Kiel have demonstrated the excellent properties of brown juice as substrate for lactic acid fermentation without additional growth factors (Kiel and Andersen 2000). In the present study it is investigated whether the two substrates are suited for lactic acid fermentation when mixed.

The quick and easy method of spectrophotometry is not applicable for monitoring growth in hemicellulose hydrolysate and brown juice because of the high light absorption by the strongly colored media. Therefore, the more complex HPLC method is used for the initial determination of the suitability of brown juice as basis for

fermentation with selected LAB strains. Figure 4.1.3 shows the concentration of lactic acid and residual sugars following a 72 hour fermentation of 2% brown juice by the different LAB strains. The initial sugar concentrations before inoculation are given in Table 4.1.3.

Table 4.1.3. Initial sugar concentrations in 2% brown juice.

Sugar concentration (g/l)		
Glucose	Fructose	Sucrose
2.0	4.2	1.2

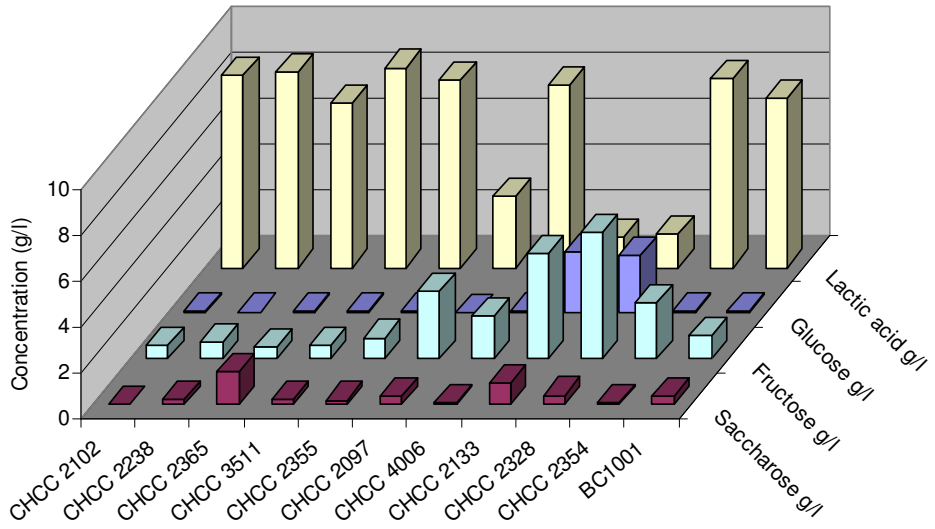

Figure 4.1.3. Lactic acid production by the different LAB strains after 72 hours fermentation on 2% Brown juice. (Saccharose = sucrose).

Before inoculation the pH of the 2% brown juice was measured to 5.6 but as lactic acid is being produced during the fermentation pH drops. In Table 4.1.4 the final pH values in the different cultures are given.

Table 4.1.4. Final pH after fermentation of 2% brown juice.

Strain	pH
CHCC 2102	3,14
CHCC 2238	3,56
CHCC 2365	3,39
CHCC 3511	3,43
CHCC 2355	3,42
CHCC 2097	4,10
CHCC 4006	3,43
CHCC 2133	4,65
CHCC 2328	4,51
CHCC 2354	3,41
BC 1001	ND

Production of lactic acid from brown juice by the two *Str. thermophilus* strains was very limited, which is also reflected in the small change in pH, see Table 4.1.4. The fermentations were done without pH control, which could cause some sensitive strains to slow down and stop production of lactic acid before depletion of substrate. To check if this was the case with *Str. thermophilus* a buffer (K_2HPO_4) was added to the 2% brown juice, giving a starting pH of 6.38. However, no improvement was seen in lactic acid production and therefore the two *Str. thermophilus* strains were omitted in subsequent experiments. Despite the fact that *Lb. brevis* only produced small amounts of lactic acid from brown juice, it was picked out for further investigation because of the unique results on hemicellulose when combined with *Lb. pentosus* (Garde *et al.* 2002).

The selected LAB, except for *Lb. Salivarius BC 1001,* which was difficult to keep active, were inoculated on 2% brown juice and the production of lactic acid and consumption of sugars were monitored. Figure 4.1.4-6 shows the concentration of glucose, fructose and sucrose as the different LAB assimilates them during fermentation of 2 % brown juice. Except for *Lb. brevis CHCC 2097*, the LAB almost completely utilized the three major sugar components. The reason why fructose assimilation stops at around 1 g/l for most of the LAB is not clear, but it could be due to an unknown component merging with the fructose peak in the HPLC analysis, causing a fructose detection when there is none. *Ped. pentosaceus CHCC 2354* had a long lag phase and exhibited together with *Lb. sake CHCC 4006* a low fructose consumption rate.

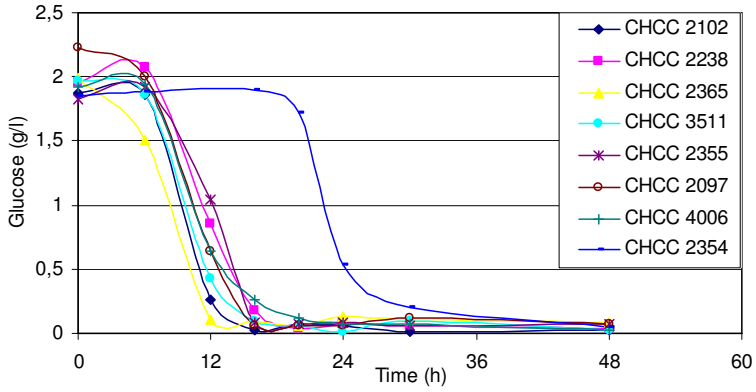

Figure 4.1.4. Concentration of glucose during fermentation of 2% brown juice by LAB.

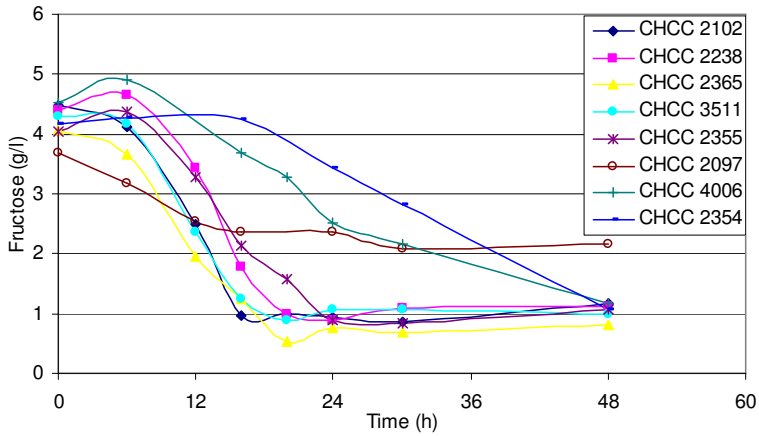

Figure 4.1.5. Concentration of fructose during fermentation of 2% brown juice by LAB.

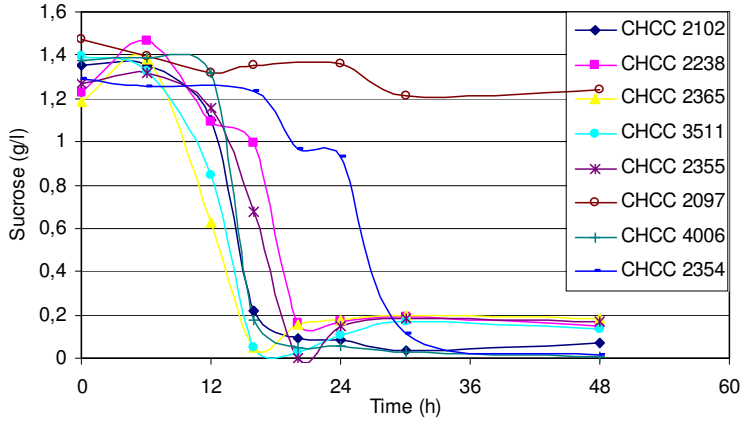

Figure 4.1.6. Concentration of sucrose during fermentation of 2% brown juice by LAB.

The final concentration of lactic acid was just above 3 g/l in the broth containing *Lb. brevis CHCC 2097*, while between 7 and 8 g/l were reached by the other strains, as shown in Figure 4.1.7.

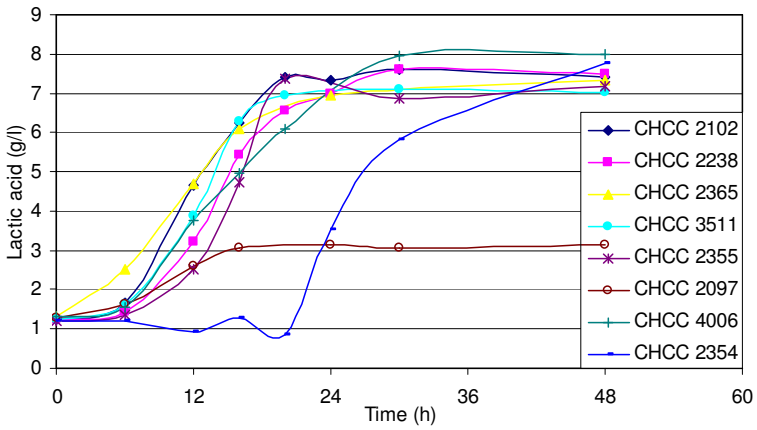

Figure 4.1.7. Production of lactic acid during fermentation of 2% brown juice by LAB.

Having verified that the major sugar components of the brown juice were assimilated by the LAB strains, they were inoculated on two different mixtures of brown juice and hemicellulose hydrolysate. Figure 4.1.8 and Figure 4.1.9 shows the production of lactic acid from a combination of brown juice and hemicellulose treated with “Risø enzymes” (WOLR) and Celluclast® (WOLC), respectively.

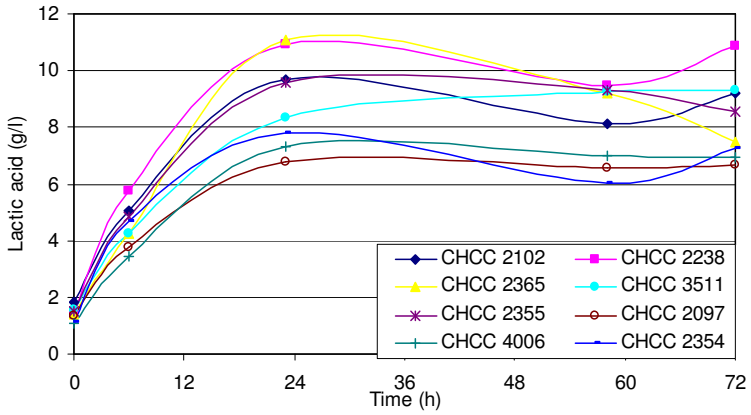

Figure 4.1.8. Production of lactic acid during fermentation of a mixture of 2% brown juice and hemicellulose treated with an enzyme product from Risø National Laboratories.

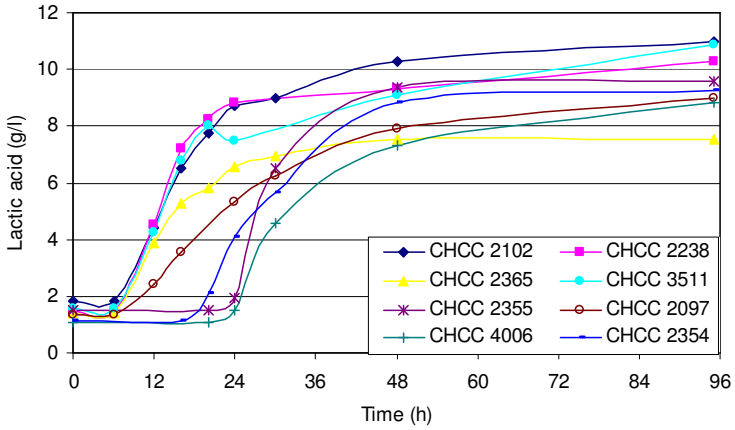

Figure 4.1.9. Production of lactic acid during fermentation of a mixture of 2% brown juice and hemicellulose treated with Celluclast®.

The concentrations of fermentable sugars in the hemicellulose fraction correspond to an extra lactic acid production of approximately 7-8 g/l. The final concentration of lactic acid in both types of broth ranges from 7-11 g/l, which is lower than the theoretical maximum value of around 14 g/l. To produce lactic acid amounts near the theoretical value the LAB must be able to utilize a whole range of different substrates in an optimal way. The WOLC mixture contains glucose, fructose, sucrose, xylose, arabinose, xylulose and to a minor extent fructans, xylobiose and different dicarboxylic acids, which are all potential substrates for conversion into lactic acid. To achieve full conversion of the substrates a combination of two or more bacteria might be the solution, like it was the case with the optimal culture on pure hemicellulose hydrolysate. Unfortunately, it was not possible to quantify all the substrates on the used HPLC column due to overlapping peaks, so attempts were not made to identify an optimal combination of LAB strains.
However, in comparison with the pure 2% brown juice, *Lb. brevis CHCC 2097* showed the largest increase, about 6 g/l, in lactic acid production on the combined medium WOLR. *Lb. pentosus* CHCC 2355, also had relatively high production of lactic acid on both pure 2% brown juice, WOLR, and WOLC. So, on this background, and in the light of the results obtained on pure hemicellulose hydrolysate a combination of these two strains could serve as a first guess on an optimal culture for production of lactic acid from a mixture of hemicellulose and brown juice.

When it comes to choosing the best kind of enzymatic treatment of the hemicellulose, the performed experiments cannot give a straight answer. Both enzyme products release fermentable sugars from the hemicellulose and there is no marked difference in the lactic acid production from the two types of medium. The choice therefore depends on treatment cost, which must be determined on the basis of an economic evaluation.

Experiments were performed to establish if addition of MRS-components would have a noticeable effect on lactic acid production from brown juice. From Figure 4.1.10 it can be seen that nearly the same amount of lactic acid is produced from the brown juice whether the MRS-components are present or not. It is hereby evident that the brown juice covers all the bacteria's need in respect to important growth factors.

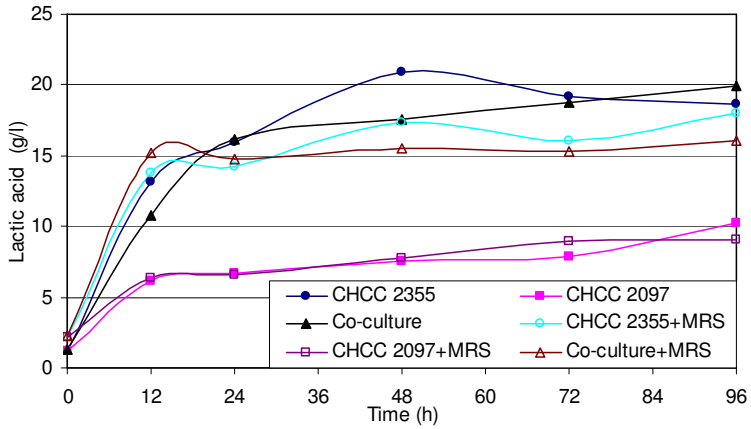

Figure 4.1.10. Lactic acid production by *Lb. pentosus*, *Lb. brevis CHCC 2097* and a co-culture of the two on 5% brown juice with and without addition of MRS components.

In the fermentations without MRS-components no buffer was added and still the concentration of lactic acid increase to around 20 g/l, which suggest that the brown juice by it self, possesses some buffer capacity.

4.1.3 Conclusion

It has been shown that by combining hemicellulose hydrolysate with brown juice, expensive MRS-components, that otherwise is a necessity in LAB fermentation of hemicellulose, can be omitted. However, a negative aspect of combining the two media types is a more complex substrate composition that makes higher demands on the LAB's ability to utilize different sugars. This problem could be solved by combining two or more strains having different substrate uptake patterns.

4.2 Paper I

ELSEVIER

Bioresource Technology 81 (2002) 217–223

BIORESOURCE TECHNOLOGY

Lactic acid production from wheat straw hemicellulose hydrolysate by *Lactobacillus pentosus* and *Lactobacillus brevis*

Arvid Garde [a], Gunnar Jonsson [a], Anette S. Schmidt [b], Birgitte K. Ahring [c,*]

[a] *Department of Chemical Engineering, Building 229, Technical University of Denmark, DK-2800 Lyngby, Denmark*
[b] *Department of Plant Biology and Biogeochemistry, Risø National Laboratory, P.O. Box 49, DK-4000, Roskilde, Denmark*
[c] *The Anaerobic Microbiology/Biotechnology Research Group, Department of Biotechnology, Building 227, Technical University of Denmark, DK-2800 Lyngby, Denmark*

Received 22 March 2001; received in revised form 21 July 2001; accepted 28 July 2001

Abstract

Lactic acid production by *Lactobacillus brevis* and *Lactobacillus pentosus* on a hemicellulose hydrolysate (HH) of wet-oxidized wheat straw was evaluated. The potential of 11–12 g/l fermentable sugars was released from the HH through either enzymatic or acidic pretreatment. Fermentation of added xylose in untreated HH after wet-oxidation, showed no inhibition on the lactic acid production by either *Lb. pentosus* or *Lb. brevis*. *Lb. pentosus* produced lactate corresponding to 88% of the theoretical maximum yield regardless of the hydrolysis method, whereas *Lb. brevis* produced 51% and 61% of the theoretical maximum yield after enzymatic, or acid treatment of HH, respectively. Individually, neither of the two strains were able to fully utilize the relatively broad spectra of sugars released by the acid and enzyme treatments; however, lactic acid production increased to 95% of the theoretical maximum yield by co-inoculation of both strains. Xylulose was the main sugar released after enzymatic treatment of HH with Celluclast®. *Lb. brevis* was able to degrade xylobiose, but was unable to assimilate xylulose, whereas *Lb. pentosus* was able to assimilate xylulose but unable to degrade xylobiose.

Keywords: Lactic acid; Wheat straw; Hemicellulose; Fermentation; *Lactobacillus brevis*; *Lactobacillus pentosus*

1. Introduction

Lignocellulosic material from agricultural waste such as wheat straw represents an abundant renewable energy source for bioconversion processes as well as a raw material for the paper and pulp industry. According to FAO, 87 and 184 million tons of wheat were produced in 2000 in North America and Europe, respectively (FAO, 2000). The average yield of straw is 1.3–1.4 kg per kg of grain, which results in a considerable amount of surplus straw (Montane et al., 1998; Wong, 1997). Before straw can be utilized a pretreatment is necessary to break down the lignocellulose into the three major polymeric constituents: cellulose, hemicellulose and lignin, where the lignin binds the cellulose and hemicellulose together in the vascular tissue of the plant. Wheat straw contains about 35–40% cellulose and 30–35% hemicellulose and this relatively high amount of hemicellulose stresses the need for utilizing the hemicellulose as well as the cellulose fraction (Sun et al., 1996).

Different pretreatment methods, such as steam explosion (Montane et al., 1998; Vlasenko et al., 1997) and wet-oxidation (Abbi et al., 1996; Bjerre et al., 1996; Curreli et al., 1997; Dominguez et al., 1997; Martinez et al., 1995; Nielsen et al., 1993; Schmidt and Thomsen, 1998; Vlasenko et al., 1997) have been proposed for the fractionation of lignocellulose. Depending on the process conditions, most of the hemicellulose and lignin degradation products will be dissolved and the cellulose will be recovered in the solid fraction. The cellulose can be used for paper production or further hydrolyzed to readily usable carbon (glucose) and energy in a fermentation process. The hemicellulose fraction can also be hydrolyzed and used for fermentation purposes, but the usage of the hemicellulose fraction is more complicated due to the fact that xylose, which is the dominating monosaccharide released, is difficult to ferment (Lee, 1997). Another problem in utilizing hydrolysate from lignocellulosic material is the possible presence of microbial inhibitors formed during the relatively harsh

* Corresponding author. Tel.: +45-45-251-566; fax: +45-45-932-850.
E-mail address: birgitte.k.ahring@biocentrum.dtu.dk (B.K. Ahring).

0960-8524/02/$ - see front matter
PII: S0960-8524(01)00135-3

pretreatment. Examples of these inhibitors include acetic acid, furfural, 5-hydroxymethyl furfural and levulinic acid (Olsson and Hahn-Hägerdal, 1996).

The worldwide production of L-lactic acid through fermentation was 60,000 tons in 1998 (McCoy, 1998). Lactic acid is an important chemical used in a wide variety of applications, being used primarily in the food industry as an acidulent, preservative, and for production of emulsifying agents. Other applications of lactic acid are for cosmetics, pharmaceuticals, metal etching or textile-finishing operations. But one of the biggest potentials is as a precursor for biodegradable polylactic acid (PLA) production. By co-polymerization with other functional monomers specific properties can be obtained, making it possibly to substitute many existing petroleum-derived polymer products (Datta, 1995).

In this study, hemicellulose hydrolysate (HH) from wheat straw was used as starting material for production of lactic acid by the lactic acid bacteria *Lactobacillus brevis* and *Lactobacillus pentosus*. One important parameter in sustaining an economically viable production of lactic acid is the interaction between feedstock and microorganism. The bacteria must be able to convert all of the available carbohydrates to lactic acid at near theoretical yield. One of the main objectives of this study was to investigate whether *Lb. brevis* or *Lb. pentosus* could convert HH effectively to lactic acid.

2. Methods

2.1. Microorganisms

The two *Lactobacillae* strains *Lb. pentosus* CHCC 2355 and *Lb. brevis* CHCC 2097 were kindly provided by Chr. Hansen A/S, Hørsholm, Denmark. *Lb. pentosus* and *Lb. brevis* showed high yields on HH in a previous screening of a large number of Lactobacillae and thermophilic anaerobes (data not shown).

2.2. Cultivation

The bacteria were maintained on de Man, Rogosa and Sharpe (MRS) medium as described in Bergey's Manual of Systematic Bacteriology (Kandler and Weiss, 1986) supplemented with 10 g/l glucose and 10 g/l xylose. Further components of the MRS media were as follows: 10 g/l casein peptone, 10 g/l meat extract, 5 g/l yeast extract, 1 g/l Tween 80, 2 g/l K_2HPO_4, 5 g/l sodium acetate, 2 g/l diammonium citrate, 0.2 g/l $MgSO_4 \cdot 7H_2O$ and 0.05 g/l $MnSO_4 \cdot H_2O$. The bacteria were transferred at least every four weeks to a fresh medium.

All experiments were performed as batch fermentations under strictly anaerobic conditions with 10 ml liquid medium in 20 ml tubes (26 ml total volume), using 10% (v/v) inoculum. *Lb. brevis* and *Lb. pentosus* were incubated at their optimum temperatures of 30 and 37 °C, respectively. A temperature of 33.5 °C was used for co-cultivation. All cultivations were carried out as triplicate experiments and all variations were less that 10%.

2.3. Substrates

HH was prepared as previously described (Schmidt and Thomsen, 1998). In all experiments, the hydrolysate was supplemented with all other components of the MRS media except for the primary carbon source. Acidic or enzymatic treatment of the HH was applied in order to release the fermentable sugars.

The acidic hydrolysis was carried out by addition of sulfuric acid to the hydrolysate from a 98% (w/w) sulfuric acid solution corresponding to 4% (w/w) and applying 100 °C for 2 h in a closed container. After cooling to room temperature, the pH was adjusted to 6.5 by addition of 10 M NaOH. A concentrated solution containing the MRS components was autoclaved at 121 °C for 20 min and added to the treated hydrolysate.

Due to both high cellulolytic and hemicellulolytic activities the enzymatic hydrolysis was performed with the enzyme preparation Celluclast®, kindly provided by Novo Nordisk A/S, Denmark. HH with MRS components was autoclaved at 121 °C for 20 min. After cooling, the enzyme product was added in a concentration of 1% (v/v). The mixture was incubated for 24 h at 40 °C and afterwards stored at 4 °C until required.

2.4. Analytical techniques

Samples taken during fermentation were centrifuged using an IEC Micromax centrifuge at 10,000 rpm for 10 min to remove solids. The supernatant was acidified to pH about 1 with 98% (w/w) H_2SO_4 and filtered through a 0.2 μm filter. Whenever hemicellulose hydrolysate was used as fermentation medium, the samples were deionized *prior* to acidification using an ion-exchange resin, Dowex MR-12 (Fluka), followed by centrifugation before filtration. Samples were stored at −18 °C until analysis. Analysis was performed at 35 °C with HPLC equipped with an Aminex HPX-87H column (Biorad) using 4 mM H_2SO_4 as eluent at a flow rate of 0.6 ml/min. Sugars and ethanol were detected on a Waters 410 differential refractometer and carboxylic acids were detected on a Waters 486 tunable absorbance detector at 210 nm. Waters Millennium Chromatography Manager software was used for quantification.

3. Results

3.1. Inhibition

Possible inhibitory effects of untreated HH on production of lactic acid were examined. Hydrolysate from wet-oxidized wheat straw was diluted with distilled water to obtain different HH concentrations in the range from 0 to 100%. As HH was not treated with acid or enzymes prior to fermentation, 20 g/l of xylose was added as carbon source, before inoculation with *Lb. pentosus* and *Lb. brevis*.

The production of lactic acid by *Lb. pentosus* and *Lb. brevis* at the different HH concentrations is shown in Fig. 1. After 72 h of fermentation, the concentration of lactic acid was relatively independent of the initial HH contents, with an increase in lactic acid concentration to approximately 9 g/l by *Lb. pentosus* and 10 g/l by *Lb. brevis*.

3.2. Growth experiments

Before the undiluted HH was used as an actual carbon source for lactic acid fermentation, it was subjected to either acidic or enzymatic hydrolysis. The contents of glucose, xylose, xylulose, and arabinose before and after hydrolysis are shown in Table 1. Nearly the same amounts of glucose and arabinose were released using the two methods, but the xylose concentration increased only slightly to 0.8 g/l following the enzymatic treatment, whereas acidic treatment resulted in 10 times higher xylose concentration. Instead of xylose the enzymatic treatment resulted in release of xylulose.

Cultivation of *Lb. brevis* CHCC 2097 and *Lb. pentosus* CHCC 2355 on MRS model media with addition of glucose and/or xylose showed high lactic acid yields on the pure sugars but considerable lower yields on a mixture of the two sugars (Table 2). *Lb. brevis* CHCC 2097 showed a final lactic acid production of 19.0 g/l from 22.6 g/l glucose and 11.5 g/l lactic acid from 20.9 g/l xylose.

Lb. pentosus and *Lb. brevis* were both cultivated on acidic and enzymatic pretreated hydrolysate and the concentrations of glucose, xylose, arabinose, and lactic acid were monitored. The concentrations of xylose and lactic acid during fermentation are shown in Fig. 2(a) and (b) for *Lb. pentosus* and *Lb. brevis*, respectively. Glucose, which was present in both the acid and enzyme hydrolysate in concentrations of 1.8–2.4 g/l, was depleted within 12 h by *Lb. pentosus* and within 24 h by *Lb. brevis*. From an initial concentration of approximately 1 g/l, arabinose was depleted within 12 h by both bacteria and on both media. When fermentation was conducted using *Lb. pentosus* the final lactic acid production reached 6.6 and 6.7 g/l for enzymatic and acidic hydrolyzed HH, respectively. *Lb. brevis* produced more lactic acid from the acid treated HH than from enzyme

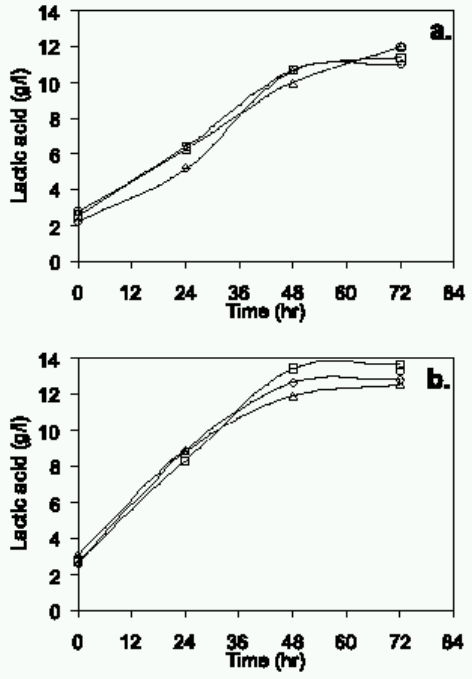

Fig. 1. *Lb. pentosus* (a) and *Lb. brevis* (b) cultivated on increasing concentrations of HH with 20 g/l xylose added as carbon source. (◇) – 0%, (□) – 30%, (Δ) – 50% and (○) – 100%.

Table 1
Monomeric sugar content in HH before and after acidic hydrolysis using 4% v/v H_2SO_4 at 100 °C for 2 h or enzymatic hydrolysis using 1% v/v Celluclast® at 40 °C for 24 h

Treatment	g/l of sugar			
	Glucose	Xylose	Xylulose	Arabinose
None	0.2	0.3	0.0	0.2
Enzymatic	1.9	0.8	7.4	0.7
Acidic	2.0	8.1	0.0	1.1

Table 2
Lactic acid yields from fermentation of treated HH and MRS model medium by *Lb. pentosus* and *Lb.brevis*

Medium	Yield	
	Lb. pentosus	*Lb. brevis*
Enzymatic treated HH	0.88	0.51
Acidic treated HH	0.90	0.61
MRS + 20 g/l glucose	0.93	0.89
MRS + 20 g/l xylose	1.13	0.92
MRS + 10 g/l glucose + 10 g/l xylose	0.69	0.56

The yields are based on pentose assimilation through the PK pathway and hexose assimilation through the EMP pathway. Refer to Section 4 for a detailed description of how yield calculations were performed.

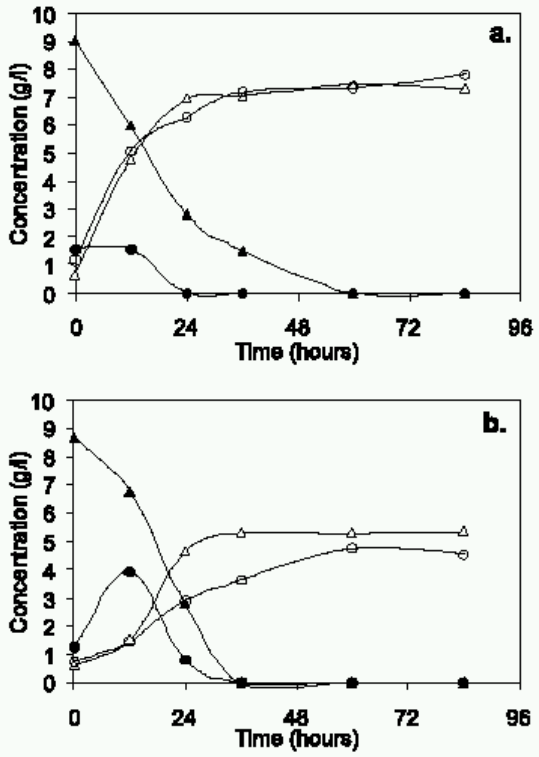

Fig. 2. *Lb. pentosus* (a) and *Lb. brevis* (b) cultivated on HH pretreated with either enzyme (1% v/v Celluclast® at 40 °C for 24 h) or acid (4% v/v H_2SO_4 at 100 °C for 2 h). Curves indicates: (○) – lactic acid, enzyme pretreated HH, (Δ) – lactic acid, acid pretreated HH, (●) – xylose, enzyme pretreated HH, (▲) – xylose, acid pretreated HH.

treated HH, but considerable less than *Lb. pentosus* (about 4.0–4.7 g/l). *Lb. pentosus* had nearly the same yield on both acidic and enzymatic treated HH, accounting for a little higher yield compared to that of the MRS media with the same concentration of glucose and xylose. The yields from acidic and enzymatic treated HH were somewhat lower when using *Lb. brevis* (Table 2).

The two strains were co-cultivated on enzymatic hydrolyzed HH (see Fig. 3) giving a yield of 95% with consumption of practically all sugars.

4. Discussion

There was no significant inhibitory effect of the hydrolysate on production of lactic acid from xylose. Approximately the same amount (9–10 g/l) of lactic acid was produced in pure MRS broth supplemented with 20 g/l xylose and in 100% HH–MRS supplemented with 20 g/l xylose. Several other researchers have reported problems with microbial inhibition when utilizing hydrolysate from lignocellulosic material (Perttunen et al., 1996; Preziosi-Belloy et al., 1997). The fact that inhibition was not encountered in this study was probably due to the dilute nature of the hydrolysate used and the fact that during wet-oxidation very low amounts of toxic compounds such as furfural and 5-hydroxymethyl-furfural are produced (Ahring et al., 1996; Schmidt and Thomsen, 1998).

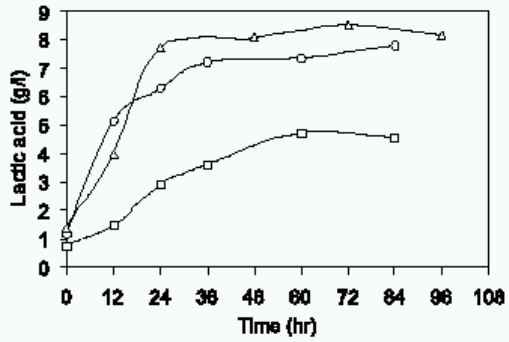

Fig. 3. Production of lactic acid from enzymatically (1% v/v Celluclast® at 40 °C for 24 h) treated HH by pure *Lb. pentosus* culture (○), pure *Lb. brevis* culture (□) and mixed culture of *Lb. pentosus* and *Lb. brevis* (Δ).

The two major pathways for assimilation of glucose and xylose in lactic acid bacteria (LAB) are the Embden–Mayerhof–Parnas (EMP) pathway and the pentose phosphoketolase (PK) pathway, simplified on the left and right side of Fig. 4, respectively. Homofermentative LAB use the EMP pathway to assimilate hexoses with lactate being the sole product, while heterofermentative

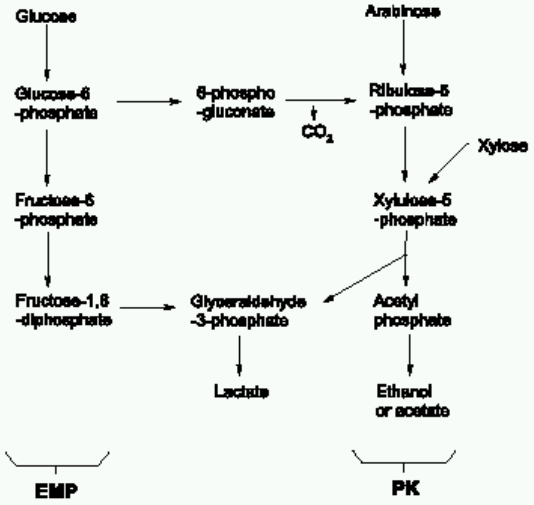

Fig. 4. Simplified illustration of EMP pathway and PK pathway in the left and right sides, respectively.

LAB use the PK pathway, generating a mixture of lactate, acetate, ethanol, and CO_2 from hexoses and pentoses (Chaillou et al., 1998).

Lb. pentosus belongs to the facultatively heterofermentative Lactobacillae that are characterized by their ability to ferment hexoses through the EMP pathway like homofermenters, and use the PK pathway for pentose assimilation (Chaillou et al., 1998). This means that *Lb. pentosus* under optimal conditions will generate 2 mole lactate/mole glucose and 1 mole lactate + 1 mole acetate or ethanol/mole xylose. In the literature, *Lb. brevis* is often listed as part of the obligate heterofermentative *Lactobacillae* (Axelsson, 1993). This term indicates a lack of key enzymes (e.g. fructose-1,6-diphosphate aldolase) of the EMP pathway (Kandler and Weiss, 1986). In this case, glucose enters the PK pathway where it is decarboxylated to ribulose-5-phosphate, resulting in 1 lactate + 1 CO_2 + 1 acetate or ethanol/glucose (Fig. 4).

The high amount of lactic acid produced by *Lb. brevis* CHCC 2097 from glucose in model media could not have been achieved if glucose was metabolized using the PK pathway, where only 1 mole lactate/mole glucose is generated. On the other hand, if the EMP pathway were operative, the results obtained correspond to a yield of 89% (Table 2), which is a reasonable lactic acid yield for glucose fermentation in homofermentative *Lactobacillae*. Compared to a yield of 92% on xylose, these observations indicate activity of both the PK and EMP pathway in *Lb. brevis* CHCC 2097 and should be termed facultatively heterofermentative and not obligate heterofermentative. This is in accordance with Saier et al. (1996) who reported that *Lb. brevis* possesses a complete sugar transporting phosphotransferase system (PTS) as well as the initial enzymes of the EMP pathway induced in the presence of fructose under anaerobic conditions. Further investigations into the enzyme activities of *Lb. brevis* CHCC 2097 are, however, needed to determine whether or not the EMP pathway is operative.

The lactic acid yield from fermentation of enzymatic and acidic hydrolyzed HH (Fig. 2(a) and (b)) and from the MRS model medium with glucose and xylose is summarized in Table 2. The yield calculations are based on hexose assimilation through the EMP pathway and pentose assimilation through the PK pathway, which imply that 1 mole of lactic acid would be obtained from 1 mole of xylose (0.6 g lactic acid produced/g xylose consumed and 2 mole of lactic acid would be obtained from 1 mole of glucose (1 g lactic acid produced/g xylose consumed).

Due to a rather complex substrate composition in enzymatic hydrolyzed HH, the yields on this medium were calculated relative to the maximum theoretical yield on acidic hydrolyzed HH where the substrate almost entirely consisted of xylose, glucose and arabinose. *Lb. pentosus* showed higher yields on all substrates compared to *Lb. brevis*, and even had a value above 1 for growth on MRS medium with xylose. This high value might be explained by utilization of co-substrates from the MRS medium.

To understand the performance of the bacteria with respect to substrate utilization, it was necessary to determine whether or not substrate components besides glucose, xylose, and arabinose were assimilated. In acid hydrolyzed HH nearly all of the carbohydrate components were at the monomeric form as glucose, arabinose or xylose, but when enzyme treatment was used, the substrate composition was more complex. Fig. 5(a) and (b) show the composition of the enzyme pretreated HH substrate during fermentation by *Lb. pentosus* and *Lb. brevis*, respectively. After 12 h, *Lb. pentosus* had used almost all the substrate except xylobiose. The deficiency to utilize xylobiose indicated a lack of β-xylosidase activity, which is present in most microbial hemicellulolytic systems for hydrolysis of xylooligosaccharides to xylose (Puls and Poutanen, 1989). The shoulder on peak 1 has not been identified, but it was obviously a component that *Lb. pentosus* was able to utilize. On the other hand, *Lb. brevis* was able to degrade xylobiose to xylose, but had a deficiency in utilization of xylulose as well as the unidentified component. The enzymatic conversion of xylobiose was faster than the xylose

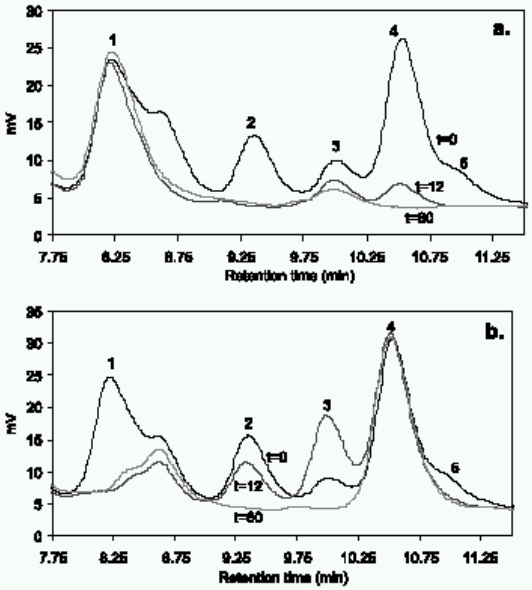

Fig. 5. Refractive index chromatograms from HPLC analysis (Aminex HPX-87H column at 35 °C, 4 mM H_2SO_4 as eluent) of during fermentation of enzymatically treated hemicellulose hydrolysate with *Lb. pentosus* (a) and *Lb. brevis* (b). The samples were taken at 0, 12 and 60 h after inoculation. Peak numbers are: 1 – xylobiose, 2 – glucose, 3 – xylose, 4 – xylulose and 5 – arabinose.

uptake, causing xylose accumulation after 12 h (Fig. 5(b), peak 3).

A xylobiose standard had the same retention time as peak 1, but due to the inability of the column to clearly separate oligomers with different degrees of polymerization, it was not certain that only the disaccharide was contained within peak 1. However, the relatively fast release of xylose indicated that the disaccharide was the major component. This was in good agreement with experiments by Kumar and Ramon (1996), where the hydrolysis patterns of xylobiose, xylotriose and xylotetraose with β-xylosidase were investigated. The degradation rate of xylobiose was found to be the fastest with 90% degradation within 6–9 h compared to 70–80% degradation of xylotriose after 16 h. As almost the entire component represented by peak 1 was converted within the first 12 h (Fig. 5(b)), this indicated that peak 1 most likely was xylobiose.

From the substrate uptake patterns of *Lb. pentosus* and *Lb. brevis* it was obvious that the potential of the medium could be better exploited if the two cultures were co-fermenting. Therefore, *Lb. pentosus* and *Lb. brevis* were co-cultivated on enzymatic treated HH as indicated in the chromatogram (Fig. 6). Virtually all substrate components were fully utilized by the bacteria. The characteristic accumulation of xylose was observed due to the fast degradation of xylobiose by *Lb. brevis* together with complete assimilation of xylulose by *Lb. pentosus*. The very small amount of xylose after enzyme hydrolysis compared to the content after acid hydrolysis (as shown in Table 1) was due to conversion of xylose to xylulose, which indicated xylose isomerase activity present in the employed enzyme preparation. In Fig. 3, the production of lactic acid from the mixed and pure cultures are compared. By combining the two cultures the complete substrate utilization led to a 7% increase in lactic acid production compared to pure *Lb. pentosus* culture, resulting in a final yield of 95%. Combination of the two strains was especially advantageous since incomplete sugar utilization could lead to increased cost for purification of the lactic acid.

In this paper we have demonstrated for the first time that complete substrate utilization from HH is of possible importance for production of environmentally friendly biodegradable plastic from lignocellulosic feedstock.

5. Conclusion

Enzymatic and acidic treated HH from wet-oxidized wheat straw was successfully used as substrate for lactic acid production by *Lb. brevis* and *Lb. pentosus* without inhibition. A lactic acid yield of 95% and complete substrate utilization were achieved with a mixed culture of *Lb. brevis* and *Lb. pentosus* on enzyme treated HH. This was a little higher than the yield of 88% on enzymatic treated HH by the pure *Lb. pentosus* culture. *Lb. brevis* was not able to utilize xylulose released from the HH during enzymatic treatment, resulting in a yield of only 51%.

Lb. pentosus and *Lb. brevis* can be used for lactic acid fermentation on HH, but the theoretical maximum lactate production from pentoses is restricted to approximately 0.6 g/g sugar in accordance with the phosphoketolase pathway.

Both enzymatic and acidic hydrolysed HH could be used for lactic acid fermentation with nearly the same yield. Therefore, the choice of hydrolysis method depends on an economic evaluation, where the impact on separation and purification costs must be considered. Enzymes are expensive compared to sulfuric acid, but a high level of inorganic ions after acidic treatment followed by neutralization could complicate the separation step.

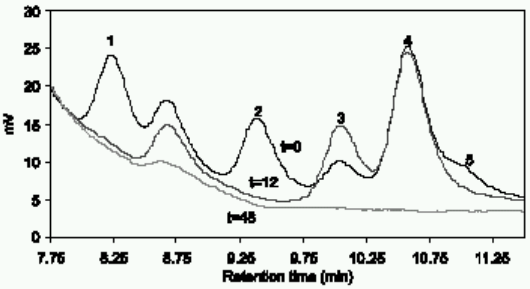

Fig. 6. Refractive index chromatograms from HPLC analysis (Aminex HPX-87H column at 35 °C, 4 mM H_2SO_4 as eluent) of batch fermentations of enzymatically treated hemicellulose hydrolysate with co-cultivated *Lb. pentosus* and *Lb. brevis*. The samples were taken at 0, 12 and 48 h after inoculation. Peak numbers are: 1– xylobiose, 2 – glucose, 3 – xylose, 4 – xylulose and 5 – arabinose.

Acknowledgements

This work was supported by the Danish Ministry of Food, Agriculture and Fisheries by grants from the program "Increased Utilization of Renewable Resources for Industrial Non-food Purposes (1997–2001)". A special thank to Susanne Grøn, Chr. Hansen A/S, Bøge Allé 10, DK-2970 Hørsholm for providing lactic acid bacteria.

References

Abbi, M., Kuhad, R.C., Singh, A., 1996. Bioconversion of pentose sugars to ethanol by free and immobilized cells of *Candida shehatae* (NCL-3501): Fermentation behaviour. Process. Biochem. 31, 555–560.

Ahring, B.K., Jensen, K., Nielsen, P., Bjerre, A.B., Schmidt, A.S., 1996. Pretreatment of wheat straw and conversion of xylose and xylan to ethanol by thermophilic anaerobic bacteria. Biores. Technol. 58, 107–113.

Axelsson, L.T., 1993. Lactic acid bacteria: Classification and physiology. In: Salminen, S., von Wright, A. (Eds.), Lactic Acid Bacteria. Marcel Dekker, New York, pp. 1–63.

Bjerre, A.B., Olesen, A.B., Fernqvist, T., Plöger, A., Schmidt, A.S., 1996. Pretreatment of wheat straw using combined wet oxidation and alkaline hydrolysis resulting in convertible cellulose and hemicellulose. Biotechnol. Bioeng. 49, 568–577.

Chaillou, S., Lokman, B.C., Leer, R.J., Posthuma, C., Postma, P.W., Pouwels, P.H., 1998. Cloning, sequence analysis, and characterization of the genes involved in isoprimeverose metabolism in *Lactobacillus pentosus*. J. Bacteriol. 180, 2312–2320.

Curreli, N., Fadda, M.B., Soddu, G., Sollai, F., Vaccargiu, S., Sanjust, E., Rinaldi, A., 1997. Mild alkaline/oxidative pretreatment of wheat straw. Process. Biochem. 32, 665–670.

Datta, R., 1995. Hydroxycarboxylic acids. In: Kirk, R.E., Othmer, D.F., Kroschwitz, J., Howe-Grant, M. (Eds.), Encyclopedia of Chemical Technology 1991–1998, vol. 13. Wiley, New York, pp. 1042–1062.

Dominguez, J.M., Cao, N., Gong, C.S., Tsao, G.T., 1997. Dilute acid hemicellulose hydrolysates from corn cobs for xylitol production by yeast. Biores. Technol. 61, 85–90.

Food and Agriculture Organization of the United Nations. [online] 2000. http://apps.fao.org/page/collections?subset=agriculture [16 February 2001 last date accessed].

Kandler, O., Weiss, N., 1986. Regular, nonsporing gram-positive rods. In: Holt, J.G. (Ed.), Bergey's Manual of Systematic Bacteriology, vol. 2. Williams & Wilkins, Baltimore, Md, pp. 1208–1234.

Kumar, S., Ramon, D., 1996. Purification and regulation of the synthesis of α-xylosidase from *Aspergillus nidulans*. Microbiol. Lett. 135, 287–293.

Lee, J., 1997. Biological conversion of lignocellulosic biomass to ethanol. J. Biotechnol. 56, 1–24.

Martinez, J.M., Granado, J.M., Montane, D., Salvado, J., Farriol, X., 1995. Fractionation of residual lignocellulosics by dilute-acid prehydrolysis and alkaline extraction: application to almond shells. Biores. Technol. 52, 59–67.

McCoy, M., 1998. Chemical makers try biotech paths. Chem. Eng. News 76 (25), 13–19.

Montane, D., Farriol, X., Salvado, J., Jollez, P., Chornet, E., 1998. Application of steam explosion to the fractionation and rapid vapor-phase alkaline pulping of wheat straw. Biomass Bioenergy 14, 261–276.

Nielsen, P., Ahring, B.K., Angelidaki, R., 1993. Report on biogas production from manure. Department of biotechnology, Technical University of Denmark (in Danish).

Olsson, L., Hahn-Hägerdal, B., 1996. Fermentation of lignocellulosic hydrolysates for ethanol production. Enzyme Microb. Technol. 18, 312–331.

Perttunen, J., Sohlo, J., Mäentausta, O., 1996. The fermentation of birch hemicellulose liquor to lactic acid. In: Proceedings of the 6th Conference on Biotechnology in the Pulp and Paper Industry. Chemical Abstracts, CAN 683172, pp. 295–298.

Preziosi-Belloy, L., Nolleau, V., Navarro, J.M., 1997. Fermentation of hemicellulosic sugars and sugar mixtures to xylitol by *Candida parapsilosis*. Enzyme Microb. Technol. 21, 124–129.

Puls, J., Poutanen, K., 1989. Mechanisms of enzymatic hydrolysis of hemicelluloses (xylans) and procedures for determination of the enzyme activities involved. In: Coughlan, M.P. (Ed.), Enzyme Systems for Lignocellulose Degradation. Elsevier, London, pp. 151–165.

Saier Jr., M.H., Ye, J.J., Klinke, S., Nino, E., 1996. Identification of an anaerobically induced phosphoenolpyruvate-dependent fructose-specific phosphotransferase system and evidence for the Embden–Meyerhof glycolytic pathway in the heterofermentative bacterium *Lactobacillus brevis*. J. Bacteriol. 178, 314–316.

Schmidt, A.S., Thomsen, A.B., 1998. Optimization of wet oxidation pretreatment of wheat straw. Biores. Technol. 64, 139–151.

Sun, R., Lawther, J.M., Banks, W.B., 1996. Fractional and structural characterization of wheat straw hemicelluloses. Carbohydr. Polym. 29, 325–331.

Vlasenko, E.Y., Ding, H., Labavitch, J.M., Shoemaker, S.P., 1997. Enzymatic hydrolysis of pretreated rice straw. Biores. Technol. 59, 109–119.

Wong, A., 1997. Agricultural fibre supply for pulp production. [Online] http://www.agripulp.com/home01/articles/index.php 1997.

4.3 Paper II

Schmidt, A.S., Garde, A., Klinke, H.B., Thomsen, A.B., Jonsson, G. and Ahring, B.K. (2001). Lactic acid production from wheat straw: Effect of pre-treatment conditions In: Proceedings of 1st World Conference on Biomass for Energy and Industry (S. Kyritsis, A.A.C.M. Beenackers, P. Helm, A. Grassi and D. Chiaramonti (eds.)), Sevilla, Spain, 5-9 June 2000. James & James Science Publisher Ltd. Vol. 2. pp. 1078-1081

ABSTRACT: Lactic acid production by a mixed culture of *Lactobacillus brevis* and *Lactobacillus pentosus* on hemicellulose from pre-treatment of wheat straw was evaluated. Different pre-treatment conditions were applied to minimise the use of alkali and oxygen in the process. Wet oxidation (no alkali) gave the highest amount of solubilised hemicellulose (measured as monosaccharides after acid hydrolysis) in particular at high oxygen pressure (25.8 g sugar/100 g straw). However, these conditions gave the lowest recovery of hemicellulose, whereas the previously found optimal conditions (alkaline wet oxidation at 12 bar oxygen) resulted in the highest hemicellulose recovery. Hence, a compromise between optimal hemicellulose recovery and solubilisation is necessary *e.g.* wet oxidation at 6-bar oxygen giving 23.8 g sugar/100 g straw with a hemicellulose recovery of 58%. The different hemicellulose-rich fractions were hydrolysed to fermentable sugars by the enzyme Celluclast® after which these sugars were fermented to lactic acid giving up to 20 g lactic acid per 100 g straw. No inhibition from degradation products on either *L. pentosus* or *L. brevis* was observed. Hence, hemicellulose substrates look promising for lactic acid production in Denmark.

1. Introduction

Lignocellulosic material such as agricultural waste *e.g.* wheat straw represents an abundant renewable raw material source for several value-added products [1,2] *e.g.* lactic acid and fibres. Lactic acid is an important chemical used in a wide variety of industrial applications, but the main potential is as precursor for production of the biodegradable polymer, polylactic acid [3].

Utilisation of starchy substrates is well known for lactic acid production [4], but these substrates are directly utilisable as foods. Alternatively, sugar solutions can be obtained from lignocellulosic materials. According to FAO, 94 and 184 million tons of wheat were produced in 1998 in North America and Europe, respectively. The average yield of straw is about 1.3 kg per kg grain providing a considerable amount of surplus wheat straw. Wheat straw consists of about 36% cellulose, 31% hemicellulose and 7% lignin, but this may vary from year to year. The high amount of hemicellulose emphasises the need to utilise hemicellulose in addition to the cellulose, however, a pre-treatment is needed for efficient utilisation of the polysaccharides [3,5]. Despite the costs of the necessary pre-treatment step, this technology shows economic promise [6].

In Denmark, the wet-oxidation process (WO), using water, oxygen pressure, and elevated temperature, has proven efficient for fractionation of wheat straw at alkaline conditions [5,7]. By this treatment most of the hemicellulose is solubilised mainly as oligomers and polymers and the cellulose is recovered in the solid fraction and could be used for fiber-based materials (Figure 1).

The ability of *Lactobacilli* to transform a wide range of carbohydrates to lactic acid is well known [4,8]. However, these micro-organisms do not produce enzymes for hemicellulose hydrolysis for which reason the hemicellulose cannot be utilised directly. Fermentable sugars can be released either by enzymatic (mainly xylulose, xylobiose and xylose, depending on enzymes used) or by acidic (mainly xylose) hydrolysis. Another problem in fermenting pre-treated lignocellulose might be the presence of potential inhibitors such as organic acids

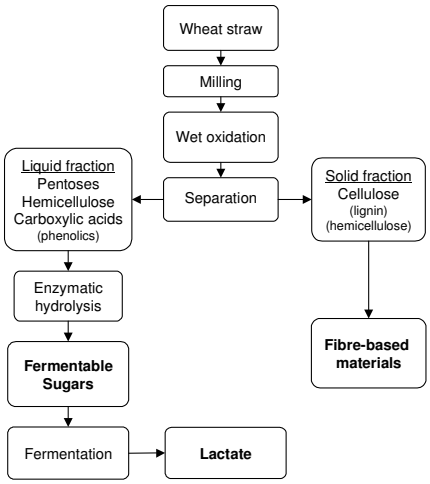

Figure 1. Flow chart of the wheat straw to lactate process.

(formic, acetic and levulinic acid) and furan derivatives (2-furfural and 5-hydroxymethyl-2-furfural) together with a whole range of phenolic compounds [9-11]. In this study, solubilised hemicellulose from pre-treatment of wheat straw was hydrolysed by the enzyme Celluclast® and used for lactic acid production by *Lactobacillus brevis* and *Lactobacillus pentosus* (Figure 1). Pre-treatment conditions were investigated to lower the amount of oxygen and alkali used in the alkaline wet oxidation process and thereby lowering the cost of lactic acid production. The composition of the solid and liquid fraction from the pre-treatment was characterised to evaluate the effect of pre-treatment conditions on the utilisation of the hemicellulose for lactic acid production by determined the amount of solubilised hemicellulose and degradation products (potential inhibitors). Fermentations were carried out on the different hemicellulose fractions to investigate whether the *Lactobacilli* could convert all sugars effectively to lactic acid.

2. MATERIALS AND METHODS

2.1 Pre-treatment process

Pre-treatments were carried out in a loop-reactor with a 1-L working volume constructed at Risø National Laboratory [7]. Ground wheat straw from 1997 (5 mm) (60 g/L) was mixed with water (and Na_2CO_3) before applying oxygen pressure and heated to 185°C for 15 minutes (Table 1). Experiments in the absence of oxygen were performed by replacing air with nitrogen or replacing the air with 12 bar nitrogen. After pre-treatment, the suspension was filtered to separate the fractions.

Table 1. Pre-treatment of wheat straw (60 g/L) at 185°C for 15 minutes.

Pre-treatment	Abbreviation	Oxygen (bar)	Na_2CO_3 (g/L)
Alkaline wet oxidation (high)	AWOH	12	6.5
Alkaline wet oxidation (low)	AWOL	6	6.5
Wet oxidation (high)	WOH	12	0
Wet oxidation (low)	WOL	6	0
No oxygen (nitrogen)	AHN	0 (12 N_2)	6.5
No oxygen	AH	0	6.5
No oxygen/alkaline	OO	0	0

2.2 Chemical composition of solid fraction

Untreated wheat straw and treated solid fibre fractions were analysed for their content of hemicellulose, cellulose, lignin, and the non-cell wall material (NCWM) (such as pectin, proteins etc.). Modification of a gravimetric method was used [12,13] taking the ash content into account in each step. Results were given as a dry matter percentage.

2.3 Analysis of liquid fraction

Solubilised hemicellulose was hydrolysed by 4% w/v H_2SO_4 at 121°C for 10 minutes. The sulfate ions were precipitated by $Ba(OH)_2$. After removal of $BaSO_4$, any remaining ions were eliminated by ion exchange treatment with Dowex MR3 (Fluka). The monosaccharides were quantified by HPLC cation exchange (Aminex HPX-87H column (Biorad)) with 4 mM H_2SO_4 as eluent [7].

Carboxylic acids was determined on Dionex 4000 i ion chromatograph (Ionpac ICE-AS-6 column) using 0.4 mM heptafluorobytyric acid as eluent at 1.0 mL/min with a combined conductivity and UV (204 nm) detection.

2-Furfural and 5-hydroxymethyl-2-furfural (HMF) was analysed by HPLC (Phenomenex Luna C18 column) using a linear eluent gradient of methanol (10-90%) in 0.02 M sodium phosphate buffer (pH 3).

Phenolic compounds were derivatised with N,O-Bis-trimethylsilyl-triflouroacetamid [14]. *Prior* to GC analysis, the samples were extracted by solid phase extraction with ethyl acetate as eluent [13]. Quantification was performed on a GC fused silica capillary column (XTI-5) (30m x 0.25 mm i.d. with a 0.25-µm film) using helium as carrier gas. The oven temperature was held at 80°C for 3 min and then increased by 8°C/min to 280°C.

2.4 Calculation of recovery

The recoveries of the hemicellulose (R_H) and cellulose (R_C) during pre-treatment were calculated by means of their mass balances based on 100 g straw:

$$R_H = \frac{H_{out} + (X_{liq} + A_{liq}) \cdot 132/150}{H_{in}} \cdot 100\%$$

$$R_C = \frac{C_{out} + G_{liq} \cdot 162/180}{C_{in}} \cdot 100\%$$

Where H_{in} and C_{in} are the amount of hemicellulose and cellulose present in 100 g untreated straw, respectively, H_{out} and C_{out} the amount of hemicellulose and cellulose present in the treated solid fraction, and X_{liq}, A_{liq} and G_{liq} the amount of xylose, arabinose and glucose (hydrolysis of hemicellulose and cellulose) present in the treated liquid fraction, respectively.

2.5 Microorganisms

The two *Lactobacillae* strains *L. pentosus* CHCC 2355 and *L. brevis* CHCC 2097 were kindly provided by Chr. Hansen A/S, Denmark.

2.6 Cultivation media

The basic substrate was a MRS medium made up directly in the liquid fraction from pre-treatment using the solubilised hemicellulose as main carbon source. The composition of the MRS media was as follows: 10 g/L Casein peptone, 10 g/L meat extract, 5 g/L yeast extract, 1 g/L Tween 80, 2 g/L K_2HPO_4, 5 g/L sodium acetate, 2 g/L diammonium citrate, 0.2 g/L $MgSO_4 \cdot 7H_2O$ and 0.05 g/L $MnSO_4 \cdot H_2O$. The pH of the media was adjusted to 6.5 with 10 M NaOH or 2 M HCl before sterilisation (140°C, 20 minutes). [15].

2.7 Enzymatic hydrolysis

The enzymatic hydrolysis was performed by aseptically adding 1% (v/v) Celluclast®, kindly provided by Novo Nordisk A/S, Denmark, to the SH substrates (with added nutrients of the MRS media, pH 6.5) [15]. The mixture was incubated for 4 hours at 40°C.

2.8 Cultivation

The separate inoculum of *L. pentosus* and *L. brevis* was made on MRS medium in water supplemented with 10 g/L glucose and 10 g/L xylose. After two days, the bacteria were transferred to fresh MRS media supplemented with 5 g/L glucose and 5 g/L xylose. The growth was followed by measurement of optical density (OD_{578}) on a Spectronic 301 spectrophotometer (Milton Roy). When the bacteria were in the

exponential growth phase, the hemicellulose substrates (with added nutrients) were inoculated with 2.5% (v/v) inoculum of each bacteria. All experiments were performed as batch fermentations at 33.5°C under strictly anaerobic conditions at 165 rpm. Samples were taken after 0, 6, 12, 24, 48, and 72 hours of cultivation.

2.9 Analysis of lactic acid and residual sugars

Fermentation samples were diluted 20 times with 10 mM H_2SO_4 and centrifuged (10.000 rpm, 0°C, and 20 minutes). Quantification was performed using HPLC (Aminex HPX-87H column (Biorad)) at 35°C with 4 mM H_2SO_4 as eluent [15].

3. RESULTS AND DISCUSSION

The previously determined optimum alkaline wet oxidation condition for wheat straw [5] was applied in this study. However, absence of alkali has proven efficient for other materials [16]. By removing the alkali from the process the production cost could be reduced. Therefore, pre-treatments with reduced oxygen, absence of oxygen and/or absence of alkali was performed to investigate the effect of conditions on utilisation of hemicellulose for lactic acid production.

3.1 Pre-treatment

The chemical composition of the solid fraction varied to some extent with the pre-treatment conditions (Figure 2), although all conditions enriched the solid fraction with cellulose compared to untreated wheat straw by solubilisation and/or degradation of mainly hemicellulose and lignin. Alkaline wet oxidations gave the highest content of cellulose (64%) especially at high oxygen pressure (12 bar). The lowest cellulose content (54%) was obtained when straw was treated in the absence of both alkali and oxygen.

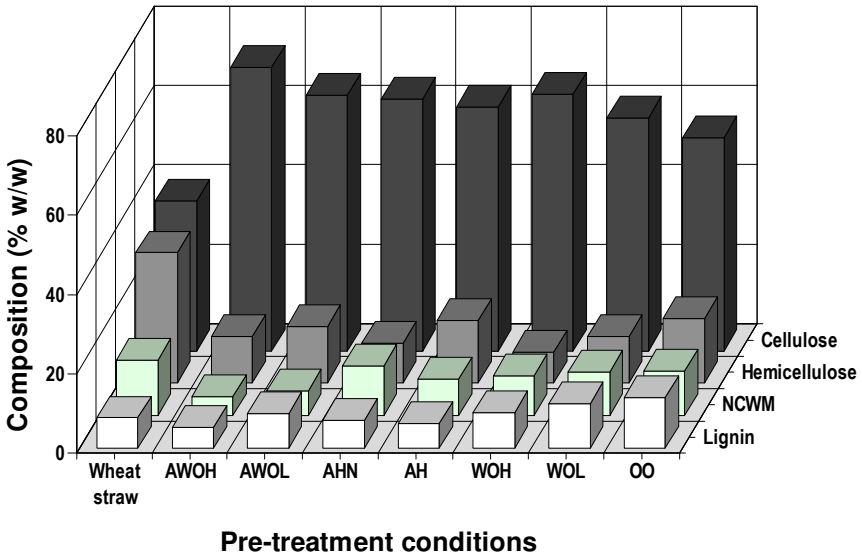

Figure 2. The chemical composition (%w/w dry weight) of the solid fraction after pre-treatment of wheat straw. NCWM: non-cell wall material. Pre-treatment conditions are given in Table 1.

A more significant effect of the pre-treatment conditions was observed on the amount of solubilised hemicellulose measured as monosaccharides after acid hydrolysis (Table 2). Wet oxidation (no alkali) gave the highest amount, in particular at high oxygen pressure (25.8 g sugar/100 g straw). In fact, most pre-treatment conditions gave a higher amount than the conditions previously found optimal (AWOH) for treatment of wheat straw (15.3 g sugar /100 g straw) [5].
For all conditions, nearly a total recovery of the original cellulose was obtained (95-99%), whereas the recovery of hemicellulose was much lower (Table 3). Alkaline wet oxidation at 12-bar oxygen (AWOH) resulted in the highest overall recovery as these conditions gave a significantly higher hemicellulose recovery (74%) than other conditions (48-65%). The recovery was lowest for wet oxidation at 12-bar oxygen (WOH), the conditions giving the highest amount of solubilised hemicellulose for fermentation. Hence, a compromise between optimal hemicellulose recovery and solubilisation is necessary. Such a compromise could be wet oxidation at 6-bar oxygen (WOL) giving 23.8 g sugar/100 g straw for fermentation with a hemicellulose recovery of 58%. This lower oxygen pressure will lower the cost of the pre-treatment process.

Table 2. Solubilised hemicellulose (g per 100 g straw) (measured as monosaccharides) after acid hydrolysis (4% w/v H_2SO_4, 121°C, and 10 minutes) of pre-treated wheat straw. Pre-treatment conditions are given in Table 1.

Pre-treatment	Glucose (g/100 g)	Xylose (g/100 g)	Arabinose (g/100 g)	Total(g/100 g)
AWOH	3.4	9.6	2.3	15.3
AWOL	1.4	10.2	1.8	13.4
WOH	6.2	17.5	2.1	25.8
WOL	6.1	15.7	2.1	23.8
AHN	2.0	14.8	2.5	19.3
AH	1.2	6.9	1.1	9.2
OO	2.8	11.3	1.4	15.5

Table 3. Calculated recovery based on mass balances for the polysaccharides (hemicellulose and cellulose) after pre-treatment of wheat straw. Pre-treatment conditions are given in Table 1.

Pre-treatment	Cellulose (%)	Hemicellulose (%)	Overall (%)	pH
AWOH	98	74	87	6.0
AWOL	98	63	81	6.5
WOH	95	48	73	3.5
WOL	95	58	78	4.0
AHN	99	52	77	7.8
AH	99	58	80	7.6
OO	99	65	83	4.3

Several products such as low molecular weight carboxylic acids, furans and phenolics from degradation of hemicellulose and lignin were formed during the different pre-treatments (Table 4). The carboxylic acids were the dominating degradation products ranging from 2.4 g to 12 g/100 g straw. Furans originating from degradation of hemicellulose were mainly formed at acidic conditions (pH around 3.5-4.3 (Table 3)) in the absence of alkali in the process. Very low amounts of furans (<5 mg/100 g straw) were formed at the previously found optimal conditions (AWOH). Aromatic acids and other phenolic compounds from lignin are typically more potent antimicrobials [9,17]. A wide range of these compounds were found in the treated liquid fractions [13] but only in low concentrations of about 0.2-0.4 g/100 g wheat straw.

Table 4. Degradation products (low molecular weight carboxylic acids, furans and phenolic compounds) after pre-treatment of wheat straw. Pre-treatment conditions are given in Table 1.

Pre-treatment	Carboxylic acids (g/100 g)	Furans (mg/100 g)	Phenolics (mg/100 g)
AWOH	12.0	4.6	175.6
AWOL	7.4	25.0	346.2
WOH	3.7	142.5	283.4
WOL	2.7	111.2	350.9
AHN	4.6	48.2	260.5
AH	2.6	51.0	187.2
OO	2.4	201.1	170.5

3.2. Lactic acid production

The liquid fraction from the different pre-treaments were hydrolysed to fermentable sugar components by Celluclast® after which these sugars were fermented to lactic acid by a mixed culture of *L. pentosus* and *L. brevis*. The maximal lactic acid production was obtained already after 24 hours cultivation (Figure 3). A mixed culture was necessary, as individually, the two organisms were not able to fully utilise the relative broad spectra of sugar components released by hydrolysis [15]. No inhibition from the present degradation products of either *L. pentosus* or *L. brevis* seemed to occur in the lactic acid production. This was also shown previously by applying an increasing concentration of solubilised hemicellulose [15].

Three different pre-treatment conditions gave the same high lactic acid production (20 g/100 g straw) (AWOH, WOH, and WOL) (Figure 3). Therefore, wet oxidation at low oxygen pressure (WOL) was identified as the most economic process using the least oxygen and no alkali. Often hemicellulose hydrolysates have to be detoxified *prior* to fermentation [9,17,18], however, the treatments used in this study do not require detoxification for the two *Lactobacillus* strains to produce lactic acid on the hemicellulose-rich fraction from wheat straw. Hence, such substrates look promising as a basis for lactic acid production in agricultural countries like Denmark.

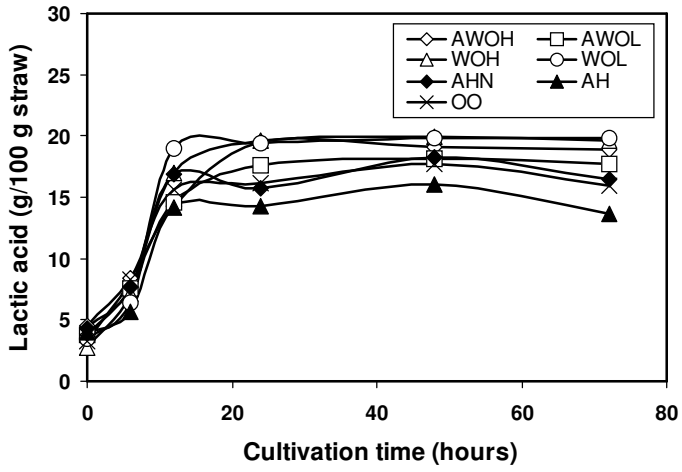

Figure 3. Lactic acid production by a mixed culture of *L. pentosus* and *L. brevis* (conditions: strictly anaerobic, 33.5°C, pH 6.5, 165 rpm) from different hemicellulose substrates after hydrolysis with Celluclast (1% (v/v) enzyme, 40°C, pH 6.5, 4 hours). Pre-treatment conditions are given in Table 1.

4. Acknowledgments

This work was supported by a grant from the program “Increased Utilization of Renewable Resources for Industrial Non-food Purposes (1997-2001)” under the Danish Ministry of Food, Agriculture and Fisheries.

5. REFERENCES

[1] BK Ahring, D Licht, AS Schmidt, P Sommer, AB Thomsen (1999) Production of ethanol from wet oxidised wheat straw by *Thermoanaerobacter mathranii*. *Biores. Technol.* 68, 3-9.

[2] LT Fan, Y-H Lee, MM Gharpura, (1982) The nature of lignocellulosics and their pretreatments for enzymatic hydrolysis. *Adv. Biochem. Eng.* 23, 157-187.

[3] JC Parajó, JL Alonso, V Santos (1996) Lactic acid from wood. *Proc. Biochem.* 31, 271-280.

[4] K Hofvendahl, B Hahn-Hägerdal (2000) Factors affecting the fermentative lactic acid production from renewable resources. *Enzyme Microb. Technol.* 26, 87-107.

[5] AS Schmidt, AB Thomsen (1998) Optimization of wet oxidation pretreatment of wheat straw. *Biores. Technol.* 64, 139-151.

[6] CE Wyman (1994) Ethanol from lignocellulosic biomass: Technology, economics and opportunities. *Biores. Technol.* 50, 3-16.

[7] AB Bjerre, AB Olesen, T Fernqvist, A Plöger, AS Schmidt (1996) Pretreatment of wheat straw using combined wet oxidation and alkaline hydrolysis resulting in convertible cellulose and hemicellulose. *Biotechnol. Bioeng.* 49, 568-577.

[8] K Melzoch, J Votruba, V Hàbová, M Rychtera (1997) Lactic acid production in a cell retention continuous culture using lignocellulosic hydrolysate as a substrate. *J. Biotechnol.* 56, 25-31.

[9] J Buchert, K Niemelä, J Puls, K Poutanen (1990) Improvement of the fermentability of steamed hemicellulose hydrolysate by ion exclusion. *Proc. Biochem.* 25, 176-180.

[10] TA Clark, KL Mackie (1984) Fermentation inhibitors in wood hydrolysates derived from the softwood *Pinus radiata*. *J. Chem. Tech. Biotechnol.* 34B, 101-110.

[11] J Zaldivar, LO Ingram (1999) Effect of organic acids on the growth and fermentation of ethanologenic *Escherichia coli* LY01. *Biotechnol. Bioeng.* 66, 203-210.

[12] HK Goering, PJ van Soest (1970) Forage fiber analyses (apparatus, reagents, procedures, and some applications). Agricultural Handbook 379, Agricultural Research Service - United States Department of Agriculture. USDA, Washington DC, pp. 1-20.

[13] Klinke HB, Ahring BK, Schmidt AS, Thomsen AB. 2002. Characterization of degradation products from wet oxidation of wheat straw. Biores Technol 82:15-26.

[14] K Niemelä, E Sjöström (1986) Simultaneous identification of aromatic and aliphatic low molecular weight compounds from alkaline pulping liquor by capillary gas-liquid chromatography – mass-spectrometry. *Holzforschung* 40, 361-368.

[15] Garde A, Jonsson G, Schmidt AS, Ahring BK. 2002. Lactic acid production from wheat straw hemicellulose hydrolysate by Lactobacillus pentosus and Lactobacillus brevis. Biores Technol 81:217-223.

[16] AB Thomsen, AS Schmidt (1999) Further Development of Chemical and Biological Processes for Production of Bioethanol: Optimisation of Pre-treatment Processes and Characterisation of Products. Risø-R-1110(EN), Risø National Laboratory, DK. 73 p.

[17] L Jonsson, E Palmqvist, NO Nilvebrant, B Hahn-Hägerdahl (1998) Detoxification of wood hydrolysates with laccase and peroxidase from the white-rot fungus *Trametes versicolor. Appl. Microbiol. Biotechnol.* 49, 691-697.

[18] E Palmqvist, B Hahn-Hägerdal, Z Szengyel, G Zacchi, K Reczey (1997) Simultaneous detoxification and enzyme production of hemicellulose hydrolyzates obtained after steam pretreatment. *Enzyme Microb. Technol.* 20, 286-293.

4.4 Fermentation using UASB reactor

4.4.1 Introduction

Continuous fermentation using an Upflow Anaerobic Sludge Blanket (UASB) reactor is evaluated to determine its suitability for lactic acid production. Operation of the bioreactor is based on immobilization of the bacteria cells in granules to form an active sludge. The ability of the lactic acid bacteria to form granules and auto-immobilize is important for obtaining high cell density in the bioreactor, and hereby also achieving high lactic acid productivity. An advantage of the UASB reactor type, apart from high cell density, is the possibility to regulate the dilution rate independent of, and especially above, the generation time of the LAB. The LAB have a specific generation time for utilization of each type of substrate, and if not immobilized properly, the culture can be flushed out of the fermenter when the dilution rate exceeds the wash out value.

4.4.2 Materials and methods

4.4.2.1 Microorganisms and cultivation

The two *Lactobacillae* strains *Lb. pentosus CHCC 2355* and *Lb. brevis CHCC 2097* were kindly provided by Chr. Hansen A/S, Denmark. The LAB were grown in MRS media as described in Paper I for 5 h at their optimum temperature, which is 37 °C for *Lb. pentosus* and 30 °C for *Lb. Brevis,* before used as inoculum. The inoculum, used in experiments to determine generation times on different sugars, was grown on 5 g/l of the respective sugar for 5 h, and applied in a concentration of 5 vol-%.

4.4.2.2 Substrate

Brown juice (produced from pressing of green biomass at 80 °C) with a dry matter content of 41.5% was received from Centre for Agro-Industrial Biotechnology, University of Southern Denmark. The concentrated brown juice was diluted with distilled water to a dry matter content of 5%, before used as substrate. MRS broth containing 5 g/l of glucose, fructose, sucrose, xylose or arabinose was used for determination of generation times on the different sugars.

4.4.2.3 Analytical techniques

Growth rates were monitored by optical density and the amounts of lactic acid and sugars were measured as described in section 4.1.1.3.

4.4.2.4 Generation time

Experiments were performed to determine the generation time (time needed for doubling the number of cells) on relevant sugars by monitoring the growth rate of *Lb. brevis* and *Lb. pentosus* in MRS broth containing 5 g/l of glucose, fructose, sucrose, xylose or arabinose. The LAB were grown in MRS media at their optimum

temperature. For each sugar component 5 test tubes were prepared, 4 containing the sugar of which 3 tubes were inoculated, and one tube where the sugar was omitted but still inoculated. The optical density was measured in all 5 tubes during 12.5 hours of incubation at optimum temperature.

4.4.2.5 UASB reactor setup and operation

Two different reactor configurations were used, one with a recycle loop and build in pH controller (see Figure 4.4.1) and one using single pass without pH control.

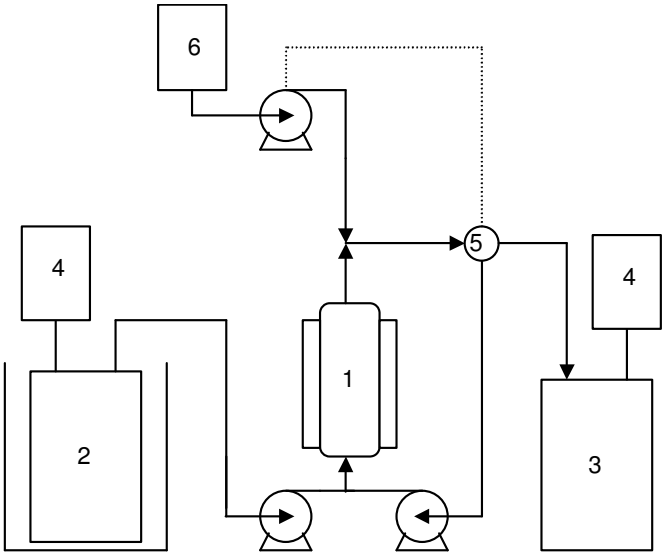

Figure 4.4.1. UASB reactor setup. 1) 200 ml Upflow anaerobic sludge blanket reactor equipped with heating jacket, 2) 20 L stirred substrate feed tank, placed on ice, 3) 20 L effluent holding tank, 4) Gasbag buffers (CO_2+N_2), 5) pH electrode and controller for NaOH dispenser, and 6) 2 L holding tank for 2 M NaOH.

A glass UASB reactor with an active volume of 200 ml and an internal diameter of 3.9 cm was used. The reactor was equipped with a water jacket connected to a water bath for temperature control. The feed was heated prior to entry of the reactor by passage through a coil within the water cap below the reactor. A glass ball in the reactor above the feed inlet prevented granules from moving down into the inlet. The settling effect of the granules prevents them from being flushed out by the up-flowing feed stream inside the fermenter.

The continuous cultivation was done in non-sterile substrate and the incubation temperature in the bioreactor was constantly kept at 33.5^{o}C. The reactor was filled with the feed substrate and 50 ml of sterilized (autoclaved 3 x 1 h at 121°C) granular material from a Dutch full-scale mesophilic UASB reactor for treatment of paper mill waste water. After inoculated with 5 ml of each of the bacterial suspensions (*Lb.*

brevis and *Lb. pentosus*), the bacteria were allowed to grow for 18 hours before continuous operation was started. All samples were taken from the effluent and analyzed for lactic acid, glucose, fructose, and sucrose. At the end of the 10 days experiment the biomass was removed from the fermenter and stored at 2°C for later use.

The fermenter setup was adapted for pH control and the reactor was sterilized and filled with 50 ml of the stored sludge/granules and 150 ml of fresh 5% brown juice. Even though the stored granules were probably still active, the reactor was inoculated with 5 ml of each of the bacterial suspensions (*Lb. brevis* and *Lb. pentosus*). The process was run as batch fermentation for 18 hours without pH control, before the continuous feed of 5% brown juice was started. The recycle rate was 0.6 times the feed rate and the pH was kept between 5.0 and 5.2.

With the setup still adapted for pH-control an experiment with continuous fermentation of 5% brown juice using only *Lb. pentosus* was carried out. The reactor was sterilized and filled with brown juice before inoculation. Again, the process was run as batch for 18 hours without pH control, before the continuous feed was started and the recycle rate and pH were the same as in the previous experiment.

4.4.3 Results and discussion

4.4.3.1 Generation time

In Figure 4.4.2 the optical density of *Lb. pentosus* cultures is shown during fermentation of the different sugars. Different uptake characteristics can be seen depending on which sugar is assimilated. When xylose is utilized the lag time is short, but there is a much slower increase in optical density compared to the other sugars. The growth curves on sucrose and glucose are very similar except for the slightly longer lag time on sucrose, which could be due to the time required for activation of the enzyme system needed for splitting sucrose into glucose and fructose.

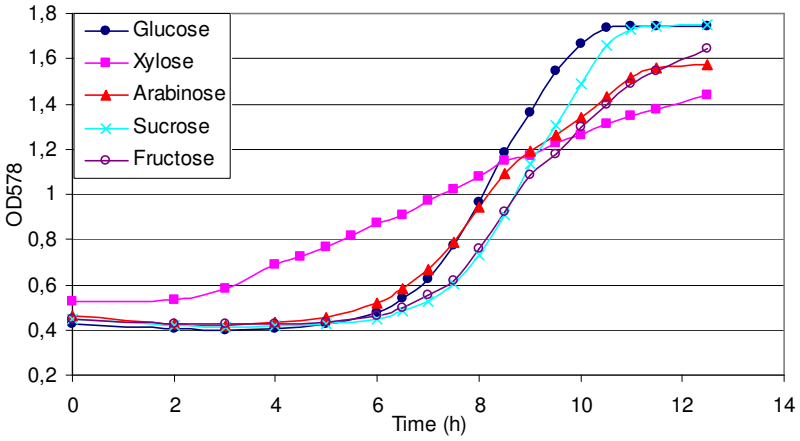

Figure 4.4.2. Optical density measured during fermentation of different sugars by Lb. pentosus.

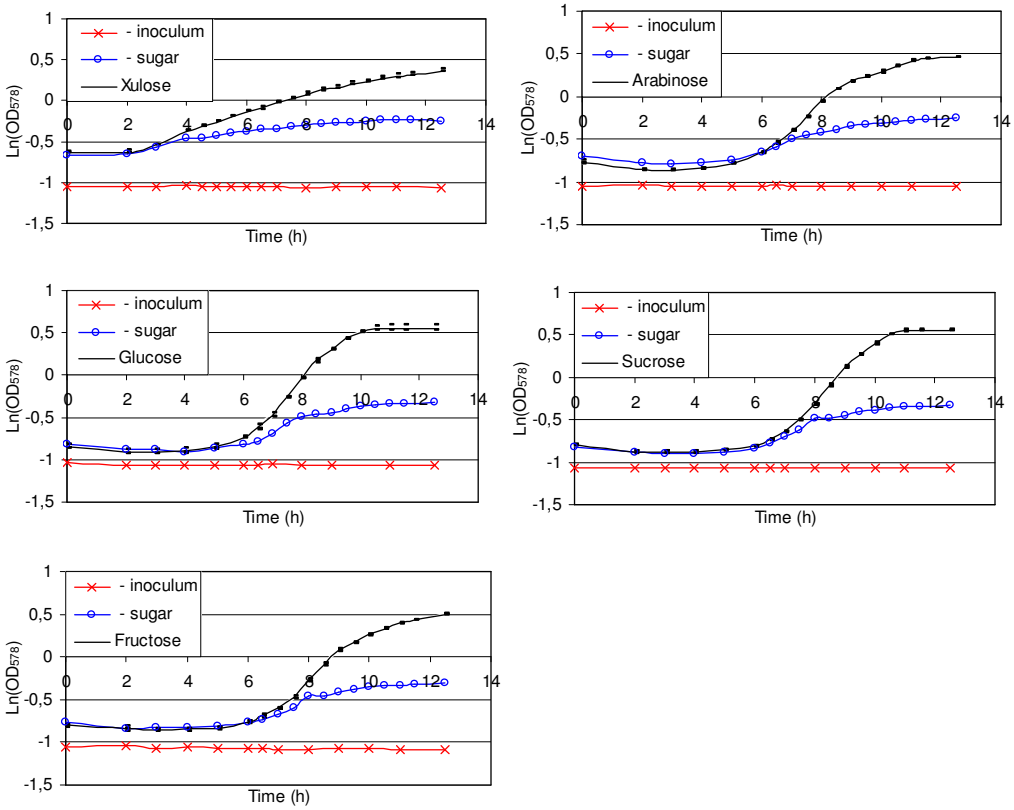

Figure 4.4.3. Assimilation of five different sugars by Lb. pentosus. The natural logarithm to the optical density vs. time is plotted. As a control/reference, measurements on tubes with no sugar (-sugar) or no inoculum (-inoculum), are also shown.

The generation time, T, for each type of sugar can be determined from the maximum slope α by:

$$T = \frac{\ln(2)}{\alpha}$$

In Table 4.4.1 the calculated generation times are given for utilization of the different sugars by *Lb. pentosus CHCC 2355* and *Lb. brevis CHCC 2097.* The generation times of *Lb. brevis* on glucose, fructose and arabinose were not determined due to difficulties starting the bacteria on the pure substrates.

Table 4.4.1. Generation time (hours) of *Lb. pentosus CHCC 2355* and *Lb. brevis CHCC 2097* on different sugars.

Strain	Xylose	Arabinose	Glucose	Fructose	Sucrose
CHCC 2355	6,12	2,01	1,61	1,85	1,65
CHCC 2097	5,81	3,23	ND	ND	ND

The fastest generation time is found for utilization of glucose and sucrose by *Lb. pentosus,* which is about 4 times faster than the growth rate that both bacteria exhibit when utilizing xylose. Assuming a homogeneous broth, a critical dilution rate for continuous fermentation of brown juice by *Lb. pentosus* is 1/1.61 h = 0.62 h^{-1}. Dilution rates higher that this value will cause the bacteria to be flushed out of the fermenter unless immobilization on the granules has taken place.

4.4.3.2 Continuous fermentation using UASB reactor

The feed, consisting of 5% brown juice, was analyzed for the major sugars, see Table 4.4.2. The initial concentration of sugars was the same in all of the continuous fermentations and the pH value of the feed was measured to 5.6.

Table 4.4.2. Initial sugar concentrations in 5% brown juice.

Sugar concentration (g/l)		
Glucose	Fructose	Sucrose
5,3	9,9	3,2

Figure 4.4.4 shows the concentration of glucose, fructose, sucrose and lactic acid during a 10 days continuous fermentation using a single pass UASB reactor without pH control. The graphs are divided into 6 time intervals corresponding to the different dilution rates, with the first interval being 18 hours batch fermentation.

During the first 18 hours the concentration of lactic acid went up from 0.8 to 12.6 g/l and the dark brown color of the broth changed into a more light brown due to increasing cell density. The 50 ml of granular initially added still had their intense black color after 18 hours of fermentation, which indicates that bacteria were not situated on the granules at this stage.

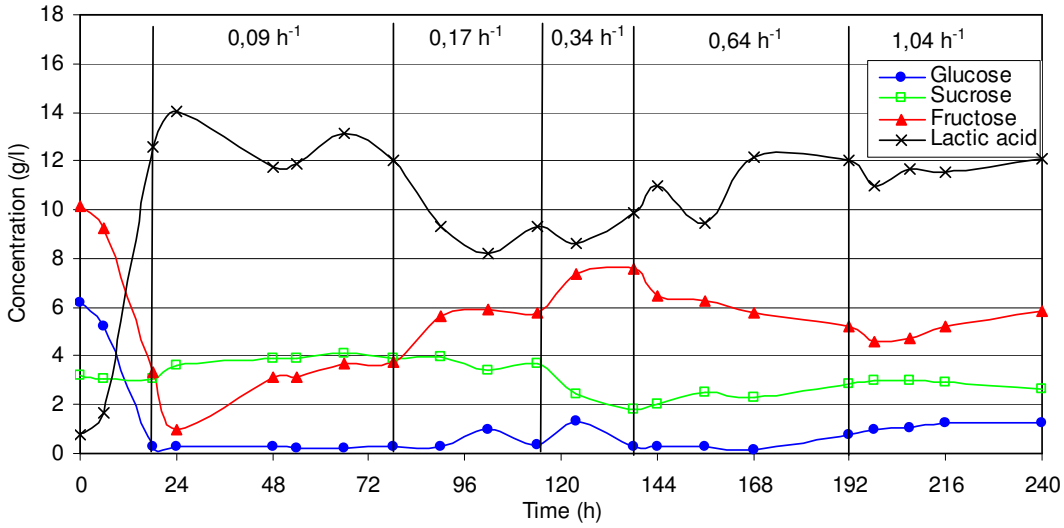

Figure 4.4.4. Fermentation of 5% brown juice by a co-culture of *Lb. pentosus* and *Lb. brevis* using an UASB reactor

6 hours after the dilution rate D was set to 0.09 h^{-1} the fructose level dropped to 1 g/l before it reached a pseudo-steady state of around 3.5 g/l. At first glance it could seem strange that the fructose concentrations experience this dive at 24 hours, but if plug flow is assumed in the fermenter, a volume segment leaving the fermenter 6 hours after the dilution rate is increased, would have experienced a hydraulic retention time of 24 hours. The hydraulic retention time for a volume segment leaving the fermenter is constant after at least 1/0.09 h^{-1} = 11 hours. By the end of the period where D = 0.09 h^{-1} a diffuse brown sludge layer had formed in the bottom of the fermenter, surrounding the initial granules. For most parts, the sludge layer probably consisted of particular matter from the feedstock. The lactic acid concentration stabilized around 12-13 g/l.

During the next two periods, where the dilution rate was increased to 0.17 h^{-1} and later 0.34 h^{-1}, white granules began to form in the sludge layer, which occupied ¾ of the fermenter volume after 138 hours. Like the new granules, the initial granules were distributed in the sludge layer, still with no visible indication of bacteria growth on their surface. The lactic acid concentration in the effluent dropped to 8-10 g/l due to the increasing dilution rate.

The fermenter was completely filled with sludge within 6 hours of changing the dilution rate to 0.64 h^{-1}, and also the number of white granular in the sludge increased. As a result of the higher cell density lactic acid concentration increased to 12 g/l in the effluent despite the higher dilution rate.

The biomass activity was increased quite fast when the dilution rate was changed from 0.64 to 1.04 h^{-1}, causing only a small temporary drop in the lactic acid concentration. The lactic acid productivity increased from 7.2 g/l/h at 192 h to 11.8 g/l/h at 240 h and the pH changed from 3.88 h to 3.96 in the same time period. At D = 1.04 h^{-1} compaction of the granules was seen and formation of channels in sludge layer became more apparent, see Figure 4.4.5. The formation of channels up through the sludge results in some of the feed passes the UASB reactor with limited contact with bacterial cells. Singhal et al. reported on increased channeling in the sludge layer as the granulation process progress in a UASB reactor causing an increase in bypassing influent from 6.55% to 36.24% (Singhal *et al.* 1998). The effect of channeling could be a contributory factor in the incomplete utilization of sugars.

Figure 4.4.5 USAB reactor after 240 hours of brown juice fermentation using *Lb. Pentosus* and *Lb. Brevis.*

The performance of the fermenter was slightly improved after introduction of pH-control compared to the results obtained without pH-control. 18 hours after inoculation with the co-culture the feed flow was adjusted to D = 0.1 h^{-1} for 25 hours before it was increased to 1.07 h^{-1}. As the dilution rate was increased to 1.07 h^{-1} free cells occupying the top half of the fermenter was flushed out and replaced with the darker feed solution. Steady state was reached within 48 hours after increasing D with a maximum productivity of 14.8 g//l/h. The lactic acid concentration was measured to 14.6 g/l and around 3 g/l of sucrose, 1 g/l of fructose, and 0.5 g/l glucose were still present in the effluent, which had a pH value of 5.12. The higher productivity observed when pH is adjusted to 5.0-5.2 can probably be attributed to two effects; the higher pH relieves some inhibition from lactic acid, as the undissociated form is a much stronger inhibitor than lactate, and the use of a recycle loop will increase he mass transfer to the granules, hereby increasing the production rate.

The following experiment, where the reactor was only inoculated with *Lb. pentosus,* showed poor substrate utilization and lactic acid productivity, compared to the co-culture. The highest productivity, 7.9 g/l/h, was reached after 224 hours of fermentation at a dilution rate of 1.14 h^{-1} and a lactic acid concentration of 7.8 g/l. The lower productivity can be explained by the inability of the pure Lb. pentosus culture to form well-defined granules, which can occupy the entire reactor volume. Instead of granular formation, part of the inner side of the reactor was covered with the white bacteria culture resulting in immobilization, but also in an incomplete utilization of the reactor volume. When the feed flow was stopped and pH kept between 5.0 and 5.2, the lactic acid concentration reached 18,2 g/l, with complete utilization of glucose, fructose, and sucrose.

4.4.4 Conclusion

It has been shown that a co-culture of *Lb. brevis* and *Lb. pentosus* are able to form granules in an UASB reactor during fermentation of brown juice. The productivity increased from 11.8 g/l/h at pH = 3.96 to 14.8 g/l/h at pH 5.12, after introduction of pH-control, but in both cases incomplete sugar utilization resulted in unwanted amounts of sugar in the reactor effluent. A very low recycle rate (0.6 times the feed rate) were used in the experiments, so if the process is limited by the mass transfer instead of by the reaction kinetics it would be possible to increase the productivity and perhaps remove sugar from the effluent by increasing the recycle rate.

5

SEPARATION AND PURIFICATION

Three different processes for separation and purification of lactic acid from fermentation broth are proposed and evaluated, see Figure 5.1-3. Extensive process control and correct proportions between equipment pieces are required to run such continuous systems, which was not possible within the scope of this project. However, as basis for the evaluation key elements of the three processes were investigated experimentally.

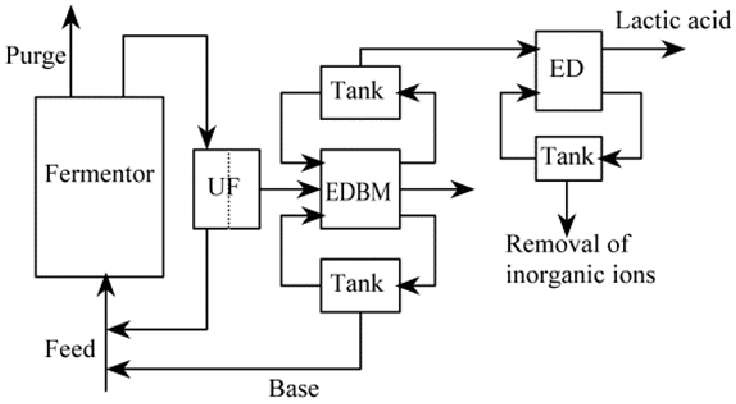

Figure 5.1. Process 1 – Separation process for relatively pure substrates e.g. wheat flour hydrolysate or cane/beet sugar.

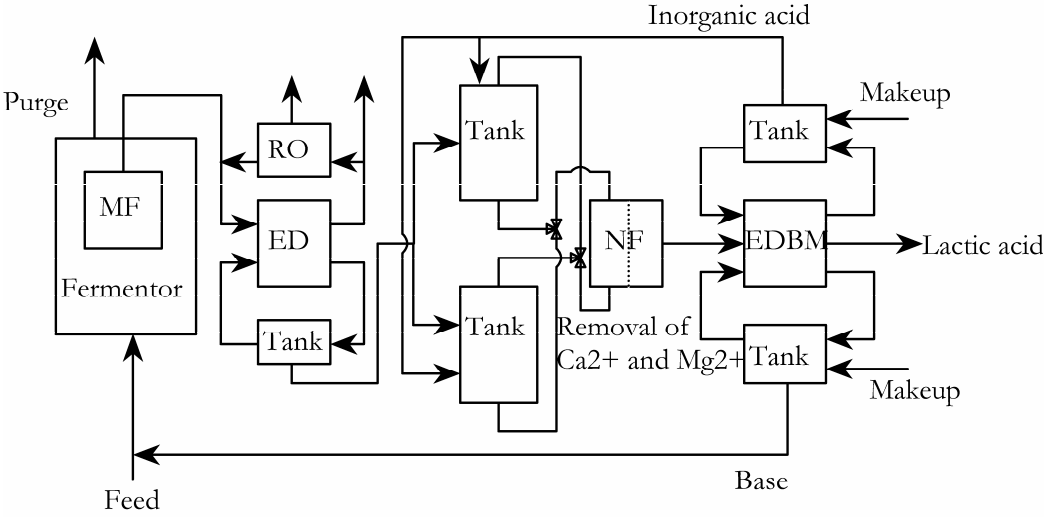

Figure 5.2. Process 2 – Separation process for impure feedstock e.g. hemicellulose from wheat straw or grass juice.

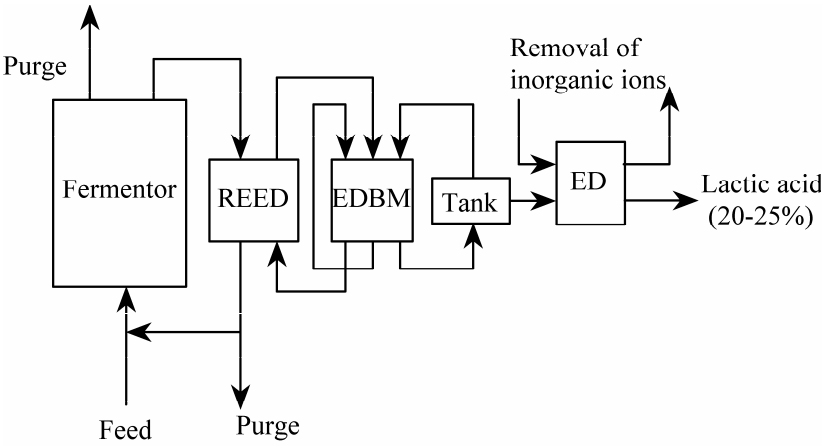

Figure 5.3. Process 3 – Separation process for impure feedstock e.g. hemicellulose from wheat straw or grass juice.

As pointed out earlier, the most suitable configuration of unit operations for the lactic acid separation process depends on the composition of the broth, and therefore also on the utilized feedstock. The heart of each of the suggested separation processes is the electrodialysis with bipolar membranes (EDBM) or bipolar electrodialysis unit. The bipolar electrodialysis generates alkaline solution for pH control of the fermenter and at the same time converts lactate to lactic acid. This is done directly, as shown in flowsheet 1 and 3 or indirectly through initial production of an inorganic acid as depicted in flowsheet 2. A sound operation of the bipolar electrodialysis unit requires a feed low in fouling materials (e.g. cells, macromolecules and proteins) and scaling materials (Ca^{2+} and Mg^{2+}).

Process 1 in Figure 5.1 was designed for a fermentation broth with low concentrations of Ca^{2+} and Mg^{2+}, as these species are not retained by ultrafiltration. Examples of feedstocks with low concentrations of Ca^{2+} and Mg^{2+} are wheat flour hydrolysate or cane/beet sugar. In Paper IV, results of EDBM experiments with UF permeate from fermentation of wheat flour hydrolysate are presented. Experiments with removal of inorganic ions by conventional ED are previously described (Garde 1997).

Process 2 in Figure 5.2 was designed for more impure fermentation broths such as hemicellulose from wheat straw or grass juice. The first separation process is a microfiltration process for removal of cells, colloids and particles. The investigated MF process utilizes a submerged hollow fiber module, as described in Paper III. In the following ED process lactate and other ionic material are concentrated. Water is removed from the diluate circuit of the ED by an RO unit to insure a satisfactorily conductivity. In the nanofiltration process divalent cations are retained and removed. By adding an inorganic acid before NF lactate is converted to lactic acid, which has lower rejection than lactate. The NF process is described in section 5.1. After nanofiltration the process stream is treated in a bipolar electrodialysis where monovalent inorganic ions are removed and converted into acid and base to be recycled in the process. The purified lactic acid leaving the EDBM can be further concentrated by evaporation.

Process 3 in Figure 5.3 was also designed for separating lactic acid from impure fermentation broth. The Reverse Electro-Enhanced Dialysis (REED) unit extracts lactic acid directly from the fermentation broth (see section 0). The lactic acid is extracted through anion-exchange membranes, driven by a combination of diffusion and electrical migration. An alkaline solution on the other side of the membranes collects the lactate ions. Hydroxide ions flows back into the fermentation broth, cleaning the ion-exchange membranes from organic buildup of fouling and replacing the removed lactate ions. By reversing the direction of the electrical current at regular intervals, the fouling is continuously countered, and the Reverse Electro-Enhanced Dialysis process runs stable for longer operations periods between cleaning cycles. This process retains cell materials, proteins, and unconverted sugars as well as inorganic cations like calcium and magnesium in the fermentation broth. Lactate is converted into lactic acid and concentrated to approximately 20% in the acid compartment of the following bipolar electrodialysis unit. Alkaline solution spent in the REED process is also regenerated in the bipolar electrodialysis. After removal of inorganic ions in the conventional electrodialysis (ED) unit the lactic acid is ready to be concentrated to 88% by removal of water by destillation.

5.1 Membrane filtration

5.1.1 Introduction

Before the broth from lactic acid fermentation of brown juice can be treated in a bipolar electrodialysis unit, removal of particles, cells, proteins, as well as calcium and magnesium ions is required. Micro- or ultrafiltration of fermentation broth has been investigated by several authors especially in connection with continuous membrane bioreactors (Boyaval *et al.* 1996;Ohashi *et al.* 1999;Tejayadi and Cheryan 1995). However, when the broth contains even small amounts of Ca^{2+} and Mg^{2+}, micro- or ultrafiltration is no longer sufficient and the pretreatment of the broth must be combined with e.g. nanofiltration (Borgardts *et al.* 1998a;Jeantet *et al.* 1996;Timmer *et al.* 1994).

The experimental work on microfiltration within this thesis is mostly centered on the development of a novel hollow fiber module, which is described in section 5.1.5. In the present chapter different micro- and ultrafiltration membranes are investigated in a batch filtration cell as pretreatment of fermented brown juice prior to experiments with nanofiltration/reversed osmosis.

5.1.2 Materials and methods

5.1.2.1 Membranes

Five different micro- and ultrafiltration membranes were tested, two UF membranes (GR61 and ETNA10A) from DSS, Denmark and three MF membranes (Durapore®) from Millipore, USA, see Table 5.1.1.

Table 5.1.1 The tested micro- and ultrafiltration membranes. The Durapore membranes have polypropylene (PP) support material and a skin layer of Polyvinylidene fluoride in hydrophilic and hydrophobic forms.

	GR61	ETNA10A	Durapore	Durapore (a)	Durapore (b)
MWCO/pore size	20,000	10,000	0.2 µm	0.65 µm	0.65 µm
Material	Polysulphone	PVDF/cellulose	PVDF	PVDF	Modified PVDF
Hydrophobicity	Hydrophobic	Hydrophilic	Hydrophobic	Hydrophobic	Hydrophilic

For removal of divalent cations five different nano- and reversed osmosis membranes were tested, four nanofiltration membranes (DL, DK and NF45, the first two from Desalination Systems, CH (now Osmonics, US) and the last from Danish Separation Systems, Denmark) and two reversed osmosis membranes (DS3-VLP and HR98-PP from Osmonics and Danish Separation Systems, respectively).

5.1.2.2 Feed solution

In all filtrations either pure water or fermented brown juice supplemented with potato starch were used. The fermentation was carried out using a Lactobacillus salivarius strain and the broth had a dry matter content of 12 %. The concentration of lactate was 82 g/l, calcium 400 ppm, magnesium 160 ppm and the pH was 5.6. The broth was kindly supplied by Centre for Agro-Industrial Biotechnology, University of Southern Denmark.

5.1.2.3 Batch cell

The feed solution was placed in a stirred batch cell with a volume of 750 ml and a 140 cm^2 flat sheet membrane fixed in the bottom of the cell, see Figure 5.1.1. The TMP was regulated by a nitrogen pressure through a reduction valve. The permeate was collected at certain time intervals and weighed to calculate the flux. The temperature of the solution was kept at 32°C-36°C using an electric heating jacket.

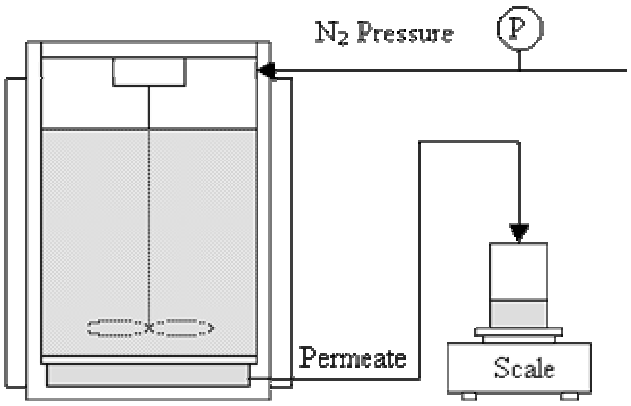

Figure 5.1.1. Set up of batch filtration cell equipped with stirrer and heating jacket.

5.1.2.4 CIP

After being flushed with water the membranes were cleaned using a 4 % solution of the chemical cleaning agent DIVOS 124 (Diversey A/S, Denmark). 500 ml of the solution was heated to 50 °C and allowed to permeate the membrane over a period of 30 min., which was sufficient to regain the initial water flux.

5.1.3 Results and discussion

5.1.3.1 Micro- and ultrafiltration

Filtration of brown juice using the five different micro- and ultrafiltration membranes at increasing pressures showed a nearly identical limiting flux around 20 $l/m^2/h$ for all the membranes, see Figure 5.1.2. The limiting flux seems to be more dependent on the properties of the feed and boundary layer mass transfer coefficient than on the actual membrane properties, such as pore size and hydrophobicity. The brown juice

probably contains some components that plug the pores, followed by a fast cake buildup on the membrane surface.

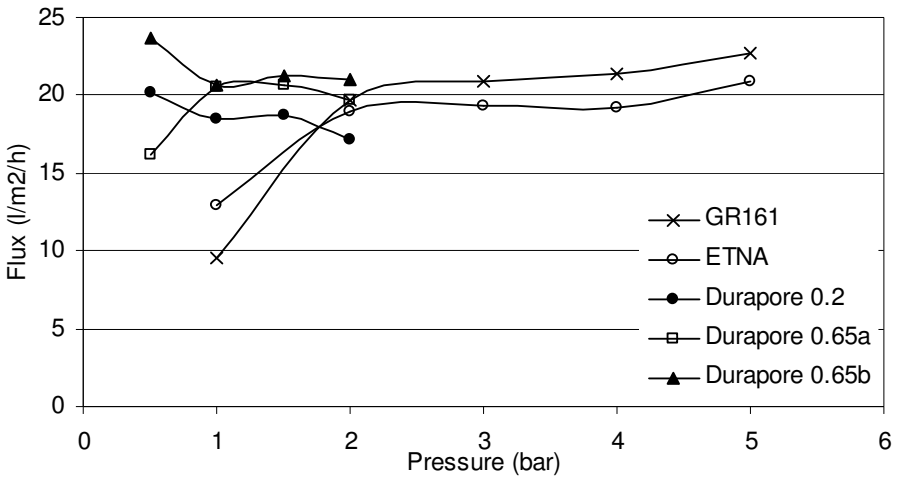

Figure 5.1.2. Limiting flux measurements for the different UF and MF membranes.

The limiting flux is reached for TMP less than 1 bar for the MF membranes and between 1 and 2 bar for the UF membranes.

A brown juice filtration was performed at 2.5 bar (TMP) with each membrane and the permeates were collected for the following nanofiltration experiments. Figure 5.1.3 shows the permeate flux vs. the natural logarithm to the concentration factor.

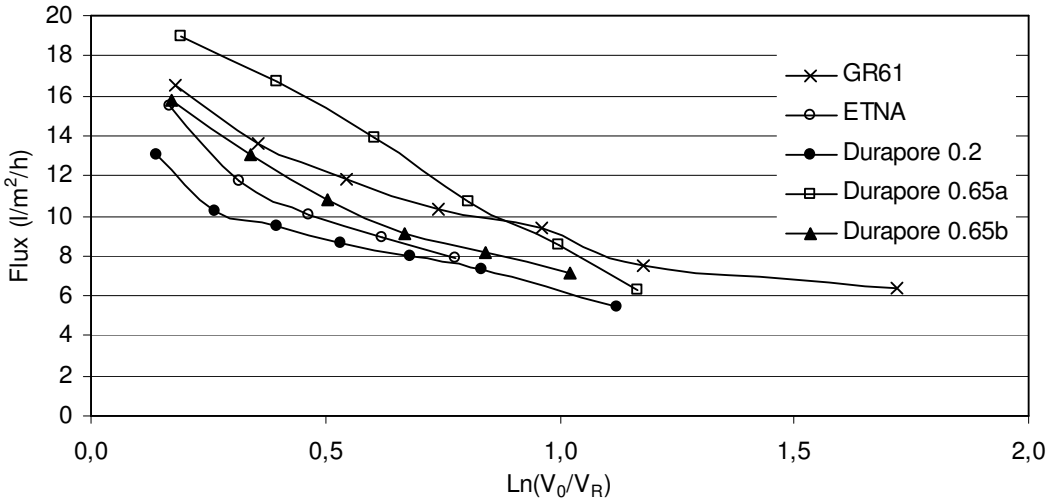

Figure 5.1.3. Permeate flux vs. the natural logarithm to the starting volume V_0 divided by the retentate volume V_R. TMP = 2.5 bar.

The initial fast drop in the flux is caused by fouling, probably a combination of pore blocking and cake layer formation, however, the data presented are insufficient for

analyzing the fouling kinetics. At 2.5 bar a theoretical maximum concentration factor of 7-10 can be determined for the ETNA, Durapore 0.2 and Durapore 0.65b membranes by extrapolating the curves from where they begin to form a straight line to the intercept with the abscissa axis.

The pure water fluxes were measured before and after the filtrations, see Table 5.1.2. After the filtrations the membranes were flushed with water before the water permeability was obtained by measuring the flux at increasing pressures, an example is given for GR61 in Figure 5.1.4.

Table 5.1.2. Pure water permeability measured before and after filtration of brown juice, and the percentage decrease in permeability due to irreversible fouling.

Permeability (l/m^2 h bar)	GR61	ETNA10A	Durapore 0.2	Durapore 0.65 a	Durapore 0.65 b
Before	57	41	1542	2008	1370
After	19	32	114	168	196
Decrease (%)	67	22	93	92	86

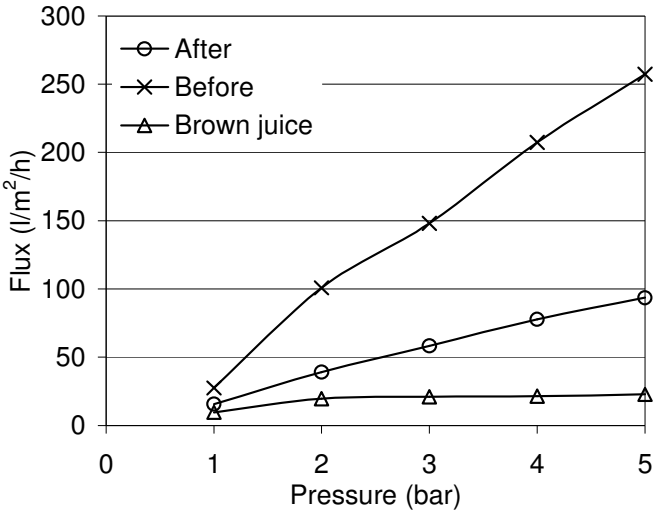

Figure 5.1.4 Permeate flux vs. trans membrane pressure for pure water before and after brown juice filtration with GR61. The permeate flux for fermented brown juice is also shown.

The irreversible fouling of the microfiltration membranes is more severe than for the ultrafiltration membranes, and the hydrophobic membranes are more susceptible to irreversible fouling than the hydrophilic membranes. However, the hydrophilic membranes have a more dense skin layer and if a membrane should be chosen solely based on flux properties as shown in Figure 5.1.3, Durapore 0.65a or GR61 are preferred.

5.1.3.2 Nanofiltration/Reverse osmosis

Experiments were performed with both untreated fermented brown juice and the collected MF/UF permeates. Based on permeate flux and rejection of Ca^{2+} and lactate during filtration of untreated juice the most suitable membrane was chosen for experiments with the different MF/UF permeates.

After compaction at 30 bar for 20 min. the water permeability of each new membrane was calculated from flux measurements at increasing TMP, see Figure 5.1.5 and Table 5.1.3. After the filtrations the membranes were flushed with clean water and the water permeability was measured once more to determine the decrease due to irreversible fouling, see Table 5.1.3. The highest water permeability reached 6.1 l/m^2 h bar, obtained with the DK membrane, followed by the NF45 membrane with 4.1 l/m^2 h bar.

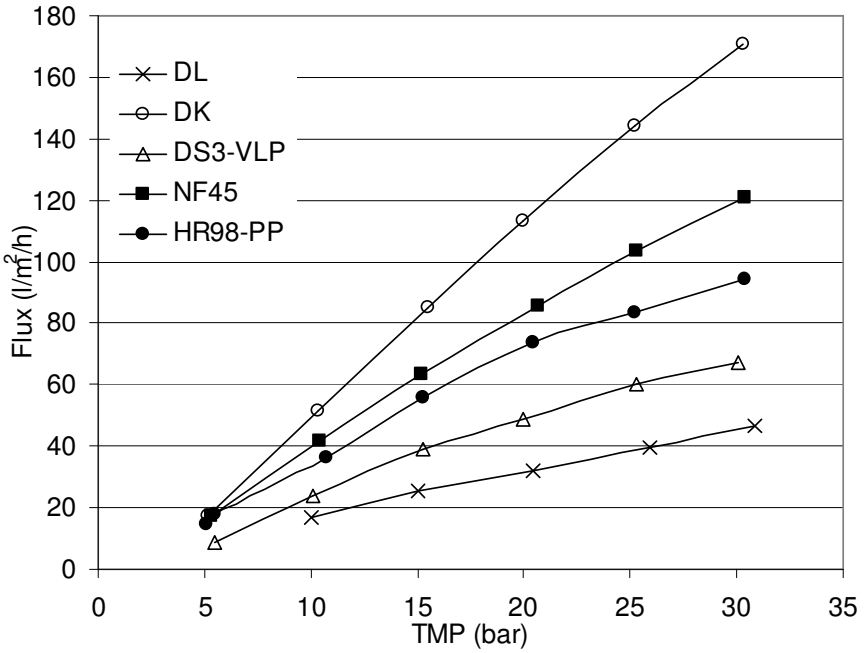

Figure 5.1.5. Pure water flux at increasing trans-membrane pressures for NF/RO membranes.

Table 5.1.3. Water permeability before and after filtration of untreated brown juice.

Permeability (l/m^2 h bar)	DL	DK	DS3-VLP	NF45	HR98-PP
Before	1.4	6.1	2,4	4,1	3,2
After	1.3	4,5	1,4	3,7	2,4
Decrease (%)	7	26	42	10	25

Figure 5.1.6 shows the permeate flux for the different NF/RO membranes when untreated fermented brown juice was filtered at increasing pressure. Approximately 10 ml of permeate was collected for each measurement. At 30 bar the permeate flux

begins to deviate from a straight line for the DK and NF45 membranes but no limiting flux where determined below 30 bar for any of the membranes. Both DK and NF45 experience high fluxes but it seems like the NF45 is less prone to fouling.

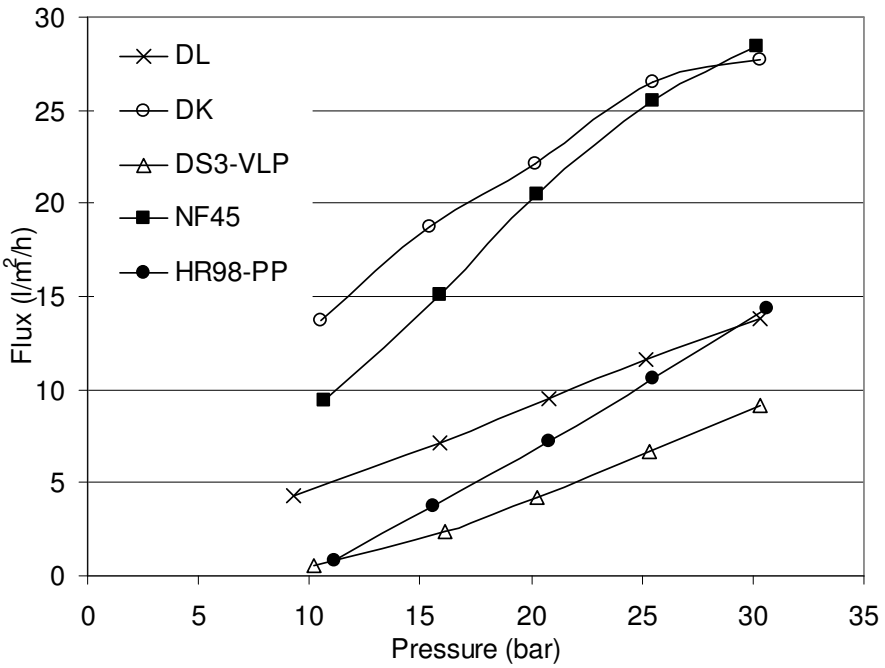

Figure 5.1.6 Permeate flux at increasing trans membrane pressures for NF/RO membranes

The filtrations were continued at a constant pressure of 30 bar and flux data collected on the computer. Figure 5.1.7 shows the flux decline after the pressure was adjusted to the final value of 30 bar using NF45.

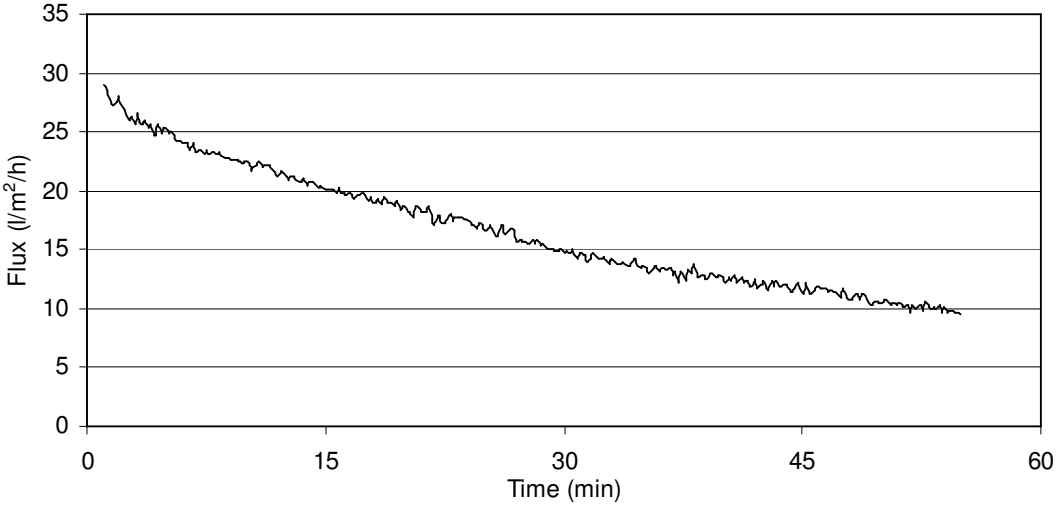

Figure 5.1.7. Flux during filtration of untreated fermented brown juice at 30 bar using NF45.

The filtrations were continued to a concentration factor of roughly 6, after which permeate was analyzed to determine rejection of lactate and calcium, see Table 5.1.4. All the filtrations were performed at pH well above the pk_a value of lactic acid which causes a relatively high rejection of lactate. The negatively charged lactate will experience higher rejection than the neutral lactic acid because of interactions with the charges on the membrane. The positive effect on transmission of lactic acid by lowering the pH have not been investigated here, but are well documented elsewhere, e.g. (Freger *et al.* 2000;Jeantet *et al.* 1996).

The brown juice contains approx. 400 ppm Ca^{2+} and even with a rejection of 99% the collected permeate will have calcium concentration of nearly 10 ppm at a concentration factor of 6. It would be unwise to perform EDBM without reducing the calcium concentration further by e.g. ion exchange or a second nanofiltration. The rejection of magnesium was only analyzed for a few samples, but was quite similar to that of calcium.

Table 5.1.4. Overall rejection of lactate and Ca^{2+} at a concentration factor of approx. 6 when filtering untreated brown juice at 30 bar.

Rejection	DL	DK	DS3-VLP	NF45	HR98-PP
Lactate	60%	30%	94%	50%	ND
Ca^{2+}	93%	84%	99%	99%	ND

By comparing permeate flux and rejection of lactate and calcium for the different membranes NF45 seems to be the most suitable membrane for filtration of brown juice. Both NF45 and DK showed high permeate fluxes, but the DK membrane only had a calcium rejection of 84 % which is not sufficient for the pre-treatment prior to electrodialysis with bipolar membranes.

It was assumed that by pre-filtering the brown juice less fouling and hereby higher fluxes could be obtained in the nanofiltration, but compared to the unfiltered juice no obvious positive effect on the permeate flux through NF45 was seen with the different MF/UF permeates. Even though the permeate flux in the nanofiltration does not increase when the broth is pre-filtered, it is doubtful whether UF/MF can be omitted on the basis of these screening experiments where the ration between liquid volume and membrane area is relatively small. If a continuous membrane bioreactor equipped with NF45 is considered, a lactate rejection of 50% would in most cases be unacceptable. The loss of product in the fermenter purge could very well be minimized, but inhibition of bacteria due to the resulting high lactate level could certainly present a problem. Considering the bacteria, pH can't be lowered directly in

the fermenter, but by lowering the pH in the permeate from a UF/MF process coupled to the fermenter, lactate rejection can be decreased in the succeeding nanofiltration.

5.1.4 Conclusion

By subjecting the fermented brown juice to nanofiltration the calcium (and magnesium) level can be reduced considerably, of importance for the subsequent bipolar electrodialysis. However, a very high concentration of calcium and magnesium in the broth combined with a high concentration factor to minimize waste of lactic acid, would likely necessitate a secondary nanofiltration process despite a high calcium rejection of 99 %.

The permeate flux through the NF membranes did not change significantly after pre-treating the brown juice using micro- or ultrafiltration. Nevertheless, due to the required pH decrease before nanofiltration, a pre-filtration is necessary if the fermentation is going to be carried out in a continuous membrane bioreactor.

5.1.5 Paper III

MICROFILTRATION USING A SUBMERGED VIBRATING HOLLOW FIBER MODULE

Garde, A., Guerra, A. and Jonsson, G.

Department of Chemical Engineering, The Technical University of Denmark, DK-2800 Lyngby, Denmark

Abstract

A novel membrane filtration system employing a submerged vibrating hollow fiber module with optional back shock is evaluated for microfiltration of baker's yeast suspensions at very low trans-membrane pressures. The filtrations were performed with 0.45 μm asymmetric hollow fibers with the skin layer on the outer side of the fibers. By stepwise increasing the permeate flux at specified rates and monitoring the transmembrane pressure in increments of 0.001 bar, critical fluxes was obtained for varying values of yeast concentration (5 and 50 g/l), vibrating frequency (5, 17.5, and 30 Hz), vibrating amplitude (1, 2, and 3 mm) and different back shock parameters. The critical flux increased with frequency and amplitude and an improvement of 325% was obtained with a 5 g/l yeast suspension by changing the vibrations from 1 mm at 5 Hz to 3 mm at 30 Hz resulting in a critical flux of 68 l/m^{2}h at a transmembrane pressure of 6 mbar. The use of back shock did not enhance the critical flux to any significant extent, and in one instance the critical flux was even reduced.

Keywords: Microfiltration, hollow fiber, vibration, back shock.

Introduction

Microfiltration (MF) is a pressure-driven membrane process that retains suspended colloids and particles while macromolecules such as proteins are allowed to pass through. Although MF is one of the oldest membrane processes, the application of MF is often limited by the occurrence of severe membrane fouling, provoked by the retained collides or particles. To reduce fouling in MF systems, it is necessary to

generate tangential forces across the membrane that can promote transport of the retained material away from the membrane surface. However, this is not an easy task as the retained materials in microfiltration systems often are colloids or small particles with very low diffusion coefficients. Several hydrodynamic approaches, which focus on increasing the mass transport of the retained materials, have been proposed in the last years (Winzeler,H.B.& Belfort G. 1993; Belfort et al 1994). In most cases this is achieved by using high cross flow velocities, generation of secondary flows at the membrane surface, feed flow pulsation, backflushing of the membrane with the permeate or air injection in the feed flow (Belfort et al 1994).

In dynamic filtration the hydrodynamic improvement is generated by the mechanical movement of the membrane itself or by movement of a body near the membrane surface.

Dynamic filtration should not be confused with dynamic membranes; in this case a secondary dynamic membrane is intentionally formed on the top of the membrane as a porous cake layer (Al-Malack M.D and Anderson, G.K 1996 Guell,C. 1999, Kuberkar, V.T. and Davis R.H. 2000).

In literature, only few examples can be found where dynamic filtration is applied to increase filtration performance. Three different dynamic filtration systems with circular flat sheet membranes and one with tubular membranes have been identified.

In the example where tubular membranes are utilized an inner membrane cylinder rotates inside a pipe (see Figure 5.1.8) generating centrifugal instabilities. These centrifugal instabilities, called Taylor vortexes, have been well analyses and modelled by a number of researches (Belfort G. et al. 1993a, Belfort G. et al 1993b, Wronski et al 1989, Tobler 1982, Murase, T. 1991a). The rotating cylindrical membrane modules, using ceramic membrane, proved to be effective in sweeping the filter cake during microfiltration of several biological solutions. The performance of the filtration was depending on the rotation rate with a more marked dynamic effect at high feed concentration. However, when high rotation speeds were used the initial permeate flux decreased due to centrifugal forces (Murase et all 1991b, Park, J.Y et al 1994.). Several researches used this type of module to study the different types of fouling as a function of the system hydrodynamics (Belfort G. et al. 1993a, Belfort G. et al 1993b). The advantages of this type of device are the excellent bulk fluid mixing, high wall shear rates, and weakly decoupled cross flow with transmembrane flux. The limitations are the high-energy consumption and the difficulties in scaling up (Belfort G. et all 1994).

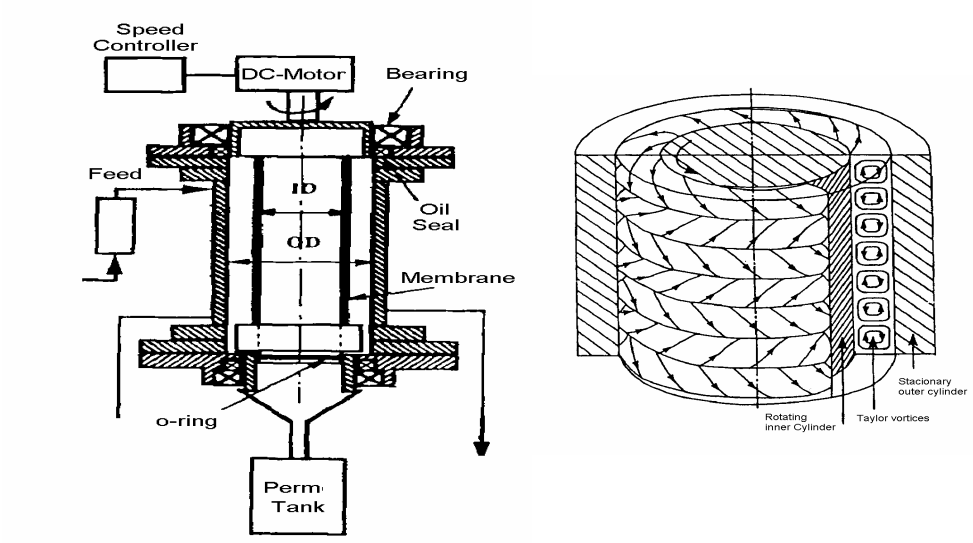

Figure 5.1.8. Rotating annular filter on the left and the Taylor vortices generate by the rotation on the right (Park et al 1994).

Several companies (Pall corp., NY and ABB flootek, Malmo Sweden) have commercialized a rotating disk system. In this system a disk rotates between two static flat sheet membranes generating spiral vortices. By partially removing the filter cake, the rotating disk dynamic filter improved both the protein transmission and the permeate fluxes (Lee S.S. et al 1995; Frenander, U and Jonsson A-S. 1996, Bouzerar R. et al 2000). However, the viscosity and solids content on the feed side adds to energy consumption and the complexity of the system makes it difficult for large-scale applications.

A second concept developed by Pall called the *vibrating membrane filtration* (VMF) system tried to overcome these problems by replacing the rotation of the membrane by torsion. In this system the circular plate and frame membrane moves forward and backwards using a torsion bar (see Figure 5.1.9).

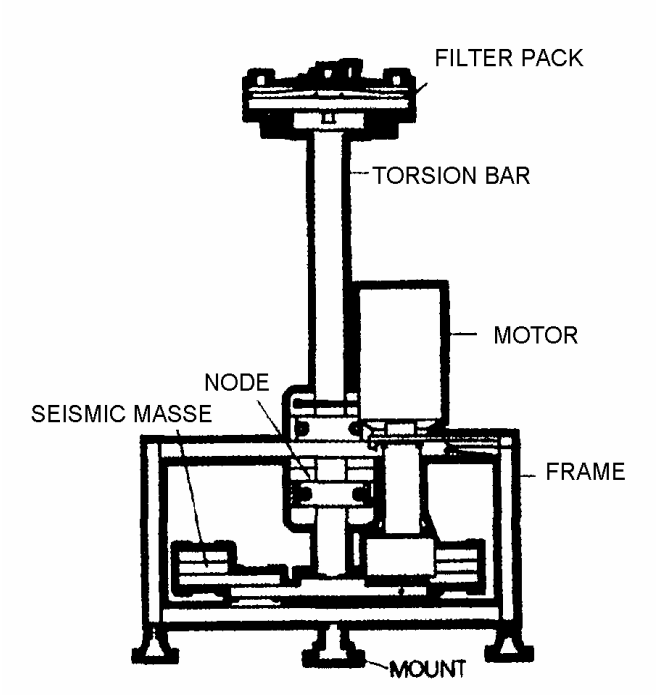

Figure 5.1.9. **The PallSep vibrating membrane filtration system (VMP). (Pall Europe 1997)**

In the VMF system the energy is directed to the membrane itself, having higher energy efficiency when compared to the rotating disk system (Pall Europe 1997). The VMP can generate shear rates about 120 000 s^{-1} and proved to be useful in preventing fouling in ultrafiltration of water coagulated by PAC (Takata, K. et al 1998). However, some problems related to pressure drop and mass transfer from the center to the edge of the membrane can occur due to the difference in the shear stress induced along this axis.

Engler J. and Wisner, M. R. (2000) assembled a circular membrane on a top of a rotating disk (see Figure 5.1.10), which was inserted inside a cylindrical vessel. By using the rotating membrane disk to filter silica particles (size 0.67μm) or glass sphere (size 3μm to 25μm) suspensions, the membrane fouling could be controlled and it was dependent on the rotation rate and transmembrane pressure. The permeate flux was relatively insensitive to particle concentration in the feed stream. However, the radial distribution of the transmembrane pressure drop generated by the high rotation rates may locally reduce or reverse the permeate flux across the membrane. A decrease of the initial water flux with the rotation speed was also observed.

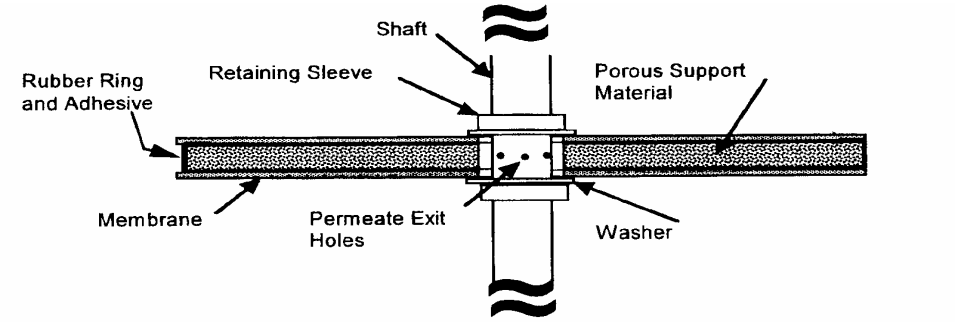

Figure 5.1.10. Schematic drawing of the Rotating Membrane Disk (Engler, J. and Wisner, M.R. 2000)

In the present work an experimental submerged vibrating filtration system using microfiltration hollow fibers was developed. The hollow fibers, submerged inside a cylindrical vessel, vibrate in a vertical movement with a specified frequency and amplitude. The system was evaluated at different vibration amplitudes and frequencies and different concentrations of yeast suspensions. The effect of short backflushings (back shocks) was also studied.

Materials and methods

Filtration rig

A bench-scale vibrating membrane system was built to evaluate performance and fouling behavior during treatment of yeast suspensions, see Figure 5.1.11. The membrane module with a total membrane area of 256 cm^2 was composed of 12 cm long hollow fibers, fixed in parallel between two circular steel plates. To prevent breakage caused by the vibrations a flexible sealing consisting of silicone tubes were placed as a transition between hollow fiber ends and the steel plates. The hollow fibers supplied by X-Flow were made of polyethersulfone with the skin layer on the outer surface and a nominal pore size of 0.45 μm. The clean water permeability of these membranes at 30°C was 12,000 $Lh^{-1}m^{-2}bar^{-1}$. The two steel plates were fixed to a hollow steel rod, which extended through the top of a cylindrical acrylic vessel to connect with a ball bearing placed acentric on the axis of an electromotor. Rotation of the motor hereby induced perpendicular movement of the steel rod, which was kept in contact with the ball bearing by a strong spring. By changing the acentric position of the ball bearing the amplitude of the vibration could be changed between 1, 2 and 3 mm. By controlling the speed of the motor, the frequency of the vibrations could be adjusted between 0 and 30 Hz. To direct the vibration only in the vertical movement a

cavity in which the steel rod could engage was placed at the bottom of the acrylic vessel. This change was only introduced in the second set of experiments.

The lower end the fibers was blocked and at the upper end they open into a small compartment, connected, through the hollow rod, to a positive displacement cavity pump (Seepex M120-0, Seeberger, Germany) where permeate was sucked out. Transmembrane pressure (TMP) was measured as the difference between permeate and module headspace pressures, using a pressure transducer (RS 286-692, RS-components, USA) linked to a computer. With this pressure transducer, it was possible to detect variations in the transmembrane pressure of the order of 1 mbar. Mass flow of permeate was measured on a balance and logged (PB3002, Mettler Toledo, Switzerland) before it was returned to a thermostatic feed tank. Feed solution was circulated from the feed tank via a gear pump (Micropump® F5734, Concord CA, USA) to an inlet in the bottom of the housing and returned from the outlet in the top above the fibers.

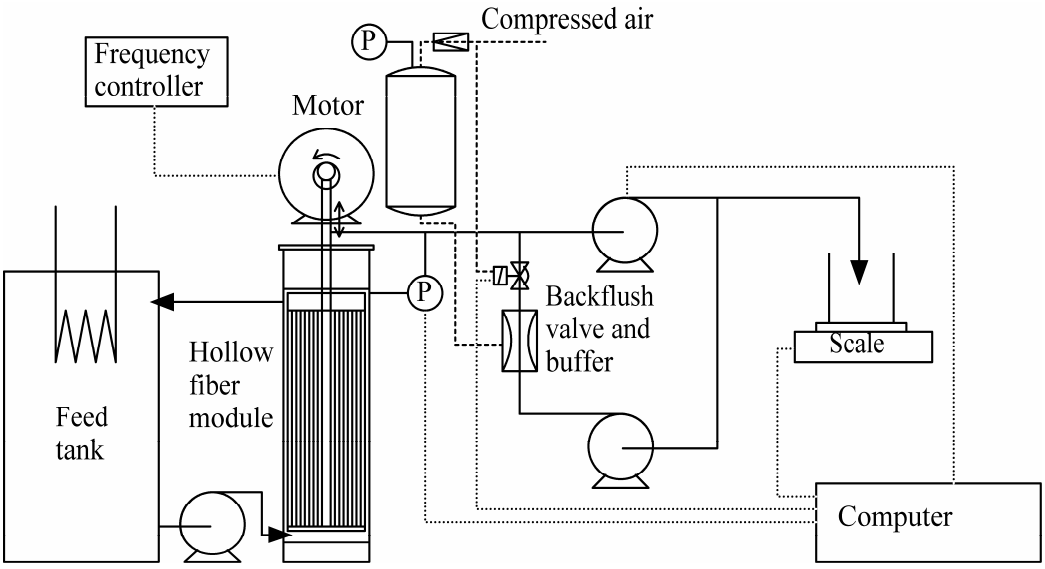

Figure 5.1.11. Schematic drawing of the experimental apparatus.

The system was also equipped with a back shock unit where part of the permeate was pressurized in a back shock buffer using a positive displacement pump (Seepex M120-0, Seeberger, Germany), before it was injected back into the permeate side in pulses. Compressed air was applied to the back shock buffer to insure a near constant pressure during the release phase or “the shoot”, where permeate was flushed from the lumen and out into the feed stream. The computer connected to a pressure valve controlled the time between shoots and duration of shoot.

Yeast cells Solution

Baker's yeast suspensions were used to test this new vibrating microfiltration system. The motive for choosing yeast suspensions as the test medium is its widespread use in the biotechnology industry, its easy availability and the large amount of studies done with microfiltration of yeast suspensions.

Yeast cell suspensions with dry weight of either 5g/l or 50g/l were prepared by using commercially available wet cake baker's yeast (Malteserkors Gær, Danisco Distillers, Grenaa - København, Denmark) suspended in 1 mM phosphate buffer and 1g/l of peptone. The average dry weight content of the initial wet yeast is 27% with small variations (± 1%).

Critical flux

The critical flux concept was used to evaluate the filtration performance. The critical flux hypothesis for microfiltration is that on start-up there exists a flux below which a decline of flux with time does not occur; above it fouling is observed. This flux is the critical flux and its value depends on the hydrodynamics and probably also on other variables (Field, R.H et al., 1995; Howell, J. A.1995).

The strong form of the hypothesis is that a flux exists corresponding to the clean water flux. The weak form of the hypothesis is that a flux exists that is rapidly established and maintained but at a lower flux than the clean water flux due to adsorption on the membrane surface (Field, R.H et al., 1995; Howell, J. A.1995). Wu, D. et al.(1999) experimentally found these two types of critical flux by using very sensitive equipment and a model solution of silica BSA and yeast.

The critical flux concept implies that it is possible to maintain a constant flux (at constant TMP) as long the constant flux is below the critical flux, which can be estimated theoretically or experimentally. (Bacchin P. et al., 1995).

Effect of vibration

A first set of experiments was performed to investigate the influence of vibrations on filtration performance. The effect of vibration on the critical flux is composed of an effect from the amplitude and an effect from the frequency. These two variables were investigated at 3 levels each for a 5g/l yeast cell solutions. The experimental plan consisted of 11 filtrations run in random order (see Figure 5.1.12). Between each filtration the clean water flux was 100 % recovered by cleaning the membrane with a

1% solution of of Divos 124 (from Scan Diversy) and a 0.1 % solution of hydrogen peroxide.

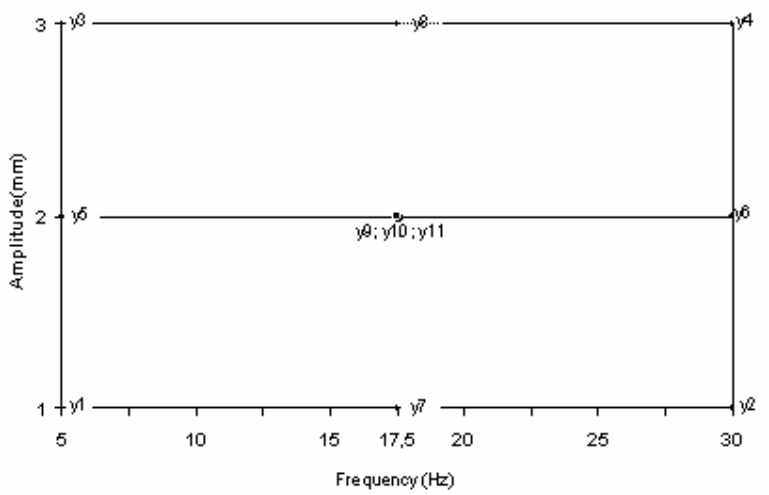

Figure 5.1.12. Three level experimental design used to study the vibration effect. The central trial y9, y10 and y11 are replicates.

In order to find the critical flux the permeate flow was controlled by a computer program in steps of approx. 4 $Lh^{-1}m^{-2}$ and intervals of 3 minutes. The flow was increased two steps for 3 minutes and when reduced one step for 3 minutes. This procedure was repeated throughout the filtration. The transmembrane pressure (TMP) and permeate flux was logged every ½ second. The critical flux (J_{pcrit}) identified as the maximum permeate flux where $\Delta P/\Delta t$ was less than 2 mbars/step and TMP was recovered when returning to the last tested permeate flux (one step back).

Effect of yeast concentration and backshock

A total of 9 experiments were completed in the second set of experiments to analyze the effect of backshock and yeast concentration on filtration performance. The frequency and amplitude of the vibration was either set to the maximum possible with this system (30 Hz, 3 mm) or the vibrations were turned off entirely. Two concentrations of yeast cells (5 and 50 g/l) were prepared and different backshock volumes were used, as shown in Table 5.1.5. The time between backshock was kept constant at 5 sec. and the duration of the backshock was 0.2 sec where the backshock volume was released at 1 bar.

Table 5.1.5. Experimental plan for investigating effects of backshock and concentration

Exp	Concentration (g/l)	Vibration		Backshock		
		Frequency (Hz)	Am (mm)	Flow (g/h)	Flux ($Lm^{-2}h^{-1}$)	Volume (ml)
B1	5	30	3	260-/+7%	10,4	0,36
B2		30	3	130+/-7%	5,2	0,18
B3		0	0	300+/-7%	12,0	0,42
B4		30	3	-	-	-
B5		0	0	-	-	-
B6	50	30	3	260-/+7%	10,4	0,36
B7		30	3	-		-
B8		0	0	490+/-9%	19,6	0,68
B9		0	0	-	-	-

The critical flux concept was used to evaluate the filtration performance. The methodology to find the critical flux was the same as described above.

Results and Discussion

Effect of vibration

Raw data analyses

The highest critical flux was obtained in trial Y4 where the vibration frequency and amplitude were at it's maximum (see Table 5.1.6 and Figure 5.1.13). The highest fluxes were obtained at the highest combination of amplitude and frequency. The effect in increasing the vibration amplitude was larger when the vibration frequency was high.

Table 5.1.6. Critical fluxes obtain for different amplitudes and frequencies using 5 g/l yeast suspension.

Experiment	Freq. (Hz)	Am (mm)	Critical Flux ($Lh^{-1}m^{-2}$)	Improvement
Y1	5	1	16	0%
Y2	30	1	36	125%
Y3	5	3	29	81%
Y4	30	3	68	325%
Y5	5	2	29	81%
Y6	30	2	50	213%
Y7	17,5	1	42	163%
Y8	17,5	3	45	181%
Y9	17,5	2	39	144%
Y10	17,5	2	42	163%
Y11	17,5	2	41	156%

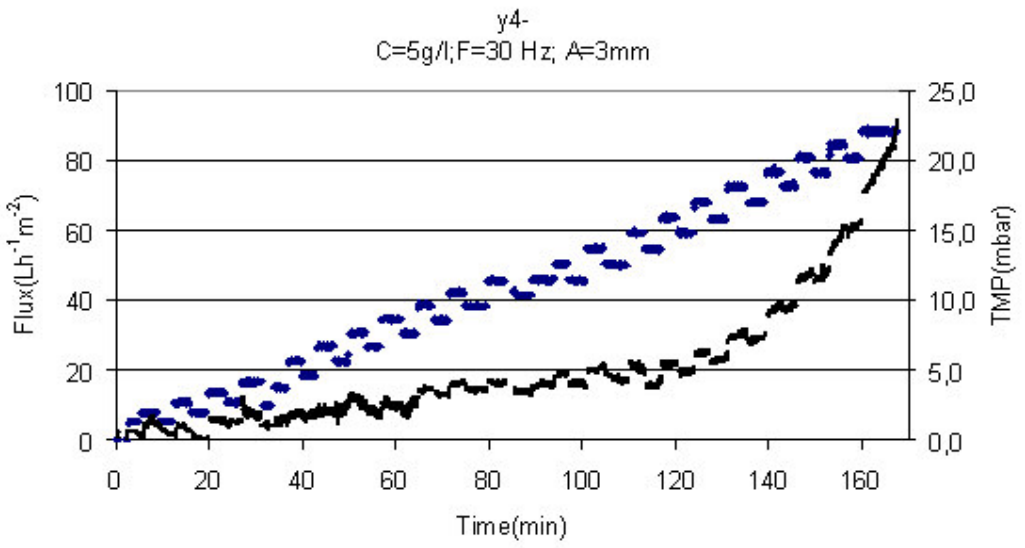

Figure 5.1.13. Permeate flux and transmembrane pressure versus time for the trial y4.

When the permeate flux was under its critical value the membrane permeability was equivalent to the clean water flux indicating that the only resistance toward permeation was the membrane resistance.

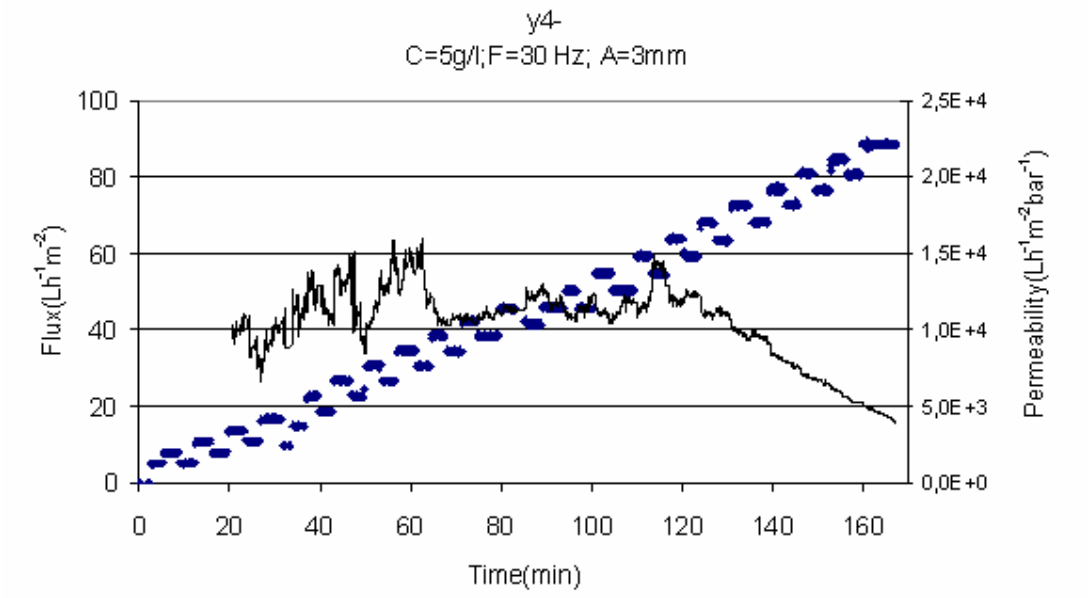

Figure 5.1.14. Permeate flux and membrane permeability versus time for the trial y4.

After passing the critical flux no visual cake formation was observed when the frequency was 30 Hz, but at 5 Hz it was possible to observe a dense deposit of yeast cells on the membrane surface (see Figure 5.1.15).

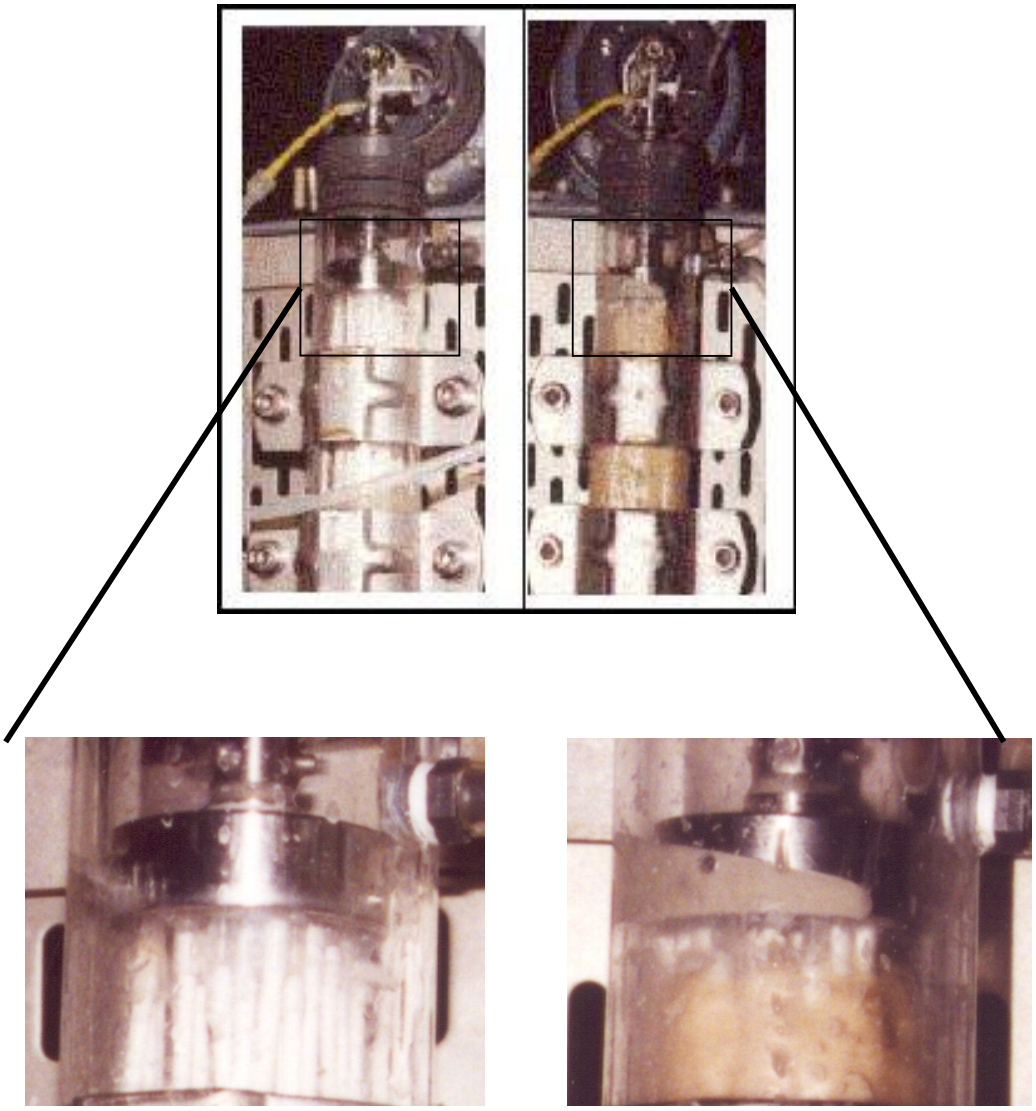

Figure 5.1.15. Photography of the filtration module after filtrations. On the left with a vibration of 30 hz amplitude 3 mm and on the right with a vibration 5 Hz amplitude 1.

Gupta, B.B. et all (1995) used helical-shaped baffles, centrally supported inside the lumen of a tubular ceramic 0.14 μm membrane to enhance mass transfer and prevent cake formation at the membrane top during filtration of a 5 % dry weight baker's yeast solution. For a transmembrane pressure of 0.2 bars a limiting flux of 45 Lh^{-1} m^{-2} after 120 minutes of filtration was reported. Using a similar system Field R.W. at all (1995) introduced the critical flux concept hypothesis, where for a 5% dry weight baker's yeast solution a critical flux of 40 Lh^{-1} m^{-2} was reported. In this work the critical flux corresponded to 80% of the clean water flux. Wu. D et all (1999)

reported on critical fluxes for a 5% yeast solution at a Reynolds number of 580. Critical fluxes for 50k and 100K MWCO membranes were 23 Lh^{-1} m^{-2} for a TMP of 44 mbar and 12 Lh^{-1} m^{-2} for a TMP of 12 mbar, respectively. They found that it was impossible to measure the critical flux for a 0.2 μm membrane, because the transmembrane pressure increased even when the permeate flux was only 8 $L.h^{-1}.m^2$.

By using the vibration submerged membrane system the strong from of critical flux (the permeate flux equals the clean water flux) was for 5 g/l yeast suspension 60 $Lh^{-1}m^{-2}$ at a transmembrane pressure of 5 mbar (see Figure 5.1.13).

Silva C.M. et al (2000) used a submerged hollow-fiber membrane system (pore size 0,1 μm) with aeration to promoted turbulence and reported for a 0,98 Wt% baker's yeast solution a permeate flux of 24,6 $Lh^{-1}m^{-2}$ at a transmembrane pressure of 16,9 kPa (169 mbar).

An interesting phenomenon common to the filtration done at high vibration amplitude and frequency, was the appearance of air bubbles in the permeate stream after passing the critical flux or for transmembrane pressures over 30 mbar. When air bubbles started to appear in the permeate stream, the transmembrane pressure started to increase exponentially indicating a possible blocking of the membrane pores with air. The reason for this could be related to the setup of the experimental system. The membrane reservoir is open to the air (atmospheric pressure) and when the system vibrates it is possible that some air is dissolved in the filtration media. Since the permeate stream is under a slight vacuum expansion of tiny air bubbles in the membrane skin layer can consequently lead to blocking of the membrane pores. It is important to mention that below the critical flux the only resistance towards the permeate flux is membrane resistance and no cake deposits are formed on top of the membrane. The absence of this cake allows the air to penetrate into the membrane pores. A possible way of solving this problem is by pressurizing the membrane container instead of applying vacuum on the permeate side. At these conditions the air expansion is minimized, which may increase the critical permeate flux even more.

Modelling of the vibration frequency and amplitude effects

The data from Table 5.1.6 were fitted an ANOVA (analysis of variance) model using the PLS (partial least squares) as fitting method. The fraction of variation of the response explained by the model (R^2) was 0,98 and the fraction of variation of the response that can be predicted by the model (Q^2) was 0.74. The model shows a significant effect of both frequency (Freq) and amplitude (am) on the critical flux (see

Figure 5.1.16). The frequency of vibration had a somewhat larger effect than amplitude on the critical flux.

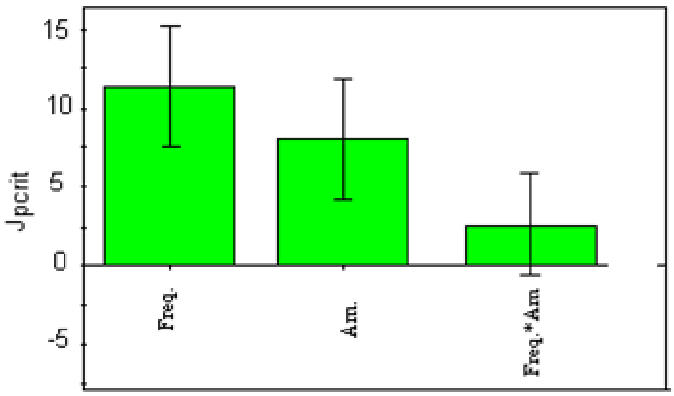

Figure 5.1.16. Resume graphic of the variables effects in the critical flux.

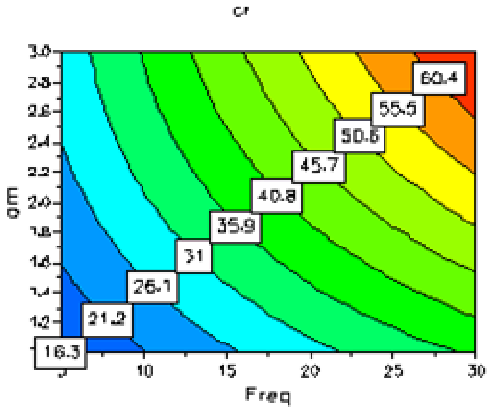

Figure 5.1.17. Responses counterplot of the critical flux. The effect of the vibration amplitude (am) can be seen versus vibration frequency (Freq). The curves separate areas with the same critical flux, given in the boxes.

For the studied range an increase of amplitude and frequency resulted in an enhancement of the critical flux (see Figure 5.1.17). This indicates that no experimental optimum was reached. The effect of increasing the intensity of the vibrations was equivalent to increasing sheer forces during cross flow filtration. The increase in vibration intensity results in high back transportation of yeast cells from the membrane to the bulk solution resulting in a more clean membrane surface and consequently a higher critical permeate flux. Although no optimum was found within

the applied frequency and amplitude range an economic optimum must exit where the energy spent on increasing the vibration intensity is not sufficiently compensated by increasing permeate flux. Vibration intensity is also limited by the structural stability of the filter.

Effect of Yeast concentration and backshock

Critical flux measurements for the second set of experiments are shown in Table 5.1.7. The variation between the critical flux obtained in run Y4 (68 $Lm^{-2}h^{-}1$) in the first set of experiments and run B5 (40 $Lm^{-2}h^{-}1$) in the present set is quite large even though identical parameters are used. This is most likely due to a modification of the experimental equipment after the first set of trials to stop small, unwanted horizontal movements of the filter during vertical vibrations (a guide for the lower end of the filter was introduced). In the case where no, or very limited vibrations were employed, only a very small difference in the critical flux exists between the two sets of experiments.

Table 5.1.7. Critical flux measurements.

Exp	Concentration (g/l)	Freq. (Hz)	Am	BSFlow (g/h)	Fcritical (Lh-1m-2)
B2	5	30	3	260-/+7%	45
B3		30	3	130+/-7%	40
B4		0	0	300+/-7%	21
B5		30	3	-	40
B6		0	0	-	18
B7	50	30	3	260-/+7%	21
B8		30	3	-	32
B9		0	0	490+/-9%	7
B10		0	0	-	7

Critical flux decreased as yeast concentration was increased from 5g/l to 50g/l and the extent of the drop in the critical flux was depending on the vibrations. With no vibrations the critical flux dropped 61%, from 18 to 7 $Lm^{-2}h^{-1}$, whereas only a 20% decrease, from 40 to 32 $Lm^{-2}h^{-1}$ was observed when vibrations were applied. The filtration system seems to be well suited for feed solutions with high dry weight contents. The energy efficiency of the vibrating filter was not investigated but is assumed to be comparable to that of Pall's VMF system since little or no pumping of feed is needed to induce shear and therefore a clear advantage over crossflow filtration is apparent for high viscosity solutions.

The backshock had no positive effect on the critical flux when 50 g/l yeast solution was filtered. Without vibrations the extra 19.6 $Lm^{-2}h^{-1}$ (cf. Table 5.1.5) of permeate spent for backshock did not pay back in the form of higher effective critical flux. When the vibrations where on, the critical flux even dropped from 32 to 21 $Lm^{-2}h^{-1}$ because of the backshock. At low yeast concentrations, backshock provided a modest increase of 13% and 17% in critical flux at high backshock volumes, when vibrations where applied or omitted, respectively. The low backshock volume used in run B3 did not have any positive effect on the critical flux. It was the intent to target a certain backshock volume (a percentage of earlier obtained critical fluxes), but due to difficulties in controlling the backshock pump precisely, it was not possible to achieve the desired volume in the shoots. Of the same reason no attempts were made to pinpoint optimal parameters for the backshock.

The most striking effect of applying vibrations was seen for the high yeast concentration where the critical flux increased 357% from 7 $Lm^{-2}h^{-1}$ to 32 $Lm^{-2}h^{-1}$.

Conclusion and recommendation for future work

A membrane filtration rig has been built that utilizes a novel combination of hollow fibers and vibrations for reduction of fouling. For a reversed 0.45 μm asymmetric hollow fiber membrane critical fluxes were measured in a constant-flux mode for baker's yeast suspensions at different vibration frequencies and amplitudes.

In the studied range of frequencies and amplitudes it was not possible to find an experimental critical flux optimum, the critical flux kept increasing with frequency and amplitude as the upper limit of the two parameters were reached. The increase of the vibration frequency had a larger effect on the critical flux than the increase of the vibration amplitude. The highest critical flux was 68 $Lm^{-2}h^{-1}$ obtained at a frequency of 30 Hz and amplitude of 3 mm with a 5 g/l yeast solution and a transmembrane pressure of 6 mbar.

The effect of employing backshock was not evident, but for the low yeast concentration (5 g/l) a moderate increase of 13-17% in the critical flux was observed. At high yeast concentration (50 g/l) the backshock had a negative effect on critical flux, but the effect of vibrations were very encouraging. Vibrations at 30 Hz and 3 mm improved the critical flux by 357% compared to filtration witout vibrations.

From an academic point of view the small, uncontrolled horizontal movements encountered during the first set of experiments was of annoyance, disturbing the standard of reference. However, this more or less elliptical movement of the filter did

increase the critical flux from 40 to 68 $Lm^{-2}h^{-1}$ and should therefore not be ignored but seen as a subject for further investigations.

At high frequency and after the critical flux was passed, air bubbles appeared in the permeate accompanied by exponential increase in transmembrane pressure. It is very important to investigate the cause of air bubbles in the permeate and it's effect on filtration performance. A possible way of solving this problem is by pressurizing the membrane container instead of applying vacuum on the permeate side. At these conditions the air expansion is minimized, which may increase the critical permeate flux even more.

References

Al-Malack, M.H. and Anderson, G.K. 1996, Formation of a Dynamic Membrane with Crossflow Microfiltration, *J Membrane Sci,* **112,** pp.287-96.

Bacchin, P., Aimar, P., and Sanchez, V. 1995, Model for Colloidal Fouling of Membranes, *AIChE J,* **41,** pp.368-76.

Belfort, G., Davis, R.H., and Zydney, A.L. 1994, The Behavior of Suspensions and Macromolecular Solutions in Crossflow Microfiltration, *J Membrane Sci,* **96,** pp.1-58.

Belfort, G., Mikulasek, P., Pimbley, J.M., Chung, K.-Y., and b). 1993, Diagnosis of membrane fouling using a rotating anular filter.2. Dilute particle suspensions pf known particle size, *J Membrane Sci,* **77,** pp.23-39.

Belfort, G., Pimbley, J.M., Greiner, A., Chung, K.-Y., and a). 1993, Diagnosis of membrane fouling using a rotating annular filter,1. Cell culter media, *Journal of the membrane Science,* **77,** pp.1-22.

Bouzerar, R., Jaffrin, M.Y., Lefevre, A., and Paullier, P. 2000, Concentration of Ferric Hydroxide Suspensions in Saline Medium by Dynamic Cross-flow Filtration, *J Membrane Sci,* **165,** pp.111-23.

Engler, J. and Wiesner, M.R. 2000, Particle Fouling of a Rotating Membrane Disk, *Water Research,* **34,** (2), , pp.557-65.

Field, R.W., Wu, D., Howell, J.A., and Gupta, B.B. 1995, Critical Flux Concept for Microfiltration Fouling, *J Membrane Sci,* **100,** pp.259-72.

Frenander, U. and Jonsson, A.-S. 1995, Cell Harvesting by Cross-Flow Microfiltration Using Shear-Enhanced Module, *Biotech Bioeng,* **52,** pp.397-403.

Gupta, B.B., Howell, J.A., and Field, R.W. 1995, A Helical Baffle for Cross-flow Microfiltration, *J Membrane Sci,* **102,** pp.31-42.

Güell, C., Czekaj, P., and Davis, R.H. 1998, Microfiltration of Protein Mixtures Using Yeast to Reduce Membrane Fouling, *J Membrane Sci,*

Howell, J.A. 1995, Sub-critical Flux Operation of Microfiltration, *J Membrane Sci,* **107,** pp.165-71.

Kuberkar, V. and Davis, R.H. Effects of Added Yeast on Protein Transmission and Flux in Crossflow Membrane Microfiltration, (In Press) *Biotechnol.Prog.* 1998,

Lee, S.S., Burt, A., Russotti, G., and Buckland, B. 1995, Microfiltration of Recombinat yeast Cells Using a Rotating Disk Dynamic Filtration System. *Biotech Bioeng,* **48,** pp.386-400.

Murase, T., Iritani, E., Chidphong, P. et al. 1991, High-speed Microfiltration Using a Rotating, Cylindrical Ceramic Membrane, *International Chemical Engineering,* **31,** (2), , pp.370-8.

Murase, T., Pradistsuwana, C., Iritani, E., Kano, K., and b). 1991, Dynamic Microfiltration of Dilute Slurries with a Rotating Ceramic Membrane, *J Membrane Sci,* **62,** pp.187-99.

Pall Europe. 1997, New Membrane Methods for Food Processing, *Filtration & Separation,* **July/August,** pp.568-70.

Park, J.Y., Choi, C.K., and Kim, J.J. 1994, A Study on Dynamic Separation of Silica Slurry Using a Rotating Membrane filter. 1. Experiments and Filtrate Fluxes, *J Membrane Sci,* **97,** pp.263-73.

Takata, K., Yamamoto, K., Bian, R., and Watanabe, Y. 1998, Removal of humic Substances with vibratory shear Enhanced Processing Membrane, *Desalination,* **117,** pp.273-82.

Tobler, W. 1982, Dynamic Filtration:Principal and Aplication of Sheer Filtration in an Annullar Gap, *Filtration & Separation,* **19,** pp.329

Winzeler, H.B. and Belfort, G. 1993, Enhanced Performance for Pressure-driven Membrane Processes: The Argument for Fluid Instabilities. *J Membrane Sci,* **80,** pp.35-47.

Wronski, S., Rundiak, L., and Molga, E. 1989, Resistance model for High-shear Dynamic Filtration, *Filtration & Separation,* **26,** pp.418

Wu, D., Howell, J.A., and Field, R.W. 1999, Critical Flux Measurement For Model Colloids, *J Membrane Sci,* **152,** pp.89-98.

5.2 Reverse Electro-Enhanced Dialysis

5.2.1 Introduction

The efforts that eventually led to a patented recovery process are founded in years of work attempting to employ electrodialysis technology for recovering lactic acid from different fermentation media.

Extracting organic acids from fermentation broth through ion-exchange membrane accomplishes many advantageous separations in one step. Only small (MW < 1000) organic molecules are extracted and of these, predominantly charged ions like inorganic ions and organic acids. Retained in the depleted broth is most bio-matter, including cells and proteins, as well as the unconverted substrates. The feed stream can be recycled to the fermentation for further substrate utilization with reduced inhibition of cell growth. If only anion-exchange membranes are utilized, scaling problems are avoided and only inorganic anions and negatively charged organic acids and amino acids are extracted.
To preserve electroneutrality of this separation process, the extracted anions can preferably be substituted by hydroxide ions. This makes the depleted fermentation broth alkaline, and the recycled stream assists or replaces the pH-control of the fermentation.

This principle resembles a Donnan dialysis process as shown in Figure 5.2.1. It was suggested and patented by Dr. Böddeker and others in 1998 (Böddeker *et al.* 1997). The feed stream, which is rich in organic acid and other bio-matter, is pumped directly from a fermenter into every second chamber in a membrane stack. The low pH (around 5-6) of the feed compared to an alkaline solution in every other second flow chamber generates a concentration difference for hydroxide ions across the anion-exchange membranes. This causes hydroxide ions to diffuse through the membranes, producing a positive potential difference across the membranes. This potential drives anions like lactate out of the feed solution in the opposite direction of the hydroxide ions. This way lactate is extracted from the feed into the alkaline solution while it passes through the Donnan dialysis stack.

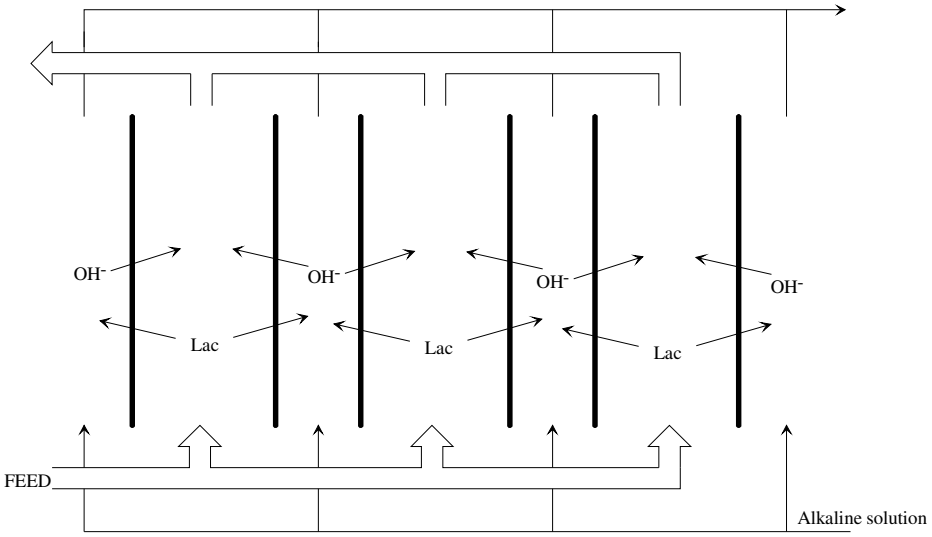

Figure 5.2.1. Extraction of lactate ions (Lac) in Donnan dialysis with just anion-exchange membranes.

Dr. Böddeker addresses the fouling issues by commenting that the high flow velocity keeps the fouling build-up at a minimum, because of high surface shear. Also the constant flux of hydroxide ions into the feed stream is assumed to continuously remove or destabilize any fouling build-up. Furthermore, the process demonstrates the advantages of high selectivity towards the organic acids as suggested above. The main disadvantage of the Donnan dialysis process is a slow flux of organic acids out of the feed, increasing demands for large membrane areas.

Previous experiments with reverse electrodialysis have demonstrated good anti-fouling results in process streams from fermentation broth (Garde and Rype 1997). Experiments with short pulses of reversed electrical current in order to destabilize a fouling layer gave no conclusive results (Garde *et al.* 2002). The scope of the continuous development process was to investigate whether it would be beneficial to enhance the lactate extraction flux utilizing electrical current while maintaining the efficient setup of the Donnan dialysis process as demonstrated in Figure 5.2.1.

A problem that must be addressed when adding electrical current to a Donnan dialysis setup is competitive ion transport. The competitive transport is demonstrated in Figure 5.2.2. When adding electrical current to the dialysis setup, the anions are the only ions allowed to travel through the stack. And lactate and hydroxide ions are both going to compete against each other for transferring the current.

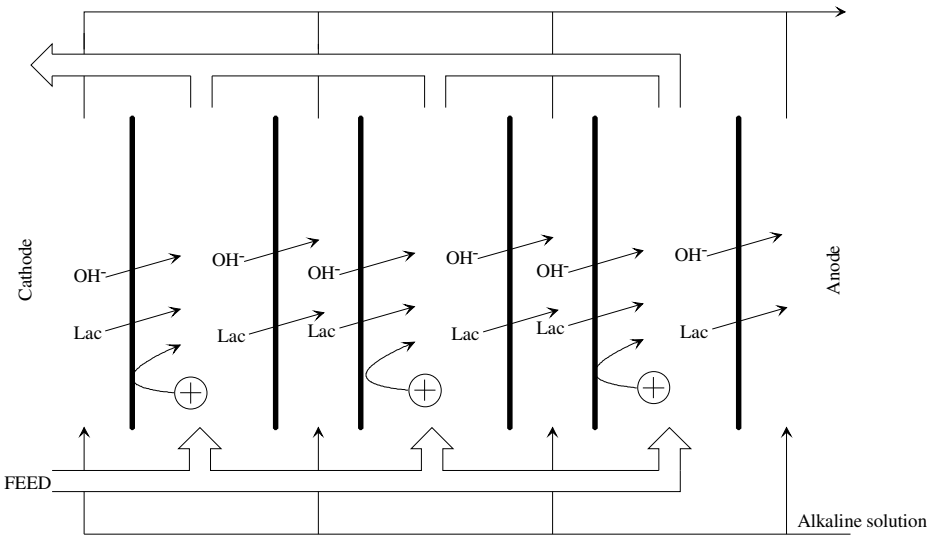

Figure 5.2.2 Competitive transport between lactate and hydroxide ions. ▌ = anion-exchange membranes.

When trying to enhance the lactate flux from feed to alkaline solution, the electrical current must enhance the lactate flux in the feed chambers while *not* enhancing hydroxide flux. When the lactate ions enter the alkaline stream, they should remain there and not continue toward the anode through the second membrane and thus return to the feed. Thus, in the alkaline process stream, the electrical current should preferably be transported by the hydroxide ions.

To ascertain the possibilities for a selective flux enhancement of lactate rather than hydroxide ions in the feed stream and of hydroxide before lactate ions in the alkaline stream, the transport numbers for both ions are compared as function of the pH.

In the following, it is assumed for the sake of simplicity that only one organic acid anion (lactate) exists in the feed from a fermenter and that the only one other anion involved is hydroxide. To balance the anions, hydrogen ions and another inorganic cation (sodium) are added to the equation. It is assumed that pH is higher than 6, so that lactic acid can be considered totally dissociated (ionic) as described in paragraph 3.1.1.

The ions must constantly maintain electro neutrality:

eq. 5.2.1 $$\sum_j z_j C_j = 0$$

and the standard water dissociation constant K_W applies:

eq. 5.2.2 $$C_{H^+} \cdot C_{OH^-} = K_W = 10^{-14}$$

The transport numbers for all ions in a solution can be calculated as described in eq. 3.5.42. Ionic mobilities for all four ions are taken or calculated from data (Atkins 1992).

Assuming a lactate concentration of 0.2 M, the transport numbers of hydroxide and lactate ions are depicted in Figure 5.2.3 as functions of pH. The transport numbers of the cations indicate how much electrical current they transport between membranes, but since they are not able to penetrate the anion-exchange membranes significantly, their contribution is of no real consequence.

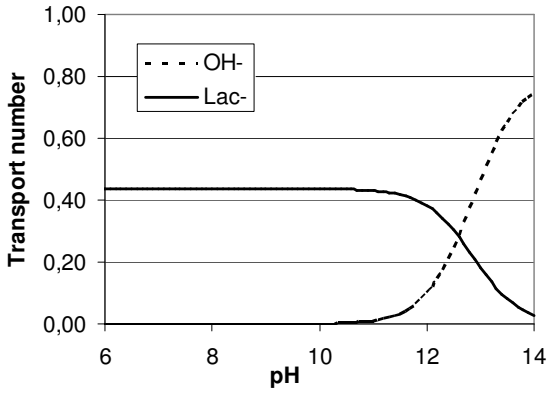

Figure 5.2.3 Transport numbers for hydroxide and lactate ions as function of pH in a solution with 0.2 M lactate.

It is obvious from this simple model that below pH 11, lactate is almost exclusively carrying electrical charges in relation to the hydroxide ions. Above pH 12.5, hydroxide ions carry an increasing amount of the current at the expense of lactate. This simple model predicts that adding electrical current to a Donnan dialysis setup as described above, should increase lactate flux from a feed stream at pH below 11, and increase hydroxide flux from an alkaline solution at pH above 13 while not returning too much lactate to the feed as sketched in Figure 5.2.4.

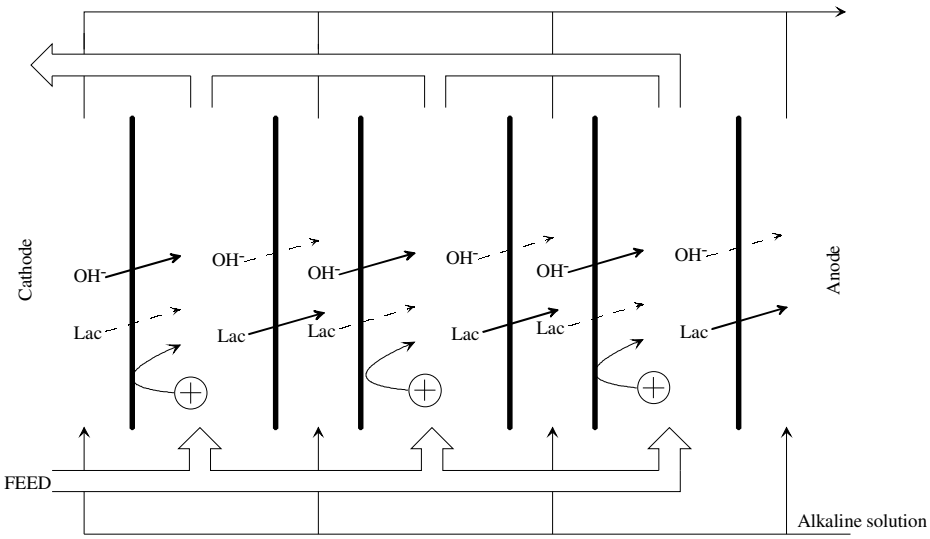

Figure 5.2.4 Theoretical result of electro-enhancement of the dialysis setup with anion-exchange membranes ▌.

To compare the transport numbers of lactate and hydroxide ions at different lactate concentrations, the relation between the transport numbers are shown as a function of pH for different lactate concentrations in Figure 5.2.5. For a linear appearance, the relations are shown on a logarithmic scale.

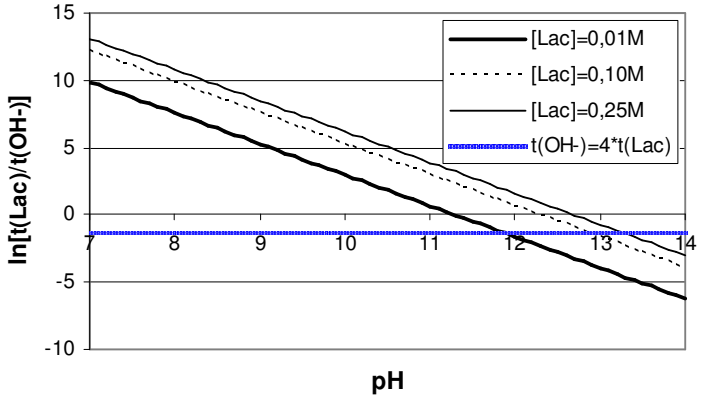

Figure 5.2.5 The relation between the transport numbers of lactate and hydroxide as function of pH at different lactate concentrations on a logarithmic scale. $t(OH^-)=4 \cdot t(Lac)$ responds to the relation where 80% of the transported anions are hydroxide.

From Figure 5.2.5, the critical pH where the transport number of lactate equals the transport number of hydroxide can be found where the lines cross 0. Assuming feed solutions are going to stay at pH-values below 10, the competition between lactate

and hydroxide heavily favors lactate being extracted from the feed. For the alkaline solution, the situation where equal amounts of lactate and hydroxide are transported back to the feed is much too inefficient to consider a turning point. The figure also shows a line ($t(OH^-)=4 \cdot t(Lac)$) where 80% of the anions returned to the feed are hydroxide ions. From the intersection between this line and the curves, it can be observed that the more lactate is collected in the alkaline solution, the higher the pH-value needs to be. If the alkaline solution only needs to sustain a 0.01 M lactate concentration, pH 12 is sufficient, while higher lactate levels demands higher pH-values. Otherwise, a severe reduction in efficiency is the outcome.

By adding electrical current to the process the ion fluxes can be greatly increased compared to diffusion fluxes. But this also increases the speed of fouling material building up at the membrane surfaces. Especially bio-matter that is charged will respond to the electrical current and cling to the membranes. As can be observed from Figure 5.2.4, hydroxide ions enter one side of the feed chambers, constantly destabilizing fouling build-up. On the other side of the feed chamber, the fouling builds up. Exploiting the symmetrical setup of the dialysis unit it is possible to reverse the electrical current without need to change manifolds and chamber designation. By changing the direction of the electrical current, the flux of hydroxide ions into the feed chambers changes side as well. This results in destabilization and removal of the fouling layer that has been building up while a new fouling layer starts building up on the opposite side of the feed chamber as demonstrated in Figure 5.2.6.

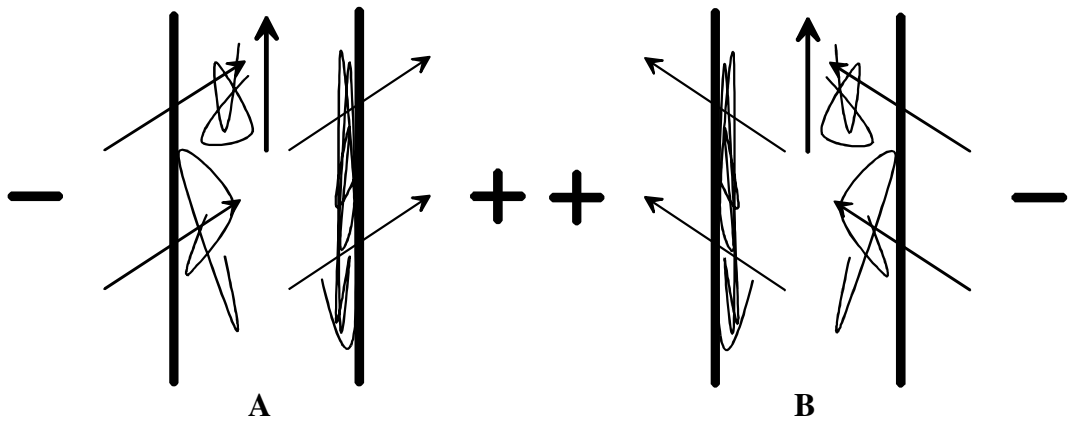

Figure 5.2.6 Build-up of fouling bio-matter on one side of feed compartments, while the opposite side is “cleaned”. When the electrical current is reversed, the cleaning process is shifted to the other side of the feed compartments.

As shown in the following paragraphs, preliminary results with this setup gave results that supported the theoretical speculations above. The process setup as shown in

Figure 5.2.4 with reversing direction of the electrical current at frequent intervals was named *Reverse Electro-Enhanced Dialysis* (REED).

Experiments with reverse electro-enhanced dialysis were carried out to evaluate the performance of this novel extraction process. Preliminary experiments were performed to investigate different parameters of the equipment and process. Experiments with both model solutions and fermented brown juice as the feed solution have been performed.

5.2.2 Materials and methods

5.2.2.1 Membranes

Tokuyama Corporation, Tokyo, Japan, kindly supplied the tree different kinds of ion-exchange membranes used in the experiments; Neosepta® AMX anion-exchange membranes, Neosepta® ACS anion-exchange membranes, and Neosepta® CMH cation-exchange membranes. The AMX membranes are standard grade membranes, whereas CMH and ACS are special grade membranes. CMH membranes have high chemical resistance and high mechanical strength and ACS are mono-anion permselective membranes

5.2.2.2 Experimental equipment

The equipment was constructed at the workshop at Department of Chemical Engineering (DTU, Lyngby, Denmark) from transparent acrylic plates. The stack was assembled with four anion exchange membranes (AEM) and two cation exchange membranes (CEM), forming two feed compartments, three base compartments, and two electrode chambers as shown in Figure 5.3.1.

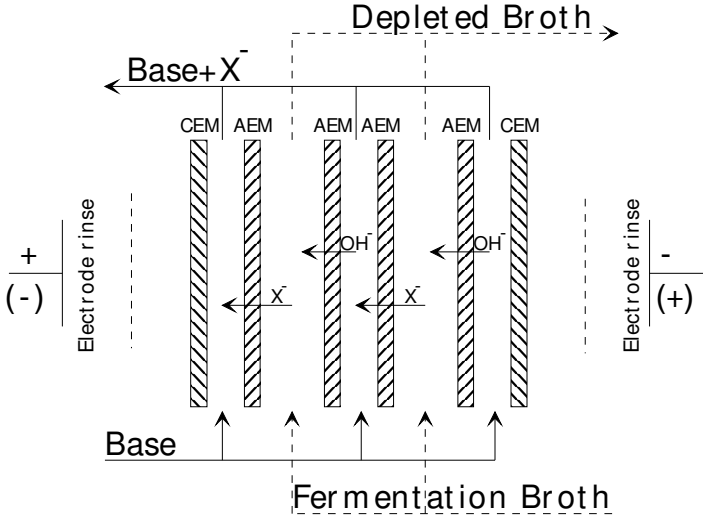

Figure 5.2.7. Membrane configuration in the Reverse Electro-Enhanced Dialysis-stack in laboratory experiments.

Each membrane had an active area of 40 cm^2. The thickness of the feed compartments, where fermentation broth entered, was 12 mm. Net spacers were omitted to minimize the risk of plugging of the flow path. The thickness of the base compartments was 6 mm and net spacers were introduced to promote turbulent flow in these compartments. The two outermost chambers had one platinum electrode each (with an electrode area of 31.5 cm^2), separated from the rest of the compartments by a set of cation exchange membrane. Solutions (feed and alkaline) were circulated from feed tank and base tank through the stack by means of two gear pumps (Micropump® F5734, Concord CA, USA). The mass flow through each gear pump was 9 g/s. The electrode solution was circulated using a centrifugal pump (Type no. 1250 21 9, EHEIM, Germany). A power supply (EA-PS 3032-10 (0-32V/0-10A), Elektro-Automatik, Germany), which delivered direct current at constant current density to the stack, was connected to a multimeter (Radio Shack LCD Digital Multimeter, Tandy Corp., US) for accurate readings of the current density. A relay (10A) reversed the direction of the current at regular intervals, controlled by a PC. In the feed chambers, Ag/AgCl electrodes were placed so the voltage drop across a cell pair could be continuously measured and data collected through a scopemeter (Fluke 123 – Industrial Scopemeter, Fluke Corporation, USA) to a PC. A titration device (TTT 80 Titrator, Radiometer, Denmark) that added lactic acid/fermentation broth to the feed tank, was controlled by the pH of the feed tank. The entire experimental setup is shown in Figure 5.3.2.

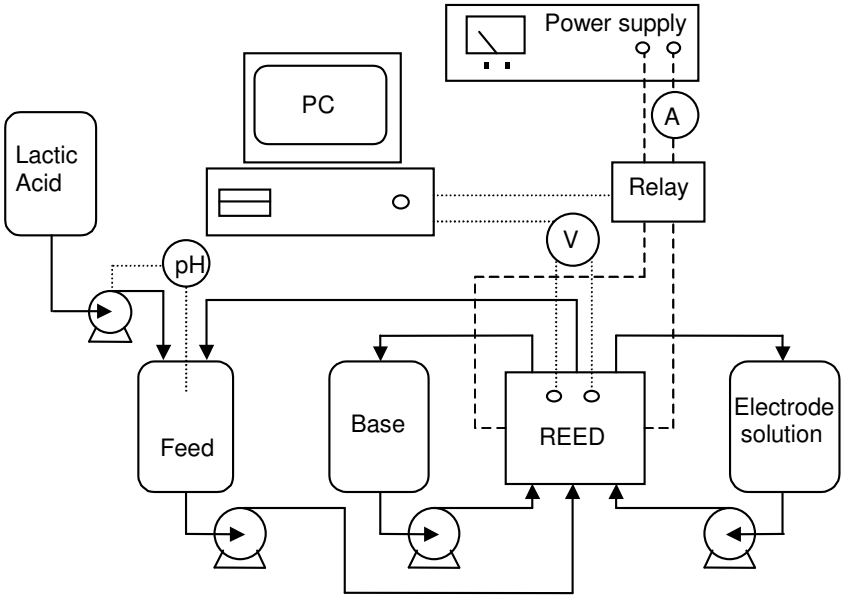

Figure 5.2.8. Setup for Reverse Electro-Enhanced Dialysis experiments.

All the tanks were equipped with heating/cooling jackets connected to a water bath.

5.2.2.3 Experimental

The feed solution was either a mixed model solution containing lactic acid or fermented brown juice. The feed solution was titrated with dry sodium hydroxide pellets to pH 5.5. In some experiments, calcium and magnesium hydroxide were added, when the calcium and magnesium retention was investigated. The alkaline solution consisted of either 0.1 M or 0.5 M sodium hydroxide or potassium hydroxide. An aqueous solution of 0.1 M Na_2SO_4 was passed through the electrode compartments. The temperature was kept at 40 °C during experiments.

When the solutions were pumped through the stack, the experiment was started by turning on the electrical current. The computer-controlled relay reversed the electrical current at given intervals, between 10 to 60 seconds.
Samples were taken from the feed and base tanks at regular intervals. pH, conductivity, and lactic acid concentration were measured in the samples. The voltage drop across the middle cell pair was continuously logged by computer.

5.2.2.4 Analytical techniques

The lactic acid concentration was measured by HPLC. 1 ml solution was taken from both the feed and the base tank and acidified using concentrated sulfuric acid (96%). Lactic acid analysis was performed at 35°C with HPLC equipped with an Aminex HPX-87H column (Biorad) using 4 mM H_2SO_4 as eluent at a flow rate of 0.6 ml/min. The acid was detected on a Waters 486 tunable absorbance detector at 210 nm. Waters Millennium Chromatography Manager software was used for quantification.
Approximately 5 ml solution was taken from both the feed tank and the combined acid and base tank and the pH and conductivity were measured using a pHM 201 portable pH-meter and a CDM92 Conductivity meter (both from Radiometer, Denmark), respectively. After measurements, the solutions were transferred back to the system to maintain mass balance.
Calcium and magnesium were measured by Atom Absorbance Spectroscopy (AAS).

5.2.3 Resume of preliminary experiments and results

Initial experiments with Reverse Electro-Enhanced Dialysis were performed using model solutions of lactic acid. To investigate fouling behavior, the model solutions were replaced by fermented brown juice.
In the following, a number of experimental parameters are investigated. The titration device was not operating in these experiments.

5.2.3.1 REED experiment #1: Initial test

For feed, 250 ml 7% lactic acid solution, adjusted to pH 5.5, was prepared. 1800 ml 0.1 M NaOH were prepared for the alkaline solution. The stack was equipped with Neosepta ASC mono-anion permselective membranes as anion-exchange membranes and Neosepta CMH membranes as cation-exchange membranes.

A constant current of 1 A (250 A/m^2) was applied across the stack. The direction of the current was reversed every 60 seconds.

The changes in lactate concentration are shown on Figure 5.2.9.

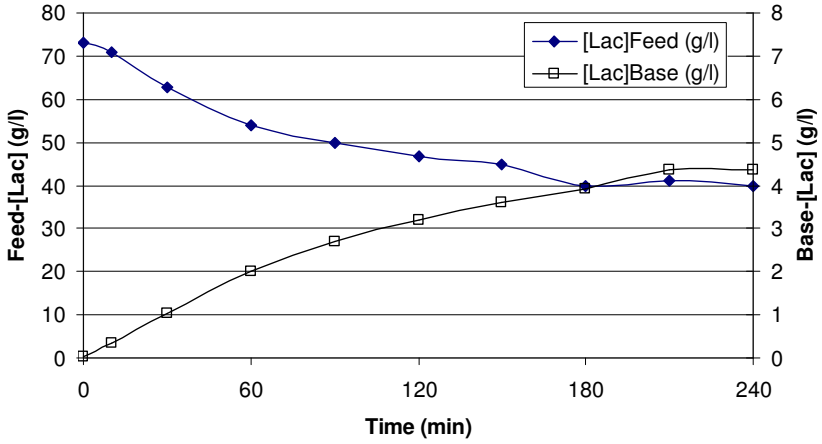

Figure 5.2.9. Lactate concentration changes in feed and alkaline solution.

The lactate concentration in the 250 ml feed decreased from around 70 g/l to 40 g/l, while the lactate concentration in the 1800 ml alkaline solution increases to 4-5 g/l. The lactate that was extracted from the feed was replaced by hydroxide ions.
It was observed how the pH in the feed solution rose, especially during the first hour, due to the replacement. The pH of the alkaline solution dropped accordingly, as shown on Figure 5.2.10.

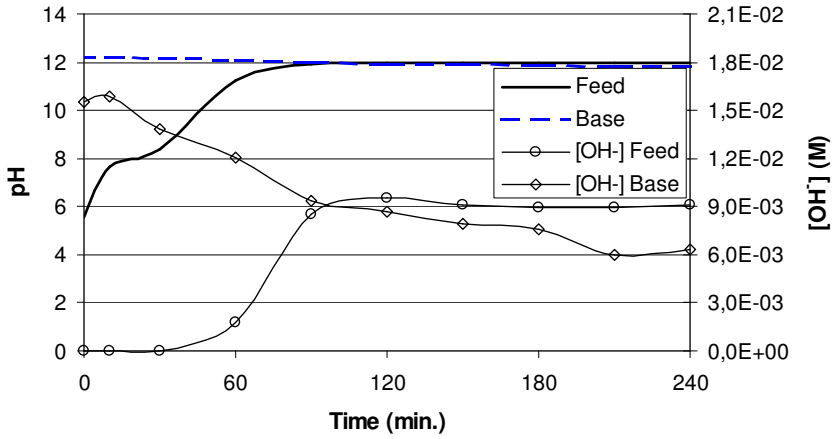

Figure 5.2.10. pH of feed and alkaline solutions during REED experiment.

The figure shows the pH-values as well as their corresponding hydroxide concentrations. When the pH-value of the feed reached the same level as in the base, the flux of hydroxide ions receded significantly. Still, the continued flux of lactate as well as hydrogen ion leakage from the electrode rinse lowers the pH in the base.

The impact of the pH in the feed stream on the lactate extraction is most evident in Figure 5.2.11, where the lactate flux and the power consumed to extract 1 kg lactate during the experiment is compared to the feed pH.

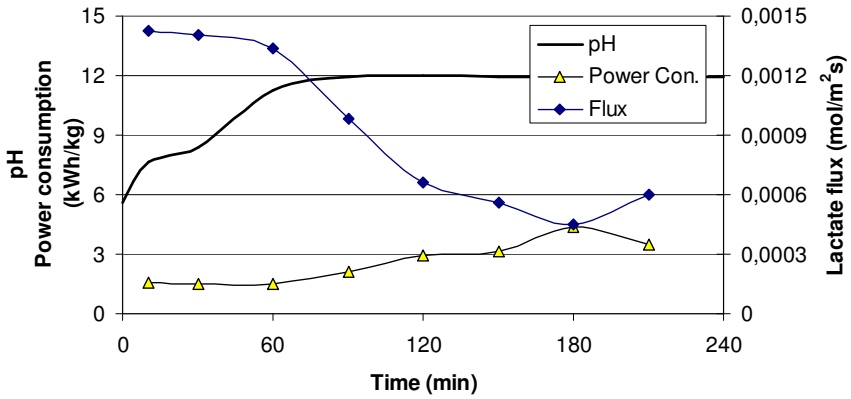

Figure 5.2.11. Lactate flux and power consumption during the experiment compared with the pH of the feed.

When the pH rises in the feed, the competition between electrical migration of lactate and hydroxide starts to favor the hydroxide ions. Thus, the efficiency of the process

decreases significantly. This increases the energy consumption necessary to extract 1 kg of lactate, because a lesser part of the current is used for lactate transport. The lactate flux and the current efficiency are depicted in Figure 5.2.12 as function of the feed pH.

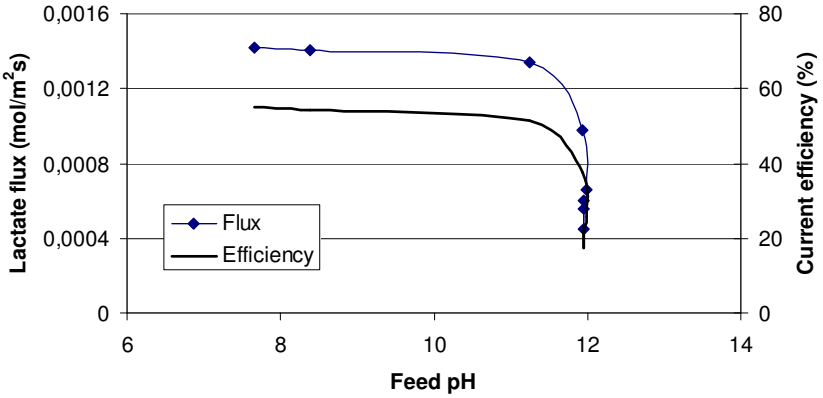

Figure 5.2.12. Lactate flux and current efficiency as function of feed pH.

In this figure, the drop in extraction efficiency is very evident. The extraction must take place at pH-values lower than the drop-off value, which is around 11.5 in this case.

From this experiment, we concluded that the process was able to extract lactate continuously from the feed solution, while the current was reversed at regular intervals. The efficiency was acceptable, when the feed pH was below 11.5. At lower pH-values, the competitive transport of hydroxide ions is less pronounced, resulting in better current efficiency and lower power consumption.

5.2.3.2 REED experiment #2: Comparison between Reverse Electro-Enhanced Dialysis and Donnan Dialysis

To investigate the effect of the added electrical current to the Donnan Dialysis setup, the two processes were compared.
Using the exact same setup and solution compositions as in the previous experiment, the experiment was repeated but without electrical current.

As before, lactate ions were extracted, and the feed alkalized, but at significantly slower rate.

The fluxes in this Donnan Dialysis experiment are compared to the fluxes of the Reverse Electro-Enhanced Dialysis experiment in Figure 5.2.13.

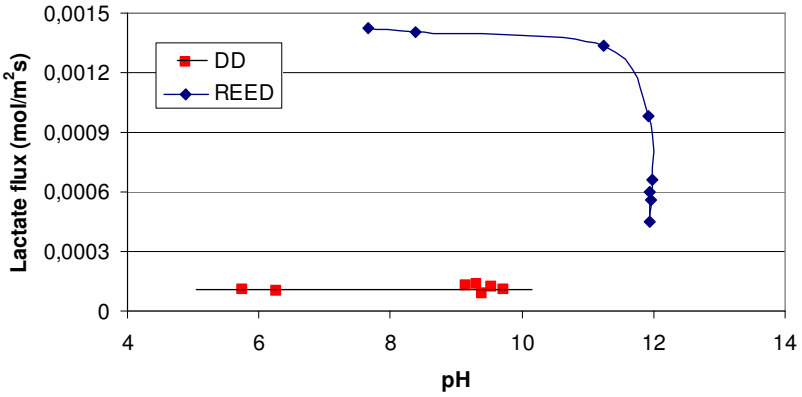

Figure 5.2.13. Flux comparisons between conventional Donnan Dialysis (DD) and Reverse Electro-Enhanced Dialysis (REED).

These results demonstrate that by electro-enhancing the dialysis, the extraction flux increases by a factor of 10.

5.2.3.3 REED experiment #3: The effect of reversing the current

To investigate the expected loss of efficiency that is an unfortunate effect of reversing the current, an experiment was performed that was similar to the first one described in this section. The only difference was that the electrical current was not reversed in this particular experiment.

The current efficiencies in the two similar experiments are compared in Figure 5.2.14.

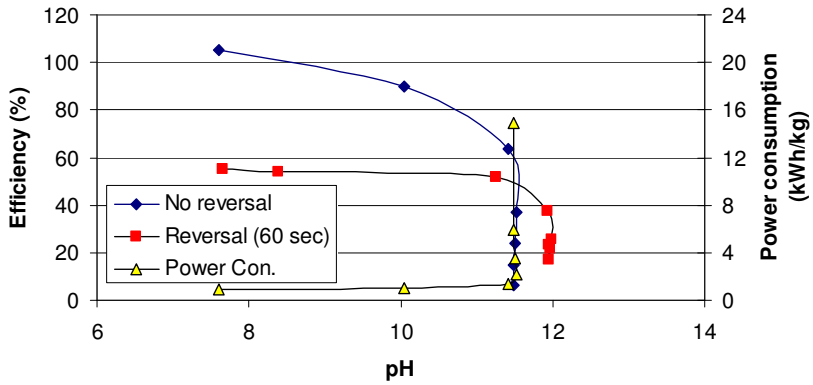

Figure 5.2.14. Current efficiency with and without current reversal. Power consumption without current reversal.

The current was much better utilized without current reversal, because of a buffer effect in the ion-exchange membranes. When the process is reversed at regular intervals, a new steady-state has to be established, resulting in the process running less time at fully developed membrane profiles. The power consumption was thus lower in this experiment.
The current efficiency in Figure 5.2.14 for the experiment without current reversal started out with a value above 100%. This is because it has been calculated from the combined fluxes of lactate migration and diffusion, which together exceeds the optimal migration flux.

This experiment demonstrates that a weakness of Reverse Electro-Enhanced Dialysis technology is decreased current efficiency.

5.2.3.4 REED experiment #4: Retention of calcium

In order for the process to be successful, it is important that the Reverse Electro-Enhanced Dialysis module can be coupled with a Bipolar Electrodialysis unit, where the lactate can be concentrated and acidified and the alkaline solution regenerated. But divalent cations like calcium and magnesium have a poisoning effect on the bipolar membranes, and it is important that the anion-exchange membranes retain enough of these ions, so the alkaline solution with the extracted lactate contain less than 2 ppm calcium and magnesium.

The initial experiment was repeated with the same feed solution of 7% lactic acid adjusted to pH 5.5, but 100 ppm calcium hydroxide was added. Samples were taken from the feed and base during the 4 hour experiment, and measured by Atom Absorbance Spectroscopy (AAS).

No traces of calcium were found in the base or the electrode rinsing solution in any of the samples. This shows that the ACS membrane is sufficiently selective to fulfill the requirement of retaining calcium.

5.2.3.5 REED experiment #5: Replacing the anion-exchange membrane

The standard experiment similar to the first was repeated with the standard Neosepta AMX anion-exchange membranes in place of the special grade ACS membranes. The feed concentration was 7.5% lactate.

The lactate flux and current efficiency were found to be very similar to the values found with the special grade anion-exchange membrane. The calcium retention was

also comparable. Any significant difference could be seen in the power consumption as shown in Figure 5.2.15.

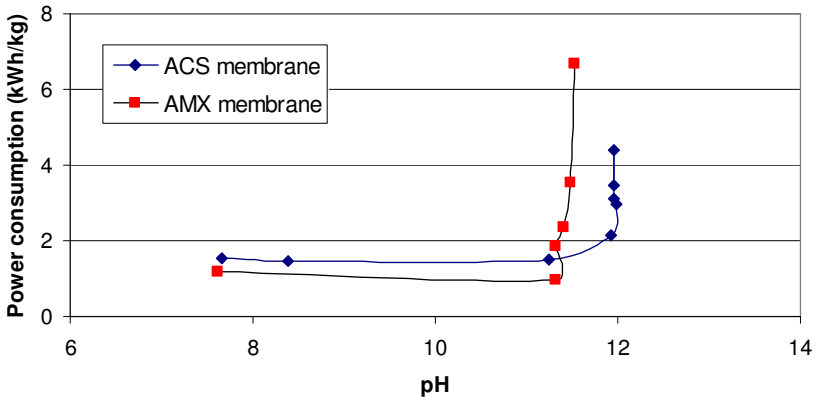

Figure 5.2.15. Difference in power consumption with regard to the chosen anion-exchange membrane.

The lower electrical resistance of the AMX membrane compared to the ACS membrane lowers the overall cell resistance, and thus, the power consumption necessary to extract 1 kg lactate.
The difference in drop-off pH-value is due to small difference in starting lactate concentrations in the feed, not because of the membranes.

The AMX membrane allows multivalent anions to pass as well as monovalent anions. In a feed solution with a high content of divalent ions, the competitive transport from these ions would lower the current efficiency with the AMX membrane compared with the ACS membrane. The mono-anion permselective ACS membrane rejects these multivalent ions, and the only competition to lactate extraction is from other monovalent anions.

5.2.3.6 REED experiment 6: The anti-fouling mechanism

REED experiments 1 and 3 were repeated, but this time the feed solutions consisted of fermented brown juice from food pellet production. The brown juice was adjusted to contain 7 % lactic acid and solid sodium hydroxide was added to reach pH 5.5 in the broth.

The first part of this experiment included a run with reversal of the electrical current, and the second part repeated the first run, but the electrical current was not reversed during the second run.

The different lactate fluxes at the changing pH-values of the feed are compared in Figure 5.2.16 for the two runs of this experiment. The lactate flux in these experiments with brown juice were lower than when using model solutions, but even with current reversal, the lactate flux from brown juice was still 5 times larger than in the Donnan dialysis experiment (REED experiment 2) using model solutions.

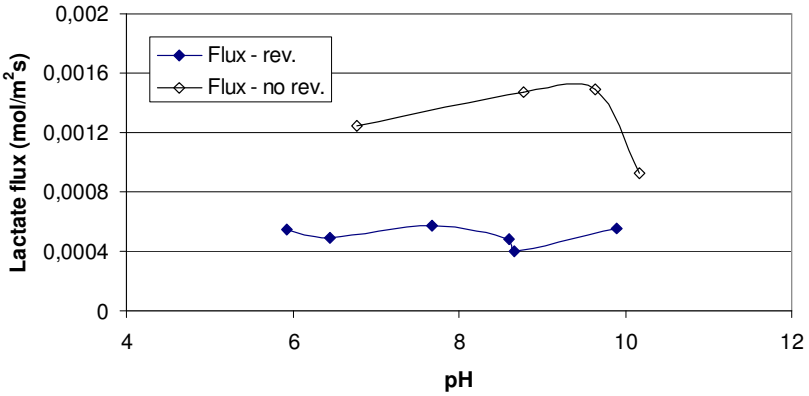

Figure 5.2.16. Lactate flux compared with and without current reversal.

As demonstrated earlier with model solutions, the lower current efficiency experienced when utilizing current reversal is reflected in the lactate fluxes shown in Figure 5.2.16. The voltage drop across a cell pair, E_{Cell} is compared in Figure 5.2.17 for experiments with and without current reversal.

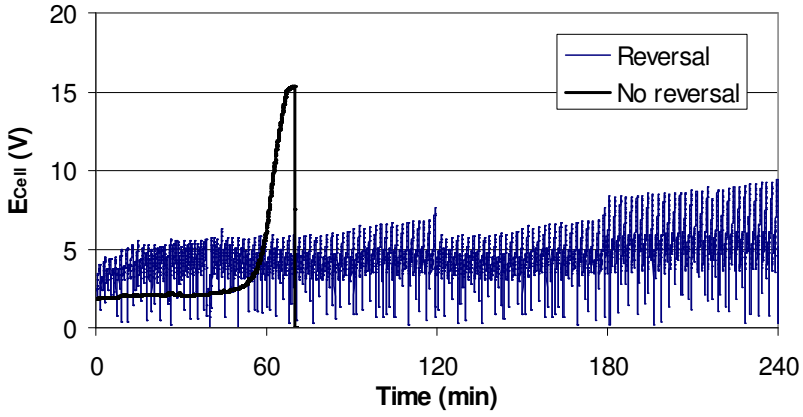

Figure 5.2.17. Numerical values of the voltage drop across a cell pair during REED experiments on fermented brown juice with and without reversal of the current. The “noise” on the potential curve for the reversal run is caused by the frequent reversal of current.

The cell voltage drop reflects the electrical resistance to ionic migration through a cell pair since the electrical current density is kept stable at 250 A/m^2.The average cell voltage drop is observed to be lower when current reversal is *not* employed during the first 50 minutes of this experiment. After 50 minutes, the cell voltage drop increases dramatically, which shortly after leads the termination of the experiment due to extreme resistance. Whether this result was due to build-up of fouling on the membrane surfaces or caused by plugging of a flow channel in the equipment from bio-matter could not be determined. The relatively sudden increase in cell voltage drop suggests that plugging is the main cause in this experiment.

Why the average cell voltage drop (and thus, the average electrical resistance) was lower when current reversal was *not* employed is not clear since the electrical conductivities of the solutions in the compared experiments were comparable. The increased resistance must be affected by the ion-exchange membranes that already demonstrate an efficiency-reducing buffer effect in connection with current reversal.

The result of this experiment suggests that current reversal should only be employed when the build-up of fouling has a sufficient impact on resistance increase, which was not observed by the fermented brown juice in these experiments. Apparently, the shear stress from the feed flow on the membrane surfaces was ample means to prevent serious fouling build-up. An increased period between the current reversals may well reduce the negative impact on resistance and efficiency, which each reversal seems to cause.

When current was reversed at regular interval (60 seconds), the experiment was seen to continuously extract lactate for a four hour period. The average cell resistance increased during this period as shown numerically on Figure 5.2.17.

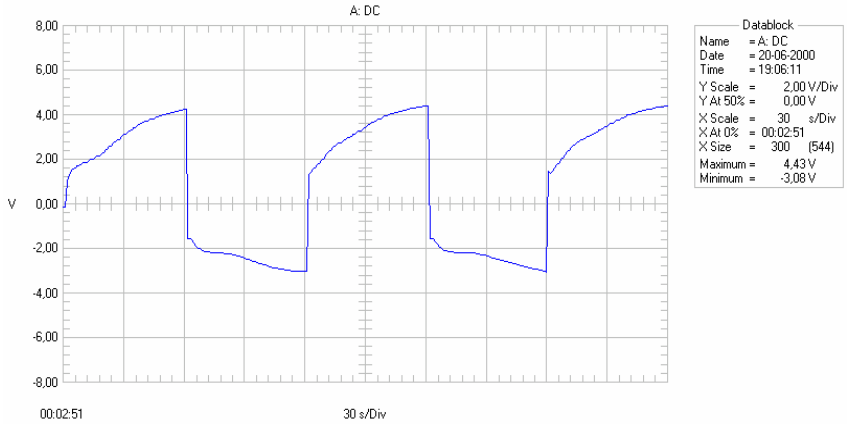

Figure 5.2.18. Extract of the voltage drop across the cell pair with current reversal every 60 seconds.

Figure 5.2.18 shows in detail how every reversal was followed by a steady increase in resistance because of fouling build-up. However, every reversal of current was followed by a regain of the cell resistance to the original level. This shows that most of the fouling buildup was reversibly removed by reversing current direction.

5.2.3.7 Conclusion on initial experiments

From initial experiments, it was concluded that the reverse electro-enhanced dialysis (REED) process acted according to theory and was worth investigating further. The self-cleaning mechanisms of reversing the electrical current were not superior to experiments where current was not reversed, when the feed contained biological material, which was surprising. Most references conclude that ion-exchange membranes are not suitable for separation and extraction directly from fermentation broth because of significant fouling, but in the initial experiments, the impact of fouling has been less severe than expected. A possible reason could be that fermentation broth with inactive bacteria was used in these experiments.

The initial experiments demonstrated that the feed pH should be kept below the observed drop-off values. The pH-value of the drop-off in efficiency and flux is slightly different from experiment to experiment, but it is mostly depending on the initial lactate content.

The conclusion of the initial REED testing showed that it was possible to combine the self-cleaning mechanism with increased lactate flux. Whether the REED process is economical superior to a dialysis process or when leaving out current reversal for higher efficiency and shorter operation times could not be determined from the few initial experiments.

5.2.4 Continuous extraction of lactic acid from fermentation broth

To start simulating the conditions that is expected when lactate is extracting in conjunction with a continuous fermentation, a titration device was added to the setup as shown on Figure 5.3.2 to simulate the continuous addition of fresh broth to the stack. A pH-sensor was introduced in the feed tank, and the titration device was programmed to maintain the pH of the feed at 5.5 by adding additional fermentation broth to the feed. Since the initial feed solution was not removed in these experiments, added broth was concentrated in respect to lactic acid (80 g/l) and had a pH of 2.1. Thus, it was only necessary to add a small volume to the feed to preserve to pH while also adding small amounts of biomaterial.

When lactate is continuously removed from a fermenter, a low lactate concentration with some unconverted sugar is more realistic. The feed solutions in the following experiments were all 2% lactic acid adjusted to pH 5.5 by potassium hydroxide.

Since the pH of the feed solution is preserved, the alkaline concentration can be increased from 0.1 M to 0.5 M. This gives the alkaline solution a much higher capacity for extracted lactate. Sodium hydroxide was replaced by potassium hydroxide, since agricultural waste is more probable to contain free potassium ions.

5.2.4.1 REED experiment #7: Retention of calcium

The calcium retention was investigated again, following the changes in procedure for the experiments.

Two experiments tested the retention of calcium: one using the special grade ACS membrane and one using the standard AMX membrane.

The feed solution was 500 ml 2% potassium lactate at pH 5.5 in both cases, and the alkaline solution 500 ml 0.5 M KOH. About 200 ppm calcium hydroxide was added to the feed.

The current was reversed every 30 seconds in these experiments.

The extraction experiments lasted for four hours each. Pure lactic acid was added to the feed tanks through titration, keeping the feed pH at 5.5. The results of one of the experiments (using AMX membranes) are depicted in Figure 5.2.19.

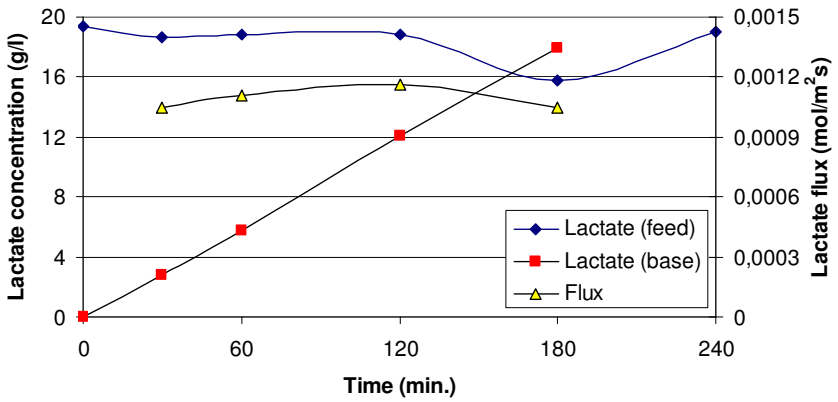

Figure 5.2.19. Lactate concentrations in feed and base during the experiment and the lactate flux.

This figure demonstrates how the lactate concentration is maintained in the feed tank through titration, which keeps the lactate flux stable and thus the lactate is easily extracted to the alkaline solution. Much higher lactate content can be sustained in the alkaline solution without significant transport of lactate back to the feed due to the increased base concentration of 0.5 M. The results for the other experiment were almost identical.

The calcium retentions of both membranes are both sufficiently great to accommodate the restrictions set for bipolar membranes, as can be seen in Table 5.2.1.

	Neosepta AMX			Neosepta ACS		
Time (min)	$[Ca^{2+}]_{Feed}$	$[Ca^{2+}]_{Base}$	$[Ca^{2+}]_{Elec}$	$[Ca^{2+}]_{Feed}$	$[Ca^{2+}]_{Base}$	$[Ca^{2+}]_{Elec}$
0	179	0.08	0.52	170	0.07	
30	182	0.22		172	0.12	
60	186	0.27		173	0.18	0.35
120	183	0.46	0.49	176	0.41	
180	180	0.67		185	0.47	
240	181		0.59	197	0.64	0.20

Table 5.2.1. Calcium concentrations in ppm in feed and base tank and electrode rinse during two experiments with different anion-exchange membranes.

No significant difference in calcium retention could be observed for the two membrane types.

5.2.4.2 REED experiment #8: Retention of calcium and magnesium in brown juice

The previous experiment was repeated with brown juice as feed solution. The brown juice contained 700 ppm calcium and 400 ppm magnesium.
The stack was equipped with ACS membranes.

During a 2 hour period, only very small amount of divalent cations was detected in the base and electrode rinse, as indicated by Table 5.2.2.

Time (min)	$[Ca^{2+}]_{Feed}$	$[Ca^{2+}]_{Base}$	$[Ca^{2+}]_{Elec}$	$[Mg^{2+}]_{Feed}$	$[Mg^{2+}]_{Base}$	$[Mg^{2+}]_{Elec}$
0	667	0.15	x	394	0.01	X
60	737	0.09	x	425	0.01	X
120	705	0.13	0.19	403	0.02	0.05

Table 5.2.2. Calcium and magnesium concentrations in ppm in feed, base, and electrode rinse during REED experiment #8. (x) marks the samples, where no traces could be detected.

Here the leakage of divalent cations is even smaller than in the previous experiments. Unlike, in the model solutions where calcium and magnesium were free ions, they were probably binding to the biomaterial in the brown juice and therefore better retained by the membranes.

Since most of the feed solution from a fermentation broth is recycled back to the fermenter, it is important to retain the unconverted sugars, too, so the conversion efficiency of the fermenter is preserved.

The unconverted sugars in the brown juice were all sufficiently retained. Only very small amounts that were hard to detect was found in the base. Some diffusion of sugars is to be expected, but most commercial anion-exchange membranes have an excellent retention of sugars.

5.2.4.3 REED experiment #9: Long time operation

The last experiment with the Reverse Electro-Enhanced Dialysis setup that is disclosed in this chapter is a fouling experiment that lasted for 7 hours.

The feed consisted of 250 ml brown juice with 2% lactic acid. Brown juice with high lactic acid content was titrated to maintain the pH-value of the feed.
The alkaline solution was 250 ml 0.5 M KOH.

The electrical current was reversed every 10 seconds in this experiment, to investigate whether the shorter intervals would result in lower overall cell resistance, and consequently lower power consumption.

After four hours, the alkaline solution was replaced with a fresh solution to continue operations without saturating the base.

The voltage drop across the central cell pair changed during the experiment as shown on Figure 5.2.20.

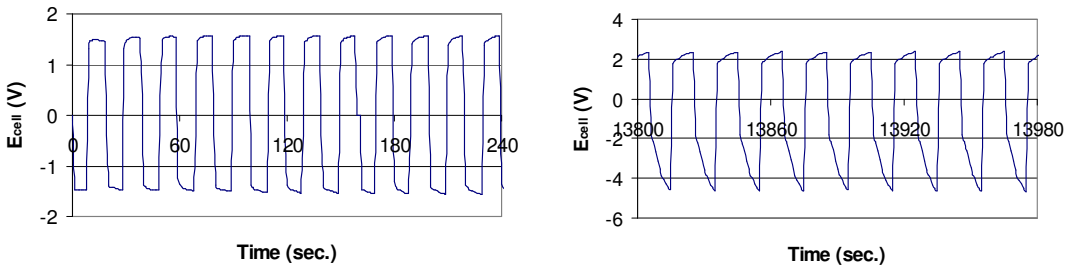

Figure 5.2.20. Comparison between the voltage drop across the cell pair in the beginning and in the middle of REED experiment #9.

The increase in cell resistance between reversals were much more pronounced later in the experiment than in the beginning. It also seems that one membrane surface was more receptive to the fouling than the opposite surface in the feed chamber, giving the graph an asymmetrical look. This can be due to uneven flow distribution in the spacers.

The overall voltage drop of the cell increased from 1.5 V in the beginning to 1.9 V near the end. The 1.9 V increased to 2.8 V or 8 V between reversals, respectively, whether the current was going left or right.

The lactate concentration in the feed was kept relatively constant as shown in Figure 5.2.21. The figure also shows the lactate concentration in the two batches of base.

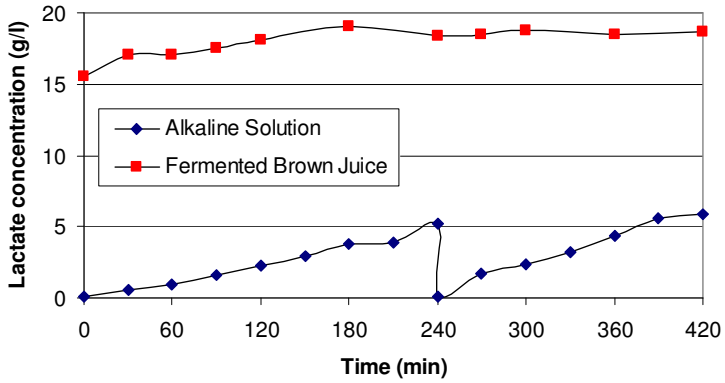

Figure 5.2.21. Lactate concentration in feed (Brown juice) and base (alkaline solution).

The flux of lactate was lower than expected from earlier experiments. Moreover, the current efficiency was found to be 3%, which is unacceptable.

The very low efficiency and fluxes were later discovered to be the result of the short intervals between current reversals. It is necessary for the membrane profiles inside the membranes to shift before acceptable current efficiencies can be reached, which takes some time. During this buffer time, only low efficiencies can be obtained as seen in this case.The self-cleaning mechanism still did the job of keeping the process running for the full 7 hours.

5.2.5 Conclusion

The reverse electro-enhanced dialysis has shown promise with regards to minimizing the harmful effects of fouling. The basic electrical resistance of a cell pair is regained after each current reversal, which makes longer operation times possible between cleaning.

The anion exchange membranes exhibit near total retention of calcium and magnesium, which enables subsequent bipolar electrodialysis. Very limited amounts of sugars diffuse through the membranes to the base compartments.

The feed to the reverse electro-enhanced dialysis becomes alkaline, which makes it ideal for pH-control of a fermenter.

A disadvantage is the low current efficiency, which must be improved through optimization of the duration of the time intervals between current reversals.

5.3 Electrodialysis with bipolar membranes

5.3.1 Introduction

Experiments with three-compartment electrodialysis with bipolar membranes (EDBM) were carried out to evaluate the performance during removal of lactate from an alkaline feed solution. The properties of the feed are made to resemble those that would be experienced if the EDBM was connected to a reverse electro-enhanced dialysis unit.

5.3.2 Materials and methods

5.3.2.1 Membranes

Tokuyama Corporation, Tokyo, Japan, kindly supplied the three different kinds of ion-exchange membranes used for the experiments; Neosepta® AMX anion exchange membranes, Neosepta® CMH cation exchange membranes, and BP-1 bipolar membranes. The AMX is a standard grade membrane, whereas the CMH is special grade membrane with high chemical resistance and high mechanical strength.

5.3.2.2 Experimental setup

The equipment was constructed at the Department of Chemical Engineering; DTU, Lyngby, Denmark from transparent acrylic plates. The stack was assembled as shown in Figure 5.3.1 with three bipolar membranes, two anion exchange membranes, and two cation exchange membranes, forming two feed compartments, two acid compartments, two base compartments, and two electrode chambers.

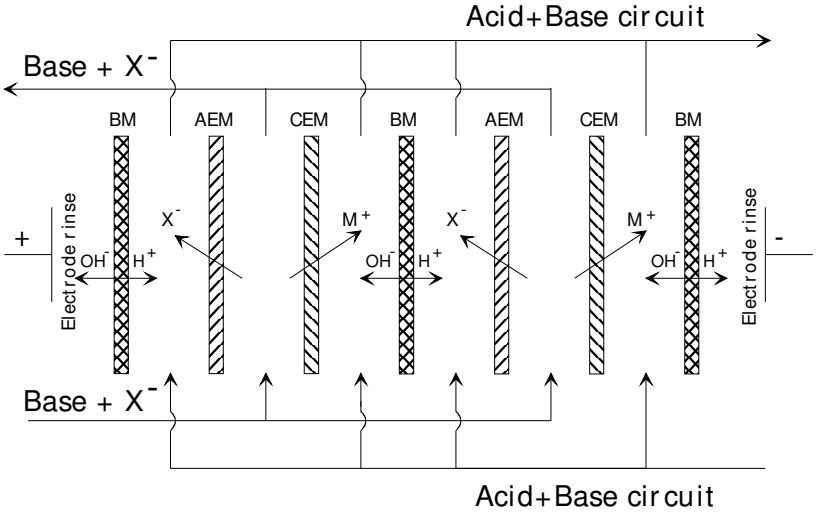

Figure 5.3.1. Membrane configuration in the EDBM-stack.

Each membrane had an active area of 40 cm^2. The thickness of the chambers between the membranes was six mm and net spacers were introduced to promote turbulent flow. In the two outermost chambers between the platinum electrodes (each

31.5 cm^2) and a set of bipolar membrane, electrode-rinsing solution was passed, consisting of an aqueous solution of 0.1M K_2SO_4. Feed solution was circulated from the feed tank through the feed chambers between the anion- and cation exchange membranes by means of a gear pump (Micropump® F5734, Concord CA, USA), see the experimental setup in Figure 5.3.2. The same type of pump was used to circulate the combined acid and base stream through the acid chambers between the bipolar membranes and anion exchange membranes, and through the base chambers between the bipolar membranes and cation exchange membranes. The mass flow through each gear pump was 3.3 g/s. The electrode solution was circulated using a centrifugal pump(Type no. 1250 21 9, EHEIM, Germany). The power supply for direct current to the stack was a (EA-PS 3032-10 (0..32V/0..10A), EA–Elektro-Automatik, Germany) connected to a multimeter (Radio Shack LCD Auto Range Digital Multimeter, Tandy Corp., US) for accurate readings of the current. In the feed chambers, silver/silver chloride electrodes were placed to continuously measure the voltage drop across a cell pair and to collect the data. (Fluke 123 – Industrial Scopemeter, Fluke Corporation, USA)

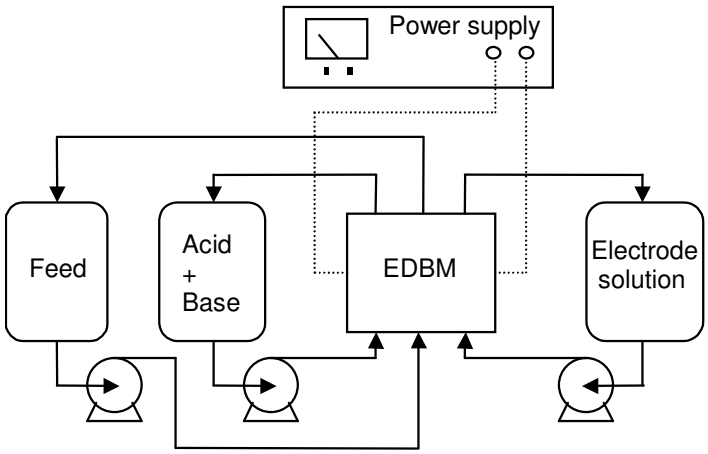

Figure 5.3.2. Experimental setup

All the tanks were equipped with heating/cooling jackets connected to a water bath and the temperature was kept at 40 °C during experiments. Samples were taken from the feed and acid/base tanks every 15 minutes the first hour and then every 30 minutes until the experiments were terminate after 3 hours. pH, conductivity and lactic acid concentration were measured in the samples.

Two experiments were carried out to investigate the influence of the lactate concentration on the current efficiency and power consumption. In the first experiment 500 ml feed solution containing 0.5 M KOH and 0.2 M lactic acid was

used and in the second experiment the lactic acid concentration was increased from 0.2 to 0.4 M. In both experiments 1000 ml of a 0.1 M KOH solution was circulated in the acid/base circuit. The experiments were started at a current of 1500 mA, corresponding to a current density of 375 A/m^2. The current was kept constant until the voltage drop across a single cell pair exceeded 11 V. The current density was then decreased to 188 A/m^2 and further down to 94 A/m^2 and finally 50 A/m^2 as the 11 V were reached.

5.3.2.3 Analytical techniques

1 ml solution was taken from both the feed tank and the combined acid and base tank and acidified using concentrated sulfuric acid (72%). Lactic acid analysis was performed at 35°C with HPLC equipped with an Aminex HPX-87H column (Biorad) using 4 mM H_2SO_4 as eluent at a flow rate of 0.6 ml/min. The acid was detected on a Waters 486 tunable absorbance detector at 210 nm. Waters Millennium Chromatography Manager software was used for quantification.

Approximately 5 ml solution was taken from both the feed tank and the combined acid and base tank and the pH and conductivity were measured using a pHM 201 portable pH meter and a CDM92 Conductivity meter, (Radiometer, Denmark), respectively.

5.3.3 Results and discussion

In the first experiment the migration of lactate from the feed chamber to the acid chamber was quite slow to begin with. Figure 5.3.3 shows only small changes in lactate concentrations during the first 60 minutes with a decrease in the feed concentration from 17.9 to 14.2 g/l.

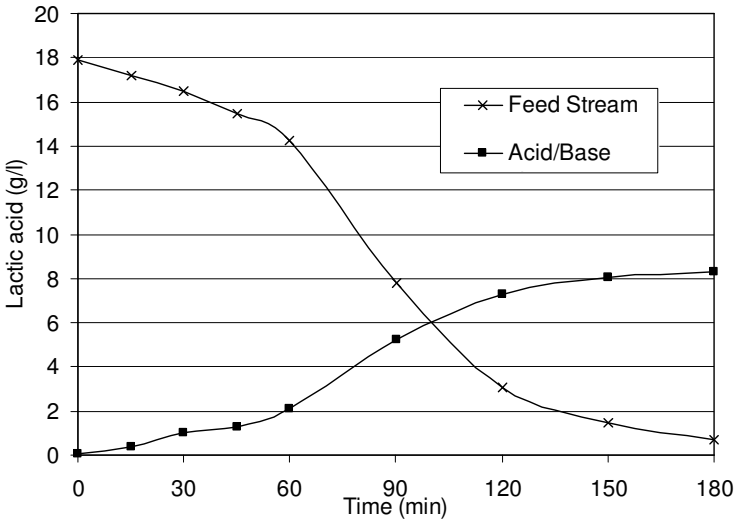

Figure 5.3.3. Concentration of lactate in the feed tank and acid/base tank during the first experiment.

The concentration changed more quickly, from 14.2 to 3.1 g/l, during the next 60 minutes, after which the process slowed down again, resulting in a concentration of 0.7 g/l in the feed at the end of the experiment.

The slow removal of lactate from the feed stream in the beginning of the experiment is due to the presence of high amounts of hydroxide ions that transports most of the current. The initial concentration of hydroxide is approximately 0.3 M compared to a lactate concentration of 0.2 M. A quick estimate of the fraction of current carried by lactate gives:

$$t_{Lac^-} = \frac{\eta_{Lac^-} C_{Lac^-}}{\eta_{Lac^-} C_{Lac^-} + \eta_{OH^-} C_{OH^-}} = \frac{C_{Lac^-}}{C_{Lac^-} + \left(\eta_{OH^-} / \eta_{Lac^-} \right) C_{OH^-}} = \frac{0.2}{0.2 + 5 \cdot 0.3} = 0.12$$

Approximately 12% of the current should be carried by lactate in the beginning of the experiment, which is in good agreement with the current efficiency obtained from the experimental data as shown in Figure 5.3.4. The current efficiency is 15% in the first 30 minutes but increases to an average of 77% between 90 and 120 minutes due to depletion of hydroxide (see the large drop in pH). By the end of the experiment the efficiency decreases again as the lactate concentration in the feed approaches zero and the effect of back-diffusion of lactate increases. The overall current efficiency is 43%, which corresponds well with only 2/5 of the anions being lactate.

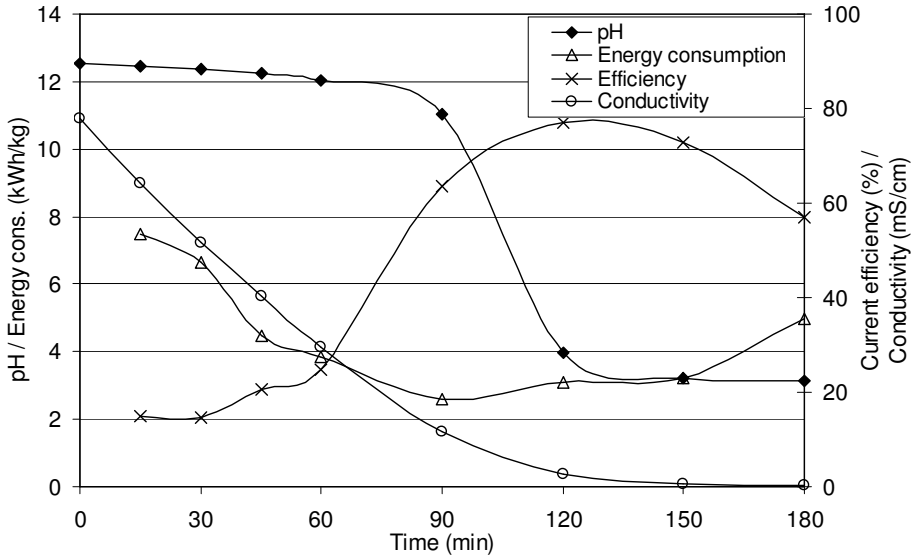

Figure 5.3.4. pH, energy consumption , current efficiency and conductivity during bipolar electrodialysis of a feed stream with 0.2 M lactic acid and 0.5 M KOH. The energy consumptions and current efficiencies in a given point are calculated as an average value in the time interval from the previous point up to the given point.

The energy needed to transfer one kilo of lactate (energy consumption) is high in the beginning of the experiment due to a low current efficiency and high again in the end mainly because of a low conductivity, see Figure 5.3.4. The energy consumption in the first 15 minutes and the last 30 minutes is 7.48 and 5.00 kWh/kg, respectively. The lowest energy consumption of 2.57 kWh/kg is observed in the interval between 60 and 90 minutes, and the overall consumption for the entire experiment is 3.67 kWh/kg. The energy consumption is an important parameter that relates to the operating costs of the EDBM unit and is directly proportional to the ohmic resistance of the cell. Figure 5.3.5 shows the resistance and the voltage drop across a single cell pair, the steep drops indicating where the current density is decreased.

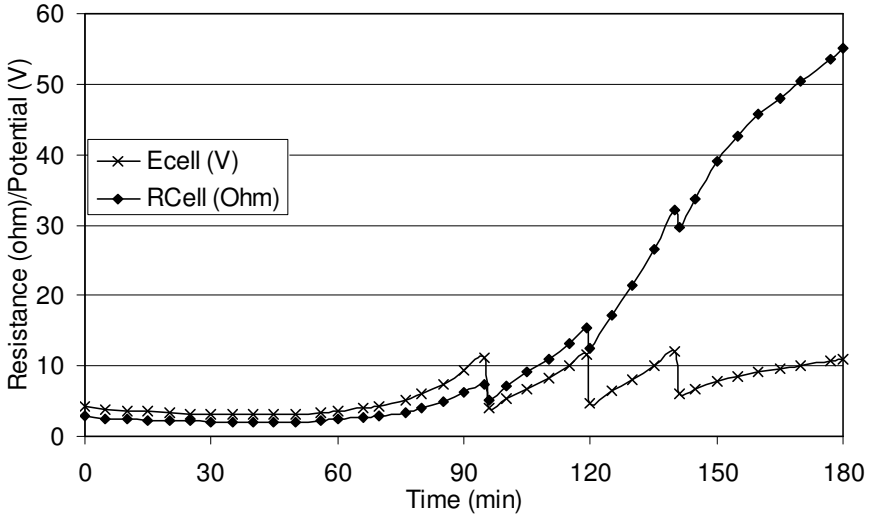

Figure 5.3.5. The electrical resistance Rcell and voltage drop Ecell across a single cell pair during bipolar electrodialysis of a feed stream with 0.2 M lactic acid and 0.5 M KOH.

In an industrial cell-stack the thickness of the flow chambers would be considerable smaller and the hydrodynamics optimised for a high mass-transfer coefficient at the membrane surface. This would result in lower electrical resistance across a cell pair and hereby reduce the energy consumption. If the better hydrodynamics were disregarded, an industrial cell with a typical spacer thickness of 1 mm would reduce the energy consumption for the above separation from 3.48 kWh/kg to 2.26 kWh/kg.

In the subsequent experiment the lactate concentration was increased to 0.4 M in the alkaline feed solution. Figure 5.3.6 shows the concentration of lactate in the feed and acid/base tanks, which changes at a high rate already from the beginning of the experiment. The lactic acid concentration in the feed drops from 35.1 to 8.2 g/l during the first 90 minutes and further down to 0.8 g/l in the next 90 minutes.

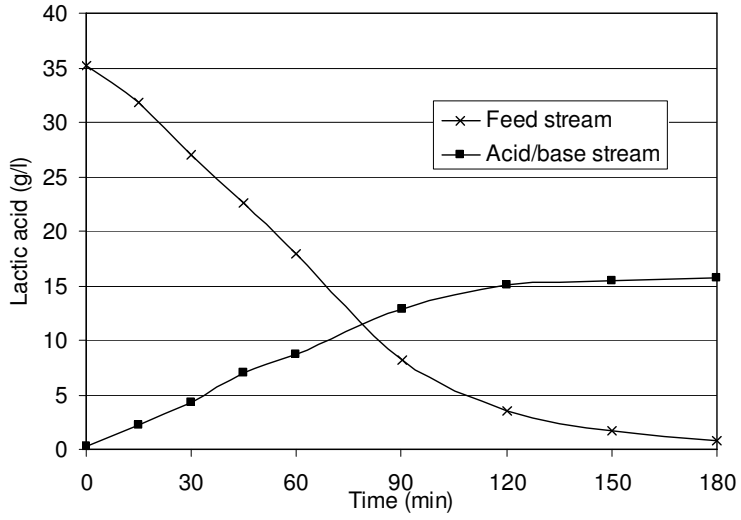

Figure 5.3.6. Concentration of lactate in the feed tank and acid/base tank during the second experiment.

The current efficiency at time = 0, can be estimated as in the previous experiment with an initial concentration of hydroxide of 0.1 M and a lactate concentration of 0.4:

$$t_{Lac^-} = \frac{C_{Lac^-}}{C_{Lac^-} + \left(\eta_{OH^-} / \eta_{Lac^-} \right) C_{OH^-}} = \frac{0.4}{0.4 + 5 \cdot 0.1} = 0.44$$

Theory gives a current efficiency of 44% at time = 0. Figure 5.3.7 shows an experimental value of the average current efficiency during the first 15 minutes of 67%, which suggests a steep increase in the beginning as the concentration of hydroxide ions diminishes. A high average current efficiency of 94% is obtained in the interval between 15 and 90 minutes and the overall current efficiency for the entire separation is 88%, or approximately twice the value that was obtained in the previous experiment.

The energy consumption is quite stable throughout the experiment with an average value of 2.15 kWh/kg lactate recovered, see Figure 5.3.7. However, in the last 30 minutes only 0.85 g/l lactate is removed at an energy expenditure of 4.28 kWh/kg. If an industrial cell-stack was used with a spacer thickness of 1 mm the energy consumption could be as low as 1.48 kWh/kg

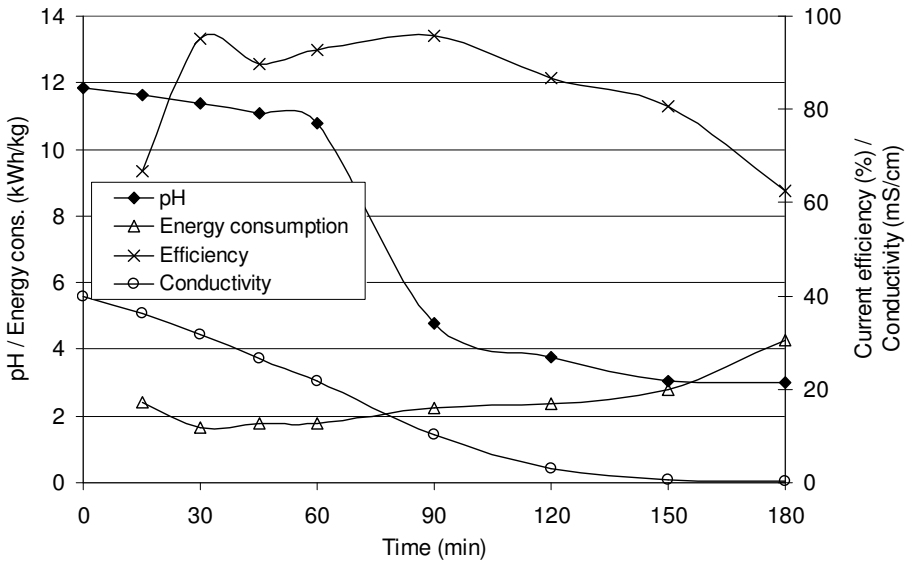

Figure 5.3.7 pH, energy consumption , current efficiency and conductivity during bipolar electrodialysis of a feed stream with 0.4 M lactic acid and 0.5 M KOH. The energy consumptions and current efficiencies in a given point are calculated as an average value in the time interval from the previous point up to the given point.

The electrical resistance and potential across a single cell-pair are shown in Figure 5.3.8. The resistance in the first 60 minutes is roughly 60-70% higher compared to that was observed in the previous experiment, as seen in Figure 5.3.5.

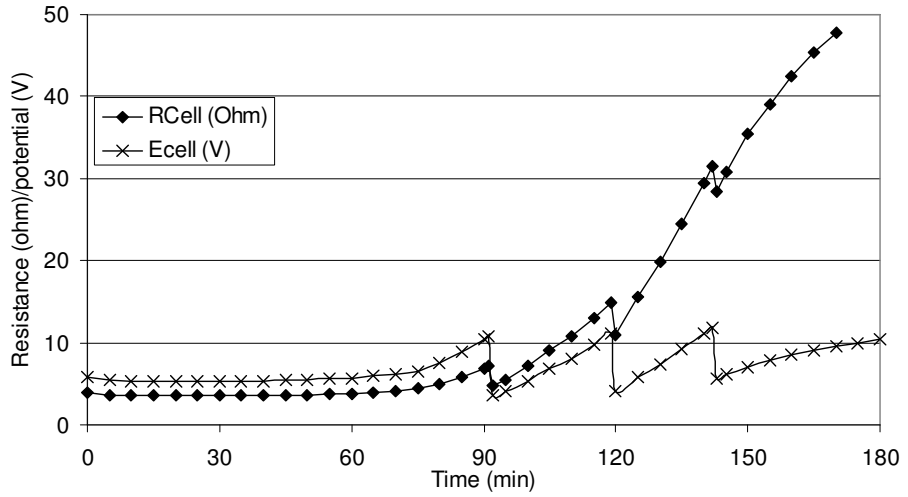

Figure 5.3.8. The electrical resistance Rcell and voltage drop Ecell across a single cell pair during bipolar electrodialysis of a feed stream with 0.4 M lactic acid and 0.5 M KOH.

Considering the large ratio of lactate to hydroxide in the second experiment, the higher resistance is due to the mobility of lactate being 5 times lower than the

mobility of hydroxide. However, the overall energy consumption is lower in the second experiment because of the much better current efficiency.

5.3.4 Conclusion

The concentration of lactate, and the ratio between lactate and hydroxide in the feed solution is of major importance for the energy consumption. At the high lactate concentration (0.4 M) an overall current efficiency of 88% was obtained and an average of 2.15 kWh/kg was necessary for decreasing the lactate concentration from 35.1 to 0.8 g/l. When the lactate concentration in the feed was 0.2 M the overall current efficiency was 43% and the energy consumption was 3.48 kWh/kg to reduce the lactate concentration from 17.9 to 0.7 g/l

The experiments showed that the last remains of lactate was expensive to remove, not just in terms of energy consumption but also because of a very low flux, which increases the necessary membrane area. At the end of the experiments the current density was 7.5 times smaller than to begin with, which for a constant current efficiency imply a necessary membrane area that is 7.5 times larger for transference of a given amount of lactate.

Since the feed circuit of the bipolar electrodialysis unit supposed to be a closed circuit connected to the reverse electro-enhanced dialysis unit, a total depletion of lactate is not essential. The level of lactate in the stream returned to the reverse electro-enhanced dialysis must depend on an optimization where the current efficiency and energy consumption of both units are taking into account.

5.3.5 Paper IV

0273-2289/01/94/0197/$13.75

Conversion of Sodium Lactate to Lactic Acid with Water-Splitting Electrodialysis

ANNA PERSSON,[1] ARVID GARDE,[2] ANN-SOFI JÖNSSON,[1] GUNNAR JONSSON,[2] AND GUIDO ZACCHI*,[1]

[1]*Department of Chemical Engineering 1, Lund University, PO Box 124, SE-221 00 Lund, Sweden, E-mail: Guido.Zacchi@kat.lth.se; and* [2]*Department of Chemical Engineering, Membrane Group, Technical University of Denmark, Building 229, DK-2800 Lyngby, Denmark*

Received October 1, 2000; Revised March 1, 2001; Accepted March 1, 2001

Abstract

The conversion of sodium lactate to lactic acid with water-splitting electrodialysis was investigated. One way of reducing the power consumption is to add a conductive layer to the acid compartment. Doing this reduced the power consumption by almost 50% in a two-compartment cell, whereas the electric current efficiency was not affected at all. Three different solutions were treated in the electrodialysis unit: a model solution with 70 g/L of sodium lactate and a fermentation broth that had been prefiltered two different ways. The fermentation broth was either filtered in an open ultrafiltration membrane (cut-off of 100,000 Dalton) in order to remove the microorganisms or first filtered in the open ultrafiltration membrane and then in an ultrafiltration membrane with a cut-off of 2000 Dalton to remove most of the proteins. The concentration of sodium lactate in the fermentation broth was 70 g/L, as well. Organic molecules present in the broth (peptides and similar organic material) fouled the membranes and, therefore, increased power consumption. Power consumption increased more when permeate from the more open ultrafiltration membrane was treated in the electrodialysis unit than when permeate from the membrane with the lower cut-off was treated, since there was a higher amount of foulants in the former permeate. However, the electrodialysis membranes could be cleaned efficiently with a 0.1 *M* sodium hydroxide solution.

Index Entries: Lactic acid; electrodialysis; bipolar membranes; fermentation broth; wheat.

*Author to whom all correspondence and reprint requests should be addressed.

Introduction

Lactic acid is a well-known organic acid that can be polymerized to polylactic acid, which is biodegradable and therefore used in the pharmaceutical industry for the production of sutures and matrices for slow-release drugs *(1)*. Lactic acid can be produced by both organic synthesis and fermentation *(2)*. Organic synthesis is most widely used for the production of lactic acid in the pharmaceutical industry, but as the cost of petroleum has increased, fermentation has become more interesting *(3)*. Fermentative production of lactic acid is inexpensive, especially when waste products such as whey are used as substrate. On the other hand, the subsequent downstream processing is difficult owing to the complexity of the media and the byproducts, such as proteins and organic acids, formed during fermentation. In addition, lactic acid has a high boiling point and polymerizes at elevated temperatures, and, thus, traditional processes, such as distillation and conventional evaporation, cannot be used for the recovery *(4)*. Because lactic acid–producing bacteria often exhibit the highest production rate at pH values over the pK_a of lactic acid, the acid is present as a salt (e.g., sodium lactate) in the fermentor. Many different processes have been suggested for the downstream processing of lactic acid/lactate, including extraction and ion-exchange chromatography *(5,6)*. Another method of recovery is to precipitate the lactic acid with calcium hydroxide, refine the calcium lactate, and convert it to lactic acid by acidification with sulfuric acid *(7)*. These processes all have disadvantages in that they are unspecific and expensive, produce waste streams, and are difficult to scale up *(4,7–9)*. Water-splitting electrodialysis is a membrane process that has been suggested as a competitive alternative for the conversion of lactate to lactic acid because the process does not produce waste streams.

Research has been conducted on electrodialysis for the desalination of seawater. However, electrodialysis has been found to be a more realistic alternative when used for desalination of brackish water *(10–12)*. It is also used to remove salts from process water in power plants and to remove radioactive substances from water in nuclear power plants *(13)*. Recently, electrodialysis has attracted interest in other areas for the recovery or removal of chemicals in process streams such as those in the pulp and paper and the iron and steel industries *(14,15)*. In the food industry, electrodialysis has been suggested for various processes such as desalination of whey, prevention of precipitation of tartrates in wine, and for purification of proteins *(16)*. In the biotechnologic industry, electrodialysis can be used for the refinement of organic acids from fermentation broths *(17,18)*. Much interest has been focused on recovery of the organic acid lactic acid from fermentation broth using electrodialysis to use the acid for the production of the biodegradable and environmentally friendly polymer polylactic acid *(19–22)*. Several mathematical models for the conversion of sodium lactate to lactic acid have also been presented *(23–25)*.

The use of bipolar membranes for the conversion of lactate to lactic acid has recently attracted interest *(24,26)*. In the bipolar membrane, water molecules are split into hydrogen and hydroxide ions. These ions can be combined with the ions in the salt, which are assumed to be converted into an acid and a base, without adding any extra chemicals, thus preventing the production of waste streams. The streams leaving the electrodialysis unit are the product (lactic acid in this case) and the base (sodium hydroxide), which can be reused as a pH adjuster in the fermentor.

The present study is part of a project on process development for the production and refinement of lactic acid from starchy raw material, mainly wheat flour *(27–31)*. The total process comprises prehydrolysis and saccharification of starch, fermentation, and separation and concentration of the product. In this article, we describe the conversion of sodium lactate to lactic acid using electrodialysis with bipolar membranes. Experiments were performed with a conventional three-compartment cell and for energy-saving reasons; a two-compartment cell was also investigated. In both cases, a model solution of sodium lactate and one or two fermentation broths containing sodium lactate were used.

Materials and Methods

Preparation and Fermentation of Medium

The lactic acid–producing bacterium *Lactococcus lactis* spp. *lactis* ATCC 19 435 was grown on a medium consisting of wheat flour hydrolysate and yeast extract. The wheat flour hydrolysate was prepared by passing the flour (4800 g) through a sieve, mesh 0.4 mm, to remove the bran. This flour was then mixed with water (20 L) and heated to 50°C, and 67 µL/L of the enzyme α-amylase (Termamyl 120 L; Novo Nordisk, Bagsvaerd, Denmark) was added. The mixture was heated to 95°C and maintained at this temperature for 50 min, while liquefaction occurred. The medium was cooled to 30°C and diluted to 50% of the original concentration using water. The medium (10 L) was then transferred to the fermentor, where 1200 µL/L of the enzyme mixture SAN Super 240 L (α-amylase and amyloglucosidase) (Novo Nordisk), 5 g/L of yeast extract, and the inoculum were added *(27)*. Fermentation was performed as simultaneous saccharification and fermentation. Owing to product inhibition of growth and thus product formation, resulting from the formation of sodium lactate, the glucose concentration had to be <73 g/L *(30)*.

The inoculum was prepared by taking a colony of *L. lactis* grown on M17 agar in a Petri dish and transferring it to a test tube with 5 mL of M17 broth (Merck, Darmstadt, Germany). This was incubated overnight at 30°C, and the mixture was then transferred to a 1-L Erlenmeyer flask containing 500 mL of M17. The flask was incubated for 12 h, and the cells were then transferred to the fermentor.

Lactic acid was produced in a 22- or a 16-L fermentor (model NLF22 and NLF16; Bioengineering, Wald, Switzerland) with baffles. The tempera-

ture was 30°C, the stirring speed 300 rpm, and the pH was maintained at 6.0 by adding 30% (w/v) NaOH. Fermentation was allowed to proceed for 3 d.

Bacterial Cell and Protein Separation

To avoid fouling in the electrodialysis unit, the flour particles, bacterial cells, and proteins had to be separated. The bacterial cells and the flour particles were separated from the broth in a shear-enhanced, crossflow, laboratory-scale ultrafiltration module (CR filter from Flootek, Malmö, Sweden) with recirculation of the retentate *(29)*. The module was equipped with two membranes: one above and one below the rotor blade. The area of each membrane was 0.05 m^2. A polymeric ultrafiltration membrane PS100 (Hoechst, Wiesbaden, Germany) with a nominal cut-off of 100,000 Dalton was used. This membrane was chosen because previous experiments with ceramic microfiltration (MF) membranes showed that MF membranes have a higher tendency toward irreversible fouling than membranes with somewhat smaller pores such as open ultrafiltration membranes (results not shown). Proteins were separated in the same module, but a membrane with a cut-off of 2000 Dalton was used (PS2; Hoechst). In the electrodialysis experiments, recovery of lactic acid from both permeate from the open ultrafiltration membrane and permeate from the ultrafiltration membrane with a lower cutoff was investigated.

Electrodialysis

In the electrodialysis unit, the sodium lactate is converted to lactic acid and sodium hydroxide. Two different membrane configurations were used: a three-compartment cell and a two-compartment cell.

Three-Compartment Cell

The membrane module used had a membrane area of 33 cm^2 (constructed at the Department of Chemical Engineering; DTU, Lyngby, Denmark). The module was equipped with four membranes, two bipolar membranes, a cation-exchange and an anion-exchange membrane, fitted between 0.6-mm-thick tortuous path spacers. The configuration is shown in Fig. 1. The three-compartment cell was used only in batch separation mode.

Two-Compartment Cell

Two different modules were used. One had a membrane area of 10 cm^2 (Micro Flow Cell; Electrocell AB, Täby, Sweden), and the other was the one used in the experiments with the three-compartment cell, adapted to a two-compartment module (membrane area of 33 cm^2). The membrane configuration (two bipolar membranes and an anion-exchange membrane) was the same for both modules (Fig. 2). Limiting current trials showed that there was only a very small difference between the two modules, so the results from the two modules are comparable. Both batch separation mode and continuous separation mode were investigated with the two-compartment cell configuration.

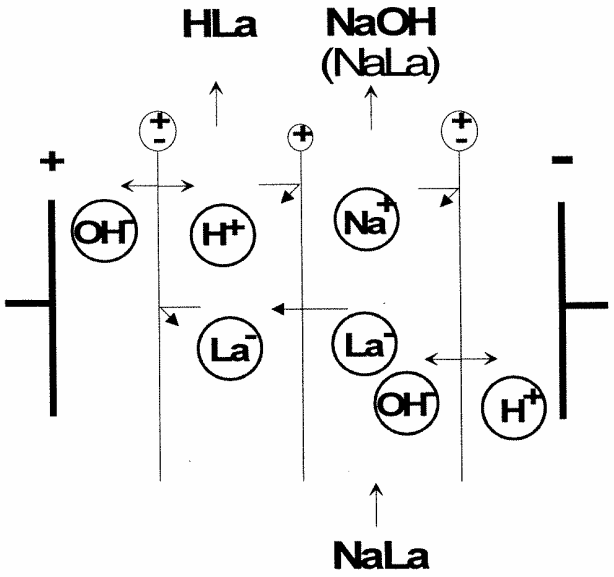

Fig. 1. Membrane configuration in the three-compartment cell. (+) anion-exchange membrane; (–) cation-exchange membrane; (±) bipolar membrane.

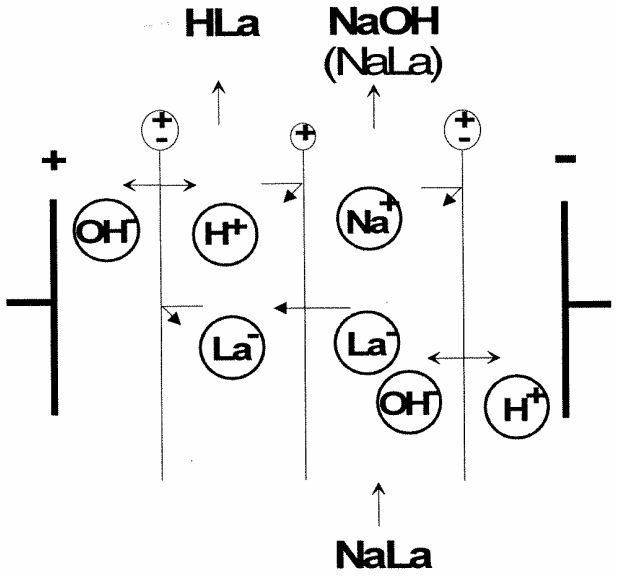

Fig. 2. Membrane configuration in the two-compartment cell. Symbols are the same as in Fig. 1.

Membranes and Experimental Conditions

The bipolar membranes used were BP-1 (Tokuyama, Tokyo, Japan). The anion-selective membrane used was Selemion AMV membrane (Asahi

Glass, Tokyo, Japan). The cation-selective membrane used in the three-compartment cell was a Neosepta CMB (Tokuyama).

In both the three-compartment and two-compartment cell experiments, the current density was 7 A/cm^2, and the crossflow velocity over the membranes was in the range of 0.05–0.07 m/s in the batch experiments and 0.0023 m/s in the continuous-mode experiments. The temperature was maintained at 25°C in all experiments. Three solutions were treated in the electrodialysis unit: one model solution with a concentration of 70 g/L of lactic acid (KEBO Lab A/S, Albertslund, Denmark) and two different ultrafilter permeates (fermentation broth with approx 70 g/L of sodium lactate). The first permeate was fermentation broth treated in an open ultrafiltration membrane (PS100) with a cut-off of 100,000 Dalton and the second permeate was broth first treated in the membrane with a cut-off of 100,000 Dalton and then in a membrane (PS2) with a cut-off of 2000 Dalton.

Analyses

The concentration of lactic acid was analyzed with high-performance liquid chromatography in an Aminex HPX-87H column (Bio-Rad, Richmond) as reported previously *(29)*.

The protein concentration was measured with the Bradford Coomassie Brilliant Blue method (Coomassie Protein Assay Reagent 23200; Pierce, Rockford, IL). The concentration of inorganic ions was measured with ion chromatography using an AS4ASC column (Dionex, Sunnyvale, CA), and the eluting buffer was 1.80 m*M* Na_2CO_3/1.70 m*M* $NaHCO_3$.

Cleaning Procedure

After filtration, the ultrafiltration membranes were rinsed with deionized water until the retentate stream was clear, and the electrodialysis membranes were rinsed until the pH was neutral. The polymeric ultrafiltration membranes were cleaned with a 0.4% alkaline cleaning agent (Ultrasil 10; Henkel, Germany), which was recirculated in the system at 50°C for 20 min. The system was then rinsed with deionized water at 20°C (5 × 5 L). A solution of 0.1 *M* NaOH at 25°C was recirculated in the electrodialysis modules for 30 min, and then the membrane was rinsed with deionized water until the pH was neutral.

Results and Discussion

The fermentation broth used was well suited for the electrodialysis step since the concentrations of small inorganic ions that could compete with the lactate ions (625 m*M*) were low (2.25 m*M* chloride ions, 1.46 m*M* phosphate ions, and 0.20 m*M* sulfate ions).

The results from the experiments using electrodialysis are presented as current efficiency, CE (%), and power consumption, PC (kWh/kg).

$$CE = [n/(I \cdot F \cdot t)] \quad (1)$$

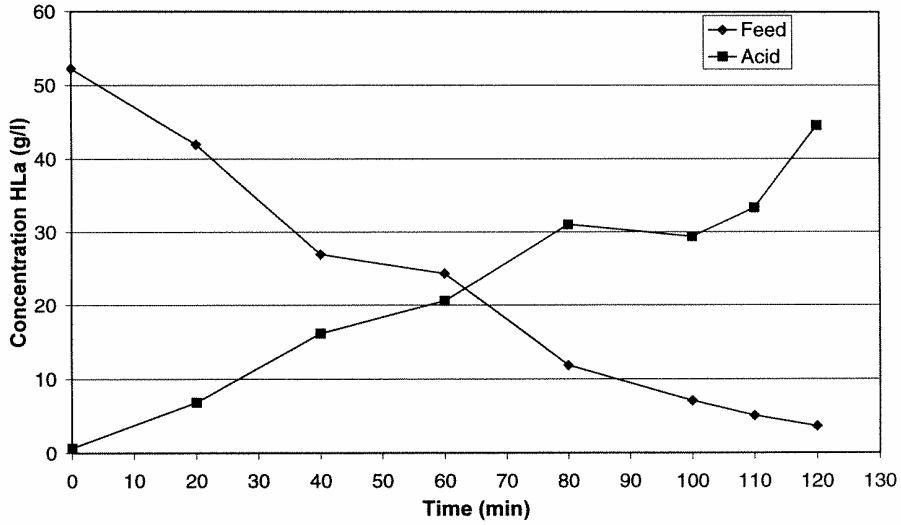

Fig. 3. Concentration in the feed and in the acid stream vs time in the three-compartment cell using a 70 g/L sodium lactate model solution.

$$PC = [U \cdot I \cdot t/(M \cdot 1000 \cdot 3600)] \quad (2)$$

in which n is the molar amount of lactate molecules transported over the membrane, I is the current (A), F is Faraday constant (As/mol), t is the time (s), U is the voltage (V), and M is the mass of the lactic acid formed (g). The current efficiency is given as the overall current efficiency, and the power consumption is based on the voltage over the whole membrane stack, including the electrode compartments.

Three-Compartment Cell

The most widely reported membrane configuration when converting lactate to lactic acid with bipolar membrane electrodialysis is the three-compartment cell. The change in concentration of lactate in the feed and in the concentrate stream can be seen in Fig. 3. In the experiment shown in Fig. 3, the model solution 70 g/L of sodium lactate at pH 6.0 was used. The overall current efficiency was 76%. The reasons for the current efficiency being <100% may be owing to a selectivity of the anion-exchange membrane <100% (i.e., cations are also transported through the membrane), back-diffusion of already converted lactic acid, or current leakage through manifolds and tubes used for the electrode rinsing solution. The overall current efficiency decreased with time (80% at 40 min, 78% at 80 min, and finally 76% at 120 min). The power consumption was 5.6 kWh/kg, calculated over the whole stack, including the electrode compartments. The resistance over the electrode compartments constitutes a significant fraction of the energy required for the process, and, thus, the energy consumption per kilogram of lactic acid can be reduced if the number of cells (per electrode pair) in the stack is increased.

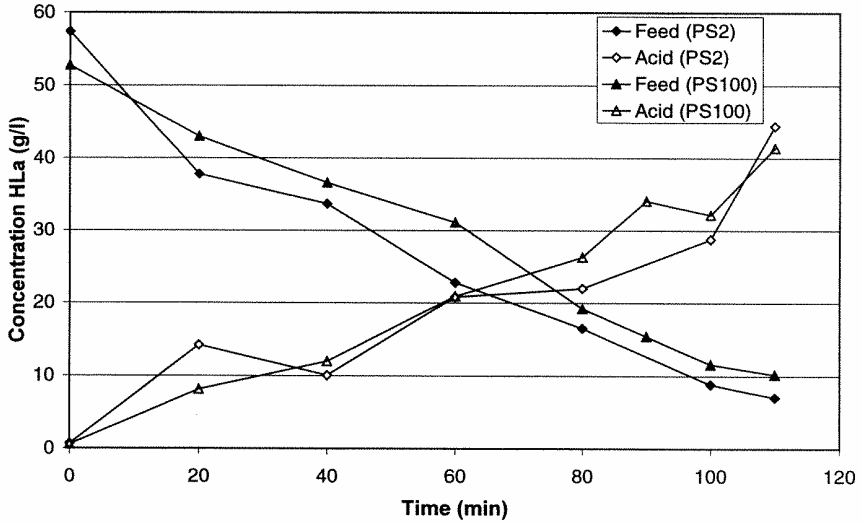

Fig. 4. Comparison of the concentration in the feed and in the acid stream vs time in a three-compartment cell using two fermentation broths treated in a PS100 and in a PS2 membrane.

Two experiments were conducted with fermentation broth: one using permeate from the PS100 membrane and one using permeate from the PS2 membrane (Fig. 4). The current efficiency for the two fermentation broths was about the same, 82% for the PS2 permeate and 77% for the PS100 permeate. However, the power consumption was higher for the PS100 permeate (7.3 kWh/kg) than for the PS2 permeate (6.5 kWh/kg). The increase in power consumption compared with the model solution was probably owing to fouling of the membranes by charged molecules (other than lactic acid), e.g., amino acids and polypeptides. The greater increase when permeate from the PS100 membrane was used is owing to the higher cut-off of the membrane, which leads to a higher concentration of foulants in the permeate. The concentration of proteins in the PS100 permeate was 0.20 mg/mL and in the PS2 permeate 0.05 mg/mL. When membrane fouling occurs, the membrane resistance increases, thus increasing the power consumption. However, the membrane properties were restored during cleaning.

The concentration of lactic acid in the acid stream was quite low (50 g/L); thus, if the concentration could be increased without extra power consumption, the gain could be considerable. To achieve this, lactate ions from a large volume (800 mL) of feed were transferred to a smaller volume of acid solution (200 mL). The results are shown in Fig. 5.

From simple mass balance calculations, the maximum theoretical concentration of lactic acid in the acid stream for this module is estimated to be about 280 g/L, which is the ratio between the total lactic acid flux and the total water flux into the acid compartment. In an investigation by Börgardts et al. *(26)*, the highest concentration reached in the acid stream

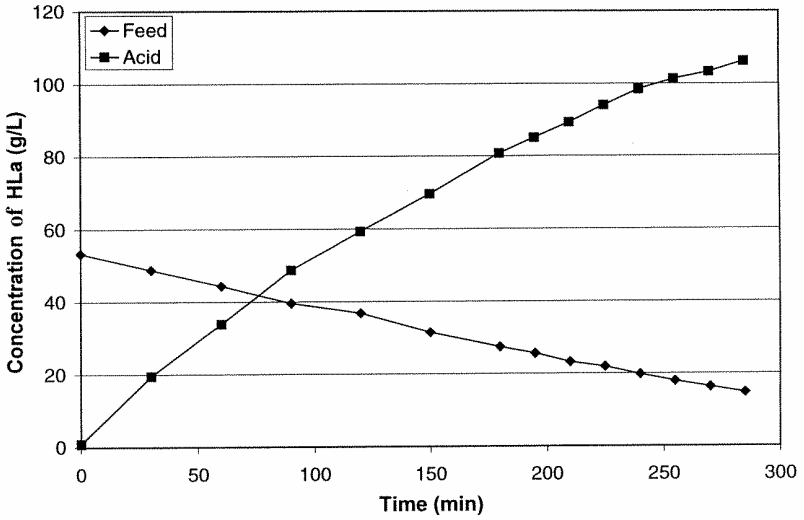

Fig. 5. Concentration in the feed and acid streams vs time in the three-compartment cell when increasing the concentration in the acid stream by transferring lactate ions from a larger volume of feed.

using the same membrane configuration was about 200 g/L. There could be several reasons for the difference between the higher estimated value in the present study and the value given in their study. The most important is that the 200 g/L is a "real" maximum value where back-diffusion of lactic acid and the osmotic water flux owing to higher ion concentration in the acid compartment is at its maximum. In the present experiment, the maximum lactic acid concentration was evaluated on the basis of the separation seen in Fig. 5 in which the concentration in the acid compartment only reached 106 g/L; that is, the process had not reached steady state. Therefore, the lower back-diffusion and lower osmotic water flux in the considered interval might lead to an overestimation of the maximum lactic acid concentration attainable. Other reasons for the difference in the two maximum values could be different concentrations of inorganic anions in the feed streams, facilitating extra electroosmotic water flux, and, of course, that different membranes might also have different water transport properties.

Two-Compartment Cell

To decrease the resistance in the module, the cation-exchange membrane was removed and the module was run with two compartments. To reduce the conductivity even further, the conductivity in the acid compartment was increased by the addition of salt. Lactic acid in a water solution has a low conductivity, even at high concentrations (Fig. 6). This low conductivity makes the voltage over the module very high, and, thus, the power consumption becomes high.

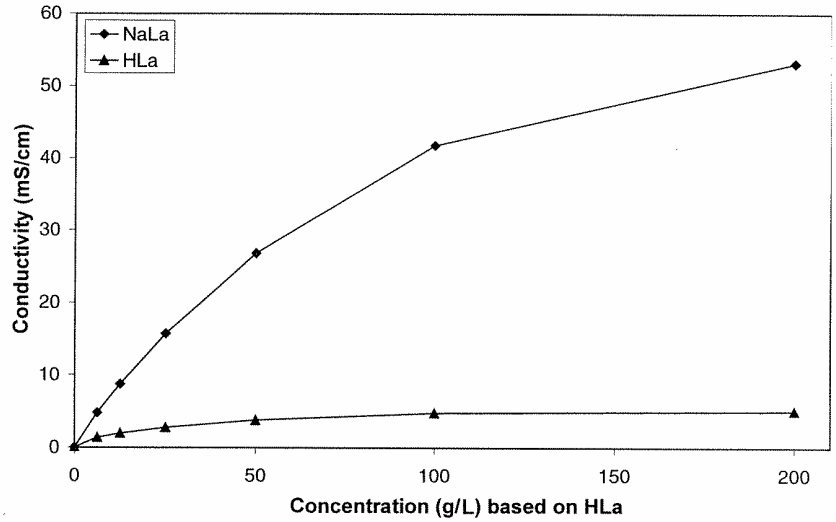

Fig. 6. Conductivity vs concentration of lactic acid and sodium lactate (based on lactic acid equivalents).

If a conductive layer is used in the acid compartment of the module, the resistance and thus the power consumption can be reduced *(32,33)*. In the present study, the resistance in the acid compartment was reduced by using a 2% sodium chloride solution as acid stream. The disadvantage of sodium chloride is that it is difficult to separate it from the lactic acid after the electrodialysis step. A more convenient way of reducing the resistance in the acid compartment is to use beads of charged chromatography gel, because they can easily be removed by filtration after electrodialysis.

Four experiments were performed with the two-compartment cell with feed solutions at pH 6.0: two with the model solution (70 g/L of sodium lactate) and two with permeate from the PS2 membrane. Continuous and batch separation were employed with both solutions.

The final concentration did not differ between continuous and batch separation, being about 20 g/L of lactic acid in the acid compartment in all cases. Figure 7A shows the results from the batch and continuous separation experiments when the fermentation broth (permeate from the PS2 membrane) was treated in the module.

The current efficiency was 33% when the model solution was treated in the module (for both batch and continuous separation mode) and somewhat lower when the fermentation broth was treated (30% for batch separation and 28% for continuous separation). The power consumption was also about the same for the two separation methods, about 8 kWh/kg for the model solution and 10 kWh/kg for permeate from the PS2 membrane. However, the current efficiency decreased and the power consumption increased when the PS2 permeate was processed in the electrodialysis unit compared with model solution (Fig. 7B). This was owing to fouling of the

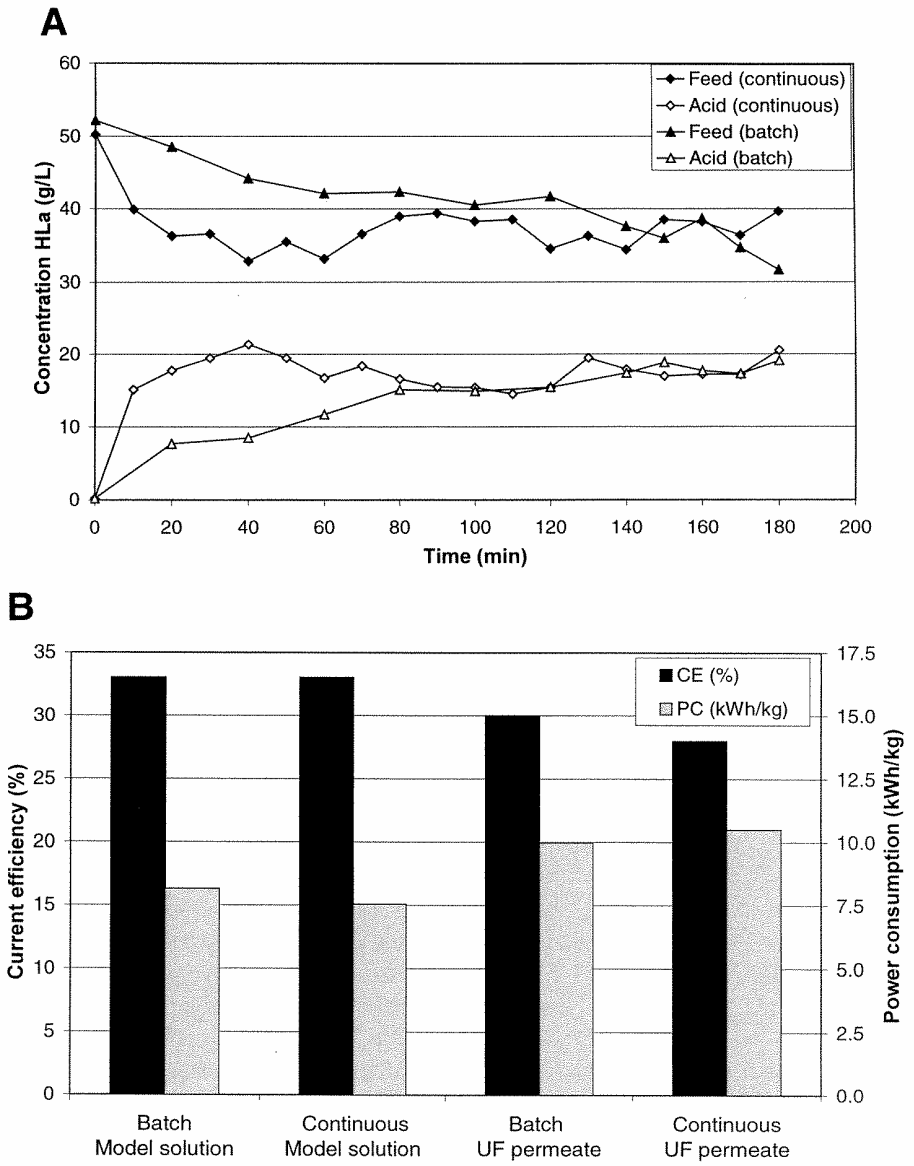

Fig. 7. **(A)** Concentration in the feed and acid compartment vs time for continuous and batch separation. PS2 permeate at pH 6.0 was used as the feed. **(B)** Current efficiency and the power consumption for batch and continuous separation when model solution and PS permeate were processed in the electrodialysis unit. UF, ultrafiltration; CE, current efficiency; PC, power consumption.

membrane, the same kind of fouling as was encountered in the three-compartment cell.

The power consumption of the two-compartment cell was higher in all cases than that of the three-compartment cell, although a conductive layer

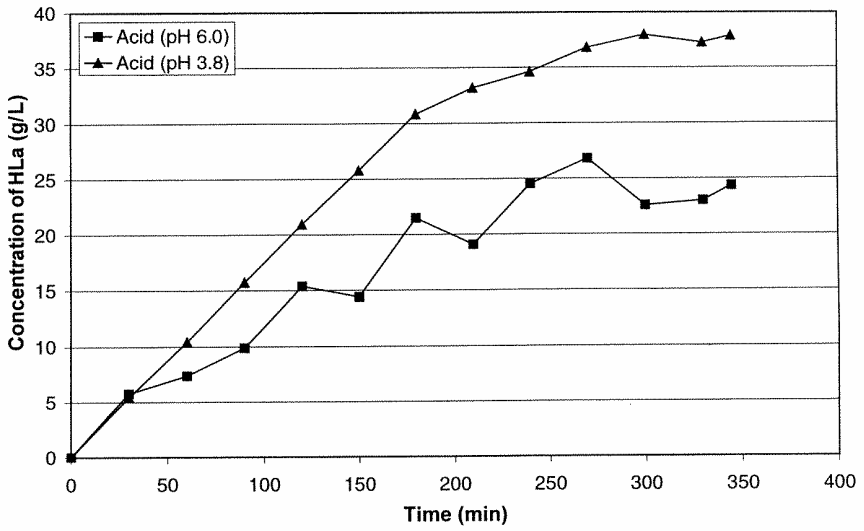

Fig. 8. Concentration of lactic acid in the acid stream vs time for a feed with low pH (3.8) and a feed with high pH (6.0). Model solutions with 70 g/L of sodium lactate molar equivalents were used.

was employed in the acid compartment in the two-compartment cell. For example, when the model solution was used in the batch experiment, the power consumption was 8.1 kWh/kg for the two-compartment cell, whereas it was 5.6 kWh/kg for the three-compartment cell. This was owing to the low current efficiency of 33% for the two-compartment cell, compared with 75% for the three-compartment cell.

This very low current efficiency was thought to be owing to competition between the lactate and hydroxide ions produced by the bipolar membrane. To elucidate this, a model solution of 70 g/L of sodium lactate equivalents at pH 3.8 was processed in the electrodialysis unit. The pK_a of lactic acid is at about pH 3.8, so 50% of the molecules are present in their acid form and 50% are present in their salt form. The first hydroxide ions produced by the bipolar membrane neutralize the molecules in the acid form, and, thus, the competition between the lactate and hydroxide ions can be avoided. It was found that the transport of lactate ions over the anion-exchange membrane increased when the pH in the feed stream decreased (Fig. 8). The current efficiency was 66% when the pH of the feed was 3.8 compared with 33% with a feed pH of 6.0. The power consumption was simultaneously reduced from 8.1 to 4.7 kWh/kg. Unfortunately, most of the bacteria used for the production of lactic acid do not have pH optima for the production of lactic acid at such a low pH as 3.8. Hence, lowering the pH is not a realistic alternative in a commercial plant for the production of lactic acid.

The final investigation was carried out to show that the conductive layer actually had a positive influence on the power consumption. The experiment with the low-pH feed was compared with an experiment under

similar conditions except that the solution in the acid compartment was pure water. When no salt was present in the acid compartment, the power consumption was doubled compared with the case in which sodium chloride was present in the acid compartment (8.3 and 4.7 kWh/kg, respectively), although the current efficiency was about the same for the two experiments, 66% with sodium chloride and 64% without sodium chloride in the acid compartment.

Conclusion

The ultrafiltered fermentation broth (lactic acid bacteria grown on hydrolyzed wheat starch) used in this investigation was well suited for use in the electrodialysis, because the concentration of inorganic ions is very low. It was found that the three-compartment cell exhibited higher current efficiency and lower power consumption than the two-compartment cell, since competition between hydroxide and lactate ions can be avoided in a three-compartment cell.

It was also shown that the power consumption could be reduced by almost 50% when a conductive layer was added in the acid compartment and that this did not effect the yield nor the current efficiency. This was found to be the case for the two-compartment cell but would probably also reduce the power consumption for the three-compartment cell.

It was also found that when fermentation broth was treated in the electrodialysis module, the power consumption increased owing to fouling by larger organic molecules present in the broth despite the fact that the broth had been pretreated with ultrafiltration. The fermentation broth treated in the membrane with a cut-off of 100,000 Dalton fouled the membranes more than the broth that also had been treated in a membrane with a cut-off of 2000 Dalton. The difference in power consumption was only about 1 kWh/kg, and because the membrane could be cleaned in both cases, it might be advantageous to omit the second ultrafiltration step, depending on the capital and operating cost of the extra ultrafiltration membrane unit. However, to be able to evaluate further the advantages or drawbacks with this process, an economical evaluation in which electrodialysis is compared with other process alternatives, such as ion-exchange chromatography or extraction, has to be made.

Appendix 1

Calculation of the maximal concentration of lactic acid is made as follows. The total mass of lactic acid in the system is calculated from the start concentrations in the acid and feed compartments:

$$M_{TOT} = C_{F0} \cdot V_{F0} + C_{A0} \cdot V_{A0} \qquad \text{A1.1}$$

in which C_{A0} and C_{F0} are the start concentrations in the acid and feed streams, respectively, and V_{A0} and V_{F0} are the start volumes of acid and feed, respec-

tively. The total mass can also be determined using the final concentrations in the acid and feed compartments (C_A and C_F):

$$M_{TOT} = C_F \cdot (V_{F0} - X) + C_A (V_{A0} + X) \quad \text{A1.2.}$$

in which X is the volume (lactic acid + water) that has been transferred from the feed compartment to the acid compartment. The mass transferred from feed to acid stream is calculated from

$$M = C_A \cdot (V_{A0} + X) \quad \text{A1.3.}$$

The theoretical maximum concentration is calculated from

$$C_{MAX} = M/X \quad \text{A1.4.}$$

Appendix 2: Notation

C_A = concentration of lactic acid in acid compartment (g/L)
C_{A0} = start concentration of lactic acid in acid compartment (g/L)
C_F = concentration of lactic acid in feed compartment (g/L)
C_{F0} = start concentration of lactic acid in feed compartment (g/L)
F = Faraday constant (As/mol)
I = current (A)
M = transferred mass of lactic acid (g)
M_{TOT} = total mass of lactic acid (g)
n = molar amount of molecules transported over membrane (mol)
PC = power consumption (kWh/kg)
t = time (s)
U = voltage (V)
V_{A0} = start volume of acid stream (L)
V_{F0} = start volume of feed stream (L)
X = volume of lactic acid and water transported over membrane (L)
η = current efficiency

Acknowledgment

We wish to thank the Absolut Company, Kristianstad, Sweden, for its kind donation of wheat flour and hydrolysis enzymes.

References

1. Seeley, R. S. (1992), *Chem. Business*, February, 28–30.
2. Lipinsky, E. S. (1981), *Science* **212,** 1465–1471.
3. Röper, H. and Koch, H. (1990), *Starch/Stärke* **42(4),** 123–130.
4. Kharas, G. B., Sanchez-Riera F., and Severson, D. K. (1994), in *Plastics from Microbes, Microbial Syntheses of Polymers and Polymer Precursors*, Mobely, D. P., ed., Carl Hanser Verlag, Munich.
5. Yabannavar, V. M. and Wang, D. I. C. (1991), *Biotechnol. Bioeng.* **37,** 716–722.
6. Jianping, L., Bo, C., Jianping, W., and Peilin, C. (1997), *Chin. J. Chem. Eng.* **5(1),** 49–55.
7. Datta, R., Tsai, S.-P., Bonsignore, P., Moon, S.-H., and Frank, J. R. (1995), *FEMS Microbiol. Rev.* **16,** 221–231.

8. Bar, R. and Gainer, J. L. (1987), *Biotechnol. Prog.* **3(2),** 109–114.
9. Katzbauer, B., Moser, A., and Narodoslawsky, M. (1992), DECHEMA Biotechnol. Conf. **5,** 711–713.
10. Seto, T., Ehara, L., Komori, R., Yamaguchi, A., and Miwa, T., (1978), *Desalination* **25(1),** 1–7.
11. Thampy, S. K., Narayanan, P. K., Harkare, W. P., and Govindan, K. P. (1988), *Desalination* **69(3),** 261–273.
12. Strauss, S. D. (1992), *Electric Power Int.* June, 21–24.
13. Hebbs, A. (1986), *Int. Power Generat.* **9(3),** 23–26.
14. Rapp, H.-J. and Pfromm, P. H. (1998), *J. Memb. Sci.* **146,** 249–261.
15. Urano, K., Ase, T., and Naito, Y. (1984), *Desalination* **51(2),** 213–226.
16. López Leiva, M. H. (1988), *Lebensm.-Wiss. U. Technol.* **21,** 177–182.
17. Glassner, D. A., Elankovan, P., Beacom, D. R., and Berglund, K. A. (1995), *Appl. Biochem. Biotechnol.* **51/52,** 73–82.
18. Novalic, S., Okwor, J., and Kulbe, K. D. (1996), *Desalination* **105,** 277–282.
19. Yao, P.-X. and Kiyoshi, T. (1990), *J. Gen. Appl. Microbiol.* **36,** 111–125.
20. Yen, Y.-H. and Cheryan, M. (1991), *Trans. IchemE* **69(C),** 200–205.
21. Yen, Y.-H. and Cheryan, M. (1993), *J. Food Eng.* **20,** 267–282.
22. Boniardi, N., Rota, R., Nano, B., and Mazza, B. (1997), *J. Appl. Electrochem.* **27,** 125–133.
23. Boniardi, N., Rota, R., Nano, B., and Mazza, B. (1997), *J. Appl. Electrochem.* **27,** 135–145.
24. Gyo Lee, E., Moon, S.-H., Keun Chang, Y., Yoo, T.-K., and Nam Chang, H. (1998), *J. Memb. Sci.* **145(1),** 53–66.
25. Xuemei, L., Jianping, L., Mo'e, L., and Peilin, C. (1999), *Bioprocess Eng.* **20,** 231–237.
26. Börgardts, P., Kriksche, W., Trosch, W., and Brunner, H. (1998), *Bioprocess Eng.* **19(5),** 321–329.
27. Hofvendahl, K. and Hahn-Hägerdal, B. (1997), *Enzyme Microb. Technol.* **20,** 301–307.
28. Hovfendahl, K., Åkerberg, C., Zacchi G., and Hahn-Hägerdal, B. (1999), *Appl. Microbiol. Biotechnol.* **52,** 781–791.
29. Toräng, A., Jönsson, A.-S., and Zacchi, G. (1999), *Appl. Biochem. Biotechnol.* **76,** 143–157.
30. Åkerberg, C., Hofvendahl, K., Zacchi, G., and Hahn-Hägerdahl, B. (1998), *Appl. Microbiol. Biotechnol.* **49,** 682–690.
31. Åkerberg, C., Zacchi, G., Torto, N., and Gorton, L. (2000), *J. Chem. Technol. Biotechnol.* **75(4),** 306–314.
32. Korngold, E. (1975), *Desalination* **16(2),** 225–233.
33. Narebska, A. and Kurantowicz, M. (1996), *Sep. Sci. Technol.* **33(7),** 959–973.

6

MODELING OF REVERSE ELECTRO-ENHANCED DIALYSIS

6.1 Model introduction

The low current efficiencies obtained during REED-experiments were thought to be related to a buffer-effect of the anion exchange membranes. It was therefore decided to use a model to investigate current efficiency and energy consumption as functions of current reversal frequency, current density and stream properties.

In this chapter, a mathematical model is used to describe the changing concentration profile inside an anion-exchange membrane located in a Reverse Electro-Enhanced Dialysis stack. The mobile ions inside the membrane are subject to periodical reversal of electrical current and react accordingly. With the model, it is possible to describe how the ions react to the changing driving forces, especially electrical migration and diffusion. The model can give estimates that help to develop and optimize the Reverse Electro-Enhanced Dialysis process.

The mathematical model was solved by a numerical method using Fortran programming. The first version of the program only simulates separation of model aqueous solutions of lactate at various pHs. The simulation takes polarization at the membrane surfaces into account, since polarization has significant influence on the boundary conditions.

6.2 Model creation

To model the changing concentration profile across an ion-exchange membrane after each reversal of electrical current, consider an elemental part of the membrane with the dimensions $\Delta x \Delta y \Delta z$ as shown on Figure 6.2.1.

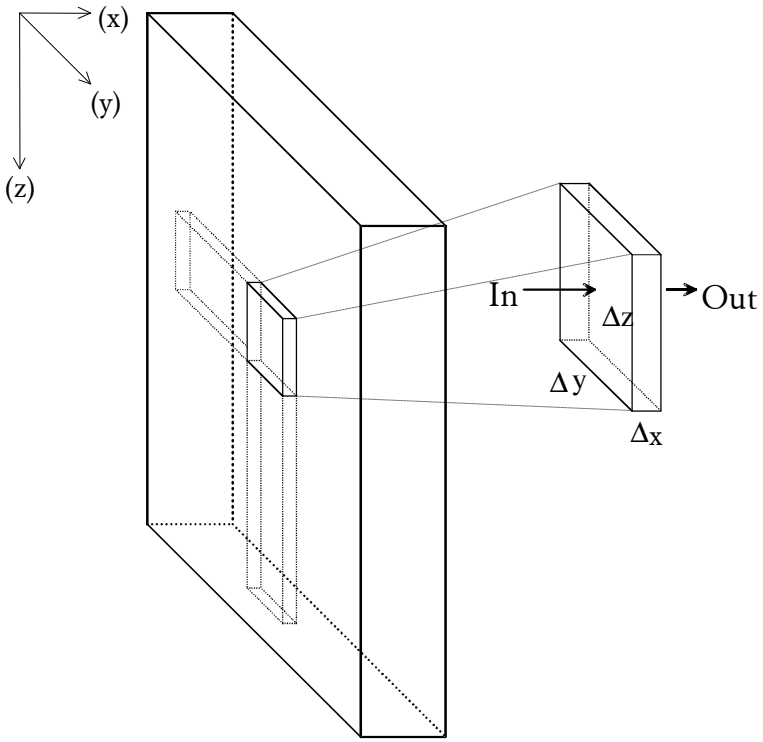

Figure 6.2.1. Membrane element as basis for modeling.

For this modeling of the changing membrane profiles, some assumptions are included.

- Only unidirectional ion-transport is considered. Ions are considered to move only along the direction of the x-axis. This assumption usually yields very satisfactory results for electrodialysis processes based on plate-and-frame modules.
- The ion-exchange membrane is assumed to be perfectly homogeneous with evenly dispersed ion-exchange groups. This assumption is probably wrong for most membranes. In polymer membranes, the ion-exchange groups are more hydrophilic than the rest of the polymeric network, and tend to collect in hydrophilic regions. Thus, the membranes tend to consist of regions with high ion-exchange capacity and thus higher degree of ion-transport and other regions with low ion-exchange capacity and corresponding lower ion-transport. However, assuming a homogeneous ion-exchange capacity, the unidirectional model results in a homogeneous ion flux through the membrane, which should reflect the average membrane flux.
- It is assumed that ions are only transported by electrical migration and diffusion. Usually, convective ion transport is driven by a pressure difference

and is insignificant in electrodialysis processes with nonporous membranes (Mulder 1991). Electro-convective transport and osmotic and electro-osmotic effects are also neglected. Electro-convective transport is not significant at the relatively low current densities, at which the process is operated. Osmotic and electro-osmotic transport mainly influences the solvent transport, which is not investigated in this model.

First objective is constructing an amount (mol) balance for the membrane element:

eq. 6.2.1 $$IN = OUT + ACCUMULATED$$

The IN part of the equation, is considered the number of moles entering the element through the element-surface of dimension $\Delta y \Delta z$ at the distance x from the membrane surface in the transport direction during a small time period described as Δt. The OUT part is similar to the IN part, except the mole-flux through the surface at $x+\Delta x$ is considered.

eq. 6.2.2
$$IN = J_i(x,t) \cdot \Delta y \Delta z \Delta t$$
$$OUT = J_i(x+\Delta x,t) \cdot \Delta y \Delta z \Delta t$$

As expression for the flux J_i of component i, the Nernst-Planck equation (eq. 3.5.40) can be used. Since constant electrical current is applied, another approach is taken in this case.

The electrical migration is defined as the part, t_i^m, of the total current density, i_d (A/m^2), that is carried by component i. t_i^m is the transport number of component i as defined in the theory part of this thesis.
Thus, the flux composed of migration and diffusion can be expressed by:

eq. 6.2.3
$$J_i(x,t) = -\frac{i_d}{z_i F} t_i^m(x,t) - D_i \frac{dC_i(x,t)}{dx},$$
$$where \qquad t_i^m = \frac{|z_i| u_i^m C_i(x,t)}{\sum_k |z_k| u_k^m C_k(x,t)}$$

The ACCUMULATION part of eq. 6.2.1 is the molar change of i during the time from t to $t+\Delta t$ in the elements volume $\Delta x \Delta y \Delta z$.

eq. 6.2.1 can be expressed as follows:

$$\left(-\frac{i_d}{z_i F} t_i^m(x,t) - D_i \frac{dC_i(x,t)}{dx}\right) \cdot \Delta y \Delta z \Delta t =$$

eq. 6.2.4 $$\left(-\frac{i_d}{z_i F} t_i^m(x+\Delta x,t) - D_i \frac{dC_i(x+\Delta x,t)}{dx}\right) \cdot \Delta y \Delta z \Delta t +$$
$$\left(C_i(x,t+\Delta t) - C_i(x,t)\right) \cdot \Delta x \Delta y \Delta z$$

Dividing the equation with $\Delta x \Delta y \Delta z \Delta t$ and assuming both Δx and Δt to approach 0, is written as a differential equation:

eq. 6.2.5 $$-\frac{i_d}{z_i F} \frac{\partial t_i^m(x,t)}{\partial x} - D_i \frac{\partial^2 C_i(x,t)}{\partial x^2} + \frac{\partial C_i(x,t)}{\partial t} = 0$$

Knowledge of the concentration of all ion species is needed to calculate the transport number, making it necessary to solve eq. 6.2.5 simultaneous for all ion species. To simplify this problem, another assumption has been added.

- Only two ion species are considered significant enough to be included: the hydroxide ions and the target acid ions, which is lactate in this instance. This assumption includes the assumption that the co-ion concentration in the ion-exchange membrane is insignificant. According to the Donnan exclusion theory; when having external solute concentrations lower than a tenth of the membrane's ion-exchange capacity, the co-ion concentration consists of less than one percent of the membrane's total mobile ions.

Hence, the sum of the concentrations of hydroxide and lactate must correspond to the ion-exchange capacity of the membrane, C_R:

eq. 6.2.6 $$C_{Lac}(x,t) + C_{OH}(x,t) = C_R$$

The membrane's ion-exchange capacity C_R is constant throughout the membrane following the assumption of a homogenous membrane. By eq. 6.2.6 the transport number can be simplified to:

eq. 6.2.7

$$t^m_{Lac}(x,t) = \frac{u^m_{Lac} C_{Lac}(x,t)}{u^m_{Lac} C_{Lac}(x,t) + u^m_{OH}\left(C_R - C_{Lac}(x,t)\right)}$$

$$= \frac{C_{Lac}(x,t)}{(1-\mu)C_{Lac}(x,t) + \mu C_R}; \qquad \mu = \frac{u^m_{OH}}{u^m_{Lac}}$$

Introducing μ as the dimensionless relation between the mobility of hydroxide and lactate ions, reduces eq. 6.2.7 a little. Differentiating eq. 6.2.7 yields:

eq. 6.2.8

$$\frac{\partial t^m_{Lac}(x,t)}{\partial x} = \frac{\mu C_R}{\left((1-\mu)C_{Lac}(x,t) + \mu C_R\right)^2} \frac{\partial C_{Lac}(x,t)}{\partial x}$$

$C_{Lac}(x,t)$ is then substituted by U(x,t), defined as:

eq. 6.2.9

$$U(x,t) = (1-\mu)C_{Lac}(x,t) + \mu C_R$$

Inserting eq. 6.2.8 and using the substitution in eq. 6.2.9, eq. 6.2.5 rearranges into the following expression for lactate:

eq. 6.2.10

$$-D_{Lac} U(x,t)^2 \frac{\partial^2 U(x,t)}{\partial x^2} - \alpha \frac{\partial U(x,t)}{\partial x} + U(x,t)^2 \frac{\partial U(x,t)}{\partial t} = 0$$

$$\textit{where} \qquad U(x,t) = (1-\mu)C_{Lac}(x,t) + \mu C_R$$

$$\alpha = \frac{i_d}{zF}\mu C_R \qquad \mu = \frac{u^m_{OH}}{u^m_{Lac}}$$

The hydroxide membrane concentration is obtained from eq. 6.2.6 after solving eq. 6.2.10 for lactate.

6.3 Determination of boundary values

6.3.1 Physical conditions

To decide on boundary values for eq. 6.2.10, consider the following:

- For this modeling, the development of concentration profile is considered for regions of continuous separation of two aqueous streams (I and II) as suggested on Figure 6.3.1. It is assumed that the composition of the solutions do not change within these regions.
- The thickness of the membrane, L, limits the development of concentration profiles to an interval between 0 and L

Polarization at the membrane surface has great influence on the membrane concentrations, since the wall concentrations are in Donnan equilibrium with the membrane concentrations just inside the membrane.

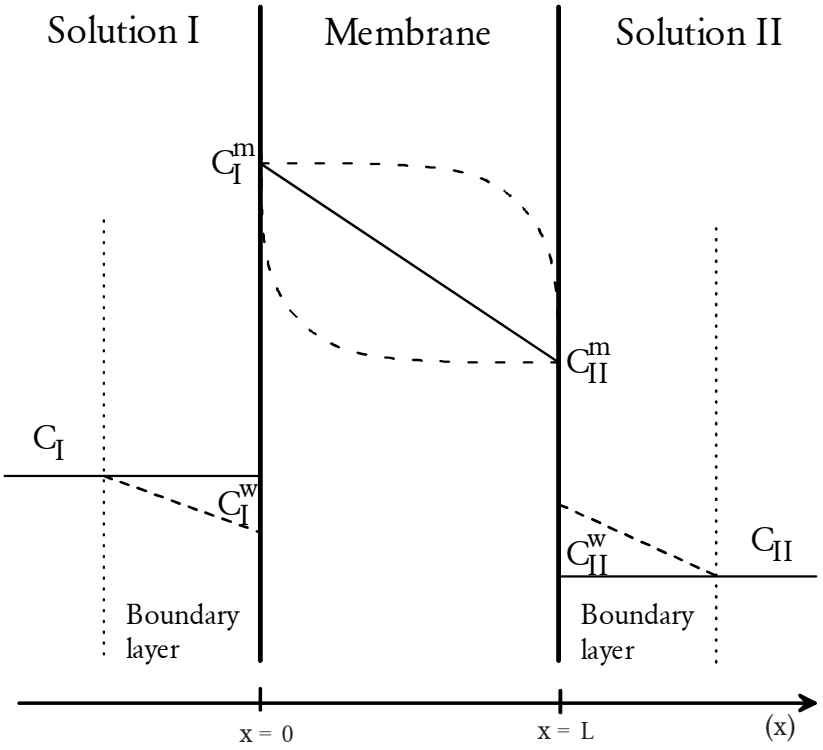

Figure 6.3.1. Assumed starting concentration profile (—), and assumed profile development (---).

Boundary conditions at x = 0:

- After polarization is stabilized outside the membrane at x = 0, the surface flux into the membrane is stable and the membrane concentration at x = 0 is constant from that time on. For simplicity, this assumption has been extended to assuming a constant membrane concentration at x = 0 at all times. The constant membrane concentration is calculated as the steady-state concentration in Donnan equilibrium with the membrane wall concentration just at the membrane surface.

Boundary conditions at x = L:

- Determination of the membrane concentration at x = L is more complex than at x = 0. As a new profile is established, the membrane concentration at x = L also changes. For this model, the membrane concentration is calculated by setting up two equations.
  1. The flux through the last membrane layer at x = L must equal the flux through the boundary layer just outside the membrane.
  2. The wall concentration and the membrane concentration at x = L are connected through the Donnan equilibrium condition.

  This means, that this boundary condition must be evaluated simultaneously with the profile.

Boundary conditions at t = 0:

- As a starting profile (t = 0), the correct choice would be too insert the final values of the concentration profile from the previous calculation, so the new profile can realistically evolve when current is reversed. However, this profile has to be found before it is accessible. Thus, a diffusion profile has been chosen for a model starting profile. The diffusion profile is assumed to be a linear profile between the membrane concentrations at the membrane surfaces as decided by Donnan equilibrium. This profile is shown on Figure 6.3.1.

6.3.2 Solving the Donnan equilibrium condition

The two boundary conditions for equation eq. 6.2.10 both depend on the Donnan equilibrium. Since only hydroxide and lactate ions are considered, the membrane concentrations can be easily determined. From eq. 3.5.29 the following equation must be satisfied:

$$E_{Don} = \frac{RT}{-1 \cdot F} \ln \frac{a^s_{Lac}}{a^m_{Lac}} = \frac{RT}{-1 \cdot F} \ln \frac{a^s_{OH}}{a^m_{OH}} \Rightarrow \frac{C^m_{Lac}}{C^w_{Lac}} = \frac{C^m_{OH}}{C^w_{OH}}$$

Electroneutrality inside the membrane must be satisfied as well:

eq. 6.3.1 $$C^m_{Lac} + C^m_{OH} = C_R$$

Combining these two equations, the membrane concentration can be calculated by this very simplified version of the Donnan equilibrium, if the lactate concentration and hydroxide concentration (or pH) of the external solution at the membrane surface (wall) is known:

eq. 6.3.2 $$C^m_{Lac} = \frac{C^w_{Lac}}{C^w_{Lac} + C^w_{OH}} \cdot C_R$$

6.3.3 Solving the polarization condition

Though polarization at the membrane surfaces follow similar conditions, the approach to calculating the membrane wall concentrations were slightly different from the side, where electrical current enters the membrane, to the side where the electrical current exits the membrane.

At the membrane surface (I), where the anions enter the membrane, the polarization is negative, meaning that this surface risks depletion of ions. If this happens, watersplitting can occur.

At the surface (II) where anions exit, the polarization is positive, thus, watersplitting is not occurring. On the other hand, an equilibrium polarization does not arise on this surface, as it is the case at the other surface.

<u>Polarization at the surface (I) where anions enter the membrane</u>

To calculate the wall concentrations C^w of lactate and hydroxide, it is necessary to consider the hydrodynamic flow-condition of the external solutions. Using a boundary-layer model, a boundary layer thickness δ must be chosen or calculated from mass-transfer (Sherwood) relations. From the boundary layer thickness, a boundary layer mass transfer coefficient k_i of each component *i* can be calculated from the relation:

eq. 6.3.3 $$k_i = D_i / \delta$$

The wall concentration of component *i* is determined by:

eq. 6.3.4 $$C_i^w = C_i^s - \frac{i_d (t_i^m - t_i^s)}{z_i F k_i}$$

t^s is the transport number of *i* in the solution. While t^m only includes the two mobile ions in the membrane, t^s includes all mobile ions in the solution.
With the assumption of no co-ions entering the membrane, eq. 6.3.4 can be expressed for a mono-valenced co-ion (like Sodium):

eq. 6.3.5 $$C_{Na}^w = C_{Na}^s + \frac{i_d \cdot t_{Na}^s}{F \cdot k_{Na}}$$

Again using electroneutrality, the wall concentrations must obey the following relation:

eq. 6.3.6 $$C_{Na}^w + C_H^w = C_{Lac}^w + C_{OH}^w$$

Normally the hydrogen ion concentration can be related to the hydroxide concentration by the water dissociation equilibrium:

eq. 6.3.7 $$C_H \cdot C_{OH} = K_W \qquad K_W \approx 10^{-14}$$

If watersplitting occurs equation eq. 6.3.7 cannot be used. This case is treated later in this section.

In the case of no watersplitting, the wall concentration can be determined by inserting the simplified Donnan relation in equation eq. 6.3.2 in the expression of the transport number, eq. 6.2.7, which yields a quadratic equation:

eq. 6.3.8 $$\begin{aligned} &\left(C_{Lac}^w\right)^2 + \left(\left(\frac{i_d}{F \cdot k_{Lac}}\right) \cdot \left(1 - t_{Lac}^s\right) - C_{Lac}^s - \mu C_{OH}^w\right) \cdot C_{Lac}^w \\ &+ \mu \frac{i_d \cdot t_{Lac}^s}{F \cdot k_{Lac}} C_{OH}^w + \mu C_{Lac}^s C_{OH}^w = 0 \end{aligned}$$

To solve equation eq. 6.3.8, it is necessary to deduct the wall concentration of hydroxide. It can be determined from eq. 6.3.5 - eq. 6.3.7, ending in another quadratic equation:

eq. 6.3.9 $$\left(C_{OH}^{w}\right)^2 + \left(C_{Lac}^{w} - C_{Na}^{w}\right)\cdot C_{OH}^{w} - K_W = 0$$

For hydroxide concentrations higher than 10^{-5} M (pH > 9), eq. 6.3.9 can be reduced to:

eq. 6.3.10 $$\underline{C_{OH}^{w} > 10^{-5} M:} \qquad C_{OH}^{w} = C_{Na}^{w} - C_{Lac}^{w}$$

Combining eq. 6.3.8 and eq. 6.3.10 yields:

eq. 6.3.11
$$(1-\mu)\left(C_{Lac}^{w}\right)^2 + \left(\mu C_{Na}^{w} - (1-\mu)C_{Lac}^{s} + \frac{i_d}{F\cdot k_{Lac}}\left(t_{Lac}^{s}(1-\mu)-1\right)\right)C_{Lac}^{w}$$
$$+\left(\frac{i_d}{F\cdot k_{Lac}}\cdot t_{Lac}^{s} - C_{Lac}^{s}\right)\cdot \mu C_{Na}^{w} = 0 \qquad (pH > 9)$$

With lower hydroxide concentrations, an iteration method can be employed between eq. 6.3.8 and eq. 6.3.9.

From the wall concentrations of lactate and hydroxide, the corresponding concentrations just inside the membrane can then be calculated from the simplified Donnan expression.

In the case of watersplitting, a different approach has to be taken. Since lactate ions are drawn into the membrane as fast as they are transported to the membrane surface, the surface concentration of lactate is close to zero, although lactate is still transferred. In that case, another method is employed to determine the membrane concentration. First, the limiting flux is determined as the sum of the limited migration flux and the diffusion flux across the boundary layer. The limited migration flux can be calculated as $i_{d,lim}/(z_iF)$ from eq. 6.3.4, setting the wall concentration of lactate to zero. The diffusion flux in this case is $k_{Lac}\cdot C^{s}_{Lac}$. The membrane concentration is then assumed to have the value that satisfies the steady-state migration flux inside the membrane, which must equal the aforementioned boundary layer flux.

Since watersplitting is best avoided, these equations are not very interesting for this model. They are included in the modeling program, though, since the program is to be further developed along with the Reverse Electro-Enhanced Dialysis pilot module. More details of the watersplitting calculations can be found in Appendix B.

Polarization at the surface (II) where anions exit the membrane

As mentioned earlier, the approach is slightly different at this surface. Since the membrane profile changes with time, the surface conditions change accordingly.

- The assumption is that the lactate and hydroxide fluxes through the last membrane "layer" must equal the corresponding fluxes through the diffusion layer.
- Another assumption is that the membrane concentration C^m is in constant equilibrium with the wall concentration C^w according to the simplified Donnan equilibrium in eq. 6.3.2.
- For simplicity, the hydrogen ions are omitted. It is assumed that all cations are sodium ions. Otherwise, the following fourth degrees equations will be fifth degree. When pH is 4 or greater, as is always the case for the simulation of the Reverse Electro-Enhanced Dialysis module in this thesis, and the corresponding lactate concentration is close to 0.1 M, the resulting error should be less than 1%.

The assumptions are described graphically in Figure 6.3.2.

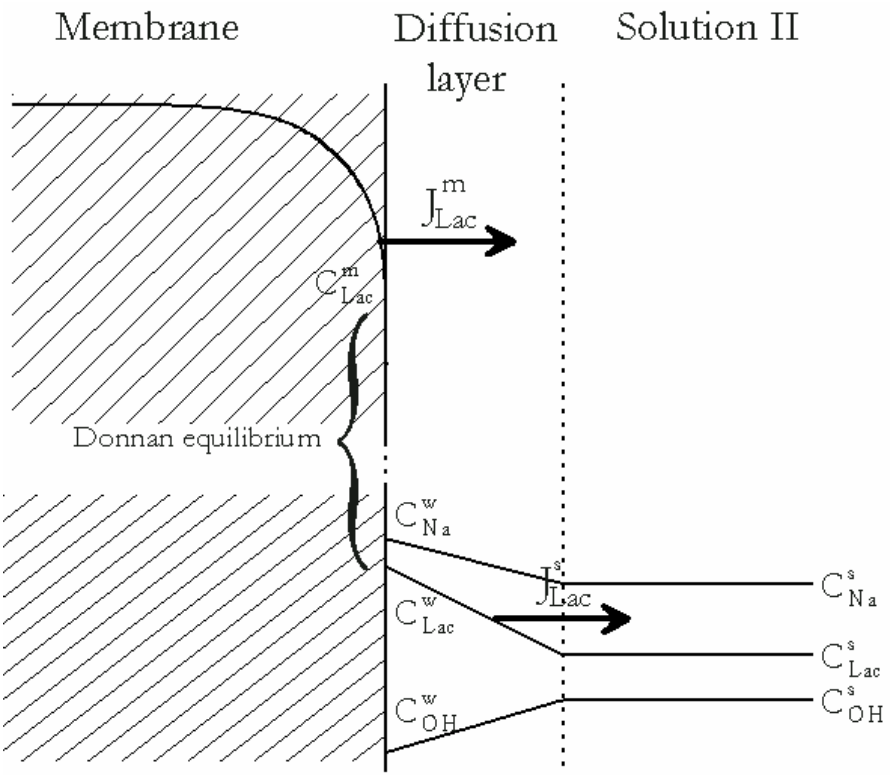

Figure 6.3.2. This is a graphic description of the expected concentration profiles through the diffusion layer during the process. The lactate fluxes (Jm and Js) that are assumed uniform are shown. The corresponding fluxes for the hydroxide ions are also assumed uniform. Finally, the surface concentrations of lactate and hydroxide are assumed to maintain Donnan equilibrium with the ions just inside the membrane.

The equations that must be satisfied and solved for each timestep of the membrane profile are:

$$J^s_{Lac} = -k^s_{Lac}(C^s_{Lac} - C^w_{Lac}) + \frac{i_d}{z_{Lac}F}\cdot t^w_{Lac}$$

$$J^m_{Lac} = -k^m_{Lac}(C^{m-1}_{Lac} - C^m_{Lac}) + \frac{i_d}{z_{Lac}F}\cdot t^m_{Lac}$$

$$J^s_{OH} = -k^s_{OH}(C^s_{OH} - C^w_{OH}) + \frac{i_d}{z_{OH}F}\cdot t^w_{OH}$$

$$J^m_{OH} = -k^m_{OH}(C^{m-1}_{OH} - C^m_{OH}) + \frac{i_d}{z_{OH}F}\cdot t^m_{OH}$$

$$C^m_i = \frac{C^w_i}{C^w_{Lac} + C^w_{OH}}\cdot C_R$$

C^{m-1} is the membrane concentration one steplength (Δx) back inside the membrane, $C_{Lac}(L-\Delta x,t)$, and C^m is $C_{Lac}(L,t)$. The index of the mass transfer coefficients k_i and of the transport numbers t_i refers to the composition that is used in calculating the transport number at the wall (w) or inside the membrane at x=L (m).

By setting J^m equal to J^s for both the lactate and hydroxide ions, two fourth degree equations are the result.

The wall concentration of lactate can be found by solving:

eq. 6.3.12 $$A_0 \cdot (C_{Lac}^w)^4 + A_1 \cdot (C_{Lac}^w)^3 + A_2 \cdot (C_{Lac}^w)^2 + A_3 \cdot C_{Lac}^w + A_4 = 0$$

where

$$A_0 = k_{Lac}^s(\mu_{Lac} + \mu_{Na})$$

$$A_1 = k_{Lac}^s(((1+\mu)(\mu_{Lac} + \mu_{Na}) + \mu_{OH} + \mu_{Na})C_{OH}^w - (\mu_{Lac} + \mu_{Na})C_{Lac}^s) + k_{Lac}^m(\mu_{Lac} + \mu_{Na})(C_R - C_{Lac}^{m-1}) + \mu_{Na}\frac{i_d}{F}$$

$$A_2 = (k_{Lac}^s(\mu(\mu_{Lac} + \mu_{OH} + 2\mu_{Na}) \cdot C_{OH}^w - (1+\mu)(\mu_{Lac} + \mu_{Na})C_{Lac}^s) + k_{Lac}^m((\mu(\mu_{Lac} + \mu_{Na}) + \mu_{OH} + \mu_{Na})C_R - (\mu_{OH} + \mu_{Na} + (1+\mu)(\mu_{Lac} + \mu_{Na}))C_{Lac}^{m-1} + 2(\mu_{OH} + \mu_{Na})\frac{i_d}{F}) \cdot C_{OH}^w$$

$$A_3 = (\mu(\mu_{OH} + \mu_{Na})(k_{Lac}^s C_{OH}^w + k_{Lac}^m C_R) - (\mu(\mu_{Lac} + \mu_{Na}) + (1+\mu)(\mu_{OH} + \mu_{Na})) \cdot (k_{Lac}^s C_{Lac}^s + k_{Lac}^m C_{Lac}^{m-1}) + (\mu_{OH} + \mu_{Na} - \mu_{Lac})\frac{i_d}{F}) \cdot \left(C_{OH}^w\right)^2$$

$$A_4 = -(k_{Lac}^s C_{Lac}^s + k_{Lac}^m C_{Lac}^{m-1})\mu(\mu_{OH} + \mu_{Na}) \cdot \left(C_{OH}^w\right)^3$$

and the wall concentration of hydroxide can likewise be found by:

eq. 6.3.13 $$A_0 \cdot (C_{OH}^w)^4 + A_1 \cdot (C_{OH}^w)^3 + A_2 \cdot (C_{OH}^w)^2 + A_3 \cdot C_{OH}^w + A_4 = 0$$

where

$$A_0 = k_{OH}^s \mu(\mu_{OH} + \mu_{Na})$$

$$A_1 = k_{OH}^s((1+\mu)(\mu_{OH} + \mu_{Na}) + \mu(\mu_{Lac} + \mu_{Na}))C_{Lac}^w + \mu(\mu_{OH} + \mu_{Na})(k_{OH}^m C_{Lac}^{m-1} - k_H^s C_{OH}^s) + \mu\mu_{Na}\frac{i_d}{F}$$

$$A_2 = (k_{OH}^s((1+\mu)(\mu_{Lac}+\mu_{Na})+\mu_{OH}+\mu_{Na})C_{Lac}^w - k_{OH}^m\mu(\mu_{OH}+\mu_{Na})C_R + ((1+\mu)(\mu_{OH}+\mu_{Na})+\mu(\mu_{Lac}+\mu_{Na}))(k_{OH}^m C_{Lac}^{m-1} - k_{OH}^s C_{OH}^s) + 2\mu\mu_{Na}\frac{i_d}{F})\cdot C_{Lac}^w$$

$$A_3 = (k_{OH}^s(\mu_{Lac}+\mu_{Na})C_{Lac}^w - k_{OH}^m(\mu(\mu_{Lac}+\mu_{Na})+\mu_{OH}+\mu_{Na})C_R + ((1+\mu)(\mu_{Lac}+\mu_{Na})+\mu_{OH}+\mu_{Na})(k_{OH}^m C_{Lac}^{m-1} - k_{OH}^s C_{OH}^s) + \mu\mu_{Na}\frac{i_d}{F})\cdot\left(C_{Lac}^w\right)^2$$

$$A_4 = (\mu_{Lac}+\mu_{Na})(k_{OH}^m(C_L^{m-1} - C_R) - k_{OH}^s C_{OH}^s)\cdot\left(C_{Lac}^w\right)^3$$

recalling that μ_i is the ionic mobility of component *i* in solution, while μ is the dimensionless relation between the ionic motilities of hydroxide and lactate inside the membrane.

As can be noted from eq. 6.3.12 and eq. 6.3.13, the wall concentrations of lactate and hydroxide are linked together. In the numerical program a simple iteration method has been employed for solving these coupled equations. The wall concentration of hydroxide is calculated using the previous value of the wall concentration of lactate. The new value of hydroxide is used to calculate a new value for lactate, which again is used for a better calculation of the wall concentration of hydroxide. This continues until the difference between recalculated wall concentrations of lactate is sufficiently low.
When the wall concentration of lactate is established, the internal membrane concentration at the surface $C_{Lac}(L,t)$ is determined from the Donnan equilibrium eq. 6.3.2.

6.4 Numerical solution

Because of the complexity of eq. 6.2.10, the solution was evaluated numerically. A program was written in FORTRAN using the Plato 2 compilation software from Salford Software Ltd., United Kingdom.

For modeling purpose, the membrane is divided into a number, *n*, of slices of equal thickness, Δx. Membrane concentrations are established at each interface between slices, and it is assumed that the thickness of the slices is sufficiently small that concentration profile can be considered linear within every slice. Furthermore, membrane profiles that are calculated from x = 0 to x = L, are spaced with regular

time intervals, Δt. Figure 6.4.1 demonstrates the numerical interpretation of the model within the membrane.

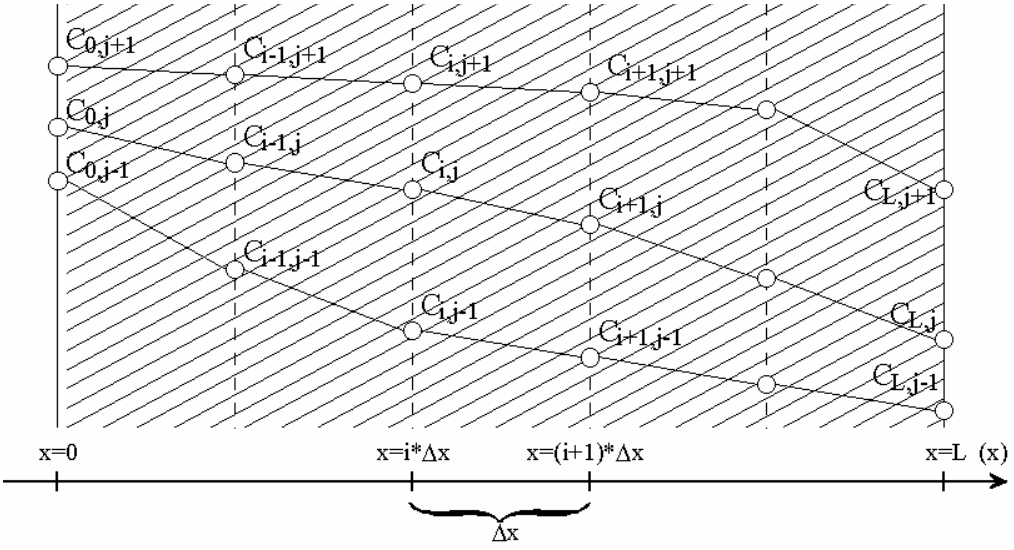

Figure 6.4.1. A graphical representation of how the numerical program perceives the membrane concentrations.

The substitution variable U(*x,t*), defined in eq. 6.2.9, is replaced by a grid point value $U_{i,j}$, where the index *i* stands for membrane thickness, and index *j* is for the time development. The membrane thickness L, limits the interval of *i* to consist of (0, n). The exact position in the membrane can be determined by $i \cdot \Delta x$, where the length between each calculated point, Δx, is calculated as L/n. The time index, *j*, starts at 0, and continues to increase until a steady profile is reached, indicating that equilibrium has been obtained. The exact time since simulation start (current reversal) can be found by $j \cdot \Delta t$.

The substitutions that are made for U as well as the first and second derivative of U:

eq. 6.4.1 $$U(x,t) = U_{i,j}$$

eq. 6.4.2 $$\frac{dU(x,t)}{dx} = \frac{U_{i,j} - U_{i-1,j}}{\Delta x}$$

eq. 6.4.3 $$\frac{dU(x,t)}{dt} = \frac{U_{i,j} - U_{i,j-1}}{\Delta t}$$

eq. 6.4.4 $$\frac{d^2U(x,t)}{dx^2} = \frac{U_{i+1,j} + U_{i-1,j} - 2U_{i,j}}{(\Delta x)^2}$$

From eq. 6.2.9 and eq. 6.4.1 -eq. 6.4.4 follows that

eq. 6.4.5 $$C^m_{Lac}(x,t) = C_{i,j} = \frac{U_{i,j} - \mu C_R}{1-\mu}$$

Inserting these substitutions in eq. 6.2.10 yields a third degree equation for $U_{i,j}$:

eq. 6.4.6 $$\begin{aligned}&(2D^m_{Lac}\Delta t + \Delta x^2)\cdot U^3_{i,j} \;-\; (D^m_{Lac}\Delta t(U_{i+1,j} + U_{i-1,j}) + \Delta x^2 U_{i,j-1})\cdot U^2_{i,j} \\ &+\; \alpha\Delta x\Delta t\cdot U_{i,j} \;-\; \alpha\Delta x\Delta t U_{i-1,j} \;=\; 0\end{aligned}$$

D^m is the membrane diffusion coefficient. Δt and Δx are the simulation stepsizes of respectively time and length axis. α is a previously defined constant.

By solving eq. 6.4.6 for $U_{i,j}$, the concentration profile can be obtained through the relation given in eq. 6.4.5. However, to calculate $U_{i,j}$, knowledge of $U_{i-1,j}$, $U_{i+1,j}$, and $U_{i,j-1}$ are necessary.
By calculating a membrane profile across the membrane from 0 to L, for every timestep, the simulation possesses the knowledge of $U_{i,j-1}$, since the index *j-1* relates to the previous timestep.
A simultaneous solution for the entire profile seems necessary and for simplicity, we have chosen an iterative solution model. For every new step in time, the new profile is assigned initial values across the membrane. The initial profile is equal to the previous profiles final form.
The first point, $U_{0,j}$, of the profile is given from border conditions. The rest of the points from *i* = 1 to *i* = n-1 are calculated in turn. Simultaneously, the points are calculated backwards from *i*=n-1 to *i*=1 to better smooth out the iteration errors. Then the last point, $U_{n,j}$, is calculated from the new values to fulfill the boundary condition at x = L. The process is then repeated until the profile changes between each iteration step are insignificant.
When a new membrane profile has been thus established, the values are recorded in a computer-file. The new profile is compared with the previous profile to establish whether steady-state is reached. If not, the time index increases by one step, and a new profile is calculated.

The order in which the profiles are calculated is given as follows:

1. Input of data. The basic compositions of the solutions on both sides of the membrane (I and II) are written into the simulation manually by the user. The user determines the size of the timestep, Δt, too. The program already holds standard information concerning the membrane's properties.
2. Initial values of all parameters are set or calculated.
3. Border values at the membrane's surfaces are calculated.
4. An initial diffusion profile between the two border values is established.
5. The time index is increased by one.
6. Initial guess for new profile.
7. Calculation of new profile based on previous values.
8. Establishment of final border-condition.
9. Check whether iteration error of new profile is insignificant. If iteration error is still significant, program returns to point 7. Otherwise, program proceeds to point 10.
10. Check whether the newly determined membrane concentration profile is significantly changed in comparison with the profile from the last time step. If not, steady-state is obtained and the program continues to point 11. Otherwise, the program returns to point 5 and starts to calculate the next profile.
11. The program shows the final output, which is the time from current reversal to steady-state. The user is offered the opportunity to save all data (concentration profiles at every timestep, membrane surface concentrations, membrane fluxes) into a data-file for later analysis.
12. The user is offered the opportunity to continue the simulation by reversing the electrical current. If the user declines, the simulation ends. If the user accepts, the final steady-state profile of the simulation is reversed. The composition of the two solutions is switched. The simulation is then repeated from point 2 except that the final steady-state solution replaces the diffusion profile in point 4.

The FORTRAN-program is recorded in Appendix C

Another version was later developed. In this second version, the current is reversed at regular interval whether the membrane profile has reached a steady-state or not. The current efficiency and energy consumption is calculated. The current efficiency is calculated for each timestep:

$$\eta_t = \frac{z_{Lac} F (J^{out}_{Lac,t} - J^{in}_{Lac,t})}{i_d}$$

where J^{out} and J^{in} represents the fluxes of lactate out of the feed solution and into the feed solution, respectively. The index *t* represents the timestep number. Since the fluxes and the current density, i_d, have opposite directions, the lactate charge, $z_{Lac} = -1$, makes the current efficiency positive, when more lactate ions are leaving the feed than entering. The current efficiency calculated for each timestep demonstrates the changes during the period until the next current reversal. The current efficiency is expected to increase until a stable membrane profile is reached, which will also stabilize the current efficiency.
The accumulated efficiency, which is the overall current efficiency calculated from the time of the last current reversal and up to the last calculated timestep:

$$\eta_{overall,t} = \frac{z_{Lac} F \sum_{j=0}^{t} (J^{out}_{Lac,j} - J^{in}_{Lac,j}) \Delta t}{i_d \cdot t \cdot \Delta t}$$

The limiting value for the overall current efficiency must be the current efficiency at steady-state, which would be reached at infinite time intervals between current reversal. This indicates that the reversal of the electrical current during the process lowers the overall efficiency of the process. Thus, without a reversible buildup of fouling, the Reverse Electro-Enhanced Dialysis process is a bad solution.

The energy consumption is calculated from the electrical resistance originating from a cell pair and an emulated fouling buildup. The resulting area-specific electrical resistance (Ωm^2) is comprised of the following parts:

$$R_{Total} = R_{SolutionI} + R_{SolutionII} + 2R_{Membrane} + R_{Polarization} + R_{Fouling}$$

The membrane resistance is taken from the manufactures information for a Neosepta AMX membrane that was the chosen membrane on most experiments (Tokoyama 1997). The polarization resistance is the resistance across the four diffusion layers at each surface of the two membranes in a cell pair. The resistances of the solutions I and II are the bulk solution resistances:

$$R_{Solution} = \frac{l}{F \sum_i |z_i| \mu_i C_i^s}$$

l is the thickness of the spacer across which the resistance is calculated. The polarization resistances are calculated by integration of the same formula across the diffusion layers.
The electrical resistance from the buildup of fouling is assumed to follow a logarithmic curve that has been estimated from experimental results.

The energy consumption, E, is calculated as the necessary energy (kWh) needed for transferring one kg of lactate ions:

$$E = \frac{i_d{}^2 R_{Total}}{(J_{Lac}^{out} - J_{Lac}^{in}) MW_{Lac}}$$

Like the current efficiency, the energy consumption is calculated both at each timestep and overall.

The energy consumption relates to the production cost of the process. The energy consumption is only calculated in respect to the electrical energy used in the extraction. It is obvious that the lower the current density of the process, the lower the energy consumption and the better the current efficiency, until the current density is zero, where the process emulates a pure Dialysis process. The flux of lactate ions is then carried by diffusion entirely, and no electrical current is necessary. Thus, another parameter must be considered to evaluate all the economical aspects.
A membrane area, A_{Mem}, based on a lactate extraction rate is chosen to represent the equipment investment cost. From the economical evaluation of a 10.000 tons lactic acid plant (Chapter 7), the Reverse Electro-Enhanced Dialysis unit is calculated to extract 1145 kg lactate per hour, which is about 300 g lactate per second. The membrane area needed for a Specific Extraction Rate (SER) of 300 g lactate per second, is found by:

$$A_{Mem} = \frac{SER}{J_{Lac}^{Total} \cdot MW_{Lac}}$$

Thus, three related factors are returned as the result of the simulation:

- Current efficiency
- Energy consumption
- Specific membrane area

6.5 Results

First, some results are presented to demonstrate the program. Then, the second version of the program is utilized in producing a response surface for some important parameters.

6.5.1 Parameters

Some parameters are known or can be assessed from experimental results. These include membrane properties and hydrodynamic conditions.

The ionic mobilities, μ_i, of the components (lactate ions, hydroxide ions, and sodium ions) are taken from literature (Atkins 1992).
The aqueous diffusion coefficients are then calculated from these mobilities. The membrane diffusion coefficients of the components are estimated from a rule of thumb that states:

eq. 6.5.1
$$D_i^m = \left(\frac{SW}{2 - SW}\right)^2 \cdot D_i^s$$

SW is the membrane swelling degree, D^m and D^s is the diffusion coefficients inside the membrane and in solution, respectively.

The membrane properties have been chosen to resemble a Neosepta AMX membrane, since this type was used in some experiments (Krol 1997;Tokoyama 1997).

- The membrane thickness, L = 200 μm
- Swelling, SW = 0.30
- The membrane's ion-exchange capacity, C_R = 2000 mol/m^3
- Membrane's area-specific resistance, R_{AMX} = 3.0·10^{-4} Ωm^2

From the hydrodynamic conditions of the experiments, plausible thicknesses of diffusion layers at the two membrane surfaces have been determined. At each surface, it was decided to use the same diffusion layer thickness, δ = 59 μm, based on formed experiments.

The remaining parameters that can be varied in the program include:

- Lactate concentration in solution I.
- Lactate concentration in solution II.
- pH of solution I.
- pH of solution II.
- Current density, i_d.

The calculation of membrane profiles continues until a steady-state is reached or 100 timesteps have passed. The length of each timestep, Δt, can also be varied.

For an evaluation of the reverse electro-enhanced dialysis process, the different stream compositions have been chosen to resemble an industrial process.

6.5.2 Case example

A simulation is performed for a case example. A small section of the Reverse Electro-Enhanced Dialysis module is considered, or more specifically, the part where the feed enters the module.

Entering the unit is a hypothetical feed stream from the fermenter carrying 200 mol/m^3 (0.2 M) lactate solution at pH 4.5. After pass, the feed stream contains 50 mol/m^3 (0.05 M) lactate. The alkaline stream passes on the opposite side of the membranes in a countercurrent setup, meaning that the alkaline solution exits the module at the same end as the fermentation stream enters as depicted on Figure 6.5.1.

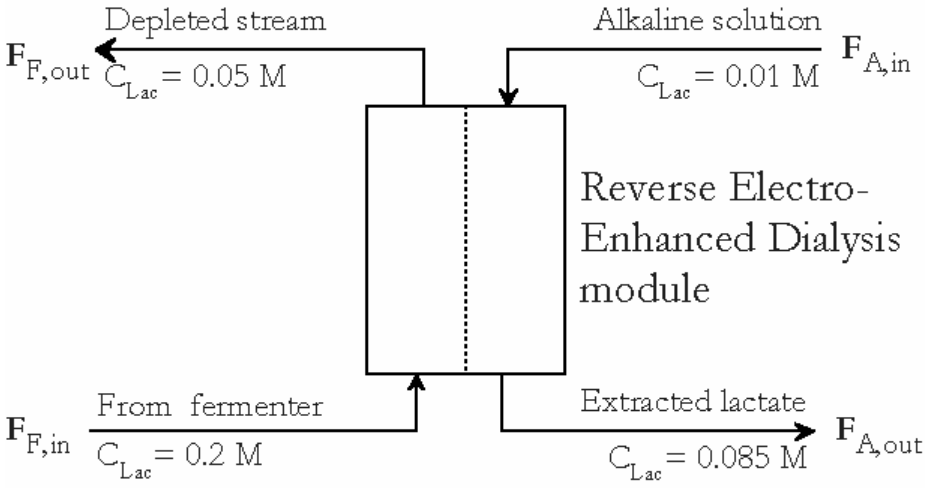

Figure 6.5.1. The hypothetical streams entering and exiting the Reverse Electro-Enhanced Dialysis module. The massflow F_A is assumed twice as fast as F_F.

When assuming that the alkaline stream enters the module with a little lactate (0.01 M) at twice the massflow of the feed stream ($F_A = 2 \cdot F_F$), the resulting lactate concentration in the exiting alkaline solution should be 0.085 M. Assuming the alkaline stream is pH 13 when entering the module, and each lactate ion collected has replaced a hydroxide ion, the exiting alkaline solution is roughly pH 12.4.

The case example examined, is the first membrane segment of the module, where the feed stream enters the membrane module.

The current is reversed at long intervals, letting a steady-state membrane profile develop every time, before current is reversed again.

The results found are presented in Figure 6.5.2 and Figure 6.5.3. These figures simulate the development of lactate concentration profiles through the anion-exchange membranes from the time of the current reversal, till the steady-state is reached.

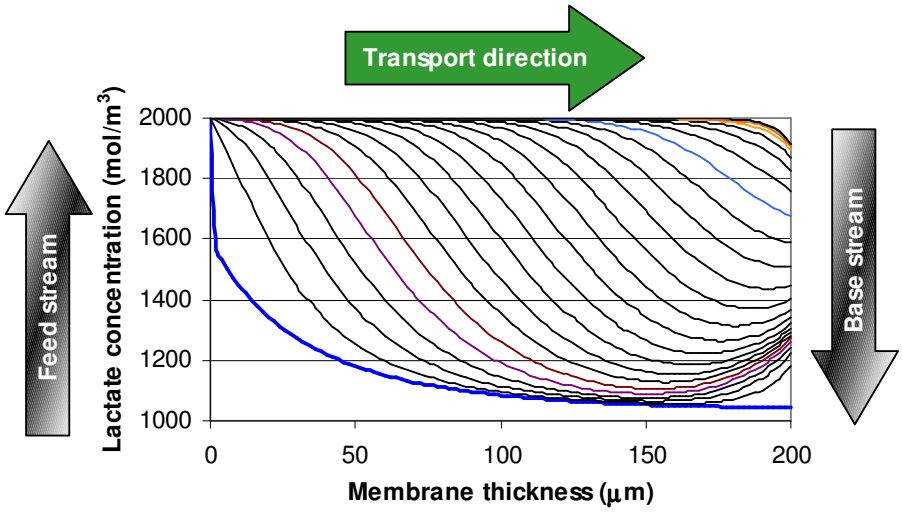

Figure 6.5.2. Membrane profiles of lactate concentration across the anion-exchange membranes, where lactate is extracted from feed to base. Profiles are presented at 5 seconds intervals. The fat line represents the starting membrane profile. Time from reversal to steady-state: 125 seconds.

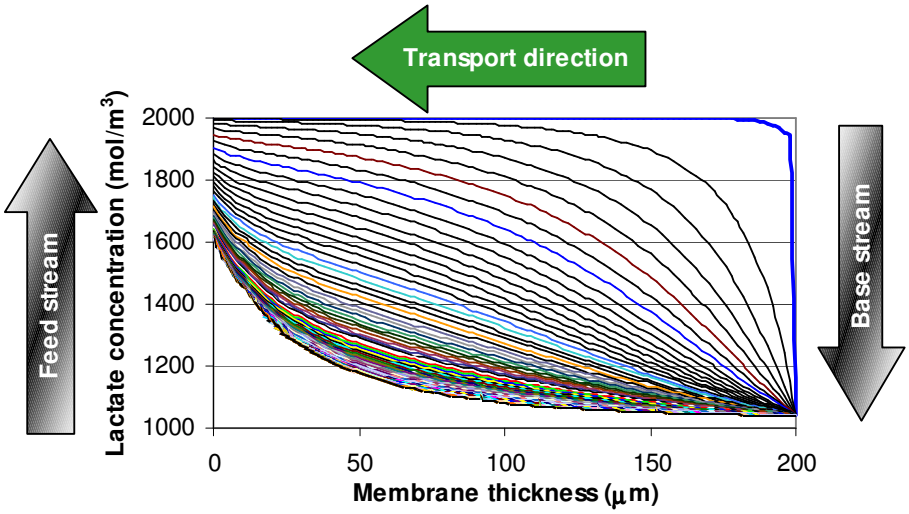

Figure 6.5.3. Membrane profiles of lactate concentration across the anion-exchange membranes, where hydroxide is driven into feed from base. Profiles are presented at 5 seconds intervals. The fat line represents the starting membrane profile. Time from reversal to steady-state: 385 seconds.

The membrane capacity is 2000 mol/m^3. At every point through the membrane, the sum of lactate and hydroxide ions corresponds to this capacity.

The two figures can be regarded in two ways. First, the figures represent the same membrane piece, where lactate ions fill up the membrane from the feed, when the electrical current is from right to left (meaning the negative ions are transported from left to right) as shown on Figure 6.5.2. After current reversal, the same lactate ions are driven out by hydroxide ions from the base, when the current is from left to right (negative ions migrate from right to left) as shown in Figure 6.5.3.

It is evident that the lactate concentration profile is more quickly established, when lactate ions are filling up the membrane, than when they are “pushed” by the more mobile hydroxide ions.

Another way to consider the two figures is to view the membrane piece in Figure 6.5.2 as every second membrane in the stack where lactate flows from feed to base, while the membrane piece in Figure 6.5.3 can be regarded as the alternate membranes, where hydroxide is transported from base to feed. Thus, by calculating the simultaneous fluxes of lactate from feed to base and from base to feed, an overall lactate flux and efficiency can be calculated.

The more time that has passed from current reversal, the higher the lactate flux from feed to base, and the lower the lactate flux from base to feed. Thus, the overall flux and efficiency of the Reverse Electro-Enhanced Dialysis process improves until steady-states are reached across all membrane pieces. The momentary current efficiency (the efficiency in an exact moment) and the overall current efficiency (accumulated from the beginning of the reversal period) are both depicted in Figure 6.5.4.

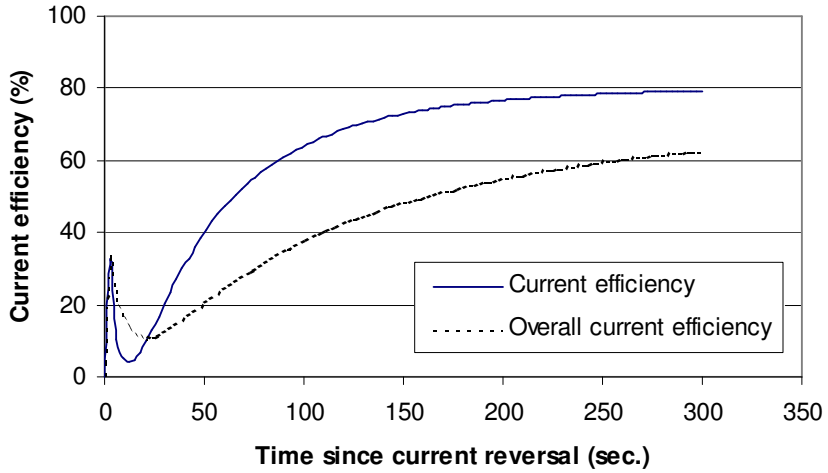

Figure 6.5.4. Momentary and overall current efficiency as function of time since last current reversal for the Reverse Electro-Enhanced Dialysis process.

A small peak in current efficiency arises just after the reversal, when the polarization layers are breaking down, followed by a drop where polarization is rebuilt. As profiles are forming, the current efficiency slowly grows. When steady-state is reached, the current efficiency has reached a plateau that corresponds to the maximum obtainable overall current efficiency.

6.5.3 "Experimental" plan

The parameters, which will be regarded in the response surface, are:

- Lactate concentration in feed stream. Range: 50 – 200 mol/m^3
- pH of feed stream. Range: 4 – 12
- Current density. Range: 250 – 1000 A/m^2
- Time between current reversals. Range: 60 – 600 seconds

Two subsequent parameters are set according to the values of these parameters:

- It is assumed that 90% of the lactate is extracted from the feed during a pass, and that the massflow of the alkaline stream is twice that of the feed stream. Thus, the effluent is assumed to have a lactate concentration of 22.5 – 90 mM. This ignores the possibility that the alkaline solution holds some lactate before entering.
- The pH of the exiting alkaline solution is calculated by assuming that every lactate ion is replacing a hydroxide ion.

The responses that are evaluated from these parameters are:

- Current efficiency (%). The amount of lactate transported during a period between two reversals in regard to the added electrical current.
- Energy consumption (kWh/kg lactate product). The overall energy used in regard to the amount of lactate transported during a period between to reversals.
- Specific membrane area (m^2). This area is calculated based on the necessary membrane area needed to extract 1145 kg lactate per hour at the current parameters. This specific lactate flux was chosen to reflect the 10,000 t capacity of a lactic acid plant as evaluated in the following section of this chapter.

An “experimental” plan has been created using the statistical software program Modde. Since the simulation program yields identical solutions with the same parameters, re-runs are pointless. The run order of the simulations is also irrelevant, but it is followed nevertheless, see Appendix D.

6.5.4 Optimization

Since the numerical values created by the simulation are only illustrative for a specific point along the separation process, and the optimization tools used in the statistical program, Modde are based on simple, linear models the resulting values can only be representative and are not able to calculate precise optimization parameters.

One of the most interesting responses from an industrial viewpoint is the separation process’s energy consumption. A contour plot of the energy consumption as function of current density and current reversal time is shown on Figure 6.5.5.

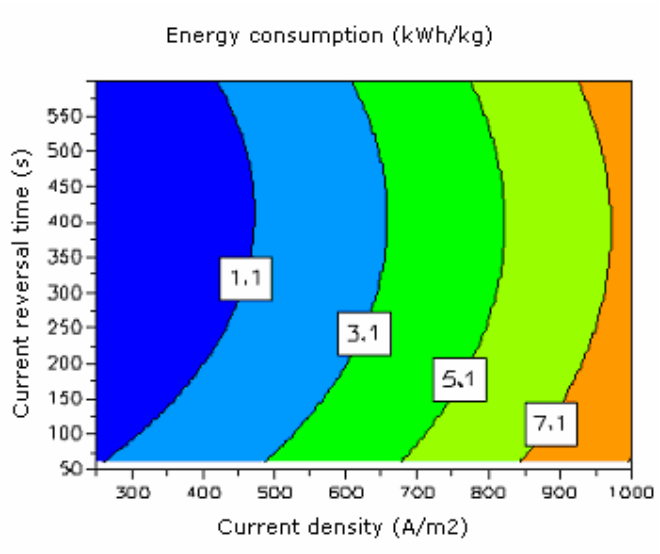

Figure 6.5.5. Contour plot of energy consumption. Feed pH = 8, $C_{Lactate,\ Feed}$ = 125 mol/m^3.

The plot suggests that low current density and current reversal time of 300-500 seconds are preferable for obtaining low energy consumption. The plot is produced for the central values of feed pH and lactate concentration. The corresponding plots at lower and higher feed pH are shown in Figure 6.5.6 and Figure 6.5.7.

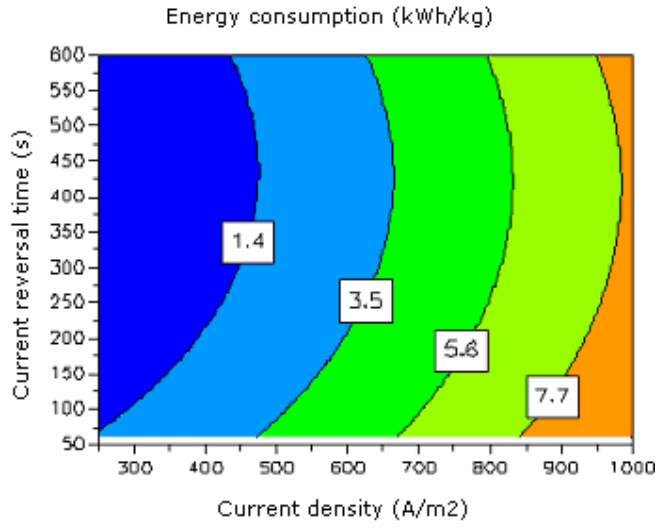

Figure 6.5.6. Contour plot of energy consumption. Feed pH = 4, $C_{Lactate,\ Feed}$ = 125 mol/m^3.

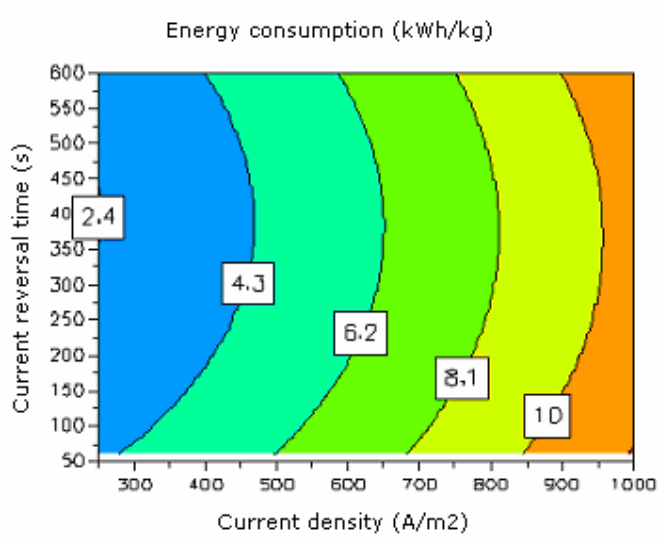

Figure 6.5.7. Contour plot of energy consumption. Feed pH = 12, $C_{Lactate,\ Feed}$ = 125 mol/m^3.

While these two plots show similar behavior, they also suggest an optimum within the feed pH. Only small changes can be observed by increasing the feed pH from 4 to 8, but at higher pH-values, the energy consumption increases significantly. The trend of lower energy consumption at lower current density is still evident, though.

The contour plots in Figure 6.5.8 and Figure 6.5.9 show the effect of lower and higher feed concentration around the central pH-value, respectively.

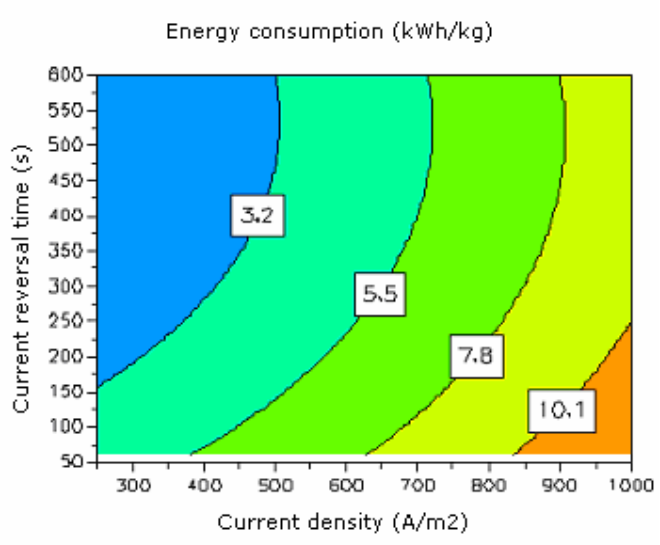

Figure 6.5.8. Contour plot of energy consumption. Feed pH = 8, $C_{Lactate,\ Feed}$ = 50 mol/m^3.

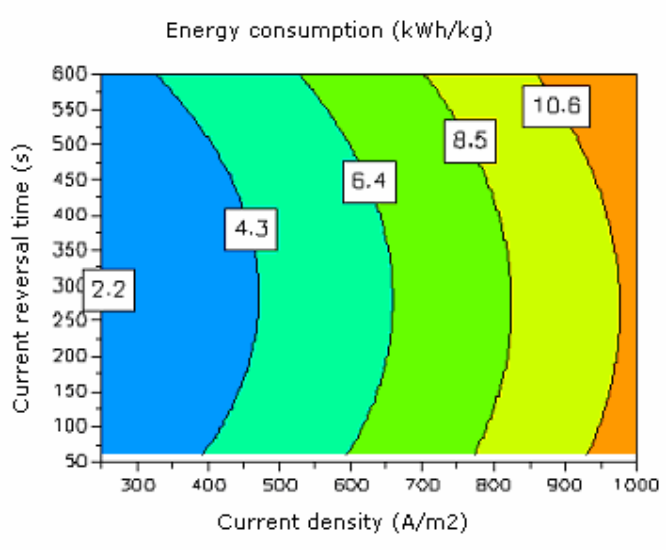

Figure 6.5.9. Contour plot of energy consumption. Feed pH = 8, $C_{Lactate,\ Feed}$ = 200 mol/m^3.

Comparison of the five plots demonstrates that an optimal region for lowest energy consumption exists within the pH-interval 4 – 12, and within the range of feed concentrations from 50 – 200 mol/m^3.

A new contour plot with the energy consumption as function of pH and feed concentration is shown in Figure 6.5.10 for central values of current density and reversal time.

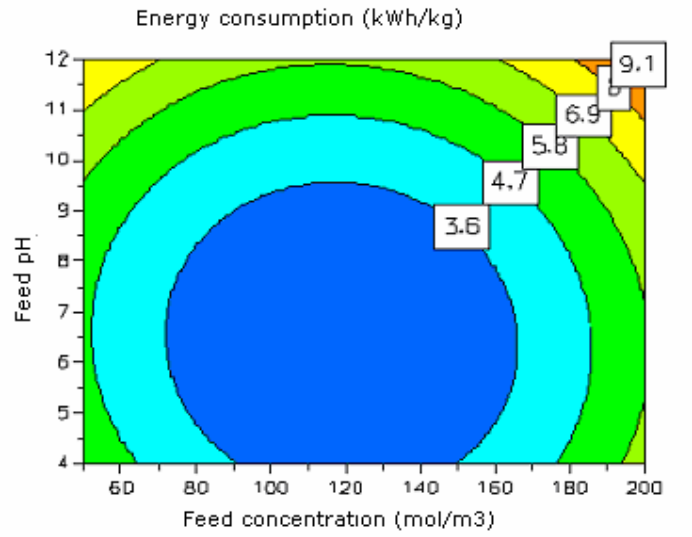

Figure 6.5.10. Contour plot of energy consumption. Current density = 625 A/m^2, reversal time = 330 seconds.

This plot confirms the previous hypothesis that the lowest energy consumption probably can be found within the chosen intervals of feed pH and concentration. From the first contour plots, the lowest energy consumption is possibly found at lower current density and reversal times of 300-500 s. The estimated contour plot with lowest current density 250 A/m^2 and central time reversal 330 seconds is depicted in Figure 6.5.11.

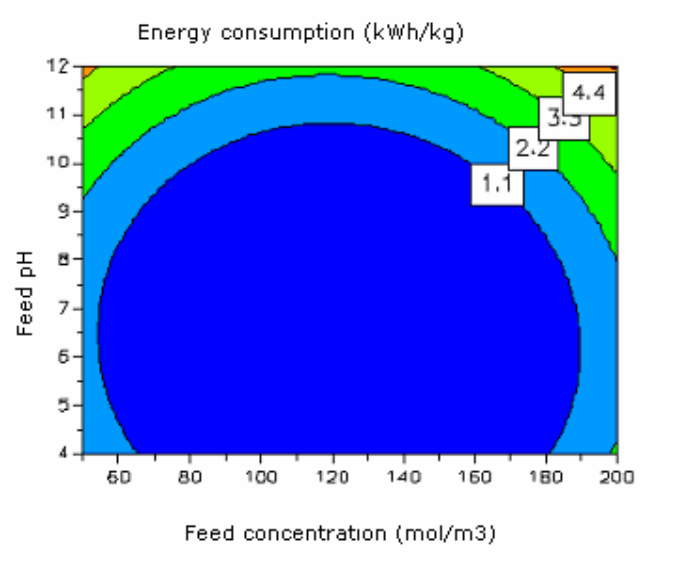

Figure 6.5.11. Contour plot of energy consumption. Current density = 250 A/m^2, reversal time = 330 seconds.

The statistical program estimates a large region of low energy consumption for feed concentration and feed pH at low current density. At these conditions, relatively large variation with feed pH and concentration are possible, and seems like optimal process conditions. Lowering the current density obviously lowers the energy consumption, but also lowers the lactate extraction flux. Thus, increased membrane area is necessary to extract the lactate.

Calculating the specific membrane area and subjecting the results to the same level of optimization reveals as expected a different optimal area. Since the membrane area represents part of the capital investment in a new plant, the optimal membrane area is as small as possible.

The contour plots are shown on Figure 6.5.12 and Figure 6.5.13. The optimal membrane area is found at the higher current densities, though the low pH and medium to high current reversal times are still close to the previously found optimum.

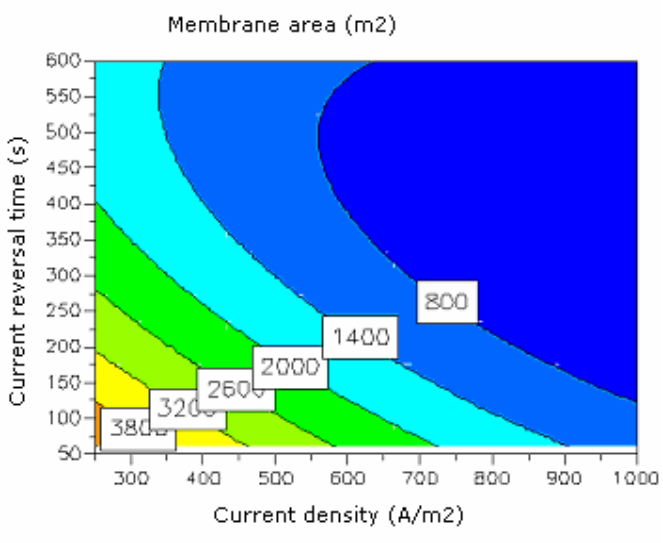

Figure 6.5.12. Contour plot of calculated specific membrane area. Feed pH = 4, $C_{Lactate,\ Feed}$ = 125 mol/m^3.

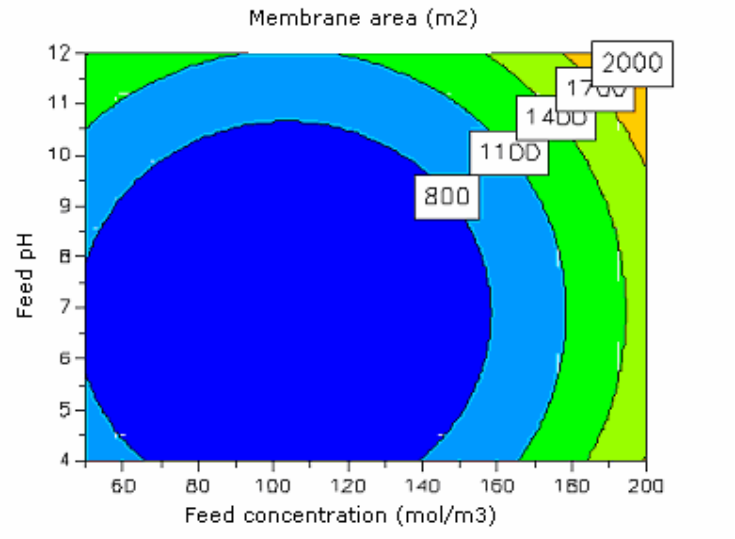

Figure 6.5.13. Contour plot of calculated specific membrane area. Current density = 1000 A/m^2, reversal time = 600 seconds.

The value of low feed pH was expected since this is part of the theoretical basis of the operation.

The big difference between the optimal operation for energy consumption and specific membrane area is heavily influenced by the current density. This is also expected as the current density is closely linked to the flux.

The current efficiency increases as the current density decreases as shown when comparing the contour plots on Figure 6.5.14 (250 A/m^2) and Figure 6.5.15 (1000 A/m^2), because a higher fraction of the lactate is carried by power free diffusion flux at lower current densities.

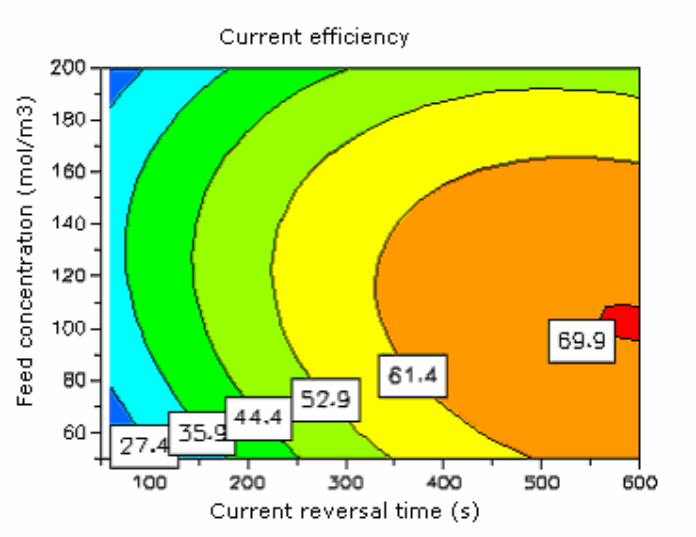

Figure 6.5.14. Contour plot of current efficiency. Feed pH = 4.5, current density = 250 A/m^2.

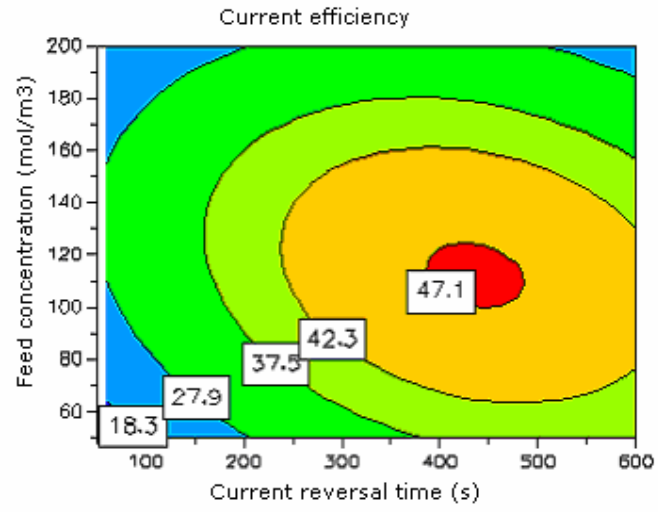

Figure 6.5.15. Contour plot of current efficiency. Feed pH = 4.5, current density = 1000 A/m^2.

To discern the optimum value for an industrial application, a new factor, based on both energy consumption and necessary membrane area, must be calculated. For this a very simple “modified” Net Present Value (NPV) expression is used. The NPV includes both the investment of the equipment (related to specific membrane area),

and the running costs (related to the energy consumption), but as it is related to a single unit operation no profit term is included. In electrodialysis applications, the investment can be assumed to be close to the total membrane area required, and the running costs close to the electrical energy consumption of the process. By assigning general membrane and power cost, a NPV for equipment ready to produce 10,000 t lactic acid per year can be calculated:

Membrane cost (installed):	3450 DKK/m^2
Power cost:	0.34 DKK/kWh

The NPV is calculated as eq. 7.8.1, which is later explained in details, setting a desired rate of return to 10% and a plant lifetime of 15 years.

Figure 6.5.16 and Figure 6.5.17 show the contour plots of the optimal region for process operation.

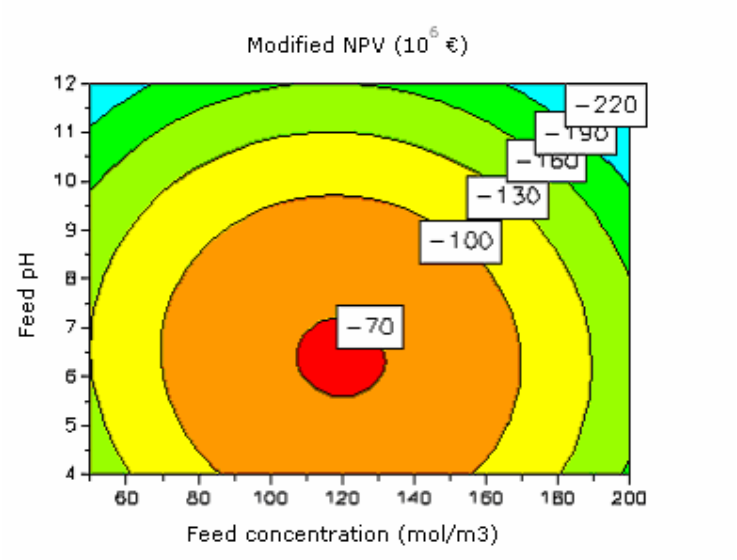

Figure 6.5.16. Contour plot of Net Present Value (NPV) in 10^6 € for a REED equipment producing 10,000 t lactic acid per year.

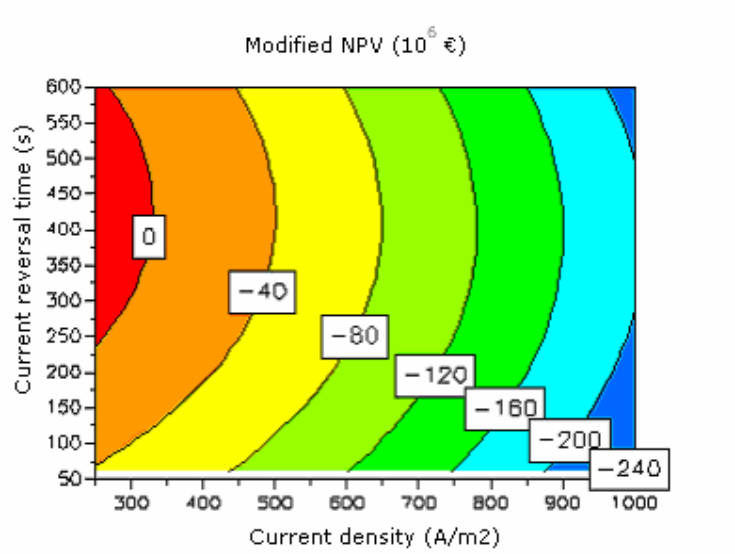

Figure 6.5.17. Contour plots of Net Present Value (NPV) in 10^6 € for a REED equipment producing 10,000 t lactic acid per year.

Since no production income is included in the NPV, the results are all negative.

As expected from earlier findings the feed pH and concentration are not crucial parameters in optimization. There is room for some variation in current reversal time, but the running cost of energy consumption weighs more heavily on the influence of current density on NPV than does the membrane investment. The great pH-variations in the equipment cause the assumption of an equipment lifetime of 15 years to be very optimistic. Shorter membrane lifetime of 3-8 years is more realistic, and this would shift the weight towards higher current density.

6.6 Conclusion

The demonstration shown here represents a very simplistic case study for a reverse electro-enhanced dialysis operation included in a designed plant producing 10,000 t lactic acid per year, as will be evaluated in the following chapter.

The simulation successfully accomplished our initial goals of simulating and establishing steady-state concentration profiles of lactate ions by a simple mathematical, two-component model. To accommodate membrane surface polarization a simple diffusion model was included to observe the significant influence from this effect. Watersplitting can greatly influence the steady-state system, when operating close to optimal conditions. By calculating overall lactate

fluxes and reworking the program to handle the current reversal of concentration profiles, whether in steady-state or in transition, it became possible to estimate current efficiency as function of current reversal times. These results were compared to experimentally determined values and found to be very comparative. The program was expanded to include other parameters and continuous evaluation of energy consumption and specific membrane area, which have been demonstrated.

The program is still lacking, as it can only predict a binary membrane profile through the membrane, which is adequate for the lactate/hydroxide system, when other anions are only present in insignificant amounts. For more complicated feed streams, a more complex solution must be employed for solving the coupled equations.
Further expansion of the program is currently planned to include mass balance segments along the membrane surface in the feed chamber to evaluate the change in lactate extraction from the point of entry to an optimal point of exit from the REED.

7

EVALUATION OF A 10,000 T LACTIC ACID PLANT

7.1 Introduction

The commercial potential in lactic acid production from renewable resources is assessed through an economical evaluation carried out for a plant capable of an annual production of 10,000 tons 88%-w/w lactic acid. The evaluation is based on a plant that utilizes a new technology for separation and purification developed at The Technical University of Denmark. The process combines different electro-membrane unit operations in a unique way that makes it fairly independent of feedstock purity. Hence, evaluation can be carried out without impact from the choice of feedstock other than the variable unit price of carbohydrates, e.g. varying amounts of Ca^{2+} and Mg^{2+} in the raw material will not change the characteristics of the separation process.

7.2 Process flowsheet

Flowsheet and process description is prepared as basis for further calculations. The process can be divided into 3 independent sub-processes as shown in Figure 7.2.1. The process flowsheet depicts one process string, but it is often advantageous to have more parallel strings, which will be discussed later.

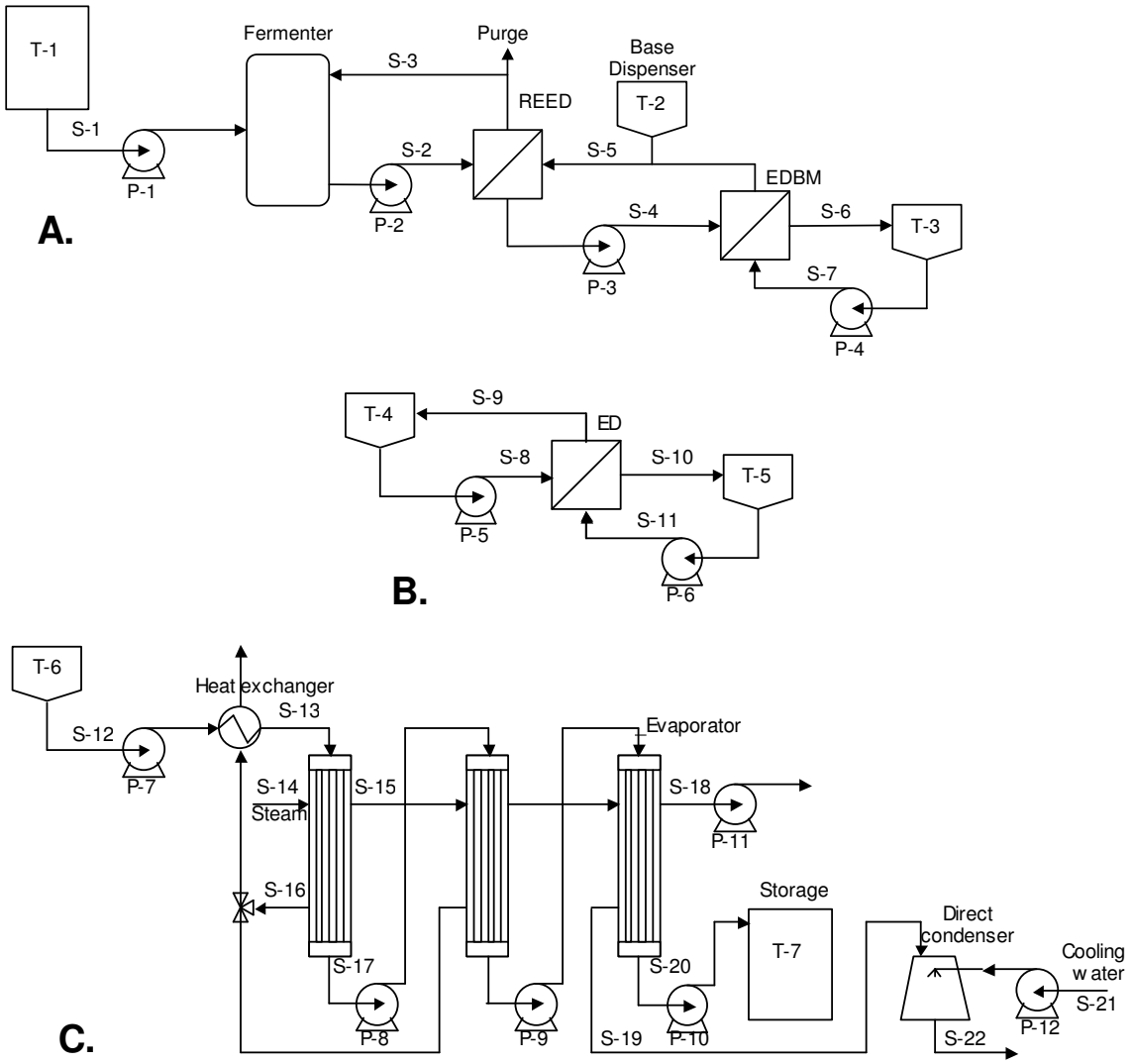

Figure 7.2.1. Process flow sheet. Flow sheet A shows the continuous or semi-continuous fermentation connected to extraction by REED and combined concentration and acidification by EDBM. Flow sheet B demonstrates a gentle electrodialysis process for removal of inorganic anions, if necessary. Flow sheet C shows a possible evaporation solution for final product concentration.

Sub-process A

From the feed tank (T-1) a substrate is pumped to the recycle fermenter, where the sugars are fermented by microorganisms producing lactic acid. From the fermenter, broth (S-2) is fed to the Reverse Electro-Enhanced Dialysis (REED) stack, where lactate ions are extracted and replaced by OH^- before the broth is returned to the fermenter along with microorganisms, unconverted sugars and the added hydroxide ions for pH control. As very little

water is transferred during the exchange in the REED, a part of the recycled stream corresponding to the substrate flow (S-1) is purged.

An alkaline stream (S-4), acting as carrier of the extracted lactate, is pumped to a Bipolar Electrodialysis (EDBM) module where lactate is transferred, concentrated and acidified in a storage tank (T-3). The alkaline solution is regenerated and returned to the REED (S-5), replenished by addition of make-up base (T-2).

When the concentration of lactic acid in the storage tank (T-3) has reached a certain level (~20-25%), the lactic acid solution is transferred to sub-process B for removal of inorganic ions.

Sub-Process B

The acidic liquid from the EDBM process is fed to an Electrodialysis (ED) stack operated as a batch process. In the ED process inorganic anions are removed from the undissociated lactic acid in tank T-4 and concentrated in T-5. At a predetermined low level of inorganic ions in the diluate circuit, tank T-4 is connected to sub-process C and treatment of a new batch from sub-process A can start.

Sub-process C

The purified lactic acid is concentrated to 88% in a series of *falling film* evaporators. The feed (S-13) is preheated with the pooled condensate from the first two effects before it is fed to the first effect. External steam (S-14) is supplied to the first effect, resulting in evaporation of water (S-15), which is used to drive the subsequent effect. The concentrated lactic acid leaves the bottom (S-17) to be fed to the next effect. From the last effect, 88% lactic acid product (S-20) is collected in a storage tank (T-7) and the partly condensed stream (S-19) is taken to a direct condenser.

7.3 Unit operations

The sizing of each unit operation is based on some overall process assumptions combined with design parameters attained through experiments or modeling.

Overall process assumptions:

- Produces 10,000 tons 88 w-% lactic acid per year.
- Operation time of 8000 h/yr.
- Substrate is brown juice from grass pellet production.

7.3.1 Recycle fermentation

The fermentation is done in an upflow anaerobic sludge blanket (UASB) reactor with a recycle loop for product removal and pH control. The lactic acid bacteria (LAB) are immobilized on granules inside the fermenter, which also minimizes the amount of biomass in the stream leaving the top of the fermenter.

7.3.1.1 Assumptions

- Three separate upflow anaerobic sludge blanket bioreactors.
- Dilution rate, D, set to 0.3 h^{-1}.
- 8.5% sugar in the feed solution.
- Yield, Y_{SP} = 95%.
- pH 5.
- Recycle rate, R = 6 times the feed flow rate.
- Degree of filling Θ = 80%.
- Production of other organic acids than the targeted acid is insignificant.
- Temperature kept at 40 °C.
- Purge, P = Q_F (8% product loss).

Three parallel operating fermenters have been chosen to minimize harmful effects of contamination or equipment break down. The dilution rate is relatively low due to the complex composition of sugars in the substrate. A 95% yield is assumed based on experiments. The fermentation is performed under non-sterile conditions and to diminish the risk of contamination the pH is kept below 5. A low recycle rate is chosen to prevent flushing the bacteria granules out of the fermenters and into the recycle loop. The filling degree is the utilized fermenter volume.
The Lactobacillus bacteria chosen for the fermentation produce mainly lactate, but minor amounts of other organic acids are present in the substrate.

7.3.1.2 Sizing of fermenters

Calculation of feed flow rate:

$$Q_F = \frac{Q_P}{Y_{SP} \cdot \theta_{REED} \cdot \theta_{EDBM} \cdot \theta_{ED} \cdot \theta_{EVAP} \cdot C_S \cdot \rho}$$

Q_p (t/yr) is the annual production rate of lactic acid, Y_{SP} is the “Substrate to Product” yield, C_s (wt-%) is the concentration of sugar in the feed, ρ is the mass density (t/m^3)

and θ is the recovery of lactic acid in each unit operation. Using the process assumptions and inserting values for the different unit operations, Q_F is calculated:

$$Q_F = \frac{10000t/yr \cdot 0.88}{0.95 \cdot 0.92 \cdot 1.00 \cdot 0.98 \cdot 0.98 \cdot 0.085 \cdot 1.0t/m^3} = 123{,}000m^3/yr = 15.4\,m^3/h$$

An operation time of 8000 hours per year is assumed in this calculation.

To design the fermenters, the volume of each of the three fermenters can be estimated from Q_F and the dilution rate, and taking into account the filling degree Θ:

$$V_{Fermenter} = \frac{Q_F}{D \cdot \Theta \cdot N_{Fermenters}} = \frac{15.7\,m^3/h}{0.3h^{-1} \cdot 0.8 \cdot 3} = 22m^3$$

7.3.2 Reverse Electro-Enhanced Dialysis (REED)

7.3.2.1 Assumptions

- Neosepta AXE-01 and CMB ion exchange membranes
- Purge, P = Q_F (8% product loss).
- Recovery of lactate, θ_{REED} = 92% (due to loss in purge).
- Current density i_d = 500 A/m^2
- Average current efficiency, $\eta_{Current}$ = 0.70
- Shadow effects from sheet flow spacers are insignificant.
- One stack is assumed for each of the three process strings.

A new commercial available anion-exchange membrane, AXE-01[1] from Tokuyama with improved alkaline resistance, is chosen.
CMB cation-exchange membranes are only installed to protect the process fluids from the electrode rinsing solutions. Thus, only two CMB membranes are necessary for each membrane stack.
Since mass balance across the fermenters must be maintained, the mass flow of purge must equal the mass flow of substrate. Thus, a high amount of lactate is lost through the purge unless a highly concentrated substrate is utilized. Or, since lactate, which is not recovered in the Reverse Electro-Enhanced Dialysis modules, is either purged or returned to the fermenter, a high degree of lactate recovery must be achieved, which also stresses the need for a very low output concentration from the REED.

[1] Commercial name of the AXE-01: Neosepta ASM

An average current density below the critical current density is chosen to avoid watersplitting. A relatively low current efficiency is expected based on a combination of results from laboratory experiments on brown juice and computer modeling.
Expecting sheet flow with open net-spacers, shadowing of membrane area from spacers is assumed to be insignificant. The extra membrane area needed for fixation along the rim of the membranes is not included as prices are obtained for installed square meters of membrane.
Laboratory experiments show that long operation times are possible without cleaning the system.
Three power supplies, one for each stack, must cover the yearly power requirements of 7809 MWh (Table 7.6.3).

7.3.2.2 Sizing of REED

The amount of lactate that is removed in the REED can be calculated from the amount of lactate produced in the fermenters, as:

$$m_{Lac} = \frac{Q_P}{\theta_{EDBM} \cdot \theta_{ED} \cdot \theta_{EVAP}} = \frac{1100\,kg/h}{1 \cdot 0.98 \cdot 0.98} = 1145\,kg/h$$

From the amount of lactate that is transferred, the corresponding active membrane area can be found, taking into account the current efficiency and current density:

$$A_{Active} = \frac{m_{Lac}}{MW_{Lac}} \cdot \frac{|z_{Lac}|F}{i_d \cdot \eta_{Current}} = \frac{1145 kg/h}{90.08 \cdot 10^{-3} kg/mol} \cdot \frac{1h}{3600s} \cdot \frac{|-1| \cdot 96487 As/mol}{500 A/m^2 \cdot 0.7} = 973 m^2$$

Since each cell pair is made up of two anion-exchange membranes, twice the calculated active membrane area is required. Shadow effects from the spacers are considered insignificant, making the necessary actual membrane area:

$$A_{REED,needed} = 2 \cdot A_{Active} = 1{,}947 m^2$$

Since only two CMB membranes are necessary for each of the three stacks, which consists of 649 m^2 (1,947 m^2/3) anion-exchange membranes the required CMB membrane is insignificant, and therefore, not included in the total cost estimation.

Three power supplies providing the yearly estimated requirement of 7809 MWh must each have an effect of at least:

$$Effect(REED \quad power \quad supply) = \frac{7809 MWh}{8000 hr \cdot 3} = 325 kW$$

7.3.3 Bipolar Electrodialysis (EDBM)

7.3.3.1 Assumptions

- BP-1, AMH, CMB ion-exchange membranes.
- 100% recovery of lactate
- Current density i_d = 1000 A/m^2
- Current efficiency, $\eta_{Current}$ = 0.72
- Shadow effects from sheet flow spacers are insignificant.

Anion-exchange membranes with high resistance to alkaline conditions are required in the three-compartment setup used in the EDBM.
Though lactate is not extracted totally during the EDBM pass, lactate is recycled between the REED and the EDBM modules. Thus, all lactate is eventually recovered as lactic acid in the acid loop. Current density and current efficiency is based on results from laboratory experiments.
The power supply must provide 10,412 MWh (Table 7.6.3) on a yearly basis.

7.3.3.2 Sizing of the EDBM

The amount of lactate that must be transferred in the EDBM is equal to the amount, transferred in the REED. The active membrane area needed for this operation can be calculated by:

$$A_{Active} = \frac{m_{Lac}}{MW_{Lac}} \cdot \frac{|z_{Lac}|F}{i_d \cdot \eta_{Current}} = \frac{1145 kg/h}{90.08 \cdot 10^{-3} kg/mol} \cdot \frac{1h}{3600 s} \cdot \frac{|-1| \cdot 96487 As/mol}{1000 A/m^2 \cdot 0.72} = 473 m^2$$

Each cell pair consists of an AMH anion-exchange membrane, a CMH cation-exchange membrane and a BP-1 bipolar membrane. Since lactate is only transferred across the anion-exchange membrane, the necessary membrane area for each membrane type equals the active membrane area.

The effect of the power supply must be adequate to yearly provide 10,412 MWh:

$$Effect(REED \quad power \quad supply) = \frac{10412 MWh}{8000 hr} = 1302 kW$$

7.3.4 Electrodialysis (ED)

7.3.4.1 Assumptions

- AXE-01, CMH ion exchange membranes.
- 98% recovery of lactate
- Current density I_d = 250 A/m^2
- Current efficiency = 0.80
- Inorganic ions corresponding to 10% of lactic acid concentration
- Shadow effects from sheet flow spacers are insignificant.

Due to the harsh conditions in the ED, membranes with high chemical resistance such as the new AXE-01 membrane are preferred.
Even though lactic acid is not charged at this stage it is assumed that around 2% is transported to the concentration loop and lost.
The amount of inorganic ions to be removed is depending on the initial concentration in the substrate, but approximately 10% compared to the lactic acid content is considered realistic.
The power supply must provide 521 MWh (Table 7.6.3) on a yearly basis.

7.3.4.2 Sizing of the ED

The membrane area needed for the ED-stacks can be calculated from:

$$A_{Active} = \frac{m_{Lac}}{MW_{Lac}} \cdot 0.1 \cdot \frac{|z_{Lac}|F}{i_d \cdot \eta_{Current}}$$

$$= \frac{1145\,kg/h}{90.08 \cdot 10^{-3}\,kg/mol} \cdot 0.1 \cdot \frac{1h}{3600s} \cdot \frac{|-1| \cdot 96487\,As/mol}{250\,A/m^2 \cdot 0.80} = 172m^2$$

The effect of the power supply must be adequate to yearly provide 521 MWh:

$$Effect(REED \quad power \quad supply) = \frac{521MWh}{8000hr} = 65kW$$

7.3.5 Evaporator

Multiple-effect vertical long tube (VLT) falling film evaporation was evaluated for concentration of the lactic acid solution leaving the ED-unit. A simulation program developed at DTU (Nordkvist and Grotkjær 2000) was applied for performed the calculations. The simulation program uses a modified Raoult's Law and UNIFAC 2 parametric model for the bubble point calculations.

7.3.5.1 Assumptions

- 98% recovery of lactate
- 18% lactic acid in the solution entering the first effect
- 88% lactic acid is leaving the last effect.
- Solution entering the first effect is at the boiling point.
- The evaporator consists of six effects.

Even though no loss of lactic acid in the vapor fraction from each effect is assumed to ease the simulation, a recovery of 98% is assumed afterwards for a more realistic evaluation. The feed to the evaporator is heated to the boiling point in a heat exchanger before entering the first effect.

7.3.5.2 Sizing of evaporator

Simulation of the evaporation process using 6 evaporator effects yields the result given in Table 7.3.1. Each effect is 55 m^2, which adds up to a total heat exchange area of **330m^2**.

Table 7.3.1. Performance of evaporator effects.

Effect	1	2	3	4	5	6
Temperature (K)	378	373	366	359	349	318
Pressure (mmHg)	858	706	558	413	265	33
BPE (K)	1,16	1,31	1,53	1,94	2,94	14,35
Liquid inflow (kg/h)	7086	6284	5427	4516	3555	2546
Liquid outflow (kg/h)	6284	5427	4516	3555	2546	1449
Vapor outflow (kg/h)	802	857	910	961	1010	1096
Lactic acid in feed (w-%)	18,0	20,3	23,5	28,2	35,9	50,1
Lactic acid in effluent (w-%)	20,3	23,5	28,2	35,9	50,1	88,0
U (W/(m^2 K))	2313	2185	2019	1787	1404	424
Heat transfer area (m2)	55,0	55,0	55,0	55,0	55,0	55,0

From a NPV (Net Present Value) analysis the optimal number of effects is found to 11, but according to APV Anhydro A/S 6 effect is a more feasible number (Nordkvist and Grotkjær 2000). As shown in Figure 7.3.1 no significant increase in NPV is obtained by installing 11 instead of 6 effects, so 6 effects are chosen.

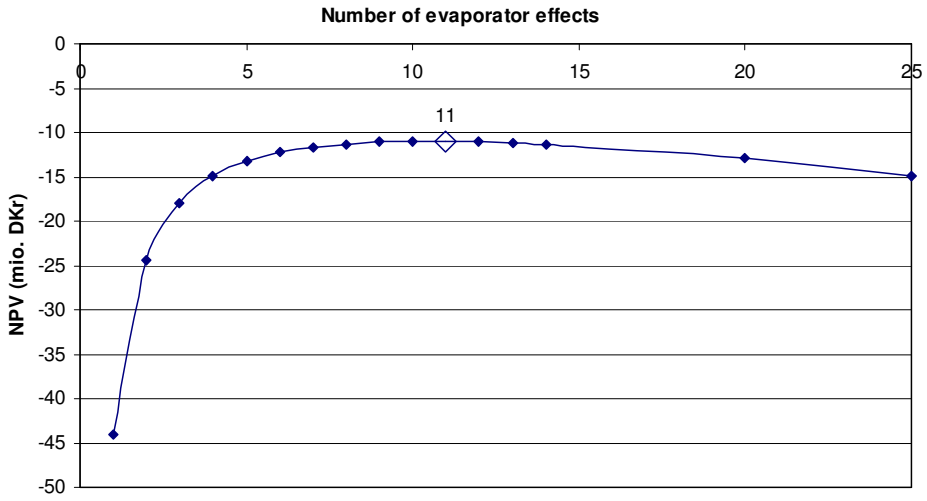

Figure 7.3.1. Net present value of evaporator operation vs. number of installed effects.

7.4 Cost estimation of equipment

Equipment prices are estimates from data, primarily obtained through vendor quotations, books or journals but also from a design project on lactic acid production completed at the Department of Chemical Engineering in 2000 (Nordkvist and Grotkjær 2000). Estimates on fermenter and evaporator costs obtained of the appropriate industries have been scaled to match the present requirements using the following exponential scaling expression (Sinnott 1993):

eq. 7.4.1 $$New\ \ \cos t = Original\ \ \cos t \cdot \left(New\ \ size \Big/ Original\ \ size \right)^{n}$$

Where *n* is a specific equipment index according to Table 7.4.1. Prices for storage and process tanks can be estimated through the following expression:

eq. 7.4.2 $$Ce = C \cdot S^{n}$$

Where Ce is the equipment cost, C is a cost constant and, S is a size parameter given in Table 7.4.1. The calculated cost is a base cost for equipment made of carbon steel, which must be adjusted if other materials are chosen. If stainless steel or monel are use the base cost is multiplied with 2.5 or 3.4, respectively (Sinnott 1993).

Table 7.4.1. Purchase cost factors for use in equation. Adapted from (Sinnott 1993) and *Eurodia, Wissous, France.

Equipment	Size range	Cost constant	Index
Process tanks	10-100m^3	1500	0.60
Storage tanks	50-8000m^3	1200	0.55
Evaporator	-	-	0.52
Electrodialysis	-	-	0.80*

The equipment cost for the electro-membrane processes are based on prices provided by Tokuyama Europe GmbH, see Table 7.4.2.

Table 7.4.2. Price in DM/m^2 for Neosepta ion-exchange membranes excluding module and utilities. The prices for the standard membranes (a) are provided by Tokuyama Europe GmbH, Düsseldorf, Germany (1999). Prices for special grade membranes are found by multiplying the prices for standard membranes with a factor of 2.28(b) or 1.62(c), provided by Eurodia, Wissous, France (2000).

Membrane area	AMX[a]	AMH[b]	AXE-1[c]	CMB[a]	CMH[b]	BP-1[a]
< 50 m^2	232	529	375	417	951	2,000
51-100 m^2	185	422	299	370	844	1,800
101-300 m^2	167	381	270	334	762	1,530
> 301 m^2	157	358	254	306	698	1,350

The price of a 500 m^2 electrodialysis stack (including spacers and clamping system) is 900.000 DM, provided by Tokuyama Europe GmbH.

Equipment prices are updated to 2002 prices using the “Chemical engineering plant cost index” in Table 7.4.3. The equipment cost for electro-membrane processes have not been adjusted to 2002 prices using Table 7.4.3, as this type of equipment belongs to a fairly young category of processes where development of better technology and growing utilization tends to lower prices. This is supported by the appearance of new and cheaper membranes with better performance, e.g. AXE-1 from Tokuyama.

Table 7.4.3. Chemical engineering plant cost index.

Year	Price index
1992	358,2
1996	381,7
1997	386,5
1998	389,5
1999	390,6
2000	394,1
2001	394,3
2002	396,4

The exchange rates used for conversion of currencies into Euro (€) are given in Table 7.4.4.

Table 7.4.4. Exchange rates to Euro (€).

Currency	Exchange rate
British Pounds	164.10
US Dollars	113.34
German Deutchmarks	51.13
Danish Kroner	13.446

7.4.1 Fermentation

The equipment cost for the fermenters are based on a resent estimates (2000) from Aage Christensen A/S who suggested AISI 304 stainless steel tanks delivered from a local supplier. The price for 6 fermenters with a volume of 11 m^3, including instrumentation and control was 2,500,000 DKK, corresponding to 338,000 € in 2002 prices.

The price for three 22 m^3 fermenters is calculated from the given price of the 11 m^3 fermenters through eq. 7.4.2:

$$Cost(22m^3\ fermenter) = Cost(11m^3\ fermenter)\cdot\left(\frac{22m^3}{11m^3}\right)^{0.6} = \frac{338{,}000€}{6}\cdot 2^{0.6} = 85{,}400€$$

$$Cost(3\ fermenters) = 3\cdot 85{,}400€ = 256{,}200€$$

7.4.2 REED

The cost of the REED equipment is found by multiplying the calculated membrane area with the prices supplied for AMX and CMB in Table 7.4.2:

Membranes:

$$1{,}947\text{m}^2\cdot 254\ \text{DM/m}^2\cdot 0.5113\ €/\text{DM} = 253{,}000\ €$$

Modules:

$$Cost(1\quad stack) = 900{,}000\quad DM\cdot\left(\frac{\left(649m^2/2\right)}{500m^2}\right)^{0.8}\cdot 0.5113€/DM = 325{,}600€$$

$$Cost(3\quad stacks) = 3\cdot 325{,}600 = 976{,}900€$$

Power supplies:

The power supply price estimates are based on prices provided by Lambda Scandinavia (2001) scaled to 2002 prices and size by an equipment index of 0.7.

$$Cost(325kW) = 31{,}823US\$ \cdot \left(\frac{325kW}{60kW}\right)^{0.7} \cdot 0.8823€/US\$ \cdot \frac{396.4}{394.3} = 92{,}100€$$

$$Cost(3x\ 325kW\ power\ supplies) = 3 \cdot 92{,}100€ = 276{,}300€$$

The total cost of the REED equipment is:

$$\text{Cost}_{\text{(REED equipment)}} = 253{,}000\ € + 976{,}900€ + 276{,}300€ = 1{,}506{,}200€$$

7.4.3 EDBM

The cost of the EDBM equipment is found by multiplying the calculated membrane area with the prices supplied for AMH, CMB and BP-1 in Table 7.4.2:

Membranes:

$$473\text{m}^2 \cdot (358\ \text{DM/m}^2 + 306\ \text{DM/m}^2 + 1{,}350\ \text{DM/m}^2) \cdot 0.5113\ €/\text{DM} = 487{,}100\ €$$

Module:

$$Cost(1\ \ stack) = 900{,}000\ \ DM \cdot \left(\frac{\left(473m^2 \cdot 3/2\right)}{500m^2}\right)^{0.8} \cdot 0.5113€/DM = 608.800€$$

The membrane area is multiplied by a factor of 3/2 because the module price provided by Tokuyama is for a two compartment system and not a three compartment EDBM.

Power supply:

$$Cost(1302kW) = 31{,}823US\$ \cdot \left(\frac{1302kW}{60kW}\right)^{0.7} \cdot 0.8823€/US\$ \cdot \frac{396.4}{394.3} = 243{,}300€$$

The total cost of the EDBM equipment is:

$$\text{Cost}_{\text{(EDBM equipment)}} = 487{,}100\ € + 608{,}800€ + 243{,}300€ = 1{,}339{,}200€$$

7.4.4 ED

The cost of the ED equipment is found by multiplying the calculated membrane area with the prices supplied for AMX and CMH in Table 7.4.2:

Membranes:

$172\text{m}^2 \cdot (167\ \text{DM/m}^2 + 762\ \text{DM/m}^2) \cdot 0.5113\ €/\text{DM} = 81{,}700\ €$

Module:

$$Cost(1\ \ stack) = 900{,}000\ \ DM \cdot \left(\frac{172m^2}{500m^2}\right)^{0.8} \cdot 0.5113\,€/DM = 196{,}000€$$

Power supply:

$$Cost(65kW) = 31{,}823US\$ \cdot \left(\frac{65kW}{60kW}\right)^{0.7} \cdot 0.8823€/US\$ \cdot \frac{396.4}{394.3} = 29{,}900€$$

The total cost of the ED equipment is:

$\text{Cost}_{\text{(ED equipment)}} = 81{,}700\ € + 196{,}000€ + 29{,}900€ = 307{,}600€$

7.4.5 Evaporator

The equipment cost for the evaporator is based on a resent estimate performed at APV Anhydro A/S for concentration of 30,000 kg/h 4%-w/w lactic solution in an evaporator with 5 effects and a total heat transfer area of 1470 m^2 (Nordkvist and Grotkjær 2000). The price for this arrangement is 8.8 mill. DKK. Inserting values of the estimate and the calculated heat transfer area, equipment cost for the evaporator can be calculated from eq. 7.4.1:

$$C_2 = 8{,}800{,}000 \cdot \left(330/1470\right)^{0.52} = 4{,}047{,}000\ \ DKK$$

The price includes pumps for recirculation, vacuum pump and condenser for the last effect and PCL/PC control.

The optimal area of the installed heat exchanger was found from a NPV analysis using the evaporator simulation program to calculate the decreasing steam requirement as function of increasing heat exchange area and FIG 6.3 in (Sinnott 1993) (Carbon steel shell and stainless steel tubes) to estimate the equipment price. An optimal heat exchange area of 35 m^2 for the pre-heating the feed to the

evaporator resulted is an equipment price of 220,000 DKK. The total price of the last concentration step when becomes 4,267,000 DKK or 573,700€.

7.4.6 Tanks

The cost of tanks are evaluated from eq. 7.4.2 and summarized in Table 7.4.5.

Table 7.4.5. Cost of tanks in 2002 prices. *Fiberglass reinforced plastic – price of tank obtained from (http://www.matche.com/EquipCost/Tank.htm)

Tank	Material	Volume	Price (€)
T1 (storage)	Carbon steel	2587	164.100
T2	AISI 304	5	14.900
T3	AISI 316	68	85.700
T4	AISI 316	68	85.700
T5	Plastic*	7	13.500
T6	AISI 316	68	85.700
T7 (storage)	AISI 316	104	95.400
Total			545.000

The feed storage tank, T1 is designed to hold substrate for 1 week's production and the product storage tank can hold three days production of 88% lactic acid.

7.4.7 Pumps

No high performance pumps are used in the plant due to the absence of filtration processes. The price for pumps suitable for this process ranges from 12,000-18,000 DKK, which is very limited compared to the other equipment pieces. An estimate for the 30 pumps used in the plant is based on data supplied by Grundfoss A/S and lands on an approx. value of 450,000 DKK or 60,500 €.

7.5 Total capital investment

The total capital investment required for the lactic acid plant is summarized in Table 7.5.1. Estimation of the total direct and indirect plant costs is based on the factor method described by Peters and Timmerhaus, where the cost of each item is found by multiplying the total equipment cost with a specific multiplication factor applicable for a fluid-processing chemical plant (Sinnott 1993). Contractor's fee and contingency are found by applying a multiplication factor to the total direct and indirect plant cost and the sum of these three numbers gives the fixed capital investment. Adding the working capital to the fixed capital investment gives the total capital investment for the project.

Table 7.5.1. Budget for total capital investment. The multiplication factor refers to: [1]Total equipment cost, [2]total direct and indirect plant cost, and [3]fixed capital investment.

Item	Investment (1,000 €)	Multiplication factor
Fermenter	256	
REED	1,506	
EDBM	1,339	
ED	308	
Evaporator	574	
Tanks	545	
Pumps	61	
Total equipment cost	*4,588*	
Installation	2,157	0.47[1]
Instrumentation and controls	1,377	0.30[1]
Piping	3,028	0.66[1]
Electrical work	505	0.11[1]
Buildings	826	0.18[1]
Yard improvement	459	0.05[1]
Service facilities	3,212	0.70[1]
Land	275	0.06[1]
Total direct plant cost	*16,426*	
Engineering and supervision	1,514	0.33[1]
Construction expenses	1,881	0.41[1]
Total direct and indirect plant cost	*19,822*	
Contractors fee	991	0.05[2]
Contingency	1,982	0.10[2]
Fixed capital investment	*22,795*	
Working capital	3,419	0.15[3]
Total capital investment	26,214	

7.6 Total production cost

The total production cost is composed of the direct production cost, the indirect production cost, fixed charges and general expenses. The method is adapted from Peters and Timmerhaus (Sinnott 1993), but the division entries follow the procedures suggested in Danish accounting (adapted from (Nordkvist and Grotkjær 2000)). The total production costs are summarized in Table 7.6.1 and the specific items are described in details in subsequent paragraphs.

Table 7.6.1 Total production cost.

Item	(1000€)
Raw materials	50
Power and utilities	1,112
Maintenance	2,280
Operating labor	605
Operating supplies	342
Total direct production cost	*4,388*
Laboratory charges	91
Supervisory labor	168
Plant overhead	874
Total indirect production cost	*1,132*
Real estate taxes	22
Insurance	228
Fixed charges	*250*
Administration	151
Distribution and marketing	247
General expenses	*398*
Total production cost	**6,168**

7.6.1 Direct production costs

7.6.1.1 Raw materials

The use of raw materials is summarized in Table 7.6.2. As a point of reference the price of substrate has been set to zero, which is true if for instance brown juice or whey permeate is utilized as feedstock. (Actually, the green crop drying industry has expenses amounting to approx. 2.7 €/ton for brown juice disposal.) If, on the other hand molasses or hemicellulose from wheat straw were used the price of substrate would be around 0.17 € or 0.27 € per kg carbohydrate in the substrate, respectively.

Table 7.6.2. Annual cost of raw materials.

Item	Amount	Unit	€/unit	Annual cost (1000 €)
Carbohydrates	10,483	ton	0/(170-270)	0/(1,782-2,830)
Sodium hydroxide	40	ton	403	16
Bacteria	-	-	-	34
Total				50/(1,832-2,880)

In the alkaline process stream that is circulated between the REED and the EDBM an estimated amount of 40,000 kg sodium hydroxide is added to makeup for loss, giving an annual cost of 16,000 €. An estimated annual price for bacteria is 34,000 €.

7.6.1.2 Power and utilities

The requirements for power and utilities are summarized in Table 7.6.3. The energy consumption in the three membrane processes is calculated based on experimental data and scaled to fit parameters of large-scale equipment. The simulation program that is also used for evaporator sizing calculates steam and cooling water requirements in the evaporator. The effluent treatment cost is taken from (Nordkvist and Grotkjær 2000).

Table 7.6.3. Annual cost of power and utilities.

Item	Amount	Unit	€/unit	Annual cost (1000 €)
Power (REED)	7,809	MWh	40	312
Power (EDBM)	10,412	MWh	40	416
Power (ED)	521	MWh	40	21
Pumping	52	MWh	40	2
Steam (Evap.)	7,400	tons	16.81	124
Cooling water (Evap.)	876,631	m^3	0.024	21
Effluent treatment	123,024	m^3	1.75	215
Total				1,112

7.6.1.3 Maintenance

Peters and Timmerhaus (Sinnott 1993) suggests that the annual maintenance cost is found as a percentage of the fixed capital investment, ranging from 2-6% if simple chemical processes is considered and 7-11% for complicated, processes with extensive instrumentation or corrosive conditions. The present process is not especially corrosive nor is extensive instrumentation required, but membranes have to be replaced after approximately 1-5 years. The average annual maintenance cost is estimated to be 10% of the fixed capital investment with 4% on labor and 6% on materials giving a total of 2,280,000 €.

7.6.1.4 Operating labor

It is considered likely that the plant can be operated by 3 operators in 8 hours shift. Since the number of production hours are 8000 and one man-year is approximately 1680 hours 15 operators needs to be employed. The annual wages are 40,338 € (300,000 DKK) per operator. Hence, the cost of operating labor is 605,000 €.

7.6.1.5 Operating supplies

Operating supplies covers many miscellaneous supplies needed to keep the process functioning efficiently. Peters and Timmerhaus (Sinnott 1993) suggest a value of 15%

of the annual maintenance cost for operating supplies, which amounts to 342,000 € annually.

7.6.2 Indirect production cost

It is considered likely that the product is sold from the factory in truck loads and thus shipping and packing are neglected is this evaluation.

7.6.2.1 Laboratory charges

The cost of laboratory tests for control of operations and for product-quality control is often taken as 10 to 20% of the operating labor (Sinnott 1993). In the present evaluation 15% is used, giving a total of 91,000 €/year

7.6.2.2 Supervisory labor

It is estimated that 2 general foremen and a works engineer are required with an annual salary 53,487 € (400,000 DKK) and 60,507 € (450,000 DKK), respectively. Thus, the annual cost of supervisory labor is 168,000 €.

7.6.2.3 Plant overhead

The plant overhead is taken as 60% of the total expenses for operating, supervisory and maintenance labor, resulting in an annual cost of 874,000 €. (Peters and Timmerhaus suggests 50-70%)

7.6.3 Fixed charges

7.6.3.1 Real estate taxes

Real estate taxes are taken to be 2% of the cost of land and buildings resulting in an annual cost of 22,000 €.

7.6.3.2 Insurance

The annual cost of insurances are normally 1% of the fixed capital investment (Sinnott 1993) giving an annual cost of 228,000 €.

7.6.4 General expenses

7.6.4.1 Administration

Administration costs correspond to 20-30% of the annual cost of operating labor. A value of 25% is used here yielding an annual cost of 151,000 €.

7.6.4.2 Distribution and marketing

Distribution and marketing costs vary widely for different chemical plants ranging from 2-20% of the total production cost. The higher figure usually applies for new

products sold in small quantities and the low figure applies to large-volume products, such as bulk chemicals (Sinnott 1993). A value of 4% have been used in this evaluation as lactic acid is a bulk chemical, but new suppliers have to operate in a market where competition is considered to be hard. Distribution and marketing expenses are estimated to 247,000 €.

7.7 Annual income and profit

Lactic acid prices began to droop in the late-1990s based on overcapacity and competition from low-grade product from China, but appear to have rebounded slightly. The price in December 2000 for 88% food grade was 70-80 cent/lbs (Mirasol 1999) and it has kept steady rising to a present day level of 75-87 cent/lbs (Jarvis 2003).

Using a lactic acid price of 1.56 €/kg (80 cent/lbs) a profit close to 50% of the turnover can still be expected as seen from Table 7.7.1. The numbers obtained in Table 7.7.1 are considered as the base case.

Table 7.7.1. Annual income, total production cost and profit.

Item	(1000 €)
Sale of lactic acid	15,560
Total production cost	6,168
Annual profit	9,392

In order to evaluate the project from an investor's point of view the total capital investment must be taken into account.

7.8 Evaluation of project

The economic evaluation of this project is based on an interest rate of 10%, which represent the minimum acceptable rate of return. Furthermore, the expected lifetime is estimated to 15 years after which the scrap value is set to zero. An estimate of the lifetime is not determined easily as this would require insight into the current and future technologies of competitors. The lifetime depends on the applied technology and is not limited by equipment as this is easily replaced.

For calculating the economic indicators the following expression is applied:

eq. 7.8.1 $$NPV = -I + P\frac{(1+i)^T - 1}{i(1+i)^T}$$

Where NPV is the net present value of the project, *P* is the annual profit, *i* is the interest rate, *T* is the plant lifetime and *I* is the capital investment. In the base case

where the annual profit is 9,392,000 €, the net present value is calculated to 45,219,000 €. In Figure 7.8.1 NPV is plotted as function of lactic acid sales price for two substrate prices of 0 and 0.17 €/kg carbohydrate in substrate, respectively.

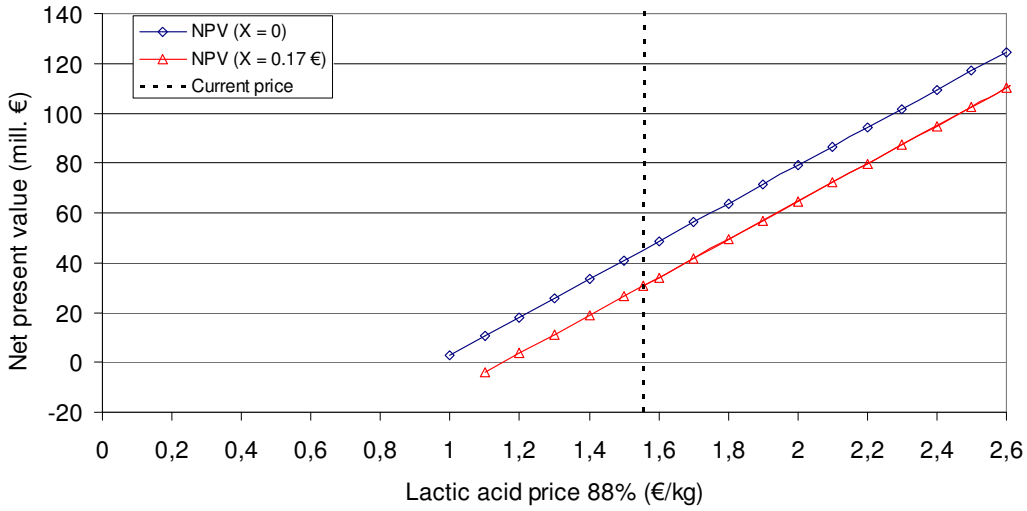

Figure 7.8.1. Net present value (NPV) of the 26.2 mill. € investment as a function of lactic acid sales price. X corresponds to the cost of substrate per kg produced lactic acid.

The internal rate of return (IRR) and break even time (BET) are in Figure 7.8.2 used to illustrate the sensitivity of the investment to different lactic acid sales-prices. The internal rate of return can be found from equation eq. 7.8.1 by setting NPV equal to zero and solving for the interest rate *i*. Break even time is the minimum period before the total capital investment is paid back and can be determined in the same way by solving for the lifetime *T.*

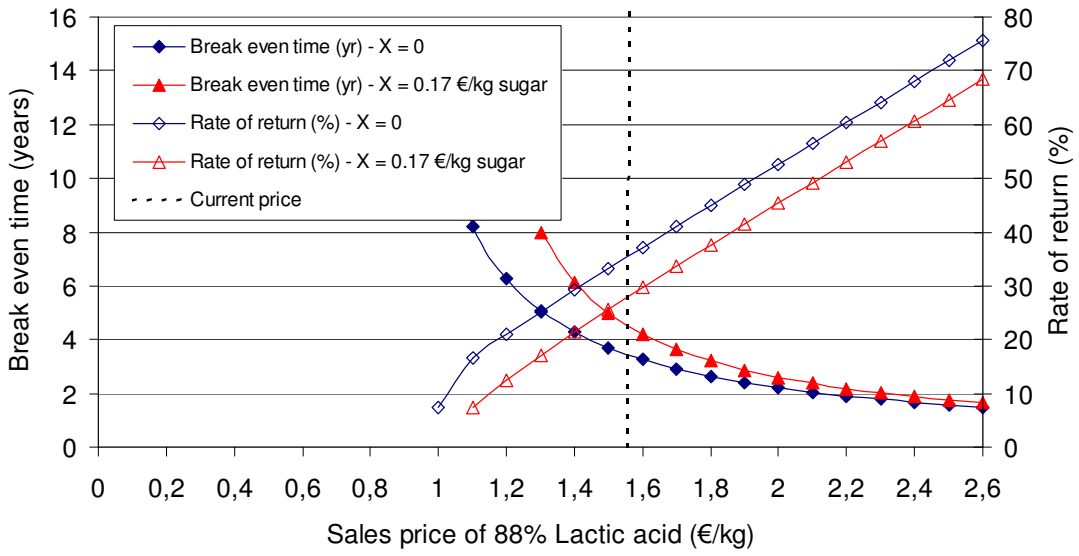

Figure 7.8.2. Break even time (BET) and internal rate of return (IRR) as function of lactic acid sales price. X corresponds to the cost of carbohydrates. The vertical line marks the base case example.

In the base case the internal rate of return is 35% and the break even time is 3.4 years. If the substrate prices increases to 0.17 or 0.27 € per kg carbohydrate internal rate of return will drop to 28 or 24%, respectively.

The economical analysis paints a rosy picture with respect to the lactic acid production, even though the parameters and assumptions applied to the analysis are considered realistic. Comparable predictions of great profit for production of different organic acids from different substrates are being put forth from many sources, but the market is hesitant, possibly considering the relatively high investment costs involved combined with the fact that much of the proposed purification technology is complicated or not yet established in the industry.

The sales price of 88% lactic acid in this case study is based on current US market level. The sales price in Europe and Asia is presently (2003) even higher.

The internal rate of return is in the region of 25-40%, which should make the lactic acid plant very attractive from an investor's point of view.

8

CONCLUSION

During the present Ph. D. study different aspects of fermentative lactic acid production from agricultural waste streams have been investigated. The focus has been on an Upflow Anaerobic Sludge Blanket (UASB) reactor for the fermentation and especially processes involving ion-exchange membranes have received mush attention for the subsequent recovery of lactic acid.

A screening of different Lactic Acid Bacterial revealed that a combination of *Lactobacillus pentosus* and *Lactobacillus brevis* were able to utillize all sugar components of wet-oxidized wheat straw hemicellulose at high yield (95%). By adding 2% brown juice to the hemicellulose fraction no extra growth-factors were necessary to sustain growth of the co-culture, which is very important for minimizing substrate costs. Successful operation of an UASB reactor was possible due to the ability of the co-culture to form granules during fermentation of brown juice, hereby enabling dilution rates above the doubling rate of the bacteria, which is important for obtaining a high productivity.

Electrodialysis with bipolar membranes (EDBM) is an efficient way of recovering and concentrating lactic acid from a stream containing lactate. The current efficiencies found were close to the theoretical maximum and energy consumptions ranged from 1.48-2.26 kWh/kg recovered lactic acid. However, the feed stream received by the EDBM unit must be very pure in terms of organic material that can cause fouling, and more imperative, inorganic multivalent cations, which will damage the membranes due to precipitations, must be avoided.

Two different approaches when were tried for generating a lactate containing stream from the brown juice fermentation broth, suitable for EDBM. By filtering the broth using a NF45 nanofiltration membrane from DSS, Denmark, with or without MF/UF

pre-filtration, a clear colorless permeate with a significant reduction of calcium and magnesium were generated. However, despite an acceptable permeate flux ranging from 10-30 l/m^{2}h and a rejection of divalent cations of approx. 99% nanofiltration was deemed inferior to the Reverse Electro-Enhanced Dialysis (REED) for separating the lactate from the fermentation broth. The main reason is the required decreasing of pH before nanofiltration, which only makes it possible to desalt the lactic acid in the EDBM unit and not concentrating it. Due to the desired high concentration factor and very high levels of divalent cations, two consecutive nanofiltrations will most likely be required for sufficient calcium and magnesium reduction.

As an alternative method, the REED process is able to selectively extract lactate (anions) from the fermentation broth with nearly total rejection of cations. By transferring lactate to an alkaline dialysate stream, the lactate can be further transported across the anion exchange membrane of the subsequent EDBM and concentrated as lactic acid. Normally, it would not be possible to perform electrodialysis directly on a very impure stream like the fermented brown juice, but the unique combination of a symmetric configuration of the REED-stack and periodical current reversal keeps the membrane fouling in check and enables longtime operation.

From this research a new and promising process for production of lactic acid has emerged based upon fermentation of agricultural waste streams in an UASB reactor and recovery using different types of electrodialysis. Judging from the economic evaluation of a 10,000 tons/year lactic acid plant, stating an internal rate of return of 35% and a break even time of 3.4 years (base case, see 7.8), the technology seems to have a fair chance as a commercial process. What still misses, however, is prove-of-concept where especially the purity of the produced lactic acid needs to be investigated.

The use of renewable resources for production of lactic acid is no longer restricted to academia. The latest achievements within commercial exploitation of renewable resources for production of lactic derived products can be found at the homepage of Cargill Dow at http://www.cargilldow.com/home.asp - indeed an inspiring view of modern production of chemicals, fibers and plastic.

9

REFERENCES

http://biorealis.com/biofilter/RightBiofNarr.html., 2001.
Ref Type: Generic

Andersen,M. and Kiel,P. (2000) Integrated utilisation of green biomass in the green biorefinery. *Industrial Crops and Products* **11**, 129-137.

Angelidaki,I., Petersen,S.P. and Ahring,B.K. (1990) Effects of lipids on the anaerobic digestion and reduction of lipid inhibition upon addition of bentonite. *Applied Microbiology and Biotechnology* **33**, 469-472.

Argonne National Laboratory. http://www.itd.anl.gov/techtour/ethyl-faqs.html ., 2001.

Atkins, P. W. (1992) *Physical Chemistry*. Oxford: Oxford University Press.

Axelsson, L. T. (1993) Lactic acid bacteria: Classification and physiology. In *Lactic acid bacteria* ed. Salminen,S. and von Wright,A. pp. 1-63. New York, Basel, Hong Kong: Marcel Dekker, Inc.

Beschkov,V., Peeva,L. and Valchanova,B. (1995) Ion-exchange separation of lactic acid from fermentation broth. *Hungarian Journal of Industrial Chemistry* **23**, 135-139.

Bizzari, S. N., Riepl, J. and Takei, N. (1999) CEH Product Review: Lactic acid. In *Chemical Economics Handbook* pp. 670.5000 A-670.5001 F. California: SRI International.

Boniardi,N., Rota,R., Nano,G. and Mazza,B. (1996) Analysis of the sodium lactate concentration process by electrodialysis. *Separations Technology* **6**, 43-54.

Boniardi,N., Rota,R., Nano,G. and Mazza,B. (1997a) Lactic acid production by electrodialysis. Part I: Experimental tests. *Journal of Applied Electrochemistry* **27**, 125-133.

Boniardi,N., Rota,R., Nano,G. and Mazza,B. (1997b) Lactic acid production by electrodialysis. Part II: Modelling. *Journal of Applied Electrochemistry* **27**, 135-145.

Borgardts, P., Krischke, W. and Troesch, W. Process for purifying dairy wastewater. [US5746920]. 1998a.

Borgardts,P., Krischke,W., Trosch,W. and Brunner,H. (1998b) Integrated bioprocess for the simultaneous production of lactic acid and dairy sewage treatment. *Bioprocess Engineering* **19**, 321-329.

Bowen,W.R., Calvo,J.I. and Hernández,A. (1995) Steps of membrane blocking in flux decline during protein microfiltration. *J. Membrane Sci.* **101**, 153-165.

Boyaval,P., Lavenant,C., Gesan,G. and Daufin,G. (1996) Transient and Stationary Operating Conditions on Performance of Lactic Acid Bacteria Crossflow Microfiltration. *Biotechnology and Bioengineering* **49**, 78-86.

Brown, B. CDP will build a huge PLA unit at Cargill's site. Chemical Market Reporter 17. January, 1. 2000.

Bunte, A. Genes and enzymes involved in maltose metabolism in *lactococcus lactis*. 1998. Applied Microbiology, Lund Institute of Technology, University of Lund, Sweden.

Böddeker, K. W., Schorm, C., Windmöller, D. and Schorm, C. G. Organic acid production process uses Donnan-dialysis anion exchanger-membrane - overcoming limited selectivity problems in efficient, highly-selective and lower cost process. GKSS FORSCHUNGSZENTRUM GEESTHACHT, G. M. B. H. [WO9729203-A1].

Chiao,Y.C., Chlanda,F.P. and Mani,K.N, (1991) Bipolar Membranes for Purification of Acids and Bases", Journal of Membrane Science, **61**, 239-252.

Czytko,M., Ishii,K. and Kawai,K. (1987) Continuous Glucose Fermentation for Lactic Acid Production: Recovery of Acid by Electrodialysis. *Chem. Ing. Tech.* **59 (12)**, 952-954.

Datta, R. (1995) Hydroxycarboxylic Acids. In *Kirk-Othmer: Encyclopedia of Chemical Technology* pp. 1042-1062. John Wiley & Sons, Inc.

Davis, R. H. (1992) Microfiltration. In *Membrane Handbook* ed. Ho,W.S.W. and Sirkar,K.K. pp. 457-460. New York: Van Nostrand Reinhold.

de Raucourt,A., Girard,D., Prigent,Y. and Boyaval,P. (1989) Lactose continuous fermentation with cell recycled by ultrafiltration and lactate separation by electrodialysis: model identification. *Appl. Microbiol. Biotechnol.* **30**, 528-534.

Donnan,F.G. (1911) The theory of membrane equilibrium in presence of a non-dialyzable electrolyte. *Z. elektrochem* **17**, 572.

Ebskamp, M. J. M. http://www.geocities.com/CapeCanaveral/4409/fructan.htm. 2001.

Endo, T., Kobayashi, E. and Yamagami, T. Prodn. of optically active lactic acid - using microorganism which stereospecifically hydrolyses DL-lactonitrile in polar solvent. [US5234826]. 1992.

Eyal, A. M., McWilliams, P., Witzke, D. R. and Gruber, P. R. A process for the recovery of lactic acid. Cargill Inc. [WO9815519]. 1998.

Fiebig, M. Skriptum zur Vorlesung Impuls-, Waerme- und Stoffuebertragung. Teil I und II. <None Specified> . 1992. Germany, Ruhr-Universitaet Bochum.

Freger,V., Howell,J.A., . and Arnot,T.C. (2000) Separation of concentrated organic/inorganic salt mixtures by nanofiltration. *Journal of Membrane Science* **178**, 185-193.

Garde, A. Oprensning og separation af mælkesyre ved hjælp af elektrodialyse. 1-67. 1997. Department of Chemical Engineering, Technical University of Denmark.

Garde, A. and Rype, J.-U. Oprensning og separation ved hjælp af elektrodialyse II (Separation using electrodialysis II). 1-181. 1997. Department of Chemical Engineering.

Garde,A., Jonsson,G., Schmidt,A.S. and Ahring,B.K. (2002) Lactic acid production from wheat straw hemicellulose hydrolysate by Lactobacillus pentosus and Lactobacillus brevis. *Bioresource Technology* **81**, 217-223.

Garvie,E.I. (1980) Bacterial lactate dehydrogenases. *Microbiol. Rev.* **44**, 106-139.

Gekas,V. and Hallstrom,B. (1987) Mass transfer in the membrane concentration polarization layer under turbulent cross flow. I. Critical literature review and adaptation of existing Sherwood correlations to membrane operations. *J. Membrane Sci.* **30**, 153-170.

Goden, B. (1993) Constituents of Cereals: Nature, Properties, and Levels. In *Bioconversion of Cereal Products* ed. Godon,B. pp. 1-22. New York: VCH Publishers.

Hermia,J. (1982) Constant Pressure Blocking Filtration Laws Application to Powerlaw Nonnewtonian Fluids. *Trans Inst Chem Eng* **60**, 183-187.

Hlavacek,M. and Bouchet,F. (1993) Constant flowrate blocking laws and an example of their application to dead-end microfiltration of protein solutions. *J. Membrane Sci.* **82**, 285-295.

Hofvendahl,K. and Hahn-Hagerdal,B. (2000) Factors affecting the fermentative lactic acid production from renewable resources. *Enzyme and Microbial Technology* **26**, 87-107.

Hongo,M., Nomura,Y. and Iwahara,M. (1986) Novel Method of Lactic Acid Production by Electrodialysis Fermentation. *Applied and Enviromental Microbiology* **August**, 314-319.

Hughes, W. F. and Brighton, J. A. (1999) *Schaums Outlines of Theory in Fuild Dynamics*. New York: McGrawHill.

Jarvis, L. (2003) Prospects for Lactic Acid Are Healthy as demand for all End Users Grows. Chemical Market Reporter, February 10, 2003, p 12

Jeantet,R., Maubois,J.L. and Boyaval,P. (1996) Semicontinuous production of lactic acid in a bioreactor coupled with nanofiltration membranes. *Enzyme and Microbial Technology* **19**, 614-619.

Jonsson,G. and Boesen,C.E. (1977) Concentration polarization in a reverse osmosis test cell. *Desalination* **21**, 1-10.

Kandler,O. (1983) Carbohydrate metabolism in lactic acid bacteria. *Antonie van Leeuwenhoek* **49**, 209-224.

Kesting, R. E. (1985) *Synthetic polymeric membranes*. New York/Chichester/Brisbane/Totonto/Singapore: John Wiley & Sons.

Kiel, P. and Andersen, M. Method for treating organic waste products. AGRO-FERM A/S. [WO200056912-A1]. 2000.

Klass, D. L. (1998) *Biomass for Renewable Energy, Fuels, and Chemicals*. London: Academic Press.

Kleerebezem,M., Hols,P. and Hugenholtz,J. (2000) Lactic acid bacteria as a cell factory: rerouting of carbon metabolism in Lactococcus lactis by metabolic engineering. *Enzyme and Microbial Technology* **26**, 840-848.

Koros,W.J., Ma,Y.H. and Shimidzu,T. (1996) Terminology for membranes and membrane processes. *Pure & Appl. Chem.* **68**, 1479-1489.

Krol, J. J. Monopolar and bipolar ion exchange membranes - Mass Transport Limitations -. 1997. Membrane Technology Group, University of Twente.

Kulozik,U. (1998) Physiological aspects of continuous lactic acid fermentations at high dilution rates. *Applied Microbiology and Biotechnology* **49**, 506-510.

Kulozik,U. and Wilde,J. (1999) Rapid lactic acid production at high cell concentrations in whey ultrafiltrate by Lactobacillus helveticus. *Enzyme and Microbial Technology* **24**, 297-302.

Lee,E.G., Moon,S.-H., Chang,Y.K., Yoo,I.-K. and Chang,H.N. (1998) Lactic acid recovery using two-stage electrodialysis and its modelling. *J. Membrane Sci.* **145**, 53-66.

Liew,M.K.H., Tanaka,S. and Morita,M. (1995) Separation and purification of lactic acid: Fundamental studies on the reverse osmosis downstream process. *Desalination* **101**, 269-277.

Lincoln,R.E. (1960) Control of stock culture preservasion and inoculum build-up in bacterial fermentation. *J. Biochem. Microbiol. Tech. Eng.* **2**, 481-500.

Lunt,J. (1998) Large-scale production, properties and commercial applications of polylactic acid polymers. *Polymer Degradation and Stability* **59**, 145-152.

Mani, K. N. and Hadden, D. K. Process for the recovery of organic acids and ammonia from their salts. Archer Daniels Midland Company. [US5814498]. 1998. US.

Matthew, H. N. MATERIALS - A biopolymers bonanza is seen beyond degradables. Plastics Technology - New York 44[1], 13-15. 1998.

Miao, F. Method and apparatus for the recovery and purificationof organic acids. Chronopol Inc. [US5681728]. 1997. US.

Mirasol, F. Lactic Acid Prices Falter As Competition Toughens. Chemical Market Reporter March 1, 16. 1999.

Mulder, M. (1991) *Basic Priciples of Membrane Technology*. Dordrecht/Boston/London: Kluwer Academic Publishers.

Mulder, M. (1996) *Basic principles of membrane technology*. Dordrecht: Kluwer Academic Publishers.

Musashino Chemical Laboratory, L. www.Musashino.com. <None Specified> . 2001.

Nomura,Y., Iwahara,M. and Hongo,M. (1987) Lactic Acid Production by Electrodialysis Fermentation Using Immobilized Growing Cells. *Biotechnology and Bioengineering* **30**, 788-793.

Nordkvist, M., Grotkjær, T. Lactic acid production. 2000. Dept. Chem. Eng., DTU.

Ohashi,R., Yamamoto,T. and Suzuki,T. (1999) Continuous Production of Lactic Acid from Molasses by Perfusion Culture of Lactococcus lactis Using a Stirred Ceramic Membrane Reactor. *Journal of Bioscience and Bioengineering* **85**, 647-654.

Orla-Jensen, S. (1919) *The Lactic Acid Bacteria*. Copenhagen: Fred Host and Son.

Orla-Jensen,S. (1924) La classification des bactéries lactiques. *Lait* **4**, 468-474.

Portner,R. and Markl,H. (2001) Dialysis cultures. *Applied Microbiology and Biotechnology* **50**, 403-414.

Ramirez,P., Aguilella,V.M., Manzanares,J.A. and Mafe,S. (1992) “Effects of Temperature and Ion Transport on Water Splitting in Bipolar Membranes”, Journal of Membrane Science, **73**, 191-201.

Reizer,J., Saier,M.H., Jr.,D.J., Grenier,F., Thompson,J. and Hengstenberg,W. (1988) The phosphoenolpyruvate:sugar phosphotransferase system in Gram-positive bacteria: properties, mechanism and regulation. *Crit. Rev. Microbiol.* **15**, 297-338.

Rincon,J., Fuertes,J., Rodriguez,J.F., Rodriguez,L. and Monteagudo,J.M. (1997) Selection of a cation-exchange resin to produce Lactic-acid solutions from whey fermentation broths. *Solvent Extraction and Ion Exchange* **15 (2)**, 329-345.

Roukas,T. and Kotzekidou,P. (1998) Lactic acid production from deproteinized whey by mixed cultures of free and coimmobilized Lactobacillus casei and Lactococcus lactis cells using fedbatch culture. *Enzyme and Microbial Technology* **22**, 199-204.

Schmidt,J.E. and Ahring,B.K. (1996) Granular sludge formation in upflow anaerobic sludge blanket (UASB) reactors. *Biotechnology and Bioengineering* **49**, 229-246.

Scholler,C., Chaudhuri,J.B. and Pyle,D.L. (1993) Emulsion liquid membrane extraction of lactic acid from aqueous solutions and fermentation broth. *Biotechnology and Bioengineering* **42**, 50-58.

Scholten,R.H.J., van der Peet-Schwering,C.M.C., Verstegen,M.W.A., den Hartog,L.A., Schrama,J.W. and Vesseur,P.C. (1999) Fermented co-products and fermented compound diets for pigs: a review. *Animal Feed Science and Technology* **82**, 1-19.

Siebold,M., Frieling,P.v., Joppien,R., Rindfleisch,D., Schügerl,K. and Röper,H. (1995) Comparison of the Production of Lactic Acid by Three Different Lactobacilli and its Recovery by Extraction and Electrodialysis. *Process Biochemistry* **30 (1)**, 81-95.

Singhal,A., Gomes,J., Praveen,V.V. and Ramachandran,K.B. (1998) Axial dispersion model for upflow anaerobic sludge blanket reactors. *Biotechnology Progress* **14**, 645-648.

Sinnott, R. K. (1993) *Chemical engineering*. Oxford: Pergamon Press.

Sollner, K., Teorell, T., Boyd, G. E., Rinaudo, M., Meares, P., Brun, T. S., Paterson, R., Cameron, R. G., Burke, I. S., Sélégny, E., Bourdillon, C., Sanfeld, A., Sanfeld-Steinchen, A., Gregor, H., Sonin, A. A., Pusch, W., Minning, C. P. and Spiegler, K. S. (1973) *Charged gels and membranes - Part I & II*. Dordrecht-Holland/Boston-U.S.A.: D. Riedel Publishing Company.

Sonne-Hansen,J., Mathrani,I.M. and Ahring,B.K. (1993) Xylanolytic anaerobic thermophiles from Icelandic hot-springs. Applied Microbiology and Biotechnology 38, 537-541.

Spang, B. (1994) *VDI-Wärmeatlas, Berechnungsblätter fuer den Wärmeuebergang*. Duesseldorf: VDI-Verlag GmbH.

Stanbury, P. F., Whitaker, A. and Hall, S. J. (1995) *Principle of Fermentation Technology*. New York: Pergamon.

Stiles,M.E. and Holzapfel,W.H. (1997) Lactic acid bacteria of foods and their current taxonomy. *International Journal of Food Microbiology* **36**, 1-29.

Strathmann, H. (1992) Electrodialysis. In *Membrane Handbook* ed. Winston Ho,W.S. and Sirkar,K.K. pp. 217-262. New York: Van Nostrand Reinhold.

Tejayadi,S. and Cheryan,M. (1995) Lactic acid from cheese whey permeate. Productivity and economics of a continuous membrane bioreactor. *Applied Microbiology and Biotechnology* **43**, 242-248.

Thomas,T.D., Ellwood,D.C. and Longyear,V.M.C. (1979) Changes from Homo- to heterofermentation by *Streptococcus lactis* resulting from glucose fermentation in anaerobic chemostat culture. *Journal of Bacteriology* **138**, 109-117.

Timmer,J.M.K., Kromkamp,J. and Robbertsen,T. (1994) Lactic acid separation from fermentation broths by reverse osmosis and nanofiltration. *J. Membrane Sci.* **92**, 185-197.

Timmer,J.M.K., van der Horst,H.C. and Robbertsen,T. (1993) Transport of lactic acid through reverse osmosis and nanofiltration membranes. *J. Membrane Sci.* **85**, 205-216.

Tokoyama. Neosepta Ion-exchange membranes. 1997. Tokuyama Corp.

Tracey,E.M. and Davis,R.H. (1994) Protein fouling of track-etched polycarbonate microfiltration membranes. *Journal of Colloid and Interface Science* **167**, 104-116.

Van Nispen et al. Process for the fermentative preperation of organic acids. Cooperatieve Vereniging Suiker. [US5002881]. 1991. US.

Vonktaveesuk,P., Tonokawa,M. and Ishizaki,A. (1994) Stimulation of the rate of L-lactate fermentation using *Lactococcus lactis* IO-1 by periodic electrodialysis. *Journal of Fermentation and Bioengineering* **77**, 508-512.

Warmington, A. Japan: Who's doing what and why the future may be Japanese. 1999. Http://www.ibpma.be/Frankfurt/Warmington/paper.htm.

Wayman, M. and Parekh, S. R. (1990) *Biotechnology of Biomass Conversion*. Manchester: Open University Press.

Zayed,G. and Winter,J. (1995) Batch and continuous production of lactic acid from salt whey using free and immobilized cultures of lactobacilli. *Applied Microbiology and Biotechnology* **44**, 362-366.

Zheleznov,A., Windmöller,D., Körner,S. and Böddeker,K.W. (1998) Dialytic transport of carboxylic acids through an anion exchange membrane. *J. Membrane Sci.* **139**, 137-143.

Appendix A

List of companies involved in production and/or end use of lactic acid:

ADM Food Additives Div (USA), AE Staley Mfg Co (USA), Acros Chemica NV (Belgium), Anhua Lactic Acid Plant (China), Archer Daniels Midland Co (USA), Boehringer Ingelheim GmbH (Germany), CSM NV (Netherlands), Cargill Inc (USA), Carlo Erba Reagenti Srl (Italy), Daicel Chemical Industries Ltd (Japan), Daiichi Pharmaceutical Co, Ltd (Japan), Dancheng Jindan Lactic Acid Co, Ltd (China), Earnest Healthcare Ltd (India), Ecochem (USA), Ellils & Everard Plc (United Kingdom), Fellesmeieriet Lillehammer (Norway), Fermented Products (USA), Fujisawa Pharmaceutical Co, Ltd (Japan), Fuso Chemical Co Ltd (Japan), Gopaldas Visram & Co (India), Guangzhou Chemical Reagent Factory (China), Hays Chemical Distribution Ltd (United Kingdom), Henan Feilong Fine Chemical Co Ltd (China), Hoechst Australia Ltd (Australia), Hunan Anhua Lactic Acid Plant (China), Hunan Biochemical Factory (China), Jarchem Industries Inc (USA), Kaltron-Pettibone (USA), Kerry Foods, Inc (USA), Kerry Ingredients (USA), Laboratoire Prod'hyg (France), Lactochem Ltd (India), Lambert Riviere SA (France), MD Foods AMBA (Denmark), Mengyin Lactic Acid Products Plant (China), Merck KGaA (Germany), Monsanto Europe SA (Belgium), Niphad Sahakari Sakhar Kharkana Ltd (India), Panreac Quemica, SA (Spain), Pfanstiehl Laboratories Inc (USA), Pureac Bioquimica SA (Spain), Quimicen 84 SA (Spain), Quzhou Zhexi Chemical Plant (China), Rhone-Poulenc SA Departement I O M (France), San Yuan Chemical Co, Ltd (China), Sangita Bio Chem Ltd (India), Shanghai Solvent Factory (China), Showa Chemical Industry Co Ltd (Japan), Showa Kako Corp (Japan), Sigma-Aldrich Chemie GmbH (Germany), Sigma Aldrich Quimica SA (Spain), Sintorgan SA (Argentina), Sterling Chemicals, Inc (USA), Sumitomo Chemical Co Ltd (Japan), Takeda Chemical Industries, Ltd (Japan), W Ulrich GmbH (Germany), Wilke Intl, Inc (USA), Wuhan Chemical Reagent Plant (China), Xiaxian Lactic Acid Factory (China), Xinji Lactic Acid Plant (China), and Zhongsang Yanshi Lactic Acid Co Ltd (China).

Appendix B

Watersplitting modeling:
The purpose of modeling the polarization at the membrane surface is to establish the border conditions, necessary for solving the membrane profile. Since polarization in extreme cases leads to watersplitting and limiting lactate flux, Donnan equilibrium is not valid in these cases. A special approach has to be employed in finding the membrane's border-concentration of lactate at x = 0.

Since it is desired that the simulation is programmed to be more versatile, and able to handle a larger range of different inputs, some simple routines have been included in the program to handle watersplitting.
This early version of the program only handles equilibrium polarization. After assuming that watersplitting does not take place, initial values of wall concentrations of lactate and hydroxide are found. If either of these values is below zero, a special situation arises. If both values are below zero, definite watersplitting takes place.

If only lactate or hydroxide concentration falls below zero, the actual physical situation arises that the flux of one ion is reduced, while the flux of the other ion increases. Thus, the linear boundary layer model cannot be employed in calculating the wall concentrations. The membrane border-concentration is calculated from a steady-state assumption:

- At steady state, the migration flux in the first membrane "slice" is equal to the collective diffusion and migration flux across the boundary layer. This assumption is illustrated for lactate on Figure B.0.1.

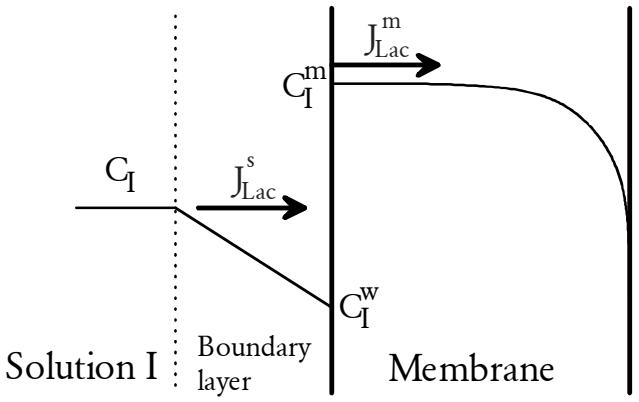

Figure B.0.1. Illustration of the assumed steady-state condition that J^s must equal J^m, when lactate concentration C^w reaches 0 at the membrane surface because of polarization.

$C_{Lac}^{w} < 0$:

The case illustrated in Figure B.0.1 shows the special case, when lactate concentration reaches zero at the membrane surface as a result of polarization. Even if current density is increased, the lactate flux cannot increase. The surplus of electrical current is then carried by hydroxide ions into the membrane and hydrogen ions away from the surface. These ions arise from watersplitting as explained earlier in the theory chapter.

The lactate flux across the boundary layer, which is the basis for determining the membrane concentration, can then be calculated as:

eq. B.1 $$J_{Lac}^{BoundaryLayer} = \frac{i_d}{z_{Lac}F} t_{Lac}^{s} + k_{Lac} C_{Lac}^{s}$$

i_d is the current density, z the ionic charge, F the Faraday number, t^s the transport number, k the mass transfer coefficient, and C^s the concentration in the bulk solution just outside the boundary layer. This flux can be readily calculated with knowledge of the bulk solution composition, the current density, and the mass transfer coefficient.
The steady-state membrane flux that the assumption uses, is calculated as a pure migration flux:

eq. B.2 $$J_{Lac}^{Inside\ \ Membrane\ \ Surface} = \frac{i_d}{z_{Lac}F} t_{Lac}^{m}$$

By setting eq. B.1 equal to eq. B.2, t^m can be determined, and from the transport number, the membrane concentration of lactate can be determined, by combining the definition of t^m with the assumption made in chapter 6
Modeling that lactate and hydroxide are the only mobile ions inside the membrane.

eq. B.3 $$C_{Lac}^{m} + C_{OH}^{m} = C_R$$

C_R is the ion-exchange capacity of the membrane. Rearranging the simplified expression of t^m in eq. 6.2.7 yields:

eq. B.4 $$C_{Lac}^{m} = \frac{\mu C_R t_{Lac}^{m}}{1-(1-\mu)t_{Lac}^{m}}, \qquad \mu = \frac{\mu_{OH}^{m}}{\mu_{Lac}^{m}}$$

$C_{Lac}^{w} > 0,\ C_{OH}^{w} < 0$:

In this special case, no watersplitting takes place, but the low concentration of hydroxide ions at the membrane surface stills increases the removal of lactate, and again, a different approach has to be taken, to calculate the lactate membrane border-concentration.

The problem is solved analogous to the previous, but this time, the hydroxide flux is considered. The two flux equations eq. B.1 and eq. B.2 written for hydroxide are:

eq. B.5 $$J_{OH}^{BoundaryLayer} = \frac{i_d}{z_{OH}F} t_{OH}^{s} + k_{OH} C_{OH}^{s}$$

and

eq. B.6 $$J_{OH}^{Inside\ \ Membrane\ \ Surface} = \frac{i_d}{z_{OH}F} t_{OH}^{m}$$

Since

$$t_{Lac}^{m} = 1 - t_{OH}^{m}$$

the membrane's border-concentration of lactate can now be determined by eq. B.4.

However, it is necessary to check the validation of this solution, since it is based on the assumption that the wall concentration of lactate is still above zero. Though, the initial estimate found a positive wall concentration, one has to take into account that the increase of lactate flux due to decrease of hydroxide flux, increases the lactate polarization.

The steady-state flux of lactate just inside the membrane surface is estimated as eq. B.2, and the steady-state assumption that the lactate flux across the boundary layer must equal the membrane's border-flux yields the following expression:

eq. B.7 $$J_{Lac}^{Inside\ \ Membrane\ \ Surface} = J_{Lac}^{BoundaryLayer} = \frac{i_d}{z_{Lac}F} t_{Lac}^{s} + k_{Lac}\left(C_{Lac}^{s} - C_{Lac}^{w}\right)$$

From eq. B.7, the lactate wall concentration can be found:

eq. B.8 $$C_{Lac}^{w} = C_{Lac}^{s} + \frac{\frac{i_d}{z_{Lac}F} t_{Lac}^{s} - J_{Lac}^{Inside\ \ Membrane\ \ Surface}}{k_{Lac}}$$

If the wall concentration of lactate is still positive, the assumption of increased polarization without watersplitting is correct, and the border-concentration as well as the wall concentration of lactate is ratified. If new estimation of the wall concentration on the other hand is *negative*, then the assumption must be discarded, since watersplitting occurs. The border-value for lactate's membrane concentration must then be found as described in the previous special case.

Appendix C

Simulation program:

This simulation program was written in FORTRAN using Plato 2 compilation software from Salford Software Ltd., United Kingdom.

```
Program Profile

Integer I,J,K,N,IREV,NUMX,Round,TID,QANSOL
Double Precision U(0:100,0:100),C(0:100,0:100)
Double Precision CLW(2,0:100),COHW(2,0:100)
Double Precision DT,DX,CLIN,CLOUT,PH(2),INISLOPE,DL,DOH
Double Precision DIFF(0:100),ERROR,UITER(0:100)
Double Precision CURDENS,FARADAY,ML,MOH,MNA,MH,DIFLAYER(2)
Double Precision MASSTL(2),MASSTOH(2),MASSTNA(2)
Double Precision IFL,IFOH,MOBL,MOBOH,ALFA,MY,COHIN,COHOUT
Double Precision L,DML,DMOH,MEMCAP,SWELLING,IDF,CNAW,TM,TS
Double Precision DNA,FLUXL(4,0:100),FLUXOH(2,0:100)
Double Precision A0,A1,A2,DISC,FLUXDIF,CUREFF(4,100)
Double Precision QACOEF(0:4),QASOL(1:4),QASOLI(1:4)
Character Answer
Logical LSPLIT,OHSPLIT

C ALFA is a composit constant, MEMCAP is the membrane's ion-capacity
C MY is the relationship between the mobility of OH and Lactate ions
C DML and DMOH are diffusion coefficients of Lactate and OH inside the membrane
C CLIN/CLOUT are the lactate concentration of the two extrenal solution on both sides
C PH is a vector containing the pH-values of IN (=1) and OUT (=2)
C INISLOPE is the initial diffusion-determined concentration slope through the mem
C MASSTL and MASSTOH are the mass transfer coefficients respectively of LACTATE and
C       OH in the external filmlayer
C IFOH and IFL are composit constants: Id/F times mobility of either OH or Lactate
C ERROR and DIFF are iteration error constants
C MOBOH and MOBL are the sum of the mobility of the cation and either OH or Lactate
C UITER is a vektor to calculate the iteration error
C CLW and COHW are membrane wall concentration vectors for Lactate and OH; IN (=1) and OUT
(=2)
C FLUX is a flux vector (mol/m2s) of the changing flux of Lactate or OH; IN (=1) and OUT (=2)
C ACF is the accumulated flux used for calculating the current efficiency CUREFF, which is
C calculated for each step (=1) and accumulated from 0 to index (=2)
C MIGIN is the constant electrical migration of lactate into the external boundary layer
C CNAW is the cation concentration at the membrane wall
C ML, MOH, and MNA are mobilities, and DL, DOH, and DNA are diffusion coefficients of either
```

```
C       Lactate, OH, or the cation

C Clearing matrices
        DO 30 I=0,100
          DO 20 J=0,100
          C(I,J)=0.D0
          U(I,J)=0.D0
          CLW(1,J)=0.D0
          CLW(2,J)=0.D0
          COHW(1,J)=0.D0
          COHW(2,J)=0.D0
          FLUXL(1,J)=0.D0
          FLUXL(2,J)=0.D0
          FLUXL(3,J)=0.D0
          FLUXL(4,J)=0.D0
          FLUXOH(1,J)=0.D0
          FLUXOH(2,J)=0.D0
   20     Continue
   30   Continue

C Setting physical constants
        TID=100
        CURDENS = 250.D0
        FARADAY = 96487.D0

        IDF=CURDENS/FARADAY

C       Solution constants
        ML = 0.00000004023D0
        MOH = 0.0000002064D0
        MNA = 0.0000000519D0
        MH = 0.0000003623D0
        DIFLAYER(1) = 0.000059D0
        DIFLAYER(2) = 0.000059D0
        DL = ML*0.0256907054836D0
        DOH = MOH*0.0256907054836D0
        DNA = MNA*0.0256907054836D0
        Do 5 I=1,2
          MASSTL(I) = DL/DIFLAYER(I)
          MASSTOH(I) = DOH/DIFLAYER(I)
          MASSTNA(I) = DNA/DIFLAYER(I)
     5  Continue
        IFL = CURDENS/FARADAY*ML
        IFOH = CURDENS/FARADAY*MOH
        MOBL = ML+MNA
        MOBOH = MOH+MNA
```

```
C       Membrane constants
        SWELLING = 0.30D0
        L = 200.D0/1000000.D0
        MEMCAP = 2.D0*1000.D0
        MY = MOH/ML
        ALFA = IDF*MY*MEMCAP
        DMOH = DOH*(SWELLING/(2.D0-SWELLING))**2
        DML = DL*(SWELLING/(2.D0-SWELLING))**2

C       INPUT of physical problem
        Write (*,*) 'Current density = ',CURDENS,'A/m2'
        Write (*,*) 'Membrane capacity = ',MEMCAP,'mol/m3'
        Write (*,*) 'Membrane thickness = ',(L*1000000.D0),'micrometer'
        Write (*,*) 'Diffusion layer´s Mass Trasfer Coefficient = ',
     1    MASSTL(1),' m/s'
        Write (*,*) 'Lactate diffusion coefficient :',DL,'m2/s'
        Write (*,*) 'Lactate diffusion coefficient in Membrane :',DML,
     1  'm2/s'
        Write (*,*) 'ALFA = ',ALFA
        Write (*,*) 'Input timestep size (sec.) :'
        Read (*,*) DT

        NUMX = 100
        DX = L/(NUMX)

        Write (*,*) 'Steplength :',(DX*1000000.D0),'micrometer'
        Write (*,*) 'Input Lactate concentration FEED (M) :'
        Read (*,*) CLIN
        CLIN=CLIN*1000.D0
        Write (*,*) 'Input Lactate concentration BASE (M) :'
        Read (*,*) CLOUT
        CLOUT=CLOUT*1000.D0
        Write (*,*) 'Input pH FEED :'
        Read (*,*) PH(1)
        COHIN=1000.D0*10**(PH(1)-14.D0)
        Write (*,*) 'Input pH BASE :'
        Read (*,*) PH(2)
        COHOUT=1000.D0*10**(PH(2)-14.D0)

C SETTING INITIAL VALUES
        C(0,0)=Donnan(CLIN,COHIN,MEMCAP)
        U(0,0)=(1.D0-MY)*C(0,0)+MY*MEMCAP
        C(NUMX,0)=Donnan(CLOUT,COHOUT,MEMCAP)
        U(NUMX,0)=(1.D0-MY)*C(NUMX,0)+MY*MEMCAP
        INISLOPE=(C(NUMX,0)-C(0,0))/L
        Round=1
C Initial Values for t = 0:
```

```
      DO 90 I=1,NUMX-1
        C(I,0)=C(0,0)+1.D0*I*DX*INISLOPE
        U(I,0)=(1.D0-MY)*C(I,0)+MY*MEMCAP
 90   Continue

C Resetting values
 100   CLW(1,0)=CLIN
       CLW(2,0)=CLOUT
       COHW(1,0)=COHIN
       COHW(2,0)=COHOUT
       CNAW=CLIN+COHIN
       CNAW=CNAW-IDF*(MNA*CNAW/(MOBL*CLIN+MOBOH*COHIN))/MASSTNA(1)
       LSPLIT=.FALSE.
       OHSPLIT=.FALSE.

C CALCULATION OF PROFILES
       TS=ML*CLIN/(MOBL*CLIN+MOBOH*COHIN)
C Calculation of Wall Concentration (IN)
 105     If (LSPLIT) Then
          Goto 130
         Elseif (OHSPLIT) Then
          Goto 120
         Else
          Goto 110
         Endif
C No Watersplitting
 110     A0=1.D0-MY
         A1=MY*CNAW-(1.D0-MY)*CLIN+IDF/MASSTL(1)*(1.D0-TS*(1.D0-MY))
         A2=-IDF*TS*MY*CNAW-MY*CNAW*CLIN
         DISC=A1**2-4.D0*A0*A2
         CLW(1,0)=(-A1-SQRT(DISC))/(2.D0*A0)
         COHW(1,0)=CNAW-CLW(1,0)
         If ((COHW(1,0) .LT. 0.D0) .AND. (CLIN .GT. MY*COHIN)) Then
          OHSPLIT=.TRUE.
          If (CLW(1,0) .LT. 0.D0) Then
           LSPLIT=.TRUE.
          Endif
          Goto 105
         Endif
         If (CLW(1,0) .LT. 0.D0) Then
          LSPLIT=.TRUE.
          Goto 105
         Endif
         If (CLW(1,0) .GT. CLIN) Then
          Write (*,*) 'C-Wall too large (wrong root selection) : '
    1      ,CLW(1,0)
          CLW(1,0)=(-A1+SQRT(DISC))/(2.D0*A0)
```

```
          Write (*,*) 'New C-Wall: ',CLW(1,0)
          COHW(1,0)=CNAW-CLW(1,0)
          Write (*,*) 'New COH-Wall: ',COHW(1,0)

        Endif
        If (COHW(1,0) .LT. 0.D0) Then
          OHSPLIT=.TRUE.
          If (CLW(1,0) .LT. 0.D0) Then
            LSPLIT=.TRUE.
            Write (*,*) 'Watersplitting!'
          Endif
          Goto 105
        Endif
        If (CLW(1,0) .LT. 0.D0) Then
          LSPLIT=.TRUE.
          Write (*,*) 'C-Wall = 0!'
          Goto 105
        Endif
        FLUXL(4,0)=IDF*TS-MASSTL(1)*(CLW(1,0)-CLIN)
        FLUXOH(1,0)=IDF*MOH*COHIN*TS/(ML*CLIN)-MASSTOH(1)*
     1    (COHW(1,0)-COHIN)
        C(0,0)=Donnan(CLW(1,0),COHW(1,0),MEMCAP)
        Goto 140
C OH-level too low
  120   If (CNAW .LT. 0.D0) Then
          LSPLIT=.TRUE.
          Goto 105
        Endif
        COHW(1,0)=0.D0
        FLUXDIF=IDF*MOH*COHIN/(MOBOH*COHIN+MOBL*CLIN)
     1    +MASSTOH(1)*COHIN
        TM=1.D0-FLUXDIF/IDF
        FLUXDIF=IDF*TM
        CLW(1,0)=CLIN+(IDF*TS-FLUXDIF)/MASSTL(1)
        If (CLW(1,0) .LT. 0.D0) Then
          LSPLIT=.TRUE.
          Goto 105
        Endif
        C(0,0)=TM*MY*MEMCAP/(1.D0-TM*(1.D0-MY))
        FLUXL(4,0)=IDF*TS+MASSTL(1)*(CLIN-CLW(1,0))
        FLUXOH(1,0)=IDF*MOH*COHIN*TS/(ML*CLIN)+MASSTOH(1)*COHIN
        Goto 140
C Watersplitting
  130   FLUXDIF=IDF*TS+MASSTL(1)*CLIN
        CLW(1,0)=0.D0
        If (CNAW .GT. 0.D0) Then
          COHW(1,0)=CNAW
```

```
      Else
        COHW(1,0)=0.D0
      Endif
      TM=FLUXDIF/IDF
      C(0,0)=TM*MY*MEMCAP/(1.D0-TM*(1.D0-MY))
      FLUXL(4,0)=FLUXDIF
      FLUXOH(1,0)=IDF*MOH*COHIN/(MOBL*CLIN+MOBOH*COHIN)
     1    +MASSTOH(1)*(COHIN-COHW(1,0))
  140   U(0,0)=(1.D0-MY)*C(0,0)+MY*MEMCAP

C Guessing first line and starting iterations
      Do 1000 J=1,TID
        CLW(1,J)=CLW(1,J-1)
        COHW(1,J)=COHW(1,J-1)
        Do 200 I=0,NUMX
          U(I,J)=U(I,J-1)
          C(I,J)=C(I,J-1)
          UITER(I)=U(I,J)
  200   Continue
      Do 990 N=1,49
        Do 210 I=0,NUMX
          DIFF(I)=C(I,J)
  210   Continue
C Finding Profile
        Do 320 K=1,49
          ERROR=0.D0
          Do 300 IREV=1,NUMX-1
            I=NUMX-IREV
            Call CalcU(U,IREV,J,DX,DT,DML,ALFA,MY,MEMCAP)
            Call CalcU(U,I,J,DX,DT,DML,ALFA,MY,MEMCAP)
  300     Continue
          Do 310 I=1,NUMX-1
            C(I,J)=(U(I,J)-MY*MEMCAP)/(1.D0-MY)
            ERROR=ERROR+(((U(I,J)-UITER(I))/U(I,J))**2)/NUMX
            UITER(I)=U(I,J)
  310     Continue
          If (K .LT. 4) Then
            Goto 320
          Endif
          If (ERROR .LT. 0.0000001D0) Then
            Goto 350
          Endif
  320   Continue
C Calculation of Wall Concentration (OUT)
  350   CLW(2,J)=CLW(2,J-1)
        COHW(2,J)=COHW(2,J-1)
        Do 370 I=1,4
```

```
      QASOL(I)=0.D0
      QASOLI(I)=0.D0
370   Continue
     Do 400 K=1,499
      ERROR=CLW(2,J)
      QACOEF(4)=MASSTOH(2)*MY*MOBOH
      QACOEF(3)=MASSTOH(2)*(MY*MOBL+(1.d0+MY)*MOBOH)*CLW(2,J)
     1          +MY*MOBOH*(DMOH/DX*C(NUMX-1,J)-MASSTOH(2)*COHOUT)
     2          -MY*MNA*IDF
      QACOEF(2)=(MASSTOH(2)*((1.d0+MY)*MOBL+MOBOH)*CLW(2,J)
     1          +((1.d0+MY)*MOBOH+MY*MOBL)*(DMOH/DX*C(NUMX-1,J)
     2          -MASSTOH(2)*COHOUT)-DMOH/DX*MY*MOBOH*MEMCAP
     3          -2.d0*MY*MNA*IDF)*CLW(2,J)
      QACOEF(1)=(MASSTOH(2)*MOBL*CLW(2,J)-DMOH/DX*(MY*MOBL+MOBOH)
     1          *MEMCAP+((1.d0+MY)*MOBL+MOBOH)
     2          *(DMOH/DX*C(NUMX-1,J)-MASSTOH(2)*COHOUT)
     3          -MY*MNA*IDF)*(CLW(2,J)**2)
      QACOEF(0)=MOBL*(DMOH/DX*(C(NUMX-1,J)-MEMCAP)-MASSTOH(2)
     1          *COHOUT)*(CLW(2,J)**3)
      Call quartic(QACOEF,QASOL,QASOLI,QANSOL)
      Do 375 I=1,QANSOL
       COHW(2,J)=QASOL(I)
       If ((COHW(2,J) .GT. 0.d0) .AND. (COHW(2,J) .LT. MEMCAP))
     1   Then
        Goto 380
       Endif
375    Continue
380    QACOEF(4)=MASSTL(2)*MOBL
      QACOEF(3)=MASSTL(2)*(((1.d0+MY)*MOBL+MOBOH)*COHW(2,J)
     1          -MOBL*CLOUT)+DML/DX*MOBL*(MEMCAP-C(NUMX-1,J))
     2          -MNA*IDF
      QACOEF(2)=(MASSTL(2)*(MY*(MOBL+MOBOH)*COHW(2,J)
     1          -(1.d0+MY)*MOBL*CLOUT)+DML/DX*((MY*MOBL
     2          +MOBOH)*MEMCAP-((1.d0+MY)*MOBL+MOBOH)
     3          *C(NUMX-1,J))-2.d0*MNA*IDF)*COHW(2,J)
      QACOEF(1)=(MY*MOBOH*(MASSTL(2)*COHW(2,J)+DML/DX*MEMCAP)
     1          -(MY*MOBL+(1.d0+MY)*MOBOH)
     2          *(MASSTL(2)*CLOUT+DML/DX*C(NUMX-1,J))
     3          +(ML-MOBOH)*IDF)*(COHW(2,J)**2)
      QACOEF(0)=-(MASSTL(2)*CLOUT+DML/DX*C(NUMX-1,J))*MY*MOBOH
     1          *(COHW(2,J)**3)
      Call quartic(QACOEF,QASOL,QASOLI,QANSOL)
      Do 385 I=1,QANSOL
       CLW(2,J)=QASOL(I)
       If ((CLW(2,J) .GT. 0.d0) .AND. (CLW(2,J) .LT. MEMCAP))
     1   Then
        Goto 390
```

```
        Endif
385     Continue
390     If ((ERROR-CLW(2,J))**2 .LT. 0.01) Then
       Goto 450
      Endif
400    Continue
450     C(NUMX,J)=Donnan(CLW(2,J),COHW(2,J),MEMCAP)
      U(NUMX,J)=(1.D0-MY)*C(NUMX,J)+MY*MEMCAP
      UITER(NUMX)=U(NUMX,J)

      ERROR=0.D0
      Do 550 I=0,NUMX
       ERROR=ERROR+(DIFF(I)-C(I,J))**2
550     Continue
      If (ERROR .LT. 10.D0) Then
       Goto 990
      Endif
990    Continue
     ERROR=0.D0
     Do 995 I=0,NUMX
      ERROR=ERROR+(U(I,J)-U(I,J-1))**2
995    Continue
     ERROR=DT*ERROR/(NUMX+1)
     Write (*,*) 'Error = ',ERROR
     If (ERROR .LT. 5.D0) Then
      Call CalcFlux(J,NUMX,C,FLUXL,FLUXOH,CLW,COHW,MASSTL,DML,
   1  DMOH,DX,IDF,MEMCAP,MY,ML,MOH,MNA,CLIN,CLOUT,CUREFF)
      Write (*,996) DT*(J)
996      Format ('Steady-state reached after ',F8.2,' seconds.')
      Write (*,*) 'FLUX (IN-mem) = ',FLUXL(1,J)
      Write (*,*) 'FLUX (IN-dif) = ',FLUXL(4,J)
      Write (*,*) 'FLUX (OUT-mem) = ',FLUXL(2,J)
      Write (*,*) 'FLUX (OUT-dif) = ',FLUXL(3,J)
      Write (*,*) 'Current efficiency = ',CUREFF(2,J)*100.d0,' %'
      Goto 1100
     Endif
1000   Continue
1010    Format ('No Steady-state reached after ',F8.2,' seconds.')
     Call CalcFlux(TID,NUMX,C,FLUXL,FLUXOH,CLW,COHW,MASSTL,DML,
   1  DMOH,DX,IDF,MEMCAP,MY,ML,MOH,MNA,CLIN,CLOUT,CUREFF)
     Write (*,1010) DT*(TID)
     Write (*,*) 'FLUX (IN-mem) = ',FLUXL(1,TID)
     Write (*,*) 'FLUX (IN-dif) = ',FLUXL(4,TID)
     Write (*,*) 'FLUX (OUT-mem) = ',FLUXL(2,TID)
     Write (*,*) 'FLUX (OUT-dif) = ',FLUXL(3,TID)
     Write (*,*) 'Current efficiency = ',CUREFF(2,TID)*100.d0,' %'
1100   Write (*,*)'Do you wish to save results in data-file (y/n)'
```

```
      Read (*,*) Answer
      If (Answer .EQ. 'y' .or. Answer .EQ. 'Y') Then
       If (Round .LT. 0) Then
        Call Reverse(C,NUMX)
        Do 1200 J=0,TID
         Call SWITCH(CLW(1,J),CLW(2,J))
         Call SWITCH(FLUXL(1,J),FLUXL(2,J))
         Call SWITCH(FLUXL(3,J),FLUXL(4,J))
         Call SWITCH(FLUXOH(1,J),FLUXOH(2,J))
1200      Continue
        Call Datafile(C,CLW,FLUXL,FLUXOH,CUREFF)
        Call Reverse(C,NUMX)
        Do 1300 J=0,TID
         Call SWITCH(CLW(1,J),CLW(2,J))
         Call SWITCH(FLUXL(1,J),FLUXL(2,J))
         Call SWITCH(FLUXL(3,J),FLUXL(4,J))
         Call SWITCH(FLUXOH(1,J),FLUXOH(2,J))
1300      Continue
       Else
        Call Datafile(C,CLW,FLUXL,FLUXOH,CUREFF)
       Endif
      Endif
C Reverse Current Direction
      Write (*,*) 'Do you wish to reverse the current (y/n) ?'
      Read (*,*) Answer
      If (Answer .NE. 'y' .AND. Answer .NE. 'Y') Then
       Goto 5000
      Endif
      If (Round .GT. 0) Then
       Round=-1
       Else
       Round=1
      Endif
      Call Clear(C,NUMX)
      Do 2010 J=0,100
       Do 2000 I=0,NUMX
        U(I,J)=(1.D0-MY)*C(I,J)+MY*MEMCAP
2000    Continue
       FLUXL(1,J)=0.D0
       FLUXL(2,J)=0.D0
       FLUXL(3,J)=0.D0
       FLUXL(4,J)=0.D0
       FLUXOH(1,J)=0.D0
       FLUXOH(2,J)=0.D0
       CLW(1,J)=0.D0
       CLW(2,J)=0.D0
       COHW(1,J)=0.D0
```

```
        COHW(2,J)=0.D0
 2010   Continue
        Call SWITCH(CLIN,CLOUT)
        Call SWITCH(COHIN,COHOUT)
        Call SWITCH(MASSTL(1),MASSTL(2))
        Call SWITCH(MASSTOH(1),MASSTOH(2))
        Call SWITCH(MASSTNA(1),MASSTNA(2))
        Call SWITCH(DIFLAYER(1),DIFLAYER(2))
        Call SWITCH(PH(1),PH(2))
        Goto 100
 5000   End


CCCC
```

```
      If ((U(I,J) .GT. MYM) .or. (U(I,J) .LT. MEMCAP)) Then
        Write (*,*) '! Illegal values - Iteration continues !'
C         U(I,J)=-(S+T)/2.D0-A1/3.D0
      Endif
      Goto 100
C     D < 0
   50 PHI = acos(R/((-(Q**3))**(1/2.D0)))
      U(I,J)=2.D0*(-Q)**(1/2.D0)*cos(PHI/3.D0)-A1/3.D0
      If ((U(I,J) .GT. MYM) .or. (U(I,J) .LT. MEMCAP)) Then
        U(I,J)=2.D0*(-Q)**(1/2.D0)*cos((PHI+pi2*2/3.D0)/3.D0)-A1/3.D0
      Elseif ((U(I,J) .GT. MYM) .or. (U(I,J) .LT. MEMCAP)) Then
        U(I,J)=2.D0*(-Q)**(1/2.D0)*cos((PHI+pi2*4/3.D0)/3.D0)
     1    -A1/3.D0
      Endif
      Continue
  100 C(I,J)=(U(I,J)-MYM)/(1.D0-MY)
      End

      Subroutine CalcFlux(MAXJ,NUMX,C,FLUXL,FLUXOH,CLW,COHW,KL,DML,
     1  DMOH,DX,IDF,MEMCAP,MY,ML,MOH,MNA,CLIN,CLOUT,EFF)
      Integer J,MAXJ,NUMX
      Double Precision C(0:100,0:100),FLUXL(4,0:100),FLUXOH(2,0:100)
      Double Precision CLW(2,0:100),COHW(2,0:100),KL(2)
      Double Precision DML,DMOH,DX,IDF,MEMCAP,MY,ML,MOH,MNA
      Double Precision CLIN,CLOUT,ACF,EFF(4,100)
      Double Precision MOBL,MOBOH
      MOBL=ML+MNA
      MOBOH=MOH+MNA
      ACF=0.d0
      Do 100 J=1,MAXJ
        FLUXL(1,J)=IDF/(1.d0+MY*(MEMCAP/C(0,J)-1.d0))
     1    +DML/DX*(C(0,J)-C(1,J))
        FLUXL(2,J)=IDF/(1.d0+MY*(MEMCAP/C(NUMX,J)-1.d0))
     1    +DML/DX*(C(NUMX-1,J)-C(NUMX,J))
        FLUXL(3,J)=IDF*ML*CLW(2,J)/(MOBL*CLW(2,J)+MOBOH*COHW(2,J))
     1    +KL(2)*(CLW(2,J)-CLOUT)
        FLUXL(4,J)=IDF*ML*CLW(1,J)/(MOBL*CLW(1,J)+MOBOH*COHW(1,J))
     1    +KL(1)*(CLIN-CLW(1,J))
        FLUXOH(1,J)=IDF*(1.d0-1.d0/(1.d0+MY*(MEMCAP/C(0,J)-1.d0)))
     1    +DMOH/DX*(C(1,J)-C(0,J))
        FLUXOH(2,J)=IDF*(1.d0-1.d0/(1.d0+MY*(MEMCAP/C(NUMX,J)-1.d0)))
     1    +DMOH/DX*(C(NUMX,J)-C(NUMX-1,J))
  100 Continue
      Do 200 J=MAXJ+1,NUMX
        FLUXL(1,J)=FLUXL(1,J-1)
        FLUXL(2,J)=FLUXL(2,J-1)
        FLUXL(3,J)=FLUXL(3,J-1)
```

```
      FLUXL(4,J)=FLUXL(4,J-1)
      FLUXOH(1,J)=FLUXOH(1,J-1)
      FLUXOH(2,J)=FLUXOH(2,J-1)
200   Continue
     Do 300 J=1,NUMX
      ACF=ACF+FLUXL(2,J)
      If (CLIN .lt. CLOUT) Then
       ACF=ACF+FLUXL(2,J)
       EFF(4,J)=ACF
      Else
       ACF=ACF+FLUXL(1,J)
       EFF(3,J)=ACF
      Endif
      If (J .gt. 1) Then
       EFF(1,J)=((EFF(3,J)-EFF(3,J-1))-(EFF(4,J)-EFF(4,J-1)))/IDF
      Else
       EFF(1,J)=(EFF(3,J)-EFF(4,J))/IDF/(J)
      Endif
      EFF(2,J)=(EFF(3,J)-EFF(4,J))/IDF/(J)
300   Continue
     End

     Subroutine Datafile(C,CLW,FLUXL,FLUXOH,EFF)
     Double precision C(0:100,0:100),CLW(2,0:100),FLUXL(4,0:100)
     Double Precision FLUXOH(2,0:100),EFF(4,100)
     Integer J
     Character*12 FILENAME
     Write (*,*) 'File-name :'
     Read (*,*) FILENAME
     Open (Unit=11,File=FILENAME)
100   Format (I3,101(';',F9.4))
     Do 200 J=0,100
      Write (11,100) J,(C(K,J),K=0,100)
200   Continue
     Write (11,*) 'Wall concentrations/Lactate fluxes/Hydroxide ',
    1  'fluxes/Current Efficiency (stepwise and accumulated)'
210   Format (I3,';Wall-C;',F9.2,';',F9.2,';L-Flux;',F8.6,';',F8.6,
    1  ';OH-Flux;',F8.6,';',F8.6,';Efficiency;',F8.6,';',F8.6,';'
    2  ,F8.6,';',F8.6)
     Do 300 J=0,100
      Write (11,210) J,CLW(1,J),CLW(2,J),FLUXL(1,J),FLUXL(2,J),
    1   FLUXOH(1,J),FLUXOH(2,J),EFF(1,J),EFF(2,J),EFF(3,J),EFF(4,J)
300   Continue
     Close (11)
     End
```

```
      Subroutine Reverse(M,NUMX)
      Double Precision M(0:100,0:100),MNEW(0:100,0:100)
      Integer I,J,NUMX
      Do 110 J=0,100
        Do 100 I=0,NUMX
          MNEW(I,J)=M(NUMX-I,J)
100     Continue
110   Continue
      Do 210 J=0,100
        Do 200 I=0,NUMX
          M(I,J)=MNEW(I,J)
200     Continue
210   Continue
      End


      Subroutine SWITCH(A,B)
      Double Precision A,B,C
      C=A
      A=B
      B=C
      End


      Subroutine Clear(M,NUMX)
      Double Precision M(0:100,0:100),INIT(0:100)
      Integer I,J,NUMX,LAST
      Logical Stability
      Stability=.FALSE.
      Do 110 J=0,100
        Do 100 I=0,NUMX
          If (M(I,100-J) .GT. 0.0001) Then
            Stability=.TRUE.
          Endif
100     Continue
        If (Stability) Then
          LAST=100-J
          Goto 150
        Endif
110   Continue
150   Do 200 I=0,NUMX
        INIT(I)=M(I,LAST)
200   Continue
      Do 310 J=1,100
        Do 300 I=0,NUMX
          M(I,0)=INIT(NUMX-I)
          M(I,J)=0.D0
```

```
 300     Continue
 310   Continue
       End

C     ***QUARTIC*************************************************25.03.98
C     Solution of a quartic equation
C     ref.: J. E. Hacke, Amer. Math. Monthly, Vol. 48, 327-328, (1941)
C     NO WARRANTY, ALWAYS TEST THIS SUBROUTINE AFTER DOWNLOADING
C     ****************************************************************
C     dd(0:4)     (i)  vector containing the polynomial coefficients
C     sol(1:4)    (o)  results, real part
C     soli(1:4)   (o)  results, imaginary part
C     Nsol        (o)  number of real solutions
C     ================================================================
      subroutine quartic(dd,sol,soli,Nsol)
      implicit double precision (a-h,o-z)
      dimension dd(0:4),sol(4),soli(4)
      dimension AA(0:3),z(3)
C
      Nsol = 0
      a = dd(4)
      b = dd(3)
      c = dd(2)
      d = dd(1)
      e = dd(0)
C
      if (dd(4).eq.0.d+0) then
        write(6,*)'ERROR: NOT A QUARTIC EQUATION'
        return
      endif
C
      p = (-3.d+0*b**2 + 8.d+0*a*c)/(8.d+0*a**2)
      q = (b**3 - 4.d+0*a*b*c + 8.d+0*d*a**2)/(8.d+0*a**3)
      r = (-3.d+0*b**4 + 16.d+0*a*b**2*c - 64.d+0*a**2*b*d +
     1     256.d+0*a**3*e)/(256.d+0*a**4)
C
C     solve cubic resolvent
      AA(3) =  8.d+0
      AA(2) = -4.d+0*p
      AA(1) = -8.d+0*r
      AA(0) =  4.d+0*p*r - q**2
      call cubic(AA,z,ncube)
C
      zsol = -1.d+99
      do 5 i=1,ncube
 5      zsol = max(zsol,z(i))
      z(1) = zsol
```

```
      xK2 = 2.d+0 * z(1) - p
      xK  = sqrt(xK2)
C-----------------------------------------------
      if (xK.eq.0.d+0) then
        xL2 = z(1)**2 - r
        if (xL2.lt.0.d+0) then
          write(6,*)'Sorry, no solution'
          return
        endif
        xL  = sqrt(xL2)
      else
        xL = q/(2.d+0 * xK)
      endif
C-----------------------------------------------
      sqp = xK2 - 4.d+0*(z(1) + xL)
      sqm = xK2 - 4.d+0*(z(1) - xL)
C
      do 10 i=1,4
 10     soli(i) = 0.d+0
      if       (sqp.ge.0.d+0 .and. sqm.ge.0.d+0) then
        sol(1) = 0.5d+0*( xK + sqrt(sqp))
        sol(2) = 0.5d+0*( xK - sqrt(sqp))
        sol(3) = 0.5d+0*(-xK + sqrt(sqm))
        sol(4) = 0.5d+0*(-xK - sqrt(sqm))
        Nsol = 4
      else if  (sqp.ge.0.d+0 .and. sqm.lt.0.d+0) then
        sol(1) =  0.5d+0*(xK + sqrt(sqp))
        sol(2) =  0.5d+0*(xK - sqrt(sqp))
        sol(3) = -0.5d+0*xK
        sol(4) = -0.5d+0*xK
        soli(3) =  sqrt(-0.25d+0 * sqm)
        soli(4) = -sqrt(-0.25d+0 * sqm)
        Nsol = 2
      else if  (sqp.lt.0.d+0 .and. sqm.ge.0.d+0) then
        sol(1) = 0.5d+0*(-xK + sqrt(sqm))
        sol(2) = 0.5d+0*(-xK - sqrt(sqm))
        sol(3) =  0.5d+0*xK
        sol(4) =  0.5d+0*xK
        soli(3) =  sqrt(-0.25d+0 * sqp)
        soli(4) = -sqrt(-0.25d+0 * sqp)
        Nsol = 2
      else if  (sqp.lt.0.d+0 .and. sqm.lt.0.d+0) then
        sol(1) = -0.5d+0*xK
        sol(2) = -0.5d+0*xK
        soli(1) =  sqrt(-0.25d+0 * sqm)
        soli(2) = -sqrt(-0.25d+0 * sqm)
        sol(3) =  0.5d+0*xK
```

```
      sol(4) =  0.5d+0*xK
      soli(3) =  sqrt(-0.25d+0 * sqp)
      soli(4) = -sqrt(-0.25d+0 * sqp)
      Nsol = 0
     endif
     do 20 i=1,4
 20    sol(i) = sol(i) - b/(4.d+0*a)
C
     return
     END

C    ***CUBIC*************************************************08.11.1986
C    Solution of a cubic equation
C    Equations of lesser degree are solved by the appropriate formulas.
C    The solutions are arranged in ascending order.
C    NO WARRANTY, ALWAYS TEST THIS SUBROUTINE AFTER DOWNLOADING
C    ********************************************************************
C    A(0:3)      (i)  vector containing the polynomial coefficients
C    X(1:L)      (o)  results
C    L           (o)  number of valid solutions (beginning with X(1))
C    ====================================================================
     SUBROUTINE CUBIC(A,X,L)
     IMPLICIT DOUBLE PRECISION(A-H,O-Z)
     DIMENSION A(0:3),X(3),U(3)
     PARAMETER(PI=3.1415926535897932D+0,THIRD=1.D+0/3.D+0)
     INTRINSIC MIN,MAX,ACOS
C
C    define cubic root as statement function
     CBRT(Z)=SIGN(ABS(Z)**THIRD,Z)
C
C    ==== determine the degree of the polynomial ====
C
     IF (A(3).NE.0.D+0) THEN
C
C      cubic problem
       W=A(2)/A(3)*THIRD
       P=(A(1)/A(3)*THIRD-W**2)**3
       Q=-.5D+0*(2.D+0*W**3-(A(1)*W-A(0))/A(3))
       DIS=Q**2+P
       IF (DIS.LT.0.D+0) THEN
C        three real solutions!
C        Confine the argument of ACOS to the interval (-1;1)!
         PHI=ACOS(MIN(1.D+0,MAX(-1.D+0,Q/SQRT(-P))))
         P=2.D+0*(-P)**(5.D-1*THIRD)
         DO 100 I=1,3
 100       U(I)=P*COS((PHI+DBLE(2*I)*PI)*THIRD)-W
         X(1)=MIN(U(1),U(2),U(3))
```

```
        X(2)=MAX(MIN(U(1),U(2)),MIN(U(1),U(3)),MIN(U(2),U(3)))
        X(3)=MAX(U(1),U(2),U(3))
        L=3
      ELSE
C       only one real solution!
        DIS=SQRT(DIS)
        X(1)=CBRT(Q+DIS)+CBRT(Q-DIS)-W
        L=1
      END IF
C
    ELSE IF (A(2).NE.0.D+0) THEN
C
C     quadratic problem
      P=5.D-1*A(1)/A(2)
      DIS=P**2-A(0)/A(2)
      IF (DIS.GE.0.D+0) THEN
C       two real solutions!
        X(1)=-P-SQRT(DIS)
        X(2)=-P+SQRT(DIS)
        L=2
      ELSE
C       no real solution!
        L=0
      END IF
C
    ELSE IF (A(1).NE.0.D+0) THEN
C
C     linear equation
      X(1)=-A(0)/A(1)
      L=1
C
    ELSE
C     no equation
      L=0
    END IF
C
C    ==== perform one step of a newton iteration in order to minimize
C         round-off errors ====
    DO 110 I=1,L
      X(I)=X(I)-(A(0)+X(I)*(A(1)+X(I)*(A(2)+X(I)*A(3))))
     1  /(A(1)+X(I)*(2.D+0*A(2)+X(I)*3.D+0*A(3)))
  110 CONTINUE
    RETURN
    END

      Function Donnan(CL,COH,CAP)
      Double Precision CL,CAP,COH
```

```
Donnan=CL*CAP/(COH+CL)
End
```

Appendix D

Inputs and responses according to experimental plan for modeling of the REED process

Exp No	Exp Name	Run Order	Incl/Excl	Current rev	Current den	Feed concn	Feed pH	Base pH	Base Concentration	Current efficien	Energy consump	Membrane area	Watersplitti
1	N1	13	Incl	60	250	50	4	12,89	22,5	23,47	2,52	5537	
2	N2	2	Incl	330	250	50	4	12,89	22,5	53,54	1,54	2428	
3	N3	10	Incl	600	250	50	4	12,89	22,5	62,04	1,46	2095	
4	N4	50	Incl	60	625	50	4	12,89	22,5	15,03	9,83	3458	
5	N5	1	Incl	330	625	50	4	12,89	22,5	42,52	4,85	1223	
6	N6	28	Incl	600	625	50,00	4	12,89	22,5	46,98	4,83	1107,00	
7	N7	59	Incl	60	1000	50,00	4	12,89	22,5	17,43	13,56	1864,00	x
8	N8	83	Incl	330	1000	50,00	4	12,89	22,5	37,71	8,76	862,00	x
9	N9	30	Incl	600	1000	50,00	4	12,89	22,5	40,20	9,03	808,00	x
10	N10	46	Incl	60	250	125,00	4	12,64	56,25	24,85	2,1	5231,00	
11	N11	19	Incl	330	250	125,00	4	12,64	56,25	68,04	1,11	1911,00	
12	N12	63	Incl	600	250	125,00	4	12,64	56,25	76,03	1,1	1710,00	
13	N13	33	Incl	60	625	125,00	4	12,64	56,25	26,65	4,89	1951,00	
14	N14	41	Incl	330	625	125,00	4	12,64	56,25	57,23	3,3	909,00	
15	N15	72	Incl	600	625	125,00	4	12,64	56,25	61,40	3,41	847,00	
16	N16	52	Incl	60	1000	125,00	4	12,64	56,25	22,34	9,34	1454,00	x
17	N17	27	Incl	330	1000	125,00	4	12,64	56,25	36,27	8,34	896,00	x
18	N18	42	Incl	600	1000	125,00	4	12,64	56,25	37,69	8,9	862,00	x
19	N19	49	Incl	60	250	200,00	4	12,00	90	16,84	3,09	7717,00	
20	N20	18	Incl	330	250	200,00	4	12,00	90	44,09	1,71	2948,00	
21	N21	9	Incl	600	250	200,00	4	12,00	90	47,35	1,77	2745,00	
22	N22	48	Incl	60	625	200,00	4	12,00	90	26,53	24,91	1960,00	
23	N23	65	Incl	330	625	200,00	4	12,00	90	35,70	5,29	1456,00	
24	N24	67	Incl	600	625	200,00	4	12,00	90	36,62	5,72	1420,00	
25	N25	66	Incl	60	1000	200,00	4	12,00	90	19,25	10,82	1688,00	
26	N26	8	Incl	330	1000	200,00	4	12,00	90	24,95	12,11	1303,00	
27	N27	7	Incl	600	1000	200,00	4	12,00	90	25,52	13,13	1273,00	
28	N28	77	Incl	60	250	50,00	8	12,89	22,5	23,47	2,52	5539,00	
29	N29	6	Incl	330	250	50,00	8	12,89	22,5	53,54	1,54	2428,00	
30	N30	5	Incl	600	250	50	8	12,89	22,5	62,04	1,46	2095	
31	N31	78	Incl	60	625	50	8	12,89	22,5	15,03	9,82	3458	
32	N32	82	Incl	330	625	50	8	12,89	22,5	42,52	4,85	1223	
33	N33	55	Incl	600	625	50	8	12,89	22,5	46,98	4,83	1107	
34	N34	36	Incl	60	1000	50	8	12,89	22,5	17,43	13,56	1864	x
35	N35	57	Incl	330	1000	50	8	12,89	22,5	37,71	8,76	862,00	x
36	N36	40	Incl	600	1000	50	8	12,89	22,5	40,20	9,03	808,00	x
37	N37	26	Incl	60	250	125	8	12,64	56,25	24,85	2,1	5232	
38	N38	4	Incl	330	250	125	8	12,64	56,25	68,03	1,11	1911	
39	N39	44	Incl	600	250	125	8	12,64	56,25	76,03	1,1	1710	
40	N40	17	Incl	60	625	125	8	12,64	56,25	26,65	4,89	1951	
41	N41	62	Incl	330	625	125	8	12,64	56,25	57,22	3,3	909	
42	N42	69	Incl	600	625	125	8	12,64	56,25	61,4	3,41	847	
43	N43	15	Incl	60	1000	125	8	12,64	56,25	22,34	9,34	1454,00	x
44	N44	14	Incl	330	1000	125	8	12,64	56,25	36,27	8,34	896,00	x
45	N45	25	Incl	600	1000	125	8	12,64	56,25	37,69	8,9	862,00	x
46	N46	56	Incl	60	250	200	8	12,00	90	16,84	3,09	7719	
47	N47	64	Incl	330	250	200	8	12,00	90	44,09	1,71	2948	
48	N48	20	Incl	600	250	200	8	12,00	90	48,35	1,77	2745	
49	N49	21	Incl	60	625	200	8	12,00	90	26,53	4,91	1960	
50	N50	60	Incl	330	625	200	8	12,00	90	35,7	5,29	1456	
51	N51	76	Incl	600	625	200	8	12,00	90	36,62	5,72	1420	
52	N52	34	Incl	60	1000	200	8	12,00	90	19,25	10,82	1688,00	
53	N53	22	Incl	330	1000	200	8	12,00	90	24,95	12,11	1303,00	
54	N54	29	Incl	600	1000	200	8	12,00	90	25,52	13,13	1273,00	
55	N55	79	Incl	60	250	50	12	12,89	22,5	6,41	8,49	20295	
56	N56	16	Incl	330	250	50	12	12,89	22,5	7,53	10,33	17254	
57	N57	51	Incl	600	250	50	12	12,89	22,5	8,5	10,12	15291	
58	N58	35	Incl	60	625	50	12	12,89	22,5	9,19	14,8	5661	x
59	N59	37	Incl	330	625	50	12	12,89	22,5	28,52	6,82	1823	x
60	N60	45	Incl	600	625	50	12	12,89	22,5	32,27	6,67	1611	x
61	N61	84	Incl	60	1000	50	12	12,89	22,5	7,99	27,22	4066	x
62	N62	39	Incl	330	1000	50	12	12,89	22,5	23,29	13,37	1395	x
63	N63	47	Incl	600	1000	50	12	12,89	22,5	25,26	13,63	1286	x
64	N64	61	Incl	60	250	125	12	12,64	56,25	10,46	4,89	12423	
65	N65	68	Incl	330	250	125	12	12,64	56,25	25,65	2,91	5067	
66	N66	81	Incl	600	250	125	12	12,64	56,25	30,67	2,7	4238	
67	N67	58	Incl	60	625	125	12	12,64	56,25	21,7	5,9	2397	
68	N68	23	Incl	330	625	125	12	12,64	56,25	49,97	3,73	1041	
69	N69	38	Incl	600	625	125	12	12,64	56,25	53,9	3,84	965	
70	N70	24	Incl	60	1000	125	12	12,64	56,25	16,91	12,11	1922	x
71	N71	71	Incl	330	1000	125	12	12,64	56,25	29	10,29	1121	x
72	N72	70	Incl	600	1000	125	12	12,64	56,25	30,24	10,96	1075	x
73	N73	32	Incl	60	250	200	12	12,00	90	0,8	64,75	162864	

Appendix E

Patent application for the *Reverse Electro-Enhanced Dialysis*.

A METHOD AND APPARATUS FOR ISOLATION OF IONIC SPECIES FROM A LIQUID
Patent Number: WO0248044
Publication date: 2002-06-20
Inventor(s): GARDE ARVID (DK); JONSSON GUNNAR (DK); RYPE JENS-ULRIK (DK)
Applicant(s): GARDE ARVID (DK); JONSSON GUNNAR (DK); RYPE JENS-ULRIK (DK); JURAG SEPARATION APS (DK)
Requested Patent: WO0248044
Application Number: WO2001DK00810 20011206
Priority Number(s): DK20000001862 20001212
IPC Classification: C02F1/00
EC Classification:
Equivalents:
Cited Documents:

Abstract

The present invention relates to a method for isolation of ionic species from a liquid and an apparatus for isolation of ionic species from a liquid. Moreover the invention relates to an electro enhanced dialysis cell and the use of the cell in the method and the apparatus.

A method and apparatus for isolation of ionic species from a liquid

The present invention relates to a method for isolation of ionic species from a liquid and an apparatus for isolation of ionic species from a liquid. Moreover the invention relates to an electro enhanced dialysis cell and the use of the cell in the method and the apparatus.

Isolation of ionic species from liquids is a very important industrial process used within such a broad technical field, as from refining metals to purification of lactic acid from a fermented liquid.

A large number of processes and apparatuses have been investigated and introduced in order to improve the processes of isolation of ionic species from liquids.

Among those processes and apparatuses are filtration with ultra- and nano-filters, exchanging ions with ion-exchangers and electrodialysis with electrodialysis cells.

Japanese patent application no. 63335032 discloses a desalting apparatus. The apparatus consists of a donnan dialysis apparatus to desalt a solution and an electric dialysis apparatus for reproducing and re-using an acidic or alkaline solution in the desalting process. The apparatus is not suitable for desalting liquid-containing particles.

US patent no. 5746920 discloses a process for purifying dairy wastewater. The process comprises first treating the wastewater with base. The treated wastewater is then introduced into a fermenting tank, where the lactose present in the wastewater is fermented to form a broth and lactic acid. The broth is subjected to purification by ion-exchanging and nano-filtration and the purified broth is subjected to bipolar electrodialysis to yield concentrated acid and base solutions from the purified broth. The process according to the US patent is complex and costly to carry out and there is a substantial loss of product during the filtration. Furthermore the process is designed to isolate specific ionic species.

Japanese patent application JP7232038 discloses a method of recovering high concentration alkali from liquid containing alkali utilizing a combination of diffusion dialysis using cation-exchange membranes and bipolar electrodialysis. No counter-measures are taken to prevent fouling of ion exchange membranes in the diffusion cell from liquids containing proteinuous material, e.g. fermentation broth. Due to the very low driving force across the cation exchange membrane in the diffusion dialysis cell only a very limited flux can be obtained.

Japanese patent application JP63291608 discloses a system for regenerating acidic waste liquid utilizing a combination of diffusion dialysis using anion exchange membranes and bipolar electrodialysis. The flux in the diffusion cell is low. Moreover impurities such as calcium and magnesium ions would prevent the

use of bipolar electrodialysis due to the fact that bipolar membranes are damaged or destroyed by presence of even very small amounts of calcium or magnesium ions.

German patent no. DE 19700044 Cl discloses a method for production of acid and alkaline products by monopolar electrodialysis followed by bipolar electrodialysis. The monopolar electrodialysis cannot selectively remove either cations or anions from a liquid, thus lactic acid cannot be removed without removing e.g. calcium, which would cause problems in the bipolar electrodialysis. The conventional monopolar electrodialysis is susceptible to fouling by biological material, proteins, etc.

Due to the drawbacks of the prior art technology there is a need for a method and an apparatus for isolation of ionic species, which is able to isolate ionic species from different kinds of liquids and furthermore is costeffective and results in a high output.

The object of the present invention is to provide an alternative method and an alternative apparatus for isolation of ionic species from a liquid.

Another object of the invention is to provide a method and an apparatus for isolation of ionic species, which method and apparatus are simple and cost-effective and provide a high output.

A further object of the invention is to provide a method and an apparatus for isolation of ionic species which method and apparatus can be used for isolation of ionic species in liquids containing solids and particles. The invention is in particular useful for separating ionic species from liquids containing particles of organic material and multivalent inorganic metal ions.

Moreover it is an object of the invention to provide a method and an apparatus for isolation of ionic species which method and appratus are useful for isolation of ionic species in a liquid containing organic material.

These objects are achieved by the present invention as defined in the claims.

By the term ionic species is meant that the species are in an ionic state. For example when sodiumchloride NaCl is dissolved in water it dissociates into the

ions Na+ (cation) and Cl- (anion). As the ions have a small electric charge, it is possible to move the ions in an electric field.

The invention provides a method and an apparatus for separating ionic species from a liquid. By using the invention it is possible to separate ionic species from liquids, which are highly contaminated, e.g. with particles. The separation can be performed without any need for a filtration step and it is possible to obtain a high output.

The method according to the invention for isolation of ionic species from a first liquid comprises the steps of: treating the first liquid in an electro enhanced dialysis cell to transfer the ionic species from the first liquid into a second liquid, and - optionally treating the second liquid in a bipolar electrodialysis cell to transfer the ionic species from the second liquid into a third liquid, - optionally separating the ionic species from the second or third liquid.

The first liquid may be provided to the electro enhanced dialysis cell from a storage tank. In a dialysis cell the ionic species are transferred into a second liquid, which has a pH value differing form the pH value of the first liquid. The difference in pH causes a difference in concentration of H+ and OH- in the first and the second liquid. The concentration difference between the first and the second liquid will be the driving forces in the electro enhanced dialysis cell. The difference in concentration will cause a flow of either H+ or OH- ions from the second liquid into the first liquid thereby building up an electric potential difference or a diffusion potential which will cause either cat-ions (M+) or an-ions (X-) of the ionic species to be transported from the first liquid into the second liquid through cation exchange membranes or an-ion membranes, respectively.

If the ionic species are cations, the second liquid will be acidic compared to the first liquid, and visa versa, if the ionic species are anions. This process has been enhanced by the electro enhanced dialysis cell according to the invention, in which the driving forces have been enhanced by use of an electric field. The electro enhanced dialysis cell will be described in more details in the following.

After treatment in the electro enhanced dialysis cell the second liquid may be treated in a bipolar electrodialysis cell. In the bipolar electrodialysis cell the ionic species will be concentrated. If the ionic species are cations, the third liquid will be basic compared to the second liquid, and visa versa, if the ionic species are

an-ions. The driving force in the bipolar electrodialysis cell is a difference in electric potential caused by a constant direct current through the cell.

The membranes, acid, bases, and pH can of course be selected depending on the ionic species to be separated.

This selection can be done by the skilled person.

When the ionic species are separated and concentrated into the third liquid, it can of course be separated from the third liquid, e.g. to obtain a dry or a substantially dry product.

The method according to the invention comprises the feature of applying an electric field of direct current through the electro enhanced dialysis cell during the treatment of the first liquid. In this way the electric potential difference or diffusion potential is enhanced and thereby increases the number of ionic species which are transferred into the second liquid from the first liquid.

In order to improve the results from the cell it is preferred to change the direction of the electric field during the treatment of the first liquid. The direction of the electric field is preferably changed by changing the direction of the direct current. By changing the direction of the electric field it is possible to give a "self-cleaning"effect to the membranes used in the electro enhanced dialysis cell and prevent fouling of the membranes during treatment of the first liquid. When an electric field of direct current is applied to the cell electrically loaded particles are driven from the first liquid onto the membrane surfaces of the cell. Here the particles will build up a layer and after a time cause fouling which will make the membranes useless. If the electric field is reversed before the particles have caused fouling, the particles will be driven back from the membranes into the first liquid and the membranes will be cleaned.

In an embodiment according to the invention the electric field can be changed at predetermined substantially regular intervals, said intervals preferably being within the range from 5 seconds to 6000 seconds, more preferably within the range from 8 to 1000 seconds and even more preferably within the range from 10 seconds to 360 seconds. More specificly the intervals are determined by the nature of the first liquid and the amount and nature of particles present herein.

In a preferred embodiment of the method according to the invention for isolation of ionic species stored in a first tank, the method comprises the steps of: - treating the first liquid in an electro enhanced dialysis cell to transfer the ionic species from the first liquid into a second liquid and optionally storing said second liquid in a second tank; - treating the second liquid in a bipolar electrodialysis cell to transfer the ionic species from the second liquid into a third liquid and optionally storing the third liquid in a third tank
By using a first, a second and a third tank for storing the first liquid, the second liquid and the third liquid, respectively, it is possible to obtain better control over the processes and optimise the treatment of the liquids in the electro enhanced dialysis cell and the bipolar electrodialysis cell. During the treatment the tanks serve as storage and/or buffers for the treated liquid or the liquid to be treated.

It is preferred that at least a part of the first liquid is recycled to the first tank after treatment in the electro enhanced dialysis cell. The liquid can be recycled via pipelines e. g. supplied with a pump and optionally a purge by which a part of the treated first liquid can be removed and/or replaced by untreated first liquid.

Moreover it is preferred that at least a part of the second liquid is recycled to the electro enhanced dialysis cell after being treated in the bipolar electrodialysis cell. The liquid can be recycled via pipelines, e.g. provided with a pump and optionally a purge by which a part of the treated second liquid can be removed and/or replaced.

Furthermore it is preferred that at least a part of the third liquid is recycled from the third tank to the bipolar electrodialysis cell. The third liquid may be recycled directly from the bipolar electrodialysis cell or from the third tank. By recycling the third liquid the ionic species will be concentrated in the liquid. It is possible to achieve very high concentrations in the third liquid. The concentration may be a factor 5 to 10 higher than in the know methods for separating ionic species from a liquid. Like in the previously mentioned recycling circuits pipelines, pumps, and a purge may be used.

In one preferred embodiment of the method according to the invention, the method further comprises the step of treating the third liquid in an electrodialysis cell to remove undesired ions, e. g. the presence of inorganic ions may be undesired, when you are separating ion of organic species from a liquid.

In a preferred embodiment of the method according to the invention the method further comprises the step of evaporating and/or crystallising and/or chromatographic treatment of the third liquid to separate the ionic species from the third liquid. By use of this embodiment of the method it is possible to achieve a very pure final product.

In a preferred embodiment of the method, the ionic species comprises anions from inorganic acids, organic acids, enzymes, peptides, hormones, antibiotics or amino acids. Moreover the ionic species comprises cat-ions from inorganic bases, organic bases, enzymes, peptides, hormones, antibiotics or amino acids. Thereby the method is useful for a wide range from of liquids containing ionic species. The method may e. g. be used for separating ionic species from streams from metal etching and food processing, including fermentation broth from fermentation of grass juice using strains of Lactobacillus bacteria, waste stream from lactic acid metal etching and waste streams from citrus oil production.

Preferably the ionic species separated according to the invention has a molar weight up to about 1000 g/mol.
The invention also relates to the use of the method according to the invention for isolating ionic species from a liquid.

Moreover the invention relates to isolated ionic species obtained by the method.

The invention also comprises an apparatus for isolation of ionic species from a first liquid which apparatus comprises - an electro enhanced dialysis cell to transfer the ionic species from the first liquid into a second liguid, - a bipolar electrodialysis cell to transfer the ionic species from the second liquid into a third liquid, - optionally means for separating the ionic species from the third liquid.

The apparatus according to the invention has excellent properties with regard to separating ionic species from a liquid. Very high output can be achieved compared to known apparatuses. The function of the electro enhanced dialysis cell and the bipolar electrodialysis cell is as explained previously in the application.

In a preferred embodiment of the apparatus the electro enhanced dialysis cell comprises means for applying an electric field of direct current. The electric field enhances the electric potential difference in the cell and thereby increases the

number of ionic species that can be transferred from the first liquid to the second liquid.

In a more preferred embodiment of the apparatus according to the invention the electro enhanced dialysis cell comprises means for changing the direction of the electric field. Preferably means for changing the direction of the direct current. The means may be in the form of electric switches, rectifiers, relays and the like. By changing the direction of the direct current a "self-cleaning"effect of the membranes is established.

In order to obtain the best possible"self-cleaning" effect the electric field can be changed at predetermined substantially regular intervals, said intervals preferably being within the range from 5 seconds to 6000 seconds, more preferably within the range from 8 to 1000 seconds and even more preferably within the range from 10 seconds to 360 seconds. The specific interval is dependent on the liquid from which it is wanted to separate the ionic species. The specific interval, which is useful for a specific liquid, can be determined by the skilled person as a matter of routine.

In a preferred embodiment the apparatus according to the invention comprises a first tank for the first liquid.

The first tank is preferably placed before the electro enhanced dialysis cell. Furthermore the apparatus preferably comprises a second tank for the second liquid.

This second tank is preferably placed after the electro enhanced dialysis cell.

Moreover the apparatus preferably comprises a third tank for the third liquid. The third tank is preferably placed after the bipolar electrodialysis cell.

In this specificly preferred embodiment of the invention the first, the second, and the third tank serve as storage and/or buffer for the first liquid, the second liquid, and the third liquid, respectively.

In another preferred embodiment of the apparatus according to the invention the apparatus comprises means for re-circulating at least a part of the first liquid from the electro enhanced dialysis cell to the first tank.

Furthermore the apparatus preferably comprises means for re-circulating at least a part of the second liquid to the electro enhanced dialysis cell after treatment in the bipolar electrodialysis cell.

Moreover the apparatus preferably comprises means for recirculating at least a part of the third liquid from the third tank to the bipolar electrodialysis cell.

The means for re-circulating the liquids are normally pipelines, which may be supplied with pumps and optionally with purges for removing/replacing liquid.

In a preferred embodiment of the apparatus according to the invention the means for applying an electric field of direct current is in the form of electrodes placed at two opposing ends in the electro enhanced dialysis cell. The electrodes may be of any known type and have any desired shape for the purpose.

In a particularly preferred embodiment of the apparatus according to the invention the electro enhanced dialysis cell is constituted by two or more electrodes placed at two opposing ends with cation-exchange membranes (CEM) and/or anion-exchange membranes (AEM) placed there between.

The electro enhanced dialysis cell is normally box-shaped with a parallel bottom and top element, two parallel side elements and two end-elements. The membranes are placed in the cell with the membrane surface parallel to the end elements of the cell.

In a more preferred embodiment of the apparatus the electro enhanced dialysis cell is constituted by two electrodes placed at two opposing ends and with two endmembranes being placed next to each of the two electrodes, the end-membranes facing each other and having cation-exchange membranes (CEM) and/or anion-exchange membranes (AEM) placed in between. The endmembranes and cation-exchange membranes (CEM) and/or anion-exchange membranes (AEM) form adjacent chambers throughout the electro enhanced dialysis cell.

Preferably the end-membranes are neutral membranes and/or cation-exchange membranes and/or anion-exchange membranes. The purpose of the end-

membranes is substantially to prevent contact between the electrodes and contaminated liquid e.g. a first liquid.

When the apparatus is used for separating cat-ionic species from a liquid it is preferred to use cat-ion exchange membranes in the electro enhanced dialysis cell.
When the apparatus is used for separating an-ionic species from a liquid it is preferred to use an-ion exchange membranes in the electro enhanced dialysis cell.

The membranes form adjacent chambers throughout the cell in a direction parallel with surfaces of the sideelements of the cell. The surfaces of the membranes are perpendicular to this direction. The adjacent chambers are preferably adapted alternately to receive the first and the second liquid. The liquids are introduced in the cell in the known way by use of tubes, pipelines, valves, etc.

In one of the most simple embodiments of the apparatus according to the invention the electro enhanced dialysis cell is constituted of at least two an-ion exchange membranes or at least two cat-ion exchange membranes which, with the end-membranes, form a central chamber for the first liquid and a chamber on each side of the central chamber for the second liquid.

In a preferred embodiment of the apparatus according to the invention an even number of an-ion exchange membranes or an even number of cat-ion exchange membranes form an uneven number of chambers between and with the two endmembranes, said chambers being adapted alternately to receive the first and the second liquid in such a way that the two chambers constituted by an end-membrane and an an-ion exchange membrane or a cat-ion exchange membrane are adapted for receiving the second liquid. By organizing the membranes in such a way, it is possible to optimise the output of the cell. The number of membranes in the cell may be several hundreds, all placed parallel to each other and optionally with spacer gaskets in between, and which constitutes the adjacent chambers.

When the apparatus according to the invention is prepared for separating cat-ionic species, preferably the electro enhanced dialysis cell for separating cat-

ionic species has cat-ion exchange membranes placed between the endmembranes
When the apparatus according to the invention is prepared for separating an-ionic species, preferably the electro enhanced dialysis cell for separating an-ionic species has an-ion exchange membranes placed between the endmembranes
In a preferred embodiment the apparatus further comprises an electrodialysis cell adapted to remove undesired ions from the third liquid, preferably the electrodialysis cell is placed after the bipolar electrodialysis cell.

In another preferred embodiment of the apparatus according to the invention the apparatus further comprises means for evaporating and/or crystallising and/or chromatographic treatment of the third liquid.

Thereby, it is possible to obtain a dry and/or pure final product by use of the apparatus.

The invention also relates to use of an apparatus according to the invention in the method according to the invention.

Furthermore the invention relates to use of the apparatus according to the invention for isolating ionic species from a liquid.

The invention also comprises an electro enhanced dialysis cell wherein the dialysis cell is enhanced with an electric field.

Preferably the electro enhanced dialysis cell is enhanced with an electric field of direct current.

In a preferred embodiment of the electro enhanced dialysis cell according to the invention the electro enhanced dialysis cell comprises means for changing the direction of the electric field, and preferably means for changing the direction of the direct current. The means for changing direction of the electric field may be electric switches, rectifiers, relays, and the like. By changing the direction of the electric field a "selfcleaning" effect of the cell can be achieved as explained previously.

Preferably the electric field can be changed at predetermined substantially regular intervals, preferably said intervals are within the range from 5 seconds to

6000 seconds, more preferably within the range from 8 to 1000 seconds and even more preferably within the range from 10 seconds to 360 seconds. Hereby it is possible to adjust the cell to have the optimal"self-cleaning" effect.

In a preferred embodiment the electro enhanced dialysis cell the electric field is applied by electrodes, which are placed at two opposing ends, in the electro enhanced dialysis cell.

Preferably the electro enhanced dialysis cell is constituted by electrodes placed at two opposing ends with cation-exchange membranes (CEM) and/or anion-exchange membranes (AEM) placed there between. When the cell is used for separation of cat-ionic species, it is preferred to use cat-ion exchange membranes. When the cell is used for separation of an-ionic species, it is preferred to use an-ion exchange membranes.

In a preferred embodiment of the electro enhanced dialysis cell the electro enhanced dialysis cell is constituted by electrodes placed at two opposing ends with two end-membranes being placed next to each of the two electrodes, said end-membranes facing each other and having cation-exchange membranes (CEM) and/or anion-exchange membranes (AEM) placed in between.

It is preferred that the end-membranes are neutral membranes and/or cat-ion exchange membranes and/or an-ion exchange membranes. The purpose of the end-membranes is to prevent contact between the electrodes and contaminated liquid.

Moreover it is preferred that in the electro enhanced dialysis cell according to the invention the end-membranes and cation-exchange membranes (CEM) and/or anion exchange membranes are forming adjacent chambers, and the adjacent chambers are adapted to receive a first and a second liquid, preferably alternately.

When the electro enhanced dialysis cell is prepared for separating cat-ionic species, it is preferred that the electro enhanced dialysis cell has a first and a second electrode where the first electrode is placed at a first end-element in the electro enhanced dialysis cell and the second electrode is placed at a second end-element of the electro enhanced dialysis cell. The first and second endelement is opposite to each other. The electro enhanced dialysis cell further

has a first and a second an-ion exchange membrane where the first an-ion exchange membrane is placed next to the first electrode and the second an-ion exchange membrane is placed next to the second electrode. The first and the second an-ion exchange membrane are facing each other and at least two cat-ion exchange membranes are placed between the first and the second anion-exchange membrane with a distance from the anion-exchange membranes and each other to provide adjacent chambers between adjacent membranes.

When the cell is used for separating anionic species the placing of the cat-ion exchange membrane and the an-ion exchange membrane is reversed.

The invention relates to use of the electro enhanced dialysis cell according to the invention in the method according to the invention.

Moreover the invention relates to use of the electro enhanced dialysis cell according to the invention in the apparatus according to the invention.

The invention will now be described in further details with examples and reference to a drawing where:

Fig. 1 shows an electro enhanced dialysis cell according to the invention, adapted to separate an-ionic species.

Fig. 2 shows a bipolar electrodialysis cell according to the invention adapted to separate an-ionic species.

Fig. 3 shows a diagram of the apparatus and method according to the invention.

Fig. 4 shows a configuration of an electro enhanced dialysis cell according to the invention.

Fig. 5 shows the concentration of lactic acid in a feed stream and alkaline solution.

Fig. 6 shows the potential drop across an electro enhanced dialysis cell pair.

Fig. 7 shows the potential drop across an electro enhanced dialysis cell pair.

Fig. 8 shows a configuration of a bipolar electrodialysis cell according to the invention.

Fig. 9 shows the transport of lactate from a feed stream to a combined acid and base stream.

Fig. 10 shows the pH and conductivity as well as current efficiency and energy consumption in a feed stream.

Fig. 11 shows the concentration profiles of citric and malic acid.

Fig. 12 shows the conductivity, pH and cell resistance in a cell.

Fig. 13 shows the concentration of glycine.

Fig. 14 shows the current through the stack.

Fig. 15 shows the concentration of lysine.

Example 1

Figure 1 shows a schematic drawing of an electro enhanced dialysis cell according to the invention. The cell has two electrodes E1 and E2, placed in electrode chambers EC1 and EC2, which are placed at opposite ends in the cell. The electrode chambers are separated from the central part of the cell by two end-membranes, which in this case are two cation-exchange membranes CEM. The two end-membranes have four anion-exchange membranes AEM placed in between. Thereby the two end-membranes and the four anion-exchange membranes form five adjacent chambers Cl, C2, C3, C4 and C5.

With this configuration the cell is adapted for separating anions X- from a liquid L1. Liquid L1 is led to the chambers C2 and C4 of the cell. The second liquid L2, which is a base when anions are separated, is led to the chambers Cl, C3 and C5 of the cell. The difference in electrical potential between the two liquids is enhanced by a direct current applied by the electrodes E1 and E2.

When the situation is as illustrated in figure 1, where E1 is the positive electrode, the anions X-move in the direction of E1 and pass through the anion-exchange

membranes from the liquid L1 in chambers C2 and C3 to liquid L2 in chambers Cl and C3 as indicated by arrows.

The anions X- from L1 are replaced by hydroxide ions OH from L2.

When the direction of the direct current is reversed, the anions X- move in the direction of E2 from the liquid L1 in chambers C2 and C4 through the anion-exchange membranes into the liquid L2 in chambers C3 and C5.

Furthermore, if the anion-exchange membranes have been covered with particles, the anion-exchange membranes will be cleaned as the particles are caused to move away from the membrane and as hydroxide ions penetrate the membrane and dissolve the fouling layer.

As it is evident from figure 1, when the second liquid L2 is running in chambers on both sides of the chambers, where the first liquid LI is running, the second liquid L2 will always receive anions X- from the first liquid L1 independently of the direction of the electric field.

Figure 2 shows a schematic drawing of the bipolar electrodialysis cell according to the invention which is used for further treatment of the second liquid L2 from the electro enhanced dialysis cell. The bipolar electrodialysis cell has an electrode in each end: a positive electrode E+ in the first end and a negative electrode E- in the second end of the cell. Between the electrodes from E+ to E- are placed repeatingly first a bipolar membrane BM, an anion-exchange membrane AEM and a cation-exchange membrane CEM. The stack of membranes forms adjacent chambers C11, C12, C13, C14, C15 and C16 and is finished with a bipolar membrane before the electrode E-.
In the case where the bipolar electrodialysis cell is used for separating anions the second liquid L2, which is basic compared to the third liquid L3, is first sent through the chambers C12 and C15 between an anion-exchange membrane AEM and a cation-exchange membrane CEM. According to the invention the second liquid L2 is further sent through the chambers C13 and C16 between a cation-exchange membrane and a bipolar membrane.

Hereafter the second liquid is recycled to the electro enhanced dialysis cell.

The third liquid L3, which is acidic compared to the second liquid L2, is sent through chambers C11 and C14 between a bipolar membrane and anion-exchange membrane.

Due to the constant electric direct current through the cell, the ions (X-, M+, OH- and H+) are drawn in directions transversely to the membrane stack as indicated with arrows. The anions X- are together with hydrogen ions H+ concentrated in the third liquid L3 in chambers Cll and C14.

It is clear that in case the bipolar electrodialysis cell is used for separating cations from the second liquid L2, the second liquid will be sent through the chambers C12 and C15 between an anion-exchange membrane and a cation-exchange membrane and further through chambers C11 and C14 between an anion-exchange membrane and a bipolar membrane.

Figure 3a shows a flow sheet of the method according to the invention. The first tank T1 contains the first liquid L1, which is fed to the electro enhanced dialysis cell EEC and treated herein. Hereafter the first liquid is recycled to the tank T1. In the electro enhanced dialysis cell EEC the ionic species are transferred from the first liquid L1 into the second liquid L2. After treatment in the electro enhanced dialysis cell EEC, the second liquid L2 is first stored in a tank T2, before it is treated in the bipolar electrodialysis cell EDBM.

After the treatment in the bipolar electrodialysis cell EDBM, the second liquid L2 is recycled to the electro enhanced dialysis cell EEC. The third liquid L3 is treated in the bipolar electrodialysis cell EDBM where the third liquid L3 receives the ionic species from the second liquid L2. After treatment in the bipolar electrodialysis cell EDBM the third liquid L3 is stored in a tank T3 and recycled trough the bipolar electrodialysis cell until a satisfactory concentration of the ionic species is obtained in the third liquid L3.

In the process it is preferred that e.g. three tanks are used parallel for storing the third liquid L3 from the bipolar electrodialysis cell EDBM. During the process one tank T3 is open for receiving the third liquid L3 and recycle it to the bipolar electrodialysis cell EDBM. The third liquid L3 in the two other tanks is optionally submitted to the processes shown in figures 3b and 3c.

Figure 3b is a flow sheet showing the process of treating the third liquid L3 in an electrodialysis cell ED to remove undesired ions which are transferred to a fifth liquid L5 and stored in a fifth tank T5.

Figure 3c is a flow sheet showing the process of evaporating the third liquid L3 in an evaporater EV to obtain a concentrated liquid, which is stored in the tank T6.

Example 2. Description of experimental extraction through an Electro enhanced Dialysis cell according to the invention

In the electro enhanced dialysis cell, the cell stack was configured with four anion-exchange membranes 1 (Neosepta AMX, Tokuyama Corp., Japan) and two cation-exchange membranes 2 (Neosepta CMH, Tokuyama Corp., Japan) as shown in figure 4. The effective membrane area was 40 cm2.

In the two end-chambers 3 between the platinum electrodes 6 and 7 (each 31.5 cm2) and each cation-exchange membrane, a flow of electrode-rinsing solution was maintained in the end-chambers. The solution was an aqueous solution of 0.1M K2SO4.

Through the chambers 4, 250 ml of an aqueous alkaline solution of 0.5M KOH (pH 12.5) was pumped from a storage container, to which the solution was returned after each passage. The volume flow was 10 g/s. The thickness of the chambers 4 between the membranes was 6 mm. Net spacers were introduced to promote turbulent flow.

Through the chambers 5, 250 ml of the feed solution, which was fermented brown juice from grass pellet production with around 16 g/1 lactic acid, was passed from a storage container. The treated feed solution was returned to the container after each pass. The fermented solution had initially been adjusted to a pH-value of 5.5 by adding KOH pellets. Nothing else had been done to the broth. The volume flow was 10 g/s. The thickness of the chambers 5 was 12 mm. No spacers were introduced in these chambers.

Each chamber 4 and 5 had a 10 cm long flow-path that was 4 cm wide.

The temperature of the electrode-rinse, the alkaline and the fermented solutions was held constant at 40 degrees Celsius during the experiment.

During the experiment, the pH was continuously measured in the fermented solution and held constant at pH 5.5 by titration of more fermented solution (pH 2) with a high lactic acid concentration (70 g/1).

In the middle of each of the chambers 5, a silver/silver chloride electrode was placed, so the voltage drop across a cell pair could be continuously measured by data collection (Fluke 123-Industrial Scopemeter, Fluke Corporation, USA).

When the experiment was started, the electrode-rinse, the fermented broth and the alkaline solution was pumped through the cell. Direct current across the cell was added by a power supply (EA-PS 3032-10 (0..32V/0..10A), EA-Elektro-Automatik, Germany) that regulates the power to uphold a constant current of 1.0 A. An IBM personal computer controlled a relay, shifting the direction of the electrical current every 10 seconds.

Samples from the fermentation broth and the alkaline solution were taken every 30 minutes. pH and conductivity were noted, and lactic content was measured by HPLC using an AMINEX HPX-87H column (Biorad, USA) at 35 degrees Celsius using 4 mM sulfuric acid as eluent.

After 4 hours, the alkaline solution was replaced by a fresh solution, and the experiment was continued.

Figure 5 shows the concentration profile of lactic acid in the feed and alkaline solutions during an eight-hour experiment. In the fermented brown juice, the initial lactic acid concentration of 16 g/1 goes up during the experiment, because pH is regulated by titration of fermentation solution having higher lactic acid content.

The alkaline solution was replaced after four hours to simulate the regeneration process in the EDBM process.

The lactate flux was found to be 1.2-10-4 mol/mrs during the first four hours, and 1.7-10"* mol/nrs during the next four hours. Some of this increase might originate from the rising lactate concentration in the feed.

Figures 6 and 7 show the potential drop across a cell pair at the beginning and at the end of the first fourhour run, respectively. The 10 second intervals were

evident as the direction of current changes between positive and negative potential drops. At the beginning of each interval, both figures show an almost constant initial drop that in figure 3 increases slightly and in figure 4 increases significantly during the 10 seconds.

These increments relate to the increase of electrical resistance partly from ionic polarization, but also from a build-up of organic matter on the membrane surface in the feed chamber.

Especially figure 8 shows that the organic fouling can be removed by changing the direction of the electric current. The reversal does not remove the organic matter completely, as an increase in initial cell-resistance from about 1.5 Ohm to 2 Ohm was evident during the experiment.

The divergence between the form of the positive and negative potential drop in figure 8 must derive from different flow conditions in the two feed chambers in the laboratory equipment.

Example 3

The electro enhanced dialysis cell was configured as in example 1 but the AMX anion-exchange membrane was replaced with a monoselective anion-exchange membrane (Neosepta ACS, Tokuyama Corp., Japan).

500 ml brown juice was circulated in the feed chambers and the pH was held constant at 5.5 by titration of lactic acid. In the base chambers 500 ml of 0.5 M KOH was passed and 500 ml 0.1 M K2SO4 was used as electrode rinsing solution.

Samples were taken at 0, 60, and 120 min. from the feed and base streams and the contents of calcium and magnesium were determined by Atom Absorption Spectroscopy (AAS).

Time (min)	[Ca2+]Feed (mg/l)	[Ca2+]Base (mg/l)	[Mg2+]Feed (mg/l)	[Mg2+]Base (mg/l)
0	667	0.15	394	0.01
60	737	0.09	425	0.01
120	705	0.13	403	0.02

From these results, it is evident that divalent cations are retained sufficiently to be non-damaging in the following EDBM process, which usually requires such concentrations to be lower than 2 ppm.

Using a mono-selective anion-exchange membrane in this experiment does not affect retention of cations significantly, but does improve retention of divalent anions such as sulfate and phosphate.

Example 4
In the experiments with the bipolar electrodialysis cell, the cell was equipped with three bipolar membranes 8 in figure 8 (Neosepta BP-1, Tokuyama Corp., Japan), two anion-exchange membranes 1 (Neosepta AMX, Tokuyama Corp., Japan) and two cation-exchange membranes 2 (Neosepta CMH, Tokuyama Corp., Japan) as shown on figure 8.

In the two end-chambers 3 between the platinum electrodes 6 and 7 (each 31.5 cm2) and a set of bipolar membranes, a flow of electrode-rinsing solution was established. The electrode-rinsing solution was an aqueous solution of 0.1M K2SO4. Through the feed chambers 9 between the anion-exchange membrane and the cation exchange membrane 500 ml of a mixture of 0.5 M KOH and 0.4 M lactic acid was circulated to a container. 1000 ml of an alkaline 0.1M KOH solution was circulated in both the acid chamber 10 between the bipolar membrane and the anion-exchange membrane and in the base chamber 11 between the bipolar membrane and the cation-exchange membrane. The streams from the acid and base chambers 10 and 11 were mixed in a container after each pass. The thickness of the chambers 9, 10, and 11 between the membranes was 6 mm. Net spacers were introduced to promote turbulent flow.

The temperature of the electrode-rinse, the feed and the base solutions was held constant at 40 degrees Celsius during the experiment.

In the feed chambers 9, silver/silver chloride electrodes were placed so the voltage drop across a cell pair could be continuously measured and data collected (Fluke 123 Industrial Scopemeter, Fluke Corporation, USA). Samples from the feed and the alkaline solution were taken every 30 minutes. pH and conductivity were noted, and lactic content was measured by HPLC using an AMINEX HPX-87H column (Biorad, USA) at 35 degrees Celsius using 4 mM sulfuric acid as eluent.

Figure 9 shows the transport of lactate from the feed stream to the combined acid and base stream, reaching a lactate concentration of 0.8 g/1 in the feed stream after 180 min., corresponding to more than 97% acid recovery.

Figure 10 shows the pH and conductivity in the feed solution during the experiment as well as the current efficiency, and corresponding effect on energy consumption. It is clear that the significant decrease in conductivity near the end of the experiment was causing a rise in cell resistance and thus energy consumption.

The current efficiency was above 80% during most of the experiment, except for the beginning and final part. The low efficiency in the final phase probably originates from polarization, leading to ineffective water-splitting at the mono-polar membranes.

Example 5
Another experiment with a bipolar electrodialysis cell was carried out exactly as example 4, except the 500 ml feed mixture was composed of 0.5M KOH, 0.1M (0.3N) citric acid, and 0.05M (0.1N) malic acid.

The acid content of the samples was measured by HPLC as before.

Figure 11 shows the concentration profiles of the citric and malic acid in the feed solution and the mixed acid/base solution.

From figure 11 it is evident that most of the citric and malic acid is extracted from the feed solution. The recovery of both citric and malic acid was higher than 97%.

However, the recovery of the last 5-10% of the organic acids is very costly, as can be seen in figure 12. As pH and conductivity in the feed decrease, cell resistance and thus energy consumption increase drastically.

Example 6
The electro enhanced dialysis cell stack was configured as in example 1, but with 4 cation-exchange membranes (Neosepta CMB, Tokuyama Corp., Japan) replacing the anion-exchange membranes and (Neosepta AMX, Tokuyama Corp., Japan) membranes replacing the cation-exchange membranes.

250 ml aqueous solution of 0.2M glycine, which is an amino acid with pKr~oH = 2.34, pH3+= 9.60 and pI = 5.97, was circulated in the feed chambers. In the dialysate chambers 1750 ml of 0.1M H2SO4 was circulated and 500 ml 0.1M Na2SO4 was used as electrode rinsing solution. The concentration of glycine was determined using HPLC. The liquids were circulated for 5 min. before the experiment was started. Current reversal was omitted, as the feed stream did not contain material that could cause fouling of the membranes.

Figure 13 shows the concentration of glycine in the feed and dialysate during the experiment. At the beginning of the experiment glycine is transported from the feed stream to the dialysate stream at a relatively low rate because the starting pH is close to the isoelectric point of the amino acid. The voltage drop across a cell pair was not allowed to exceed 14 V, which resulted in a current starting very low and slowly increasing as pH went down and conductivity increased in the feed, see figure 14. Within 180 min. 84% of the glycine is removed from the feed at a current efficiency of 580.

Example 7
The electro enhanced dialysis cell stack was configured as in example 5.

250 ml aqueous solution consisting of 50 g/1 bakers yeast and 0.2M lysine, which at the experimental conditions was a positively charged amino acid, was circulated in the feed chambers. In the dialysate chambers 1750 ml of 0.1M H2SO4 was circulated and 500 ml 0.1M Na2S04 was used as electrode rinsing solution. The liquids were circulated for 5 min. before the experiment was started.

Direct current across the cell was added by a power supply (EA-PS 9072-040 (0.. 72V/0.. 40A), EA-Elektro Automatik, Germany) regulating the power to keep a constant current of 1.0 A. The concentration of lysine is determined using HPLC.

Without current reversal the experiment had to be terminated as the voltage drop across a single cell pair increased from 10V to 30 V during the first 8 minutes in order to keep a current of 1 A (25 mA/cm2).
When the experiment was repeated with a current reversal time of 300 sec., it was possible to keep the average voltage drop across a cell pair at approx. 15 V. Figure 15 shows the concentration of lysine in the feed and dialysate during the

experiment. During the first 60 min. of the experiment the lysine concentration in the feed decreased 30% at a current efficiency of 24%.

Claims

1. A method for isolation of ionic species from a first liquid comprising the steps of: - treating the first liquid in an electro enhanced dialysis cell to transfer the ionic species from the first liquid into a second liquid, and - optionally treating the second liquid in a bipolar electrodialysis cell to transfer the ionic species from the second liquid into a third liquid, - optionally separating the ionic species from the second or third liquid.

2. A method according to claim 1 wherein the electro enhanced dialysis cell is enhanced by applying an electric field of direct current through said electro enhanced dialysis cell during the treatment of the first liquid, the direction of said electric field preferably being changed during the treatment of the first liquid, preferably by changing the direction of the direct current.

3. A method according to claim 2 wherein the electric field is changed at predetermined substantially regular intervals, said intervals preferably being within the range from 5 seconds to 6000 seconds, more preferably within the range from 8 to 1000 seconds and even more preferably within the range from 10 seconds to 360 seconds.

4. A method according to claims 1-3 for isolation of ionic species stored in a first tank comprising the steps of: - treating the first liquid in an electro enhanced dialysis cell to transfer the ionic species from the first liquid into a second liquid and optionally storing said second liquid in a second tank - treating the second liquid in a bipolar electrodialysis cell to transfer the ionic species from the second liquid into a third liquid and storing said third liquid in a third tank 5. A method according to claim 4 wherein at least a part of the first liquid is recycled to the first tank after treatment in the electro enhanced dialysis cell.

6. A method according to any one of claims 4-5 wherein at least a part of the second liquid is recycled to the electro enhanced dialysis cell after being treated in the bipolar electrodialysis cell.

7. A method according to any one of claims 4-6 wherein at least a part of the third liquid is recycled from the third tank to the bipolar electrodialysis cell.

8. A method according to any of the preceding claims wherein the method further comprises the step of treating the third liquid in an electrodialysis cell to remove undesired ions.

9. A method according to any one of the preceding claims wherein the method further comprises the step of evaporating and/or crystallising and/or chromatographic treatment of the third liquid to separate the ionic species from the third liquid.

10. A method according to any one of claims 1-9 wherein the ionic species comprises anions or an-ions from inorganic acids, organic acids, enzymes, peptides, hormones, antibiotics, or amino acids.

11. A method according to any one claims 1-10 wherein the ionic species has a molar weight up to about 1000 g/mol.

12. Use of the method according to claims 1-11 for isolating ionic species from a liquid.

13. Isolated ionic species obtained by the method according to claims 1-11 14. An apparatus for isolation of ionic species from a first liquid comprising - an electro enhanced dialysis cell to transfer the ionic species from the first liquid into a second liquid, - a bipolar electrodialysis cell to transfer the ionic species from the second liquid into a third liquid, - optionally means for separating the ionic species from the third liquid.

15. An apparatus according to claim 14 wherein said electro enhanced dialysis cell comprises means for applying an electric field of direct current.

16. An apparatus according to claim 15 wherein the electro enhanced dialysis cell comprises means for changing the direction of said electric field, preferably by changing the direction of the direct current.

17. An apparatus according to claim 16 wherein the electric field can be changed at predetermined substantially regular intervals, preferably said intervals are within the range from 5 seconds to 6000 seconds, more preferably within the

range from 8 to 1000 seconds and even more preferably within the range from 10 seconds to 360 seconds.

18. An apparatus according to claims 14-17, which further comprises means for storing and recirculating said liquids, said means preferably being tanks and pumps.

19. An apparatus according to any one of claims 14-18 wherein said means for applying an electric field of direct current are in the form of electrodes placed at two opposing ends in the electro enhanced dialysis cell.

20. An apparatus according to any one of claims 14-19 wherein the electro enhanced dialysis cell is constituted by two or more electrodes placed at two opposing ends with cation-exchange membranes (CEM) and/or anion-exchange membranes (AEM) placed there between.

21. An apparatus according to any one of claims 14-19 wherein the electro enhanced dialysis cell is constituted by two electrodes placed at two opposing ends and with two end-membranes being placed next to each of the two electrodes, said end-membranes facing each other and having cation-exchange membranes (CEM) and/or anion-exchange membranes (AEM) placed in between, and said endmembranes and cation-exchange membranes (CEM) and/or anion-exchange membranes (AEM) forming adjacent chambers throughout the electro enhanced dialysis cell.

22. An apparatus according to claim 20 wherein said end-membranes are neutral membranes and/or cation-exchange membranes and/or anion-exchange membranes.

23. An apparatus according to claims 14-22 wherein the electro enhanced dialysis cell is prepared for separating cat-ionic species, said electro enhanced dialysis cell for separating cationic species having cation-exchange membranes placed between the end-membranes 24. An apparatus according to claims 14-22 wherein the electro enhanced dialysis cell is prepared for separating an-ionic species, said electro enhanced dialysis cell for separating an-ionic species having anion-exchange membranes placed between the end-membranes 25. An apparatus according to any of the preceding claims 14-24 wherein the apparatus further comprises an electrodialysis cell adapted to remove undesired ions from

the third liquid, the electrodialysis cell preferably being placed after the bipolar electrodialysis cell.

26. An apparatus according to any one of claims 14-25 wherein the apparatus further comprises means for evaporating and/or crystallising and/or chromatographic treatment of the third liquid.

27 Use of an apparatus according to any one of claims 1426 in the method according to claims 1-11.

28. Use of the apparatus according to any one of claims 14-26 for isolating ionic species from a liquid.

29. An electro enhanced dialysis cell wherein the dialysis cell is enhanced with an electric field, preferablythe electro enhanced dialysis cell is enhanced with an electric field of direct current.

30. An electro enhanced dialysis cell according to claim 29 comprising means for changing the direction of said electric field, preferably means for changing the direction of the direct current.

31. An electro enhanced dialysis cell according to claim 30 wherein the electric field can be changed at predetermined substantially regular intervals, said intervals preferably being within the range from 5 seconds to 6000 seconds, more preferably within the range from 8 to 1000 seconds and even more preferably within the range from 10 seconds to 360 seconds.

32. An electro enhanced dialysis cell according to any one of claims 29-31 wherein said electric field is applied by electrodes placed at two opposing ends in the electro enhanced dialysis cell.

33. An electro enhanced dialysis cell according to any one of claims 29-32 wherein the electro enhanced dialysis cell is constituted by electrodes placed at two opposing ends with cation-exchange membranes (CEM) and/or anion-exchange membranes (AEM) placed there between.

34. An electro enhanced dialysis cell according to any one of claims 29-33 wherein the electro enhanced dialysis cell is constituted by electrodes placed at

two opposing ends with two end-membranes being placed next to each of the two electrodes, said end-membranes facing each other and having cation-exchange membranes (CEM) and/or anion-exchange membranes placed in between.

35. An electro enhanced dialysis cell according to claim 34 wherein said end-membranes are neutral membranes and/or cation-exchange membranes and/or anion-exchange membranes.

36. An electro enhanced dialysis cell according to any one of claims 33-35 wherein said end-membranes and cation-exchange membranes (CEM) and/or anion-exchange membranes are forming adjacent chambers, said adjacent chambers being adapted to receive a first and a second liquid, preferably alternately.

37. Use of an electro enhanced dialysis cell according to any one of claims 29-36 in the method according to claims 1-11.

38. Use of an electro enhanced dialysis cell according to any one of claims 29-36 in the apparatus according to claims 14-26.

Drawings

Fig. 1

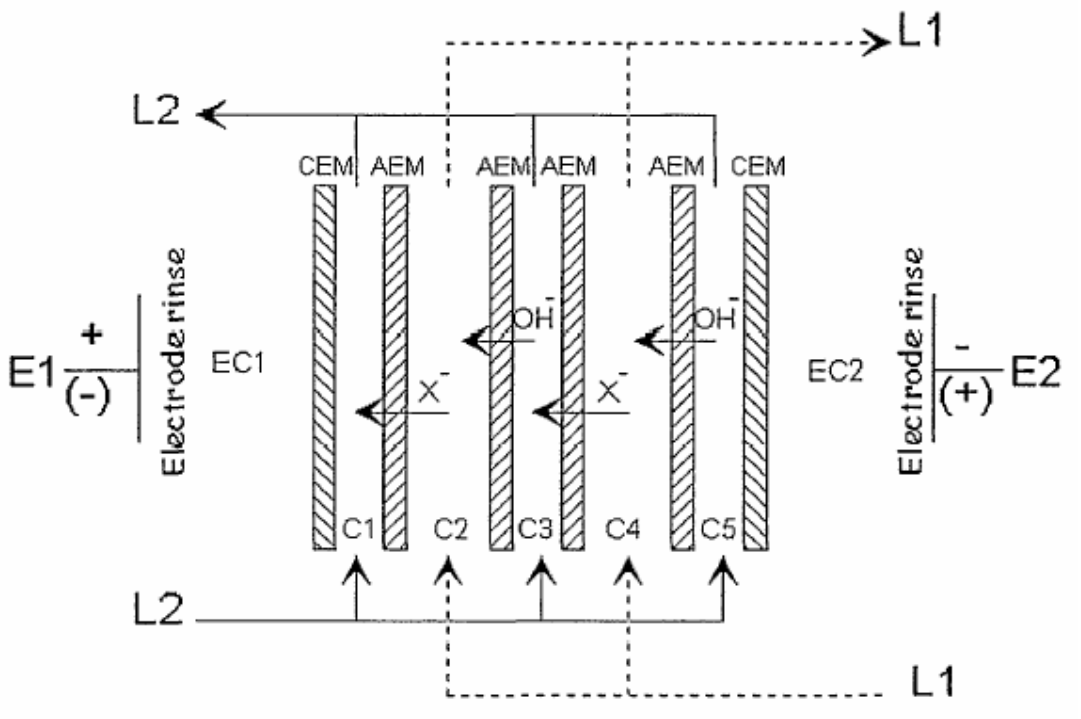

Fig. 2

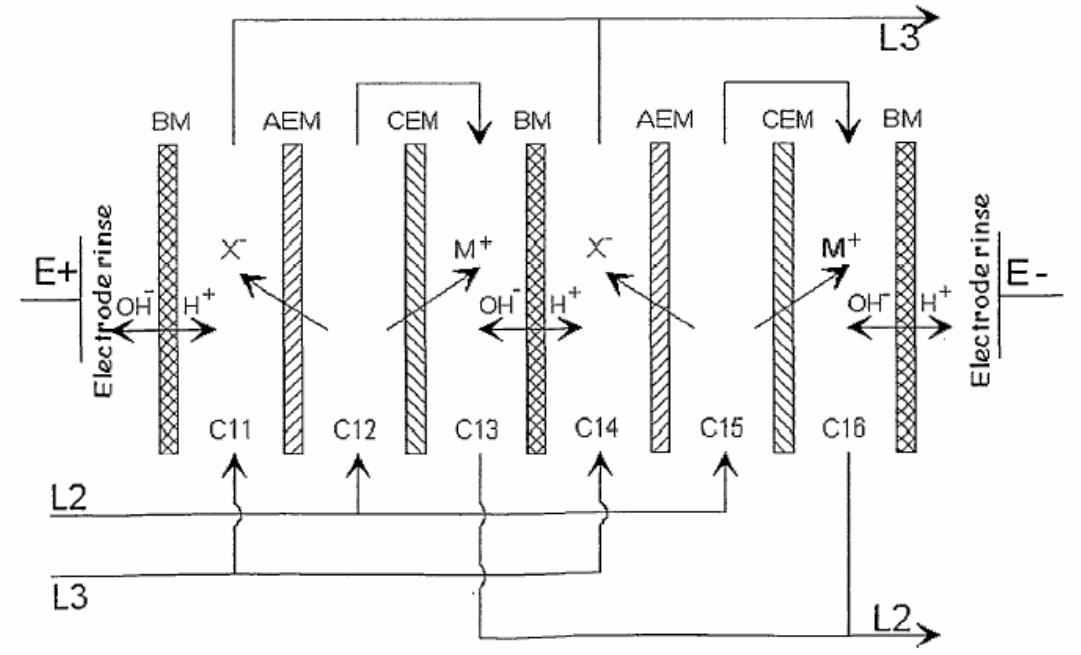

Fig. 3A

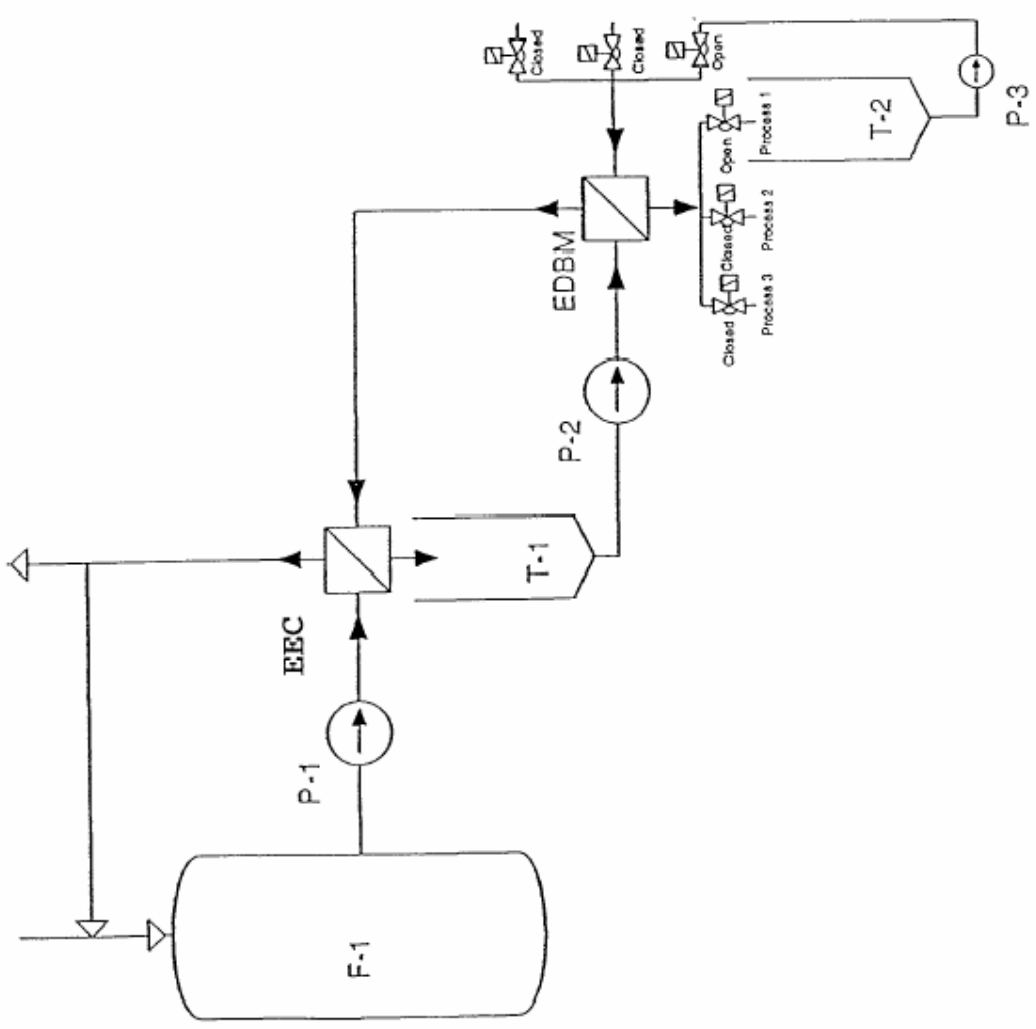
Closed
Closed
Open
Process 1
Open
Process 2
Closed
Process 3
Closed
T-2
P-3
EDBM
P-2
T-1
EEC
P-1
F-1

Fig. 3B

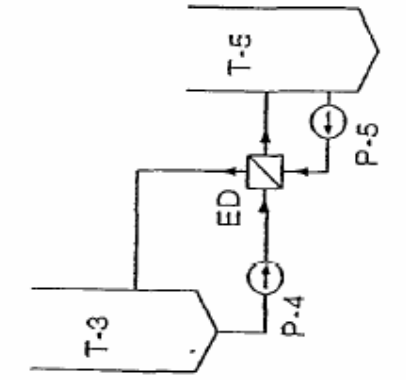
T-5
P-5
ED
P-4
T-3

Fig. 3C

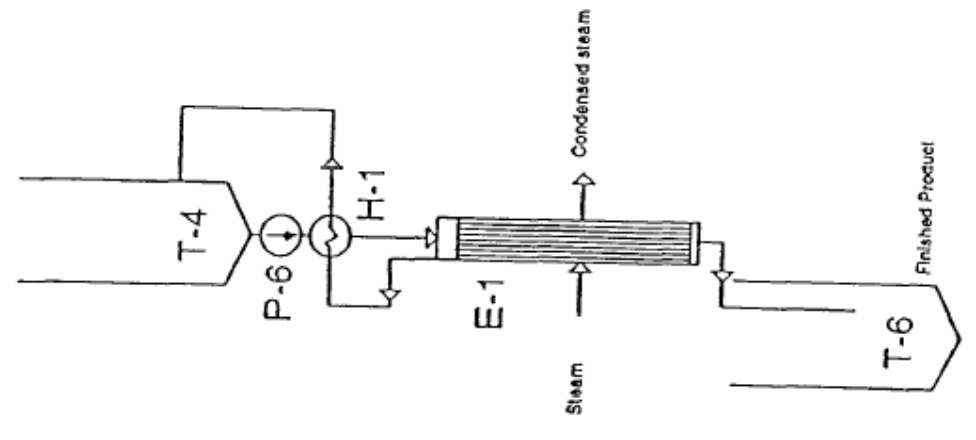
Condensed steam
H-1
T-4
P-6
E-1
Finished Product
T-6
Steam

Fig. 4

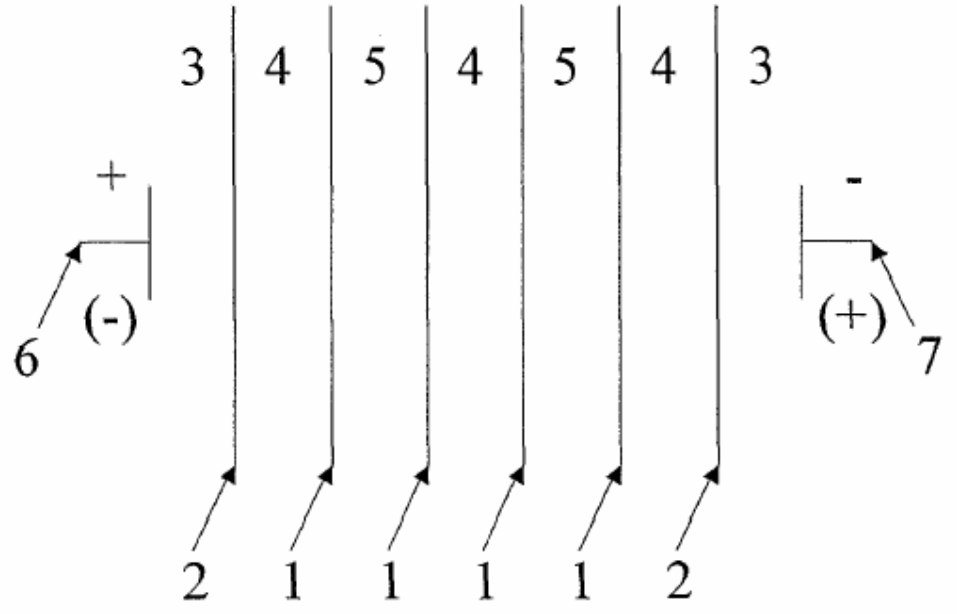
3
4
5
4
5
4
3
+
-
6
(-)
(+)
7
2
1
1
1
1
2

Fig. 5

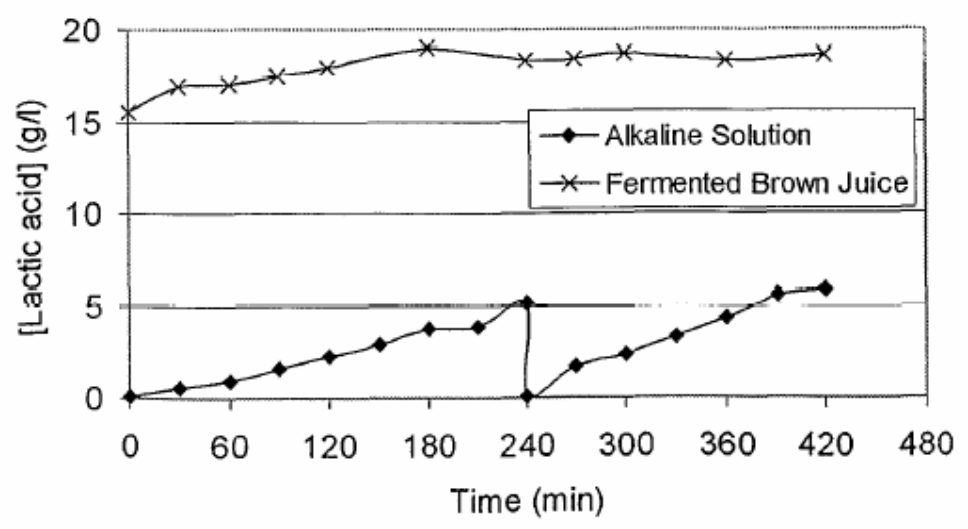

Fig. 6

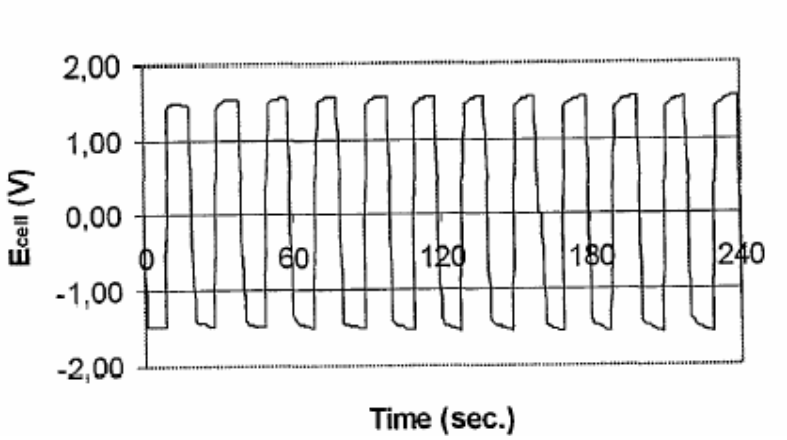

Fig. 7

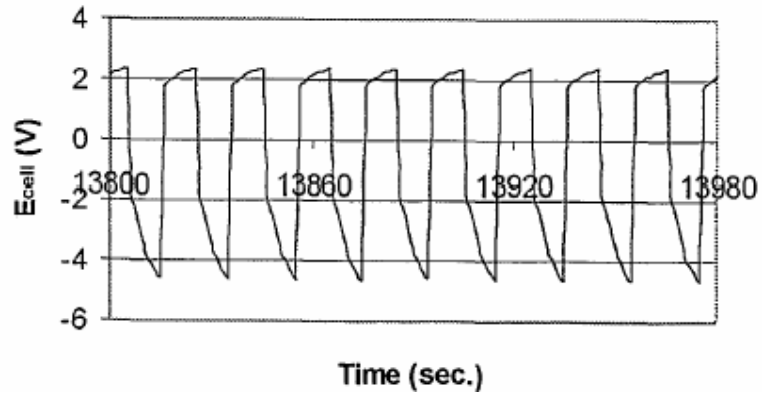

Fig. 8

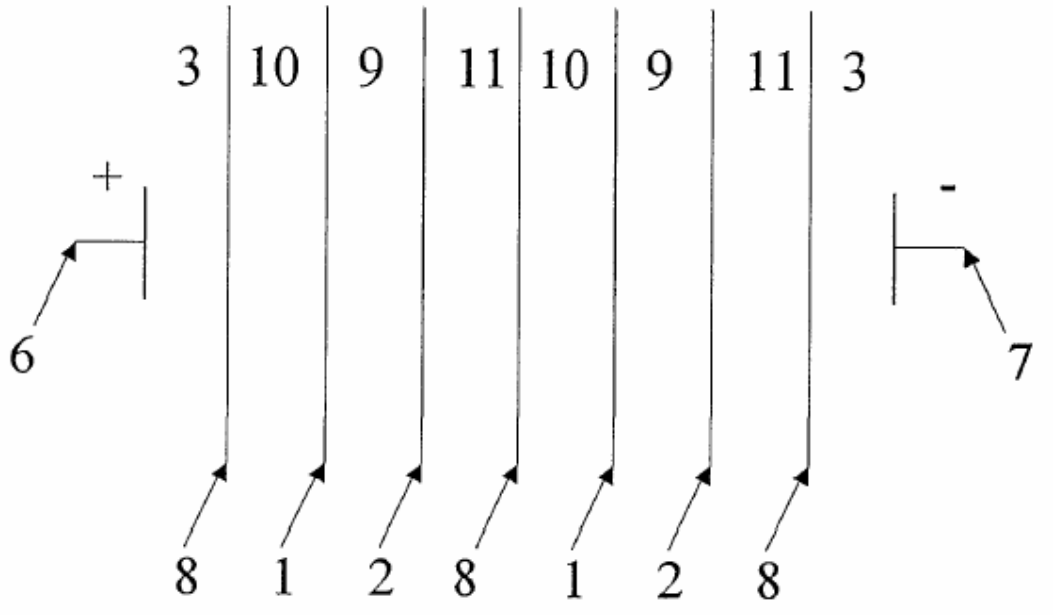
3
10
9
11
10
9
11
3
+
-
6
7
8
1
2
8
1
2
8

Fig. 9

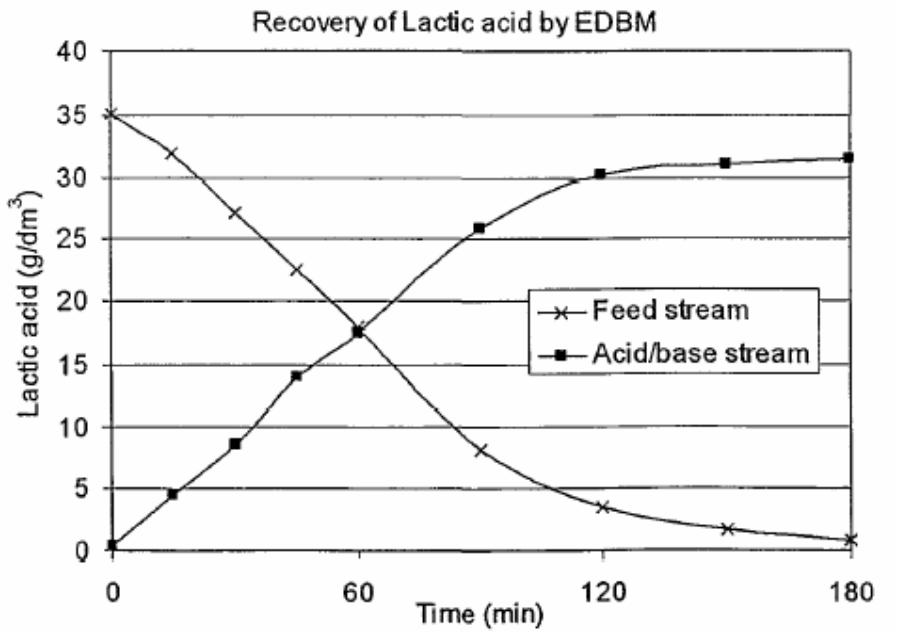
Recovery of Lactic acid by EDBM
Lactic acid (g/dm3)
40
35
30
25
20
15
10
5
0
0
60
120
180
Time (min)
Feed stream
Acid/base stream

Fig. 10

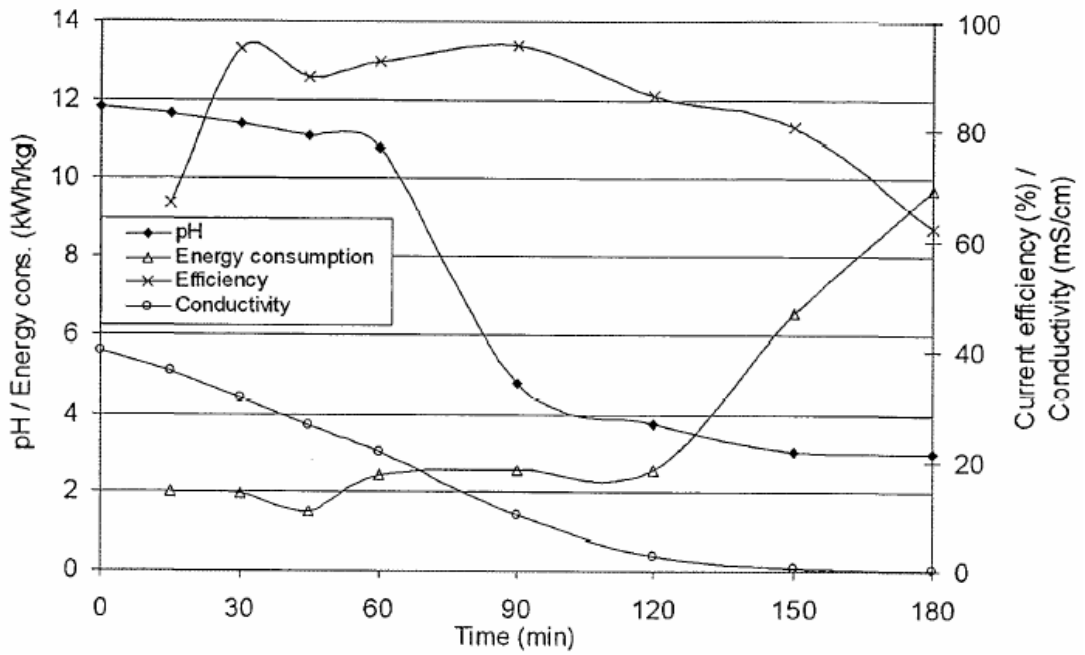
pH / Energy cons. (kWh/kg)
Current efficiency (%) / Conductivity (mS/cm)
Time (min)
pH
Energy consumption
Efficiency
Conductivity
0
2
4
6
8
10
12
14
0
20
40
60
80
100
0
30
60
90
120
150
180

Fig. 11

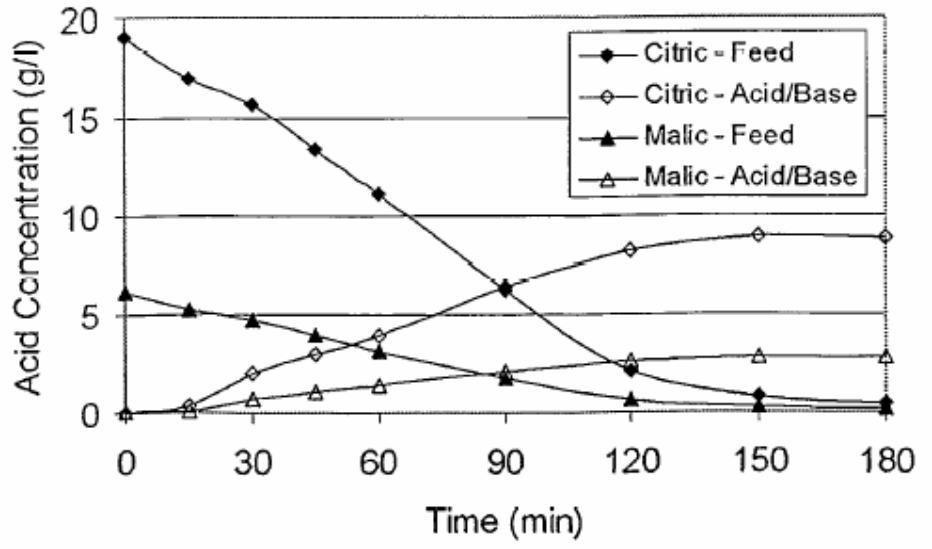
Acid Concentration (g/l)
Time (min)
Citric - Feed
Citric - Acid/Base
Malic - Feed
Malic - Acid/Base
0
5
10
15
20
0
30
60
90
120
150
180

Fig. 12

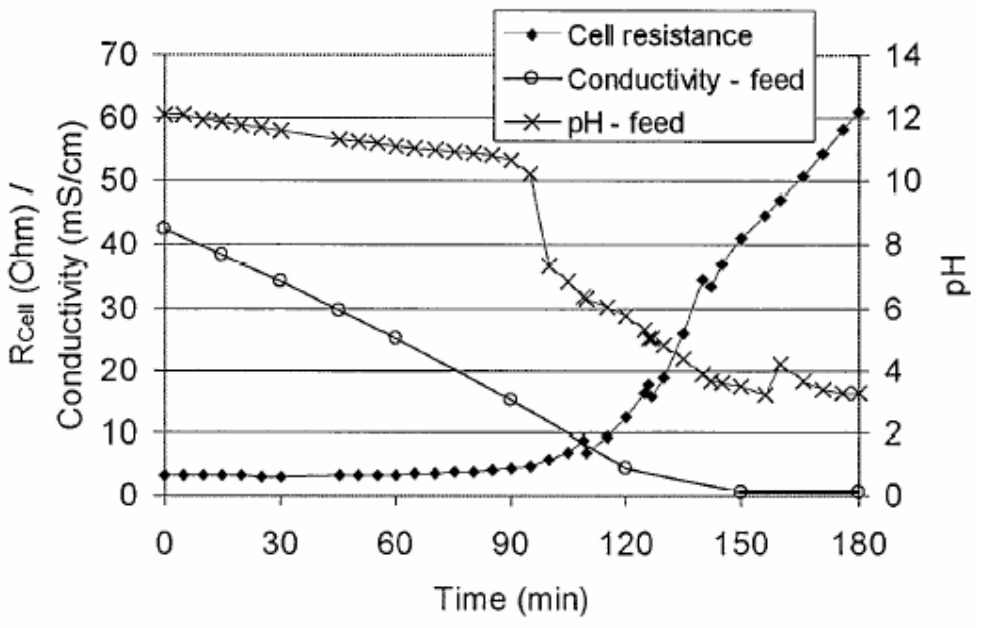
Cell resistance
Conductivity - feed
pH - feed
Rcell (Chm) / Conductivity (mS/cm)
pH
Time (min)
0
10
20
30
40
50
60
70
0
2
4
6
8
10
12
14
0
30
60
90
120
150
180

Fig. 13

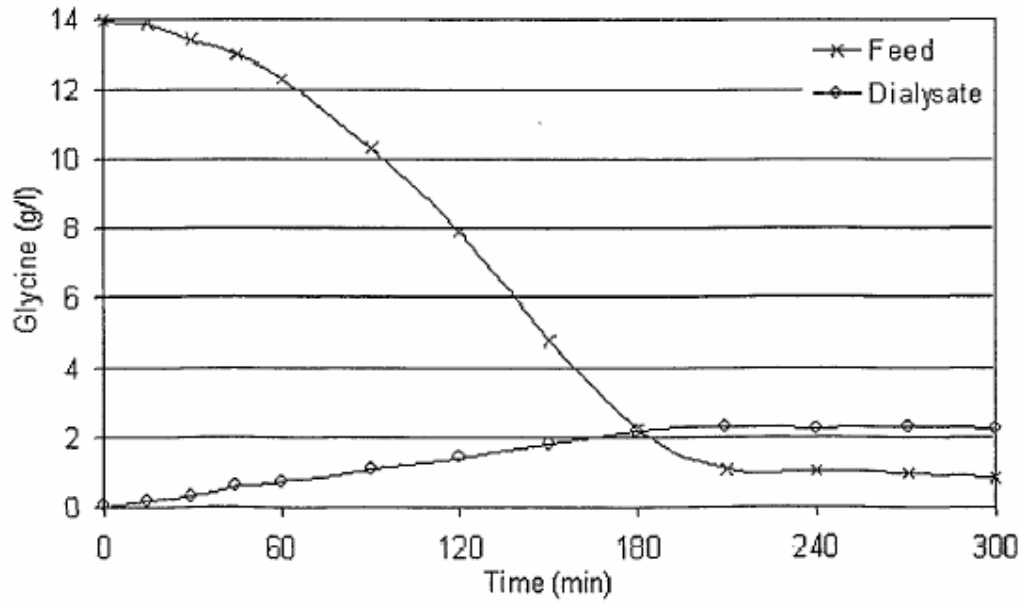
Feed
Dialysate
Glycine (g/l)
Time (min)
0
2
4
6
8
10
12
14
0
60
120
180
240
300

Fig. 14

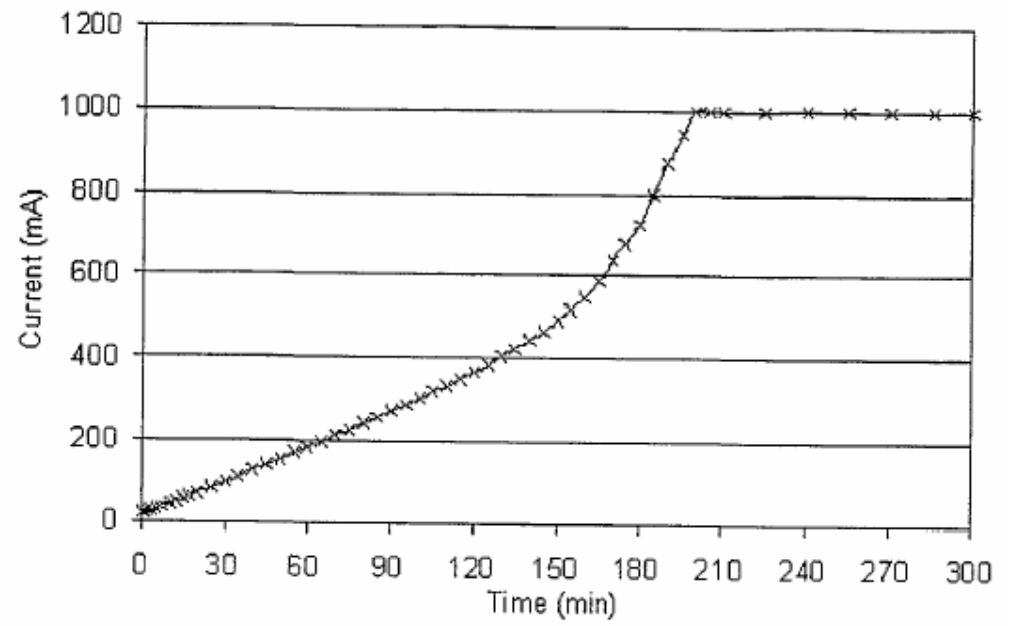
1200
1000
800
600
400
200
0
Current (mA)
0
30
60
90
120
150
180
210
240
270
300
Time (min)

Fig. 15

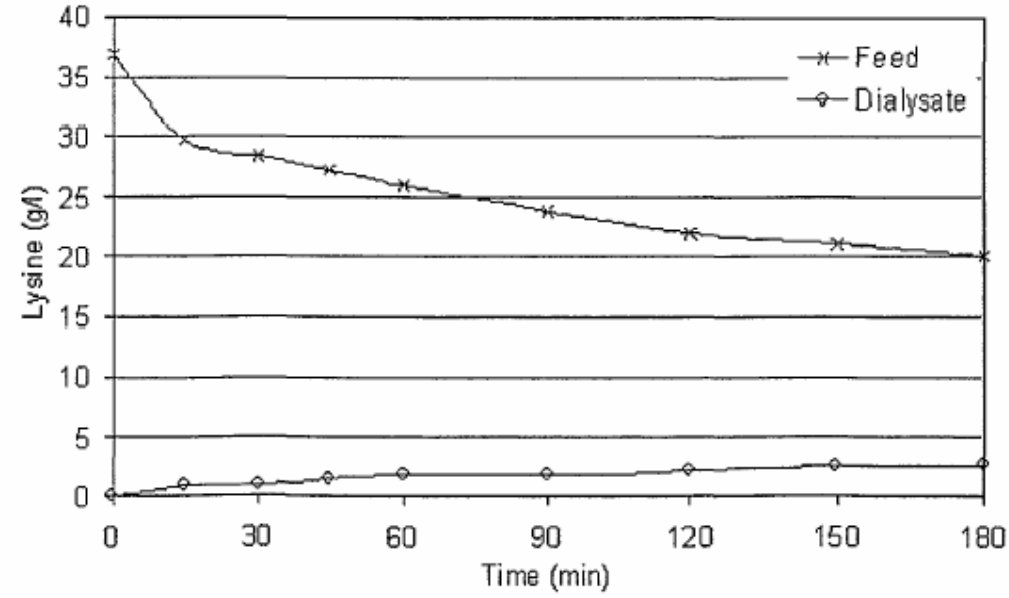
40
35
30
25
20
15
10
5
0
Lysine (g/l)
Feed
Dialysate
0
30
60
90
120
150
180
Time (min)